

University of Southampton Research Repository  
ePrints Soton

Copyright © and Moral Rights for this thesis are retained by the author and/or other copyright owners. A copy can be downloaded for personal non-commercial research or study, without prior permission or charge. This thesis cannot be reproduced or quoted extensively from without first obtaining permission in writing from the copyright holder/s. The content must not be changed in any way or sold commercially in any format or medium without the formal permission of the copyright holders.

When referring to this work, full bibliographic details including the author, title, awarding institution and date of the thesis must be given e.g.

AUTHOR (year of submission) "Full thesis title", University of Southampton, name of the University School or Department, PhD Thesis, pagination

# **The determination of pure beta-emitters and their behaviour in a salt-marsh environment**

**A thesis presented for the degree of**

**DOCTOR OF PHILOSOPHY**

**(Faculty of Science, University of Southampton)**

**Phillip Edward Warwick BSc CChem MRSC**

**Supervisors : Dr I W Croudace (School of Ocean & Earth Science)  
& Dr A G Howard (Dept. of Chemistry)**

**Submitted : April 1999**

**Abstract**

**FACULTY OF SCIENCE**  
**School of Ocean and Earth Science / Dept. of Chemistry**

**Doctor of Philosophy**

**The determination of pure beta-emitters and their behaviour in a salt-marsh environment**

**By**  
**Phillip Edward Warwick**

The thesis describes the development of analytical procedures for the isolation and measurement of anthropogenic pure beta-emitting radioisotopes in low-level radioactive wastes and environmental samples. The research focussed on three key pure beta-emitting radioisotopes, namely  $^{63}\text{Ni}$ ,  $^{90}\text{Sr}$  and  $^{99}\text{Tc}$ . Iron-55, which decays by electron capture, was also investigated. Source preparation and measurement techniques based on liquid scintillation counting were developed and optimised to permit the low-level measurement of all four radioisotopes. In particular, a technique was developed for increasing the amount of stable Fe that may be loaded into scintillant, reducing the limit of detection achievable for  $^{55}\text{Fe}$  measurement and increasing the sensitivity of analysis for  $^{55}\text{Fe}$  in Fe-rich materials such as sediments and steels.

Chemistries for the isolation of the four radioisotopes were studied and optimised. Solvent extraction was chosen for the specificity offered by the technique. In most instances, improvements in separation efficiency were achieved by adsorbing the extractant onto an inert support producing an extraction chromatographic material. Key separation techniques were then combined to produce a sequential separation scheme that permitted a more rapid analysis of the four radioisotopes on a single sample. The sequential separation technique was then optimised for the analysis of  $^{55}\text{Fe}$ ,  $^{63}\text{Ni}$ ,  $^{90}\text{Sr}$  and  $^{99}\text{Tc}$  in both low-level wastes and environmental matrices (mainly sediments). Such separation schemes are crucial to the efficient analysis of samples in limited time spans and are vital when the amount of sample available is restricted.

The optimised methods were used to investigate levels of anthropogenic pure beta-emitters in a saltmarsh sediment core collected from the Esk Estuary in Cumbria. Analysis of the four beta emitting radioisotopes was complemented by the analysis of major elements, trace elements and gamma emitting radioisotopes. This information was used to determine the behaviour of the beta emitters following deposition within the saltmarsh environment. Although all four beta emitters were detected in the core, only  $^{90}\text{Sr}$  and  $^{99}\text{Tc}$  were at sufficiently high levels to permit a more thorough investigation. The combination of geochemical analysis and radiochemical analysis of this range of radioisotopes with widely varying chemistries has allowed a range of possible pre- and post-depositional processes to be investigated as well as providing data on the levels of previously unmeasured beta emitters in the saltmarsh environment. Such information is essential in assessing the long-term retention and potential re-release of these radioisotopes and their importance in radiological dose assessment. The information also has wider implications to the behaviour of inorganic pollutants in coastal waters.

## **Acknowledgements**

I would like to thank Dr Ian Croudace and Dr Alan Howard for their valued supervision, contribution, support and patience during this study; Mike Bains, Dr Bob Carpenter and Paul Foster (AEA Technology), for their support of the PhD; Chris Dale (NNC Environmental Consultancy), Jane Caborn and Frank Wigley (University of Southampton), for working with me on aspects of the project and Richard Shaw, Eichrom Industries, for supplying some of the analytical materials. I would also like to thank Dr Andy Milton and Prof. R Nesbitt (University of Southampton) for ICP-MS measurements and Darryl Green (Challenger Division, SOC) for ICP-AES measurements and many helpful discussions.

The project has been considerably helped by fruitful interactions with all those in the Department but especially, Dom, Sonia, Wink, Alison, Andy Milton, Rex, Bob, John, Posy, Jung-Suk, Anneke, Keith, Andy Cundy and Jim.

I would like to dedicate this thesis to my mother, father, family and in particular Sue for standing by and supporting me through those stressful years; without their help I would have never been able to complete this work.

**To Dad, Mum, Sue, Daniel and Mina**

*‘Scientists first have a responsibility of ordinary citizens, but then they have a responsibility because of their understanding of science, and of those problems of society in which science is closely involved, to help their fellow citizens to understand, by explaining to them their own understanding of these problems.’*

*Linus Pauling*

### **Declaration**

This study predominantly represents research conducted by myself. However, some data presented have resulted from collaboration with individuals both within the School and from industry. In all cases this has involved a significant intellectual contribution from myself and has largely resulted in the publication of papers in peer-reviewed journals. Where such collaboration has occurred, this is clearly stated at the beginning of the relevant section and in the list of authors on the papers.

## Contents

### Introduction

<b>1. Beta emitters in the environment</b>	<b>1</b>
1.1 Occurrence of beta emitters	
1.2 Sources of pure beta emitters in the marine environment	
1.3 Beta decay	
1.4 Sources of anthropogenic radioactivity in UK coastal waters	
1.5 Behaviour of radioisotopes in coastal waters and sediments	
1.6 The importance of pure beta-emitting radioisotopes	
1.7 Summary and aims of the study	
1.8 References	
<b>2. A review of techniques for the determination of pure beta emitters</b>	<b>30</b>
2.1 Detection of beta emitting radioisotopes	
2.2 Liquid scintillation counting	
2.3 Liquid scintillation counters	
2.4 Preparation of samples for liquid scintillation counting	
2.5 Review of Cerenkov counting	
2.6 Comparison of liquid scintillation counters with non-radiometric techniques	
2.7 Review of chemical separation techniques employed prior to liquid scintillation counting	

## Experimental

<b>3. Development of source preparation and measurement techniques</b>	<b>68</b>
3.1 Stability of the Wallac 1220 Quantulus liquid scintillation counter	
3.2 Deconvolution of isotopes of the same element	
3.3 Optimisation of source preparation techniques for liquid scintillation counting	
3.4 The extraction of radioisotopes into an organic solvent	
3.5 Measurement of acidic solutions by liquid scintillation analysis	
3.6 <b>Paper</b> : An optimised method for the measurement of $^{55}\text{Fe}$ using liquid scintillation analysis	
3.7 Counting precipitates by liquid scintillation analysis	
3.8 Optimisation of $^{90}\text{Sr}$ measurement by Cerenkov counting	
3.9 <b>Paper</b> : Simplified determination of $^{90}\text{Sr}$ activity and $^{90}\text{Sr}$ : $^{89}\text{Sr}$ ratios in low-level wastes using Cerenkov counting and mathematical deconvolution	
3.10 Conclusions	
3.11 References	
<b>4. Solvent extraction and extraction chromatography</b>	<b>123</b>
4.1 Introduction	
4.2 Definition of partition coefficient, distribution coefficient and $k'$	
4.3 Separation and purification of iron-55	
4.4 Nickel-63	
4.5 Strontium-90	
4.6 Technetium-99	
4.7 <b>Paper</b> : An optimised method for technetium-99 determination in low-level waste by extraction into tri-n-octylamine	
4.8 <b>Paper</b> : Solid-phase extraction of technetium-amine complexes onto a C <sub>18</sub> -silica and its application to the analytical separation of $^{99}\text{Tc}$	
4.9 Use of TEVA resin for the purification of Tc	
4.10 Conclusions to Chapter 4	
4.11 References	

<b>5. Sequential separation of beta emitters</b>	<b>165</b>
5.1 Introduction	
5.2 Extraction chromatographic techniques in the sequential separation of beta emitting radioisotopes in low-level waste	
5.3 Sequential separation of $^{55}\text{Fe}$ , $^{63}\text{Ni}$ , $^{90}\text{Sr}$ and $^{99}\text{Tc}$ from sediments	
5.4 <b>Paper</b> : An optimised method for the routine determination of technetium-99 in environmental samples by liquid scintillation counting	
5.5 Conclusions	
5.6 References	
<b>6. Environmental study</b>	<b>209</b>
6.1 Introduction	
6.2 Methodology	
6.3 Analytical results for core RC-96-007	
6.4 Conclusions	
6.5 References	
<b>7. Overall Conclusions</b>	<b>252</b>
<b>8. Appendices</b>	<b>257</b>
A1 Conferences / meetings / courses attended / publications	
A1.1 Conferences / meetings	
A1.2 Papers in refereed journals	
A1.3 Official reports	
A2 Major and trace element results for core RC-96-007	
A3 Detection limits in routine XRF analysis at Southampton using a Rh anode X-ray tube	
A4 Results for gamma emitters in core RC-96-007	
A5 Results for beta emitters in core RC-96-007	
A6 Sellafield aqueous discharge data	
A7 Table of principle decay energies for Nirex priority radioisotopes	

## Notes on the structure of the thesis

**Chapter 1** sets the context of the research. The main routes for production and release of pure beta-emitting radioisotopes are discussed along with their behaviour in the environment following release. The objectives of this study are then presented.

**Chapter 2** is a review of the measurement techniques employed in the determination of pure beta-emitters. Both radiometric and certain non-radiometric techniques are discussed and their application to this study are investigated. A review of relevant chemical purification techniques is also presented.

**Chapter 3** details the development and optimisation of measurement techniques that have been developed as part of this study for the quantitative measurement of  $^{55}\text{Fe}$ ,  $^{63}\text{Ni}$ ,  $^{90}\text{Sr}$  and  $^{99}\text{Tc}$ . In all cases liquid scintillation counting is employed as the preferred measurement technique.

**Chapter 4** is involved with the development of techniques for the isolation of  $^{55}\text{Fe}$ ,  $^{63}\text{Ni}$ ,  $^{90}\text{Sr}$  and  $^{99}\text{Tc}$  and separation of these radioisotopes from other interfering radioisotopes. Optimisation of solvent extraction techniques followed by the development of these techniques into chromatographic methods is discussed.

**Chapter 5** presents the incorporation of the separation techniques discussed in Chapter 4 into sequential separation schemes permitting the isolation and purification of all four radioisotopes from a single sample. The Chapter is divided into three main sub-sections concentrating on the sequential separation of the radioisotopes from low-level wastes and from environmental samples with the final sub-section focussing on the specific isolation of  $^{99}\text{Tc}$  from environmental samples.

**Chapter 6** discusses the application of the sequential separation techniques to the study of pure beta-emitters in a saltmarsh environment. The profile of the beta emitters in a saltmarsh core collected from the Esk estuary is presented in the context of discharges from the nearby BNFL site at Sellafield and the geochemistry of the sediment core.

### Notes on the presentation of papers

In a number of instances, the research has been published in papers in peer-reviewed journals. These papers have been presented in their entirety as discrete sections within Chapters in the thesis. Where this is the case, for clarity of the thesis, Figure and Table numbering are prefixed with 'P'. Referencing is in the style consistent with the overall thesis rather than that of the original paper. However, lists of references that are specific to the paper are given at the end of the paper rather than at the end of the thesis chapter.

## Chapter 1

# **Introduction**

## **Beta emitters in the environment**

## 1 Beta emitters in the environment

### 1.1 Occurrence of beta emitters

Alpha, beta and beta/gamma emitting radioisotopes are routinely released into the environment by nuclear power stations, nuclear fuel reprocessing facilities and other nuclear facilities as part of their authorised discharge. These releases are either to the atmosphere as gaseous discharges or to rivers or the sea via aqueous effluent discharges. In addition, significant quantities of radioactivity have been released to the environment as a result of the atmospheric testing of nuclear weapons<sup>1</sup> and as a result of nuclear accidents.

The behaviour and ultimate fate of a radioisotope released into the marine environment may depend on the oxidation state and chemical speciation of the radioisotope on discharge, complexation and oxidation/reduction of the radioisotope following discharge as well as the environment into which it is being discharged. The isotope may be scavenged by particulates in the seawater column or assimilated by marine biota leading to the accumulation of the isotope where it may be fixed or subsequently remobilised. If none of these interactions occur, the isotope could remain dispersed in the water column and may be used as a tracer for water movements.

The behaviour of alpha and beta/gamma emitting radioisotopes in the marine environment has been extensively studied both due to their radiological significance and their use as tracers in the study of natural processes in the environment. Natural radioisotopes including the U and Th decay series and cosmogenic radioisotopes, such as  $^{3}\text{H}$ ,  $^{14}\text{C}$  and  $^{129}\text{I}$ , have found widespread application in the study of a range of environmental processes. These have been complemented in environmental studies by the use of anthropogenic radioisotopes, with their associated discrete and well-characterised source term. Following the testing of nuclear weapons in the 1950s and 1960s the behaviour of  $^{55}\text{Fe}$  in the oceans was studied (e.g. Livingston *et al*, 1979). Dispersion of the European Coastal Current has been studied using  $^{90}\text{Sr}$ ,  $^{99}\text{Tc}$ ,  $^{125}\text{Sb}$  and  $^{137}\text{Cs}$  discharged from La Hague (Dahlgaard, 1995).  $^{99}\text{Tc}$  and  $^{137}\text{Cs}$  discharged from Sellafield have also been used in the study of water transport from the Irish Sea to the North Sea.  $^{137}\text{Cs}$  is, however, scavenged by particulate clays and once bound within the interstitial sites of the clay is effectively immobilised. The extent of this effect depends on water salinity and on the composition of the sediment (Beneš *et al*, 1989). An advantage of this scavenging process

is that  $^{137}\text{Cs}$ - and  $^{134}\text{Cs}$ -derived from weapons fallout and the Chernobyl accident can be used to determine accumulation rates.

Pure anthropogenic beta emitters have not been so thoroughly studied, mainly due to difficulties associated with their measurement, their lower concentrations and hence their perceived relatively low radiological importance. Of the anthropogenic pure beta-emitting radioisotopes discharged, only  $^3\text{H}$ ,  $^{90}\text{Sr}$  and  $^{99}\text{Tc}$  have been studied in depth as they are discharged in considerable quantities.  $^{90}\text{Sr}$  is the most important radiologically due to the high-energy beta emission of its daughter  $^{90}\text{Y}$ . Although of less significance radiologically,  $^{99}\text{Tc}$  in the marine environment has become more intensely studied following the commissioning of EARP (Enhanced Actinide Recovery Plant) at Sellafield, Cumbria, in 1994. Reprocessing of previously stockpiled Magnox wastes has resulted in a significant increase in the levels of  $^{99}\text{Tc}$  discharged to the Irish Sea.

Few studies of the behaviour of other pure beta emitters in the marine environment have been undertaken. Some work has been published on the behaviour of radioactive  $^{63}\text{Ni}$  (Koide and Goldberg, 1985) and  $^{121}\text{m}+^{126}\text{Sn}$  in the marine environment (Koide and Goldberg, 1985; Patton and Penrose, 1989). Levels of  $^{147}\text{Pm}$  along with  $^3\text{H}$ ,  $^{14}\text{C}$ ,  $^{90}\text{Sr}$  and  $^{99}\text{Tc}$  are routinely monitored as part of British Nuclear Fuels Ltd (BNFL) and Ministry of Agriculture, Fisheries and Foods (MAFF) surveillance programmes (e.g. BNFL, 1995).

## **1.2 Sources of pure beta emitters in the marine environment**

There are three sources of radioisotopes in the marine environment, namely

- a) Primordial
- b) Cosmogenic
- c) Anthropogenic

### *1.2.1 Primordial radioisotopes*

These are radioisotopes that were present when the Earth was formed and which have sufficiently long half lives, compared to the age of the Earth ( $4.5 \times 10^9$  years), to have survived to the present day. The most well known primordial radioisotopes are those of uranium and thorium and  $^{40}\text{K}$ . Many elements also have isotopes which, although very

long lived, are unstable and decay usually via alpha or beta decay or electron capture.

Table 1.1 summarises such isotopes

**Table 1.1 Primordial radioisotopes**

Nuclide	Isotopic abundance	Decay mode and particle energy (MeV)	Half-life (years)	Bq/g nuclide	Bq/g of element*
<sup>40</sup> K	0.0117	$\beta^-$ EC 1.31	$1.26 \times 10^9$	$2.6 \times 10^5$	30.7
<sup>50</sup> V	0.250	$\beta^-$ EC (0.601)	$> 1.4 \times 10^{17}$	0.0019	$4.7 \times 10^{-6}$
<sup>87</sup> Rb	27.83	$\beta^-$ 0.273	$4.88 \times 10^{10}$	3118	868
<sup>115</sup> In	95.72	$\beta^-$ 1.0	$4.4 \times 10^{14}$	0.26	0.250
<sup>123</sup> Te	0.905	EC (0.052)	$1.3 \times 10^{13}$	8.28	0.075
<sup>138</sup> La	0.092	$\beta^-$	$1.06 \times 10^{11}$	905	0.833
<sup>144</sup> Nd	23.80	$\alpha$	$2.1 \times 10^{15}$	0.044	0.010
<sup>147</sup> Sm	15.0	$\alpha$ 2.23	$1.06 \times 10^{11}$	850	127
<sup>148</sup> Sm	11.3	$\alpha$ 1.96	$7 \times 10^{15}$	0.013	0.0014
<sup>176</sup> Lu	2.59	$\beta^-$ (1.188)	$3.8 \times 10^{10}$	1979	51.3
<sup>174</sup> Hf	0.162	$\alpha$	$2 \times 10^{15}$	0.04	$6.2 \times 10^{-5}$
<sup>187</sup> Re	62.6	$\beta^-$ (0.0025)	$4.2 \times 10^{10}$	1686	1055
<sup>190</sup> Pt	0.012	$\alpha$	$6.5 \times 10^{11}$	107	0.013
<sup>232</sup> Th	-	$\alpha$	$1.41 \times 10^{10}$	4061	-
<sup>238</sup> U	-	$\alpha$	$4.49 \times 10^9$	12444	-

Values in parenthesis are decay energies. Derived from Choppin, 1996.

\*Specific activity corrected for natural isotopic abundance

Many of these isotopes have found widespread application in geochemistry for dating purposes. However, as the half-lives of these isotopes are so long, the specific activities are extremely low and hence these isotopes are of limited interest in this study.

### 1.2.2 Cosmogenic radioisotopes

Cosmogenic radioisotopes are continually formed in the upper atmosphere through the interaction of neutrons and protons with the gaseous elements of the atmosphere. The neutrons and protons are produced either as a direct result of primary cosmic radiation or from secondary cosmic radiation resulting from the annihilation of pions in the atmosphere. The radioisotopes produced are washed out by rainfall and subsequently deposit on land and water masses. Table 1.2 summarises the most important cosmogenic radioisotopes. The isotopes tend to be neutron-rich and decay via beta-particle emission although some are proton-rich, decaying via positron emission or electron capture.

**Table 1.2 Cosmogenic radioisotopes**

Nuclide	Half life	Decay mode and particle energy (MeV)	Atmospheric production rate (atoms m <sup>-2</sup> s <sup>-1</sup> )
<b>Long lived</b>			
<sup>3</sup> H	12.32 y	$\beta^-$ 0.0186	2500
<sup>10</sup> Be	$1.52 \times 10^6$ y	$\beta^-$ 0.555	300
<sup>14</sup> C	5715 y	$\beta^-$ 0.1565	17 000 - 25 000
<sup>22</sup> Na	2.605 y	$\beta^+$ 0.545	0.5
<sup>26</sup> Al	$7.1 \times 10^5$ y	$\beta^+$ 1.16	1.2
<sup>32</sup> Si	160 y	$\beta^-$ 0.213	1.6
<sup>35</sup> S	87.2 d	$\beta^-$ 0.167	14
<sup>36</sup> Cl	$3.01 \times 10^5$ y	$\beta^-$ 0.709	60
<sup>39</sup> Ar	268 y	$\beta^-$ 0.565	56
<sup>53</sup> Mn	$3.7 \times 10^6$ y	EC (0.596)	-
<sup>81</sup> Kr	$2.2 \times 10^5$ y	EC (0.28)	-
<sup>129</sup> I	$1.57 \times 10^{10}$ y	$\beta^-$	-
<b>Short lived</b>			
<sup>7</sup> Be	53.28 d	EC (0.862)	81
<sup>24</sup> Na	14.96 h	$\beta^-$ 1.389	-
<sup>28</sup> Mg	21.0 h	$\beta^-$ 0.459	-
<sup>32</sup> P	14.28 d	$\beta^-$ 1.710	-
<sup>33</sup> P	25.3 d	$\beta^-$ 0.249	-
<sup>39</sup> Cl	55.6 m	$\beta^-$ 1.91	16

Values in parenthesis are decay energies - adapted from Choppin (1996)

As there is a relatively well-defined input of cosmogenic radioisotopes into the environment they have been extensively used as tracers for environmental processes. Such applications include determining exposure of meteorites to cosmic radiation (<sup>81</sup>Kr), marine sediment dating (<sup>10</sup>Be and <sup>26</sup>Al), hydrological studies (<sup>3</sup>H and <sup>36</sup>Cl), glacial ice dating (<sup>10</sup>Be), carbon dating (<sup>14</sup>C) and as natural tracers for atmospheric mixing and precipitation processes (<sup>39</sup>Cl and <sup>35</sup>S).

### 1.2.3 Anthropogenic radioisotopes

Anthropogenic, or man-made, radioisotopes are produced in nuclear reactors, particle accelerators and during the production and detonation of nuclear weapons. The majority of the radioisotopes released into the environment originate from nuclear weapons detonation and nuclear industry operations (in particular nuclear fuel reprocessing) with a much smaller input from hospitals and research institutes.

Anthropogenic radioisotopes found in the environment are mainly produced by either nuclear fission or neutron activation. Radioisotopes produced by nuclear fission (such as  $^{90}\text{Sr}$  and  $^{137}\text{Cs}$ ) are known as fission products. Isotopes produced via neutron activation (such as  $^{55}\text{Fe}$  and  $^{63}\text{Ni}$ ) are known as activation products.

#### 1.2.3.1 *Fission products*

When certain isotopes of the actinides are struck by a neutron the isotope may capture a neutron forming a heavier isotope or split into two smaller fragments (fission). Uranium-233,  $^{235}\text{U}$ ,  $^{239}\text{Pu}$  and  $^{241}\text{Pu}$  will all undergo fission when struck by thermalised neutrons in a reactor. Uranium-238 and  $^{232}\text{Th}$  will undergo fission with fast neutrons. Other actinide isotopes, such as  $^{252}\text{Cf}$ , undergo fission spontaneously. During the fission process, further neutrons are released along with a significant amount of energy. These neutrons strike other atoms and the process continues as a chain reaction. This reaction can be carefully controlled and the energy released used to power turbines and generate electricity forming the basis of the nuclear reactor. Under very exacting conditions the chain reaction can be made to propagate rapidly, resulting in the release of very large amount of energy in a very short period of time. This is the basis of nuclear fission weapons.

The fission process is dependent on the neutron energy and for  $^{235}\text{U}$  the most effective neutron energy is  $< 1\text{ eV}$  (thermal neutrons). Between  $1\text{ eV}$  and  $10^5\text{ eV}$  neutron capture reactions leading to the formation of heavier isotopes is dominant. Neutrons in this energy region are known as epithermal neutrons. Above  $10^6\text{ eV}$   $^{235}\text{U}$  fission dominates although the neutron cross-section is far lower than for thermal neutrons and hence fission occurs at a much slower rate. However, at this energy other actinides may undergo fission and this is most important for the fission of  $^{238}\text{U}$ . Neutrons with energies greater than  $10^5\text{ eV}$  are known as fast neutrons.

Whilst effective fission of  $^{235}\text{U}$  requires thermal neutrons, neutrons released during fission tend to have energies in the range of  $10^5 - 10^7\text{ eV}$  (i.e. fast neutrons). In a thermal nuclear reactor these fast neutrons are slowed down (moderated) to thermal energies to encourage subsequent fission of more  $^{235}\text{U}$  nuclei. However, in a nuclear weapon, little moderation is possible and subsequent fission reactions tend to be instigated by fast

neutrons. The characteristics of fission are therefore different for nuclear reactors and nuclear weapons. This is particularly noticeable in the formation of fission products.

When a fissile nucleus is struck by a neutron the resulting split is unsymmetrical. For thermal neutrons and  $^{235}\text{U}$ , the most probable split leads to the formation of one nuclide having a mass around 97 and one with a mass around 137. In fact the range of masses produced is much larger. Over 400 fission fragments have been identified associated with elements ranging from zinc to gadolinium. A typical thermal neutron fission yield curve is shown in Figure 1.1

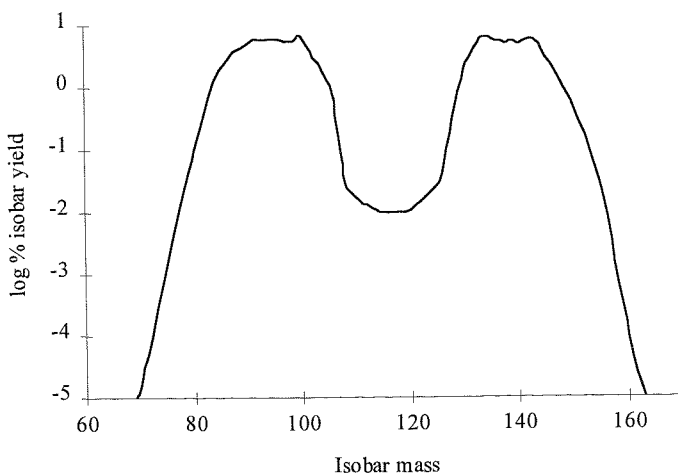
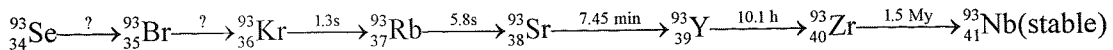


**Figure 1.1 Fission yield curve for  $^{235}\text{U}$  irradiated with thermal neutrons**  
(adapted from Steinberg and Glendenin, 1956)

The fission of heavier nuclides yields similar curves to that shown in Figure 1.1 although the left peak shifts to heavier masses. With increasing neutron energy, the trough between the two peaks becomes less pronounced until, at very high energies, a single symmetrical peak is found. Hence for nuclear weapons employing  $^{239}\text{Pu}$  and fast neutron irradiation, the peaks would be shifted to higher masses with a less pronounced trough compared to a nuclear reactor where the  $^{235}\text{U}$  fuel is irradiated with thermal neutrons.

The fission fragments formed during nuclear fission are unstable and neutron rich. These fragments usually decay via beta emission to produce a less neutron rich daughter. Some nuclides, however, will decay via a delayed emission of a neutron and approximately 0.016% of neutrons produced during the fission of  $^{235}\text{U}$  are delayed neutrons produced in this manner. This process continues until a stable daughter is attained. In this way isobaric chains are produced. One example is the  $A = 93$  isobar shown below.



The total yield for  $A = 93$  is 6.375%. Delayed neutrons are produced by  $^{93}\text{Se}$ ,  $^{93}\text{Br}$ ,  $^{93}\text{Kr}$  and  $^{93}\text{Rb}$ . The highest individual fission fragment yield is for  $^{93}\text{Rb}$  (2.96%) and  $^{93}\text{Sr}$  (2.66%). The fission fragment yield for  $^{93}\text{Zr}$  is only  $3 \times 10^{-4}\text{ %}$ . However, because of its very long half life, compared to the other nuclides in the chain,  $^{93}\text{Zr}$  is the predominant  $A = 93$  nuclide found in fission product waste. There is normally a displacement of several atomic numbers between the most probable isotope and the stable end isotope. In general the distribution of isotopes in an isobar follows a Gaussian curve described by the equation

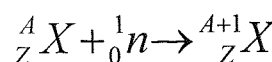
$$y(A, Z) = y(A)s^{-1}(2\pi)^{-\frac{1}{2}}e^{-(Z-Z_p)^2/(2s^2)}$$

where  $y(A, Z)$  is the initial yield of the fission fragment with atomic number  $Z$  and mass  $A$ ,  $y(A)$  is the total yield of isobar mass  $A$ ,  $s$  is the width parameter for the charge distribution at mass  $A$  and  $Z_p$  is the most probable atomic number. A discussion of the distribution of  $Z$  for a given isobar may be found in Pappas (1956)

It can be seen that fission of any fissile nucleus leads to the production of numerous fragments which decay via a series of beta emissions to form a range of products which are predominantly beta and beta/gamma emitters.

### 1.2.3.2 Activation products

When a nucleus of an atom is struck by a neutron, the neutron may be captured to produce a heavier isotope of the same element. The process is summarised as



The isotope produced is neutron rich and may decay via the emission of a beta particle. In a reactor or during the detonation of a nuclear weapon the fissile material, construction material and atmospheric gases may all undergo neutron activation producing a series of

unstable beta-emitting radioisotopes. The nature and quantities of these activation products will vary depending on the materials present and the energy and exposure time of the irradiating neutrons. The probability of neutron interaction for a given isotope of an element is known as the neutron cross section and is measured in units of barns ( $\sigma$ ). The higher the neutron cross section, the more probable a given interaction is likely to occur and the more of the particular product is formed. The neutron cross section will depend on the energy of the neutron. More than one reaction may occur during the interaction of an isotope with a neutron and cross sections for each reaction are quoted. For example when a thermal neutron strikes  $^{235}\text{U}$ , the neutron may be elastically scattered with no change to the  $^{235}\text{U}$  nucleus, captured to form  $^{236}\text{U}$ , or the  $^{235}\text{U}$  may undergo fission. The cross sections for each reaction are  $\sigma_{\text{scat}} = 10\text{b}$ ;  $\sigma_{\text{act}} = 107\text{b}$ ;  $\sigma_{\text{f}} = 582\text{b}$ . The total reaction cross section ( $\sigma_{\text{tot}}$ ) is equivalent to the sum of the individual cross sections.

A wide range of beta and beta/gamma emitting radioisotopes are produced during reactor operation and weapons detonation through the neutron activation of reactor or weapon components. Typical reaction cross sections for a range of materials used in the construction of reactors and weapons along with the neutron activation products are given in Table 1.3

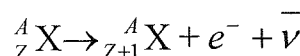
**Table 1.3 : Neutron capture cross sections for some common reactor / weapon materials**

Element	Stable isotope	Component	Thermal neutron cross section ( $\sigma$ )	Reaction	Isotope formed
H	$^2\text{H}$	$\text{H}_2\text{O}$ cooling water	$5.0 \times 10^{-4}$	$^2\text{H}(\text{n},\gamma)^3\text{H}$	$^3\text{H}$
O	$^{16}\text{O}$	$\text{H}_2\text{O}$ cooling water		$^{16}\text{O}(\text{n},\text{p})^{16}\text{N}$	$^{16}\text{N}$
	$^{18}\text{O}$	$\text{H}_2\text{O}$ cooling water		$^{18}\text{O}(\text{n},\gamma)^{19}\text{O}$ $^{18}\text{O}(\text{n},\text{p})^{18}\text{F}$	$^{19}\text{O}$ $^{18}\text{F}$
Li	$^6\text{Li}$	trace in cooling water	940.5	$^6\text{Li}(\text{n},\text{t})^3\text{He}$	$^3\text{He}$
		weapon component			
Be	$^9\text{Be}$	weapon component	$7.6 \times 10^{-3}$	$^9\text{Be}(\text{n},\gamma)^{10}\text{Be}$	$^{10}\text{Be}$
B	$^{10}\text{B}$	boric acid moderator (PWR)	3843	$^{10}\text{B}(\text{n},\alpha)^7\text{Li}$	$^7\text{Li}$
C	$^{13}\text{C}$	carbon in steel		$^{13}\text{C}(\text{n},\text{p})^{13}\text{N}$	$^{13}\text{N}$
		$\text{CO}_2$ in coolant water or as coolant			
N	$^{14}\text{N}$	N in cooling water	n.a 1.82	$^{14}\text{N}(\text{n},2\text{n})^{13}\text{N}$	$^{13}\text{N}$
				$^{14}\text{N}(\text{n},\text{p})^{14}\text{C}$	$^{14}\text{C}$
S	$^{34}\text{S}$		0.224	$^{34}\text{S}(\text{n},\gamma)^{35}\text{S}$	$^{35}\text{S}$
Cl	$^{35}\text{Cl}$	Contaminant in graphite etc.		$^{35}\text{Cl}(\text{n},\gamma)^{36}\text{Cl}$	$^{36}\text{Cl}$
Ar	$^{40}\text{Ar}$	atmospheric gas found in cooling water	0.68	$^{40}\text{Ar}(\text{n},\gamma)^{41}\text{Ar}$	$^{41}\text{Ar}$
Cr	$^{50}\text{Cr}$	Stainless steel	15.97	$^{50}\text{Cr}(\text{n},\gamma)^{51}\text{Cr}$	$^{51}\text{Cr}$
Mn	$^{53}\text{Mn}$				$^{54}\text{Mn}$
Fe	$^{54}\text{Fe}$	Ferrous metals / steel	2.59	$^{54}\text{Fe}(\text{n},\gamma)^{55}\text{Fe}$	$^{55}\text{Fe}$
	$^{58}\text{Fe}$	Ferrous metals / steel	1.27	$^{58}\text{Fe}(\text{n},\gamma)^{59}\text{Fe}$	$^{59}\text{Fe}$
Co	$^{59}\text{Co}$				$^{58}\text{Co}$
			37.22	$^{59}\text{Co}(\text{n},\gamma)^{60}\text{Co}$	$^{60}\text{Co}$
Ni	$^{58}\text{Ni}$	Steel	4.62	$^{58}\text{Ni}(\text{n},\gamma)^{59}\text{Ni}$	$^{59}\text{Ni}$
	$^{62}\text{Ni}$	Steel	14.43	$^{62}\text{Ni}(\text{n},\gamma)^{63}\text{Ni}$	$^{63}\text{Ni}$
Zn	$^{64}\text{Zn}$		0.76	$^{64}\text{Zn}(\text{n},\gamma)^{65}\text{Zn}$	$^{65}\text{Zn}$
Sb	$^{123}\text{Sb}$		4.33	$^{123}\text{Sb}(\text{n},\gamma)^{124}\text{Sb}$	$^{124}\text{Sb}$

Neutron cross section data from Jef-PC database (version 2) for thermal neutrons with Maxwellian distribution around 0.0253eV

### 1.3 Beta Decay

Neutron rich radioisotopes (such as those produced by neutron activation or during nuclear fission) may decay by a number of routes but the most dominant is through the emission of an electron from the nucleus. This process is known as  $\beta^-$  decay. A neutron in the nucleus decays into a proton and an electron and hence the atomic number,  $Z$ , increases by one unit but the mass,  $A$ , remains unchanged. Although this decay is quantised, the emitted  $\beta^-$  particle (the electron) can have an energy distribution between near zero and the maximum of the decay energy. This was explained by W. Pauli who suggested that a second particle must be emitted with the electron and that the decay energy is shared between the two particles. The second particle was subsequently identified as the anti-neutrino,  $\bar{\nu}$ . The beta decay process can therefore be summarised as



The continuous distribution of the beta particle energy prevents spectrometric identification and quantification of a mixture of beta-emitting radioisotopes (*c.f.* alpha and gamma spectrometry) although some information as to the identity of particular beta emitters may be obtained using a spectrometric technique such as liquid scintillation counting. The most probable beta decay energy is approximately one third of the maximum beta decay energy. Either the maximum ( $E_{\max}$ ) or most probable ( $E_{\text{ave}}$ ) beta particle energies are quoted in decay tables.

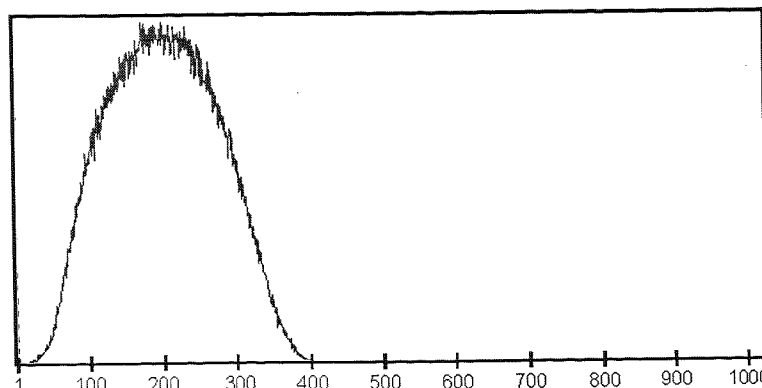
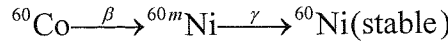


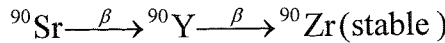
Figure 1.2 : Typical liquid scintillation beta spectrum for  ${}^{63}\text{Ni}$  ( $E_{\max} = 65.9$  keV). The data is plotted as counts registered versus channel numbers (proportional to log energy).

The daughter isotope produced by beta decay may itself be in a metastable state and will decay via the emission of gamma photons. In these cases the metastable state is usually short lived and gamma spectrometry may be used to identify and quantify the original beta

emitter. For example,  $^{60}\text{Co}$  is routinely determined by measurement of the two gamma photons at 1.173 and 1.332 MeV associated with the  $^{60m}\text{Ni}$  daughter



However, many other beta-emitting isotopes do not emit gamma photons as part of their decay scheme. Such radioisotopes are known as pure beta emitters. These isotopes can only be positively identified by specific chemical separation followed by some form of beta counting technique. One of the best known pure beta-emitting radioisotope is the fission product  $^{90}\text{Sr}$ .



## 1.4 Sources of anthropogenic radioactivity in UK coastal waters

Anthropogenic radioisotopes are released into the marine environment as part of authorised discharges from nuclear power and reprocessing sites, military establishments, and medical facilities. Significant quantities of anthropogenic radioisotopes have also been released as a result of nuclear weapons testing in the 1950s and 1960s and catastrophic nuclear accidents such as the Chernobyl accident in 1986.

### 1.4.1 Authorised releases from nuclear sites

The majority of UK nuclear sites are located on the coast (Figure 1.3) and discharge directly into the marine environment. The main reactor types in the UK are Magnox and Advanced Gas-Cooled Reactors (AGR) with one Pressurised Water Reactor (PWR) at Sizewell. The magnitude and composition of any radioactive discharge will depend on the operations being performed on the site with the greatest discharges being observed for sites involved in nuclear fuel reprocessing (i.e. Sellafield and Dounreay). In general, nuclear reprocessing operations release the whole range of fission products, activation products and actinides. Nuclear power stations release lower levels of mainly activation products, with Magnox reactors also releasing a proportion of  $^{137}\text{Cs}$ . Uranium enrichment and fuel fabrication at Capenhurst and Springfields results in the release of uranium, uranium-daughter radioisotopes and some fission products (originating from reprocessed uranium). Airborne discharges from nuclear sites will also contribute to marine radioactivity (although to a lesser extent than direct discharge to sea) with airborne

radioisotopes returning to land via precipitation and subsequently being transported to the sea via surface water run-off and river transport.

#### *1.4.2 Atmospheric weapons testing*

Atmospheric nuclear weapons testing began on July 16<sup>th</sup> 1945 with the Trinity test in New Mexico and the subsequent nuclear weapons strikes at Hiroshima and Nagasaki. Atmospheric weapons testing continued through the 1950s until a moratorium on atmospheric weapons testing was agreed in 1958. A peak in release of fission product radioactivity was observed in 1958. Levels of radioactivity then fell until Russia broke the moratorium in 1961 leading to a massive increase in atmospheric weapons testing and resultant release of radioactivity. A second, much larger peak in weapons fallout was recorded in 1963 at the height of the atmospheric weapons testing programmes. The signing of a test ban treaty in 1963 by USA, UK and Russia led to a decrease in radioactivity in the atmosphere through the 1970s and 1980s although China, India and France continued to conduct atmospheric testing up until 1980.

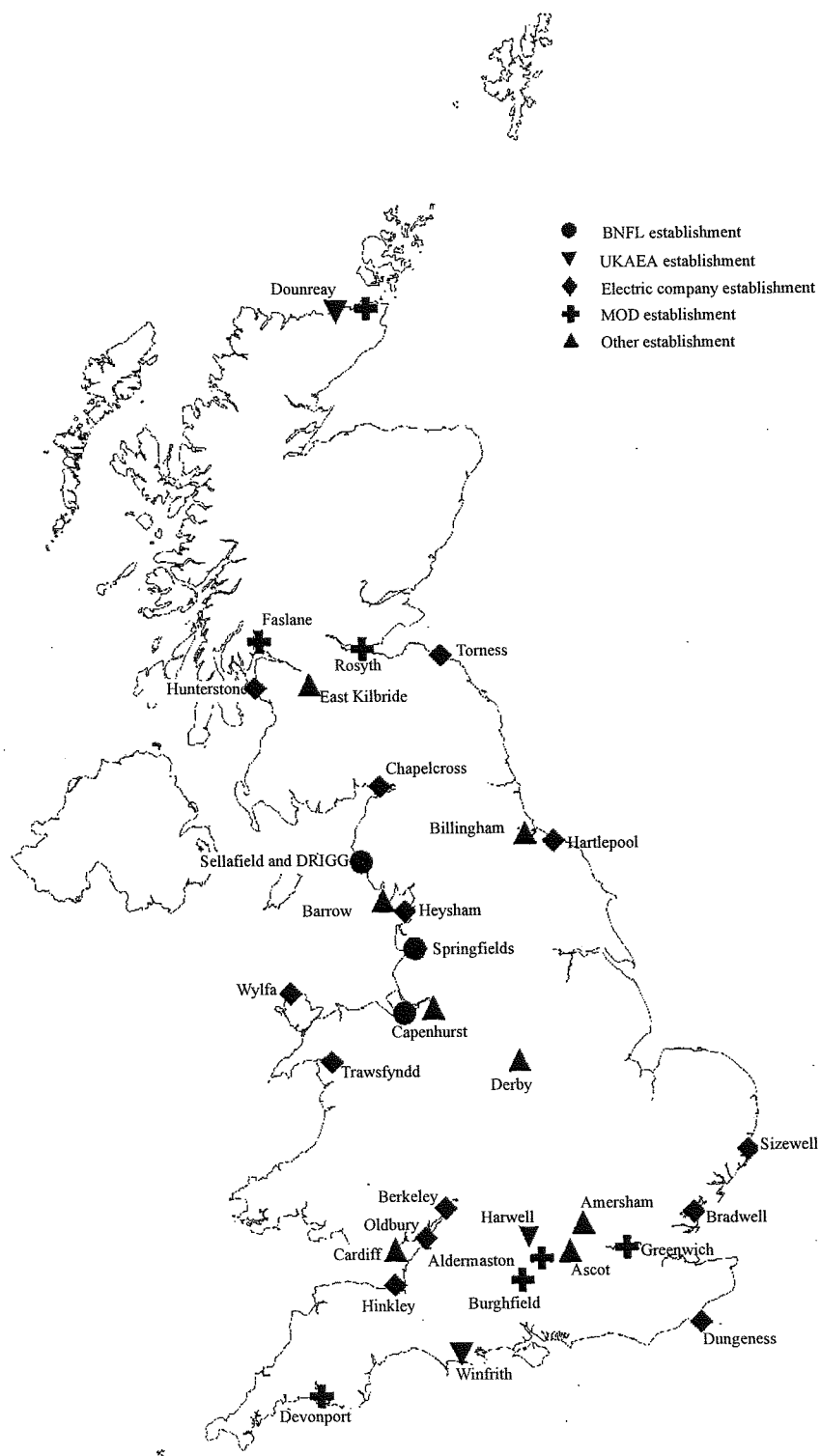
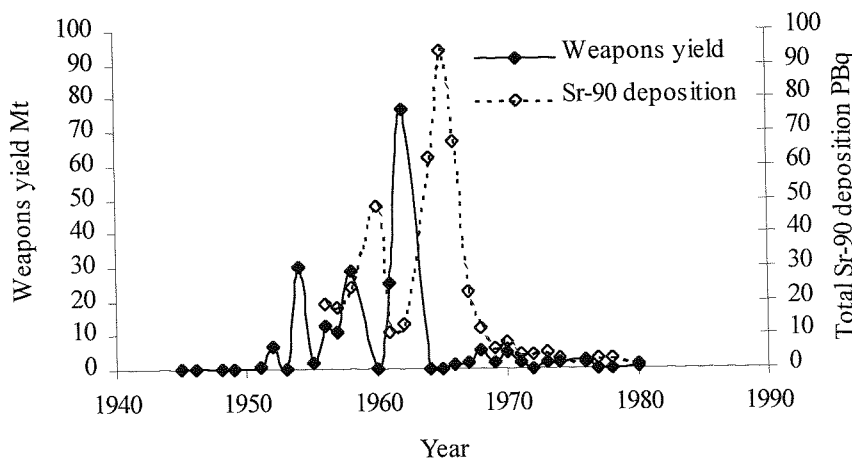


Figure 1.3 :Location of UK nuclear sites

Table 1.4 : Estimated fission yields of atmospheric tests

Year	Country	Number of detonations	Fission yield (~Mt)
1945	USA	3	0.05
1946	USA	2	0.04
1948	USA	3	0.1
1949	USSR	1	0.02
1951	USA/USSR	17	0.54
1952	UK/USA	11	6.62
1953	UK/USA	13	0.29
1954	USA/USSR	7	30.1
1955	USA/USSR	17	1.67
1956	UK/USA/USSR	27	12.3
1957	UK/USA/USSR	45	10.89
1958	UK/USA/USSR	83	28.94
1960	France	3	0.11
1961	France/USSR	51	25.42
1962	USA/USSR	77	76.55
1964	China	1	0.02
1965	China	1	0.04
1966	France/China	8	1.3
1967	France/China	5	1.92
1968	France/China	6	5.3
1969	China	11	2
1970	France/China	9	4.55
1971	France/China	6	1.97
1972	France/China	5	0.24
1973	France/China	6	1.65
1974	France/China	8	1.55
1976	China	3	2.37
1977	China	1	0.02
1978	China	2	0.04
1980	China	1	0.45
Total		423	217

Source : UNSCEAR (1982)

Figure 1.4 : Atmospheric weapons yield and total  $^{90}\text{Sr}$  deposition in the Northern Hemisphere  
(note the delay between the peak in weapons testing and the peak in  $^{90}\text{Sr}$  deposition)

#### 1.4.2.1 Production of radioisotopes during detonation

The atmospheric weapons tests resulted in a significant input of radioisotopes into the environment. Radioisotopes released during the weapons detonation originate either from the fission of uranium and plutonium (**fission products**) or from the activation of weapon components, rock, debris and the air in the vicinity of the test (**activation products**).

The quantity of fission-derived radioisotopes will depend on the flux and energy spectrum of the neutrons produced during the detonation. The relative ratios of fission products will be a function of their fission yields, which is again dependent on the neutron energy spectrum as well as the isotope undergoing fission. Edvarson *et al* (1959) suggested that the majority of the fission products released during nuclear weapons' testing originated from fast neutron fission.

The formation of activation products such as  $^{3}\text{H}$ ,  $^{14}\text{C}$ ,  $^{55}\text{Fe}$  and  $^{63}\text{Ni}$  will depend on the composition of materials in the nuclear weapon and on the environment surrounding the detonation site. The quantity of activation products will also depend on the neutron flux and neutron energy spectrum associated with the particular detonation. It is interesting to note that  $^{134}\text{Cs}$  is not produced during a nuclear weapon's detonation as the fission yield is low. However, in a reactor, the A=133 isobar is produced which has sufficient time to decay to  $^{133}\text{Cs}$ . This isotope may in-turn undergo neutron capture to produce  $^{134}\text{Cs}$ . The presence of  $^{134}\text{Cs}$  is therefore a clear indication of a fresh reactor source as opposed to a weapons source

#### 1.4.2.2 Fractionation of weapons fallout radioisotopes

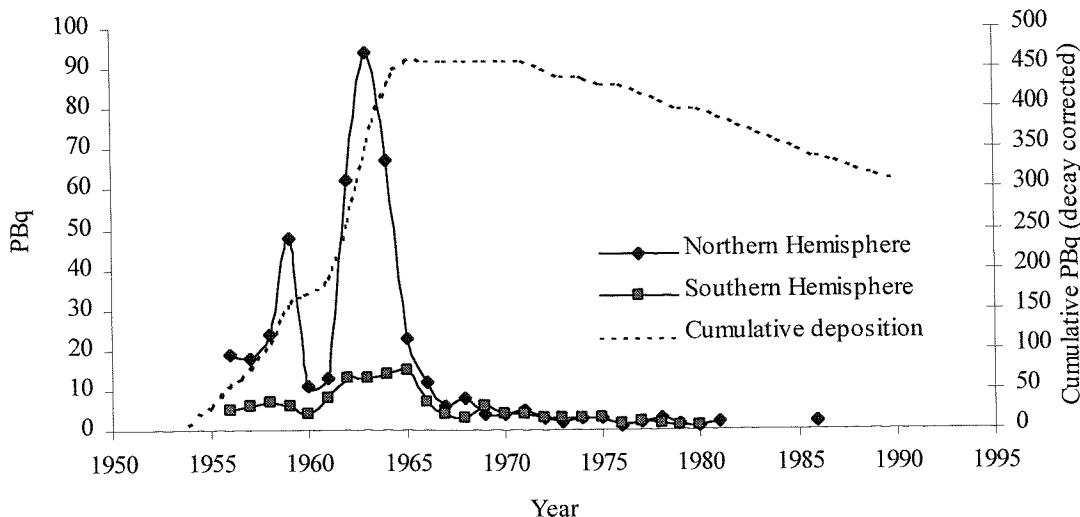
During a nuclear detonation soil, rock and other materials in the vicinity of the detonation are volatilised and this debris is carried up into the expanding fireball. As the fireball expands the volatilised debris condenses forming an aerosol 0.4 - 4.0  $\mu\text{m}$  in diameter on which the radioisotopes may condense. Large particle aerosols are formed at the early stages of condensation within the fireball carrying radioisotopes that form refractory oxides. The more volatile radioisotopes condense as the fireball continues to expand and cool and tend to be associated with smaller particle sizes ( $< 0.4 \mu\text{m}$ ). The larger particles tend to settle more rapidly in the vicinity of the test whereas the smaller particles, carrying the more volatile radioisotopes, are carried further afield leading to fractionation of the radioisotopes. The aerosol particle diameters will also be affected by the height of detonation of the weapon above ground level. If a weapon is detonated near to the ground

large quantities of rock and soil are volatilised, later condensing to form larger particle-diameter aerosols. These processes result in **primary fractionation** of the radioisotopes (Freiling, 1961). Further fractionation of the radioisotopes will then occur due to environmental processes acting on the condensed fallout. In this way, more soluble radioisotopes will be leached from the condensed fallout by seawater and small fallout particles may be preferentially separated from larger particles. This leads to **secondary fractionation** of the radioisotopes present in the fallout.

#### *1.4.2.3 Transport of radioisotopes in the atmosphere*

In low-yield (kilotonne) fission explosions, the radioactive aerosol is injected into the troposphere whereas for thermonuclear explosions the aerosol is carried into the stratosphere where the aerosol is distributed globally before being deposited back to Earth. Stewart *et al* (1957) demonstrated that the physical half-life for dust in the lower atmosphere was in the order of 20 days whilst the mean residence time for  $^{90}\text{Sr}$  in the stratosphere has been estimated as 1 year (UNSCEAR, 1977). Much work has been performed on the deposition on the fission products  $^{90}\text{Sr}$  and  $^{137}\text{Cs}$  and such data may be used to estimate the deposition of other fission products.

The deposition of fallout varies with latitude and is greater in the Northern Hemisphere than in the Southern Hemisphere. This variation has been quantified through the measurement of  $^{90}\text{Sr}$  at numerous sampling stations located at various latitudes and has enabled the total  $^{90}\text{Sr}$  deposited in the two Hemispheres to be determined (Playford *et al*, 1992).

**Figure 1.5 : Global deposition of  $^{90}\text{Sr}$ .**

From 1966-1987  $^{90}\text{Sr}$  deposition has been estimated from  $^{137}\text{Cs}$  measurements adjusted by the  $^{137}\text{Cs}$  to  $^{90}\text{Sr}$  ratio. Cumulative  $^{90}\text{Sr}$  activity adjusted for radioactive decay. (After Playford *et al*, 1992)

#### 1.4.3 Nuclear accidents

A number of accidents have occurred which have had a detectable impact on anthropogenic radioisotope activities in UK coastal waters. The most notable of these are the Windscale Pile fire in 1957 and the Chernobyl disaster in 1986. Both accidents resulted in a substantial release of fission and activation products into the environment (Table 1.6).

**Table 1.6 : Major nuclear accidents and releases affecting the UK**

Location	Date	Isotope	Activity $\times 10^{12}$ Bq
Windscale, UK	10 <sup>th</sup> October 1957	$^{131}\text{I}$	600
		$^{137}\text{Cs}$	18
		+ others	
Chernobyl, USSR	26 <sup>th</sup> April 1986	$^{131}\text{I}$	1760 000
		$^{137}\text{Cs}$	85 000
		+ others	

Data from Sanderson *et al*, 1997

## 1.5 Behaviour of radioisotopes in coastal waters and sediments

### 1.5.1 Dispersion of radioisotopes in seawater

The behaviour of a radioisotope once it has been released into the marine environment may be described as either conservative or non-conservative depending on its affinity for particulate materials in the seawater. Conservative radioisotopes only interact weakly with the particulate phases in seawater and tend to remain predominantly in the aqueous phase. The dispersal of these radioisotopes will therefore be controlled by local current patterns. Examples of conservative elements are alkali and alkaline earth elements such as Na and Cs and low-charged anionic species such as  $\text{TcO}_4^-$ . Non-conservative radioisotopes interact more strongly with the particulate phase of seawater and rapidly become incorporated within seabed sediments. Such radioisotopes can become concentrated in the local environment and their dispersal is dependent on sediment transport mechanisms. Examples of non-conservative elements are highly charged transition metal, lanthanide, actinide and metalloid species. The oxidation state and speciation of the element will determine the extent to which it associates with the particulate phase and variable behaviour of an element may be observed depending on the prevailing local conditions.

Conservative and non-conservative radioisotopes may also be adsorbed and / or assimilated by marine biota. The mechanism of uptake will depend on the organism and the radioisotope being considered. Filter feeding and scavenging organisms are more likely to concentrate non-conservative radioisotopes associated with particulate matter whereas other marine biota will concentrate radioisotopes directly from the aqueous phase. For example fucoid seaweeds are particularly effective at concentrating iodine and technetium isotopes and other species of seaweed including *Porphyra umbilicalis* have been shown to concentrate  $^{106}\text{Ru}$  to a significant extent (Mauchline *et al*, 1964).

### 1.5.2 *Sea-to-land transfer*

Liquid effluents discharged to the sea can also have a significant impact on the radioactivity detected on land. Mechanisms for sea-to-land transport of particle-bound actinides include (1) direct suspension of the sea surface in the wind as sea-spray; (2) conversion of the sea surface into an aerosol by bubble bursting; (3) injection of seawater and suspended sediment into the air by waves breaking in the surf zone; (4) movement of sediment to intertidal regions with subsequent resuspension by wind (Cambray and Eakins, 1982). One characteristic of the sea-to-land transfer is that the actinides are preferentially enriched in the spray compared with  $^{137}\text{Cs}$  suggesting that the mechanism is related to sediment transport. It is estimated that  $10^{-4}$  of the discharged Pu returns to coastal areas via this process.

### 1.5.3 *Interaction of radioisotopes with particulates*

In general, most radioisotopes will show some affinity for uptake on particulate matter present in seawater. Even radioisotopes that are considered conservative in their behaviour, such as  $^{137}\text{Cs}$  and  $^{99}\text{TcO}_4^-$  may be detected at appreciable levels in particulate matter. The mechanism of interaction will depend heavily on the radioisotope and the composition of the aqueous and particulate phases. In the Sellafield area, Pu and Am are mainly associated with iron and manganese oxyhydroxides (as determined by sequential leaching experiments – Tessier *et al*, 1979; Malcolm *et al*, 1990). Geochemical cycling of Fe and Mn may play an important role in the uptake and redistribution of certain radioisotopes in sediments although initial studies by Malcolm *et al* (1990) found no evidence for the redissolution of Pu and Am from marine sediments where reductive dissolution of Fe and Mn had occurred. Cations, such as  $\text{Cs}^+$ , will exchange with cations present within clays effectively locking the cation into the clay lattice. More exchangeable substitutions may also occur with the clay acting as an ion exchanger. Some radioisotopes, including  $^{129}\text{I}$ , are biophilic, being associated with organic matter in the sediment. In the Irish Sea, organic coatings on particulate matter have been observed to increase during the summer months with a corresponding decline over the winter (Hamilton, 1998). Such a fluctuation in organic matter may potentially result in a biannual fluctuation in the concentration of biophilic radioisotopes on particulate matter. Such radioisotopes may also be absorbed by phytoplankton and will therefore be subject to the effect of algal blooms.

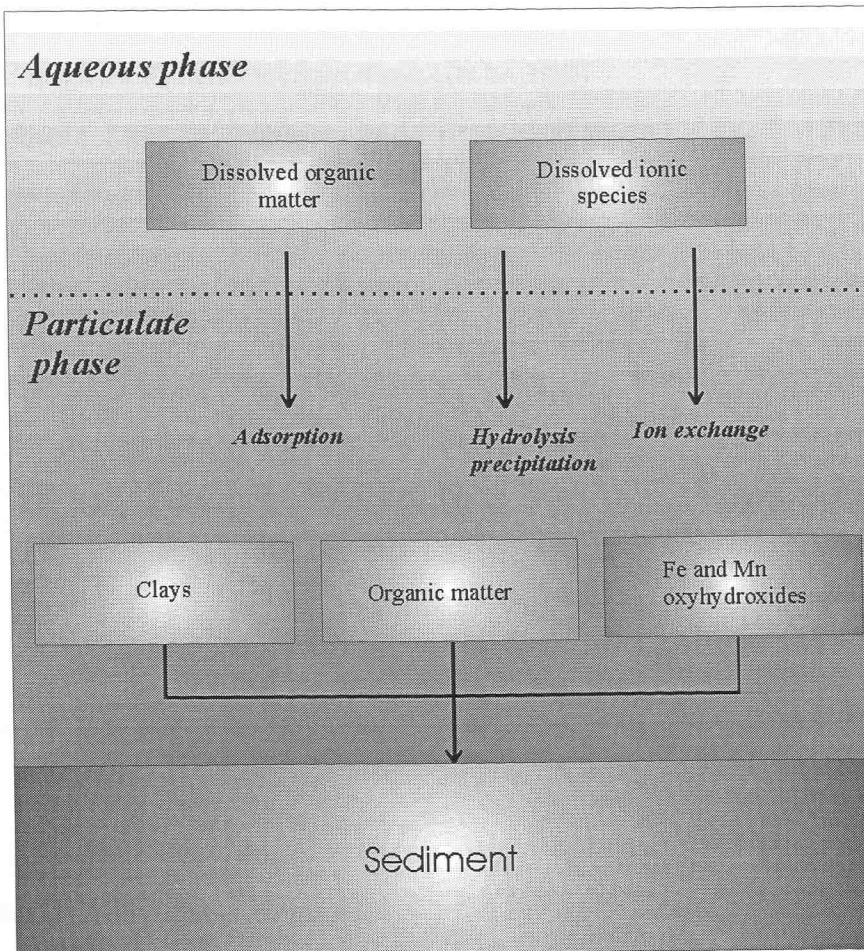


Figure 1.6 : Transfer of radioactivity from the water column to sediment

One way of quantifying the magnitude of radioisotope uptake on particulate matter is through the use of the distribution coefficient or  $K_d$ . The distribution coefficient is defined as the ratio between the concentration of a radioisotope per gram of particulate to the concentration of the radioisotope per gram of seawater. The  $K_d$  will depend heavily on the mechanism of adsorption and hence on the composition of the seawater and particulate matter as well as the chemical form of the radioisotope. For this reason,  $K_d$ 's for a given element will vary markedly with location, season, discharge source etc. and published  $K_d$ 's can therefore only be treated as an approximation. The IAEA (1985) have reviewed existing data on  $K_d$  values for the majority of elements (Table 1.7).

**Table 1.7 : Reported  $K_d$  values for coastal areas (IAEA,1985)**

Element	Mean	Maximum	Minimum
Fe	$5 \times 10^4$	$2 \times 10^5$	$1 \times 10^4$
Ni	$1 \times 10^5$	$5 \times 10^5$	$2 \times 10^4$
Co	$2 \times 10^5$	$1 \times 10^6$	$2 \times 10^4$
Sr	$1 \times 10^3$	$5 \times 10^3$	$1 \times 10^2$
Zr	$1 \times 10^6$	$5 \times 10^6$	$2 \times 10^5$
Tc	$1 \times 10^2$	$1 \times 10^3$	$1 \times 10^1$
Sn	$1 \times 10^3$	$5 \times 10^3$	$2 \times 10^2$
I	$2 \times 10^1$	$1 \times 10^2$	$5 \times 10^0$
Cs	$3 \times 10^3$	$2 \times 10^4$	$1 \times 10^2$
Pu	$1 \times 10^5$	$1 \times 10^6$	$1 \times 10^4$
Am	$2 \times 10^6$	$2 \times 10^7$	$1 \times 10^5$

#### 1.5.4 Post-depositional migration of radioisotopes in sediments

Following the deposition of radioisotope-labelled sediments, the radioisotope may remain bound to the sediment in the location where it was deposited or the radioisotope may subsequently migrate through the sediment column. This migration may be a physical or chemical process.

In physical mixing, the labelled sediment is mixed with depth down the core. Physical mixing mainly results from tidal and storm action on the surface of the sediment or through bioturbation of the sediment both by roots of surface vegetation penetrating down the sediment or through the action of burrowing fauna. Species known to be active in the Irish Sea area include *Amphiura filiformis*, *Maxmulleria lankesteri* and *Callianassa subterranea* (Swift and Kershaw, 1987; Swift 1990). Lateral transport of sediment over considerable distance will also occur. The transport of the radioisotope-labelled sediment will be governed by local sediment transport mechanisms with finer-grained sediments being transported the greatest distance. Tracking of radioisotope-labelled sediments has therefore permitted the study of sediment transport mechanisms (Olsen *et al*, 1980).

Chemical migration of certain radioisotopes occurs when changes in the prevailing chemistry render the radioisotope soluble. The radioisotope may then pass from the

sediment into the porewaters where it may migrate laterally and down the sediment column.

Sediment cores normally possess three distinct regions, known as the oxic, post-oxic and sulphidic zones. The oxic zone is characterised by lack of Fe(II) in porewaters. As oxygen penetrates the sediment this zone is relatively oxidising. At a given depth, the atmospheric oxygen can no longer penetrate effectively. The oxygen that is present is utilised by bacteria to oxidise organic carbon in the sediment. This post-oxic zone is oxygen deficient and is characterised by reductive dissolution of Fe and Mn, the presence of Fe(II) and Mn(II) in porewaters and a subsequent reduction in particle-associated Fe(III) and Mn(IV) oxyhydroxides. At greater depth, sulphate-reducing bacteria produce a sulphide-rich or sulphidic zone at depth in the sediment core. The presence and depth of these zones will depend on the sediment type and local environmental conditions. For areas with relatively coarse-grained sediments, oxygen penetration will occur to a much greater depth and the post-oxic and sulphidic zones will be correspondingly deeper.

The variation in redox potential within the sediment column may potentially affect the post-depositional migration of radioisotopes down the sediment column. The change in redox potential down the sediment column will affect the solubility and speciation of the radioisotopes and the presence of high concentration of sulphides may lead to the precipitation or adsorption of certain radioisotopes as sulphides. A key example is the case of Tc. Tc is present normally as the soluble  $\text{TcO}_4^-$  anion. This anion would be expected to migrate rapidly through the sediment column. However, at the oxic/post-oxic boundary, the concentration of Fe(II) may be expected to increase. Fe(II) reduces Tc(VII) to the more particle-reactive Tc(IV) which would be more strongly retained on the sediment. In addition, any  $\text{TcO}_4^-$  migrating as far as the sulphidic zone would be rapidly converted to the highly insoluble  $\text{Tc}_2\text{S}_7$  again rendering the species highly immobile. Both mechanisms would result in the retention of Tc within the sediment column.

### 1.5.5 *The saltmarsh environment*

A saltmarsh is a sediment flat high in the intertidal zone that has been colonised by halophytic plants and which is regularly inundated by seawater. It is estimated that around 44,370 ha of active saltmarsh exist around the UK (Allen and Pye, 1992). Saltmarshes in the vicinity of Sellafield act as sinks for radioactivity discharged from the Sellafield site. Relatively high sedimentation rates and stabilisation of the sediment resulting from the

vegetative root mat result in a high-resolution record of pollution history covering a period of approximately 50 years. As well as providing a record of depositional history, the study of radioisotope uptake in the saltmarsh environment is vital in determining the potential effect of saltmarsh-bound radioisotopes on human dose assessment. Saltmarsh vegetation may absorb radioisotopes from the sediment substrate or be contaminated with sediment-bound radioisotopes. This vegetation may be grazed by herbivores which in-turn may be consumed by man. In addition the erosion of the saltmarsh may result in the re-release of radioisotopes into the marine environment long after nuclear operations have ceased in the area.

## 1.6 The importance of pure beta-emitting radioisotopes

Numerous beta-emitting radioisotopes are produced during nuclear reactor operations, nuclear fuel reprocessing and testing of nuclear weapons. Certain of these pure beta-emitting isotopes, such as  $^3\text{H}$ ,  $^{14}\text{C}$  and  $^{90}\text{Sr}$  have been extensively studied due to their radiological impact on the environment and man. Others, such as  $^{55}\text{Fe}$ ,  $^{63}\text{Ni}$  and  $^{99}\text{Tc}$ , occur at much lower activities. Although the presence of these radioisotopes is not of radiological concern compared to other fission products such as  $^{90}\text{Sr}$  and  $^{137}\text{Cs}$  the long half lives of these radioisotopes means that they are of considerable concern in the long term storage of nuclear waste (Figures 1.7 and 1.8).

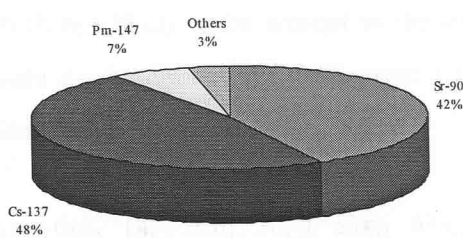


Figure 1.7 : Composition of fission products in low-level waste (LLW) on disposal

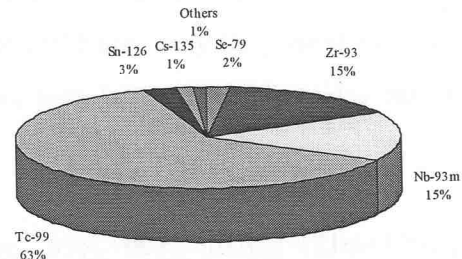


Figure 1.8 : Composition of fission products in high-level waste (HLW) 1000 years after reprocessing

Data from Chapman and McKinley, 1987

The Royal Society (1994) listed the radioisotopes of concern in radioactive waste disposal and commented on the characteristics of these nuclides. The section pertaining to beta-emitting radioisotopes is reproduced in Table 1.8

**Table 1.8 : Key characteristics in the context of waste disposal (from Royal Society, 1994)**

Radioisotope	Characteristic
Tritium ( $^3\text{H}$ )	Abundant in waste, soluble, non-sorbed
Carbon-14 ( $^{14}\text{C}$ )	Long-lived, soluble, non-sorbed
Chlorine-36 ( $^{36}\text{Cl}$ )	Long-lived, non-sorbed
Cobalt-60 ( $^{60}\text{Co}$ )	Abundant, high energy gamma emissions
Nickel-59 ( $^{59}\text{Ni}$ )	Long-lived, fairly abundant, not strongly sorbed
Selenium-79 ( $^{79}\text{Se}$ )	Long-lived, not strongly sorbed
Strontium-90 ( $^{90}\text{Sr}$ )	Abundant
Zirconium-93 ( $^{93}\text{Zr}$ )	Long-lived, may not be strongly sorbed
Niobium-94 ( $^{94}\text{Nb}$ )	Long-lived, high energy gamma emissions
Technetium-99 ( $^{99}\text{Tc}$ )	Long-lived, non-sorbed in some conditions
Tin-126 ( $^{126}\text{Sn}$ )	Long-lived, not strongly sorbed
Iodine-129 ( $^{129}\text{I}$ )	Very long lived, non-sorbed
Caesium-135 ( $^{135}\text{Cs}$ )	Long-lived
Caesium-137 ( $^{137}\text{Cs}$ )	Abundant, high energy gamma emission

**Sorbed refers to the extent to which the radioisotopes are retained by man-made and geological media during their transport from the repository with groundwaters**

The above information can be used to select pure beta emitters with significant half-lives which are likely to be present in the nuclear waste and hence may be present in liquid waste discharges. Using these criteria the following pure beta-emitting nuclides can be identified.

$^3\text{H}$ ,  $^{10}\text{Be}$ ,  $^{14}\text{C}$ ,  $^{35}\text{S}$ ,  $^{36}\text{Cl}$ ,  $^{55}\text{Fe}$ ,  $^{63}\text{Ni}$ ,  $^{79}\text{Se}$ ,  $^{90}\text{Sr}$ ,  $^{93}\text{Zr}$ ,  $^{99}\text{Tc}$ ,  $^{107}\text{Pd}$ ,  $^{121\text{m}+126}\text{Sn}$ ,  $^{129}\text{I}$ ,  $^{147}\text{Pm}$ ,  $^{151}\text{Sm}$  and  $^{210}\text{Pb}$ .

Of the above list of radioisotopes,  $^{55}\text{Fe}$ ,  $^{63}\text{Ni}$ ,  $^{90}\text{Sr}$ , and  $^{99}\text{Tc}$ , were chosen for the current study as there is a significant interest in measuring these radioisotopes in routine low-level and decommissioning wastes and their discharge from certain nuclear sites has been reported.

## 1.7 Summary and aims of the study

From the above it can be seen that there is a real need for the development of techniques for the effective determination of pure beta-emitting radioisotopes and to understand how these long-lived radioisotopes may behave in the marine environment. In addition it is important to assess the potential for sediment deposits and saltmarshes to act as sinks for these long-lived radioisotopes and the potential for re-release into the environment. Finally, there is an opportunity to exploit the routine discharge of these radioisotopes for studies of environmental processes and in particular the interaction of trace elements (radioisotopes) with particulate matter.

The aims of this study were three-fold

1. To develop methods for the determination of pure beta emitters in low-level wastes and environmental samples
2. To determine whether levels of key beta-emitters in saltmarsh sediments are detectable
3. To interpret the above results in terms of the behaviour of pure beta-emitters in the saltmarsh environment

The thesis is therefore divided into three main research themes. Firstly, a review of techniques suitable for the determination of the relevant pure beta emitters was performed (Chapter 2). From this suitable techniques were identified and developed for the routine and sensitive measurement of the pure beta-emitting radioisotopes of interest (Chapter 3).

Once suitable measurement techniques had been developed, chemical separation techniques were required to separate the isotope of interest from any other isotopes likely to be present in a complex mixture of fission and activation products. A review was made of the specific chemistries of the elements of interest (Chapter 2) and this information was used to develop an efficient sequential separation scheme that could be used to isolate all the isotopes of interest from a range of matrices including effluents, swabs, laboratory wastes and environmental samples (Chapter 4 & 5).

Finally, levels of pure beta-emitting radioisotopes in a saltmarsh environment in the vicinity of the nuclear fuel reprocessing plant at Sellafield were investigated. A sediment

core sample was collected from the Ravenglass saltmarsh in Esk Estuary. Full geochemical investigation of the core was performed along with an assessment of the gamma and beta radioisotope activities of the core. This information was used to assess the potential mobility of these isotopes in the saltmarsh environment (Chapter 6).

## 1.8 References

Allen J.R.L. and Pye K. (1992). Saltmarshes; morphodynamics, conservation and engineering significance. Cambridge University Press, Cambridge, UK.

Beneš P., Lam Ramos P. and Poliak R. (1989). Factors affecting interaction of radiocaesium with freshwater solids. I. pH, Composition of water and the solids. *J. Radioanalyst. Nucl. Chem. Articles*, **133** (2), 359-376.

BNFL (1995). Annual report on radioactive discharges and monitoring the environment 1994, vol 1. Health and Safety Directorate, British Nuclear Fuels plc, Risley, UK.

Cambray R.S. and Eakins J.D. (1982). Pu,  $^{241}\text{Am}$  and  $^{137}\text{Cs}$  in West Cumbria and a maritime effect. *Nature*, **300** (5887), 46-48.

Chapman H.A. and McKinley I.G. (1987). The geological disposal of nuclear waste. John Wiley, Chichester, UK

Choppin G., Lilzenkin J.O. and Rydberg J. (1996). Radiochemistry and Nuclear Chemistry. Reed Elsevier plc group, Oxford, UK.

Dahlgaard H. (1995). Radioactive tracers as a tool in coastal oceanography: An overview of the MAST-52 project. *J. Mar. Sys.*, **6**, 381-389.

Edvarson K., Löw K. and Sisefsky J. (1959). *Nature*, **184**, 1771-1774.

Freiling E.C. (1961). Radionuclide fractionation in bomb debris. *Science*, **133**, 1991-1998.

Hamilton E.I. (1998). Marine environmental radioactivity – the missing science. *Mar. Poll. Bullet.*, **36**(1), 8-18.

IAEA (1985). Sediment Kd's and concentration factors for radionuclides in the marine environment. Technical report series no 247, IAEA, Vienna.

Koide M., and Goldberg E.D., (1985). Determination of  $^{99}\text{Tc}$ ,  $^{63}\text{Ni}$  and  $^{121\text{m}+126}\text{Sn}$  in the marine environment. *J. Environ. Radioactivity*, **2**, 261-282.

Livingstone H.D., Casso S.A., Bowen V.T. and Burke J.C. (1979). Soluble and particle-associated fallout radionuclides in Mediterranean water and sediments. *Comm. Int. Explor. Sci. Mer. Mediterr.*, **25-6** (5), 71-76.

Malcolm S.J., Kershaw P.J., Cromar N.J. and Botham L. (1990). Iron and manganese geochemistry and the distribution of  $^{239,240}\text{Pu}$  and  $^{241}\text{Am}$  in the sediments of the North East Irish Sea. *Sci. Tot. Env.*, **95**, 69-87.

Mauchline J., Taylor A.M. and Ritson E.B. (1964). The radioecology of a beach. *Limnol. Oceanog.*, **9**(2), 187-194.

Olsen C.R., Biscaye P.E., Simpson H.J., Trier R.M., Kostyk N, Bopp R.F., Li Y.-H and Feely H.W. (1980). Reactor-released radioisotopes and fine-grained sediment transport and accumulation patterns in Barnegat Bay, New Jersey and adjacent shelf waters. *Estuarine Coast. Mar. Sci.*, **10**, 119-142.

Pappas A.C. (1956). The distribution of nuclear charge in low energy fission. In Proceedings of the International Conference on the peaceful uses of atomic energy, Volume 7. Nuclear chemistry and effects of irradiation. United Nations, New York, USA.

Patton T.L. and Penrose W.R. (1989). Fission product tin in sediments. *J. Environ. Radioact.*, **10**, 201-211.

Playford K., Lewis G.N.J. and Carpenter R.C. (1992). Radioactive fallout in air and rain: results to the end of 1990. Report AEA-EE-0362, AEA Technology, Harwell, UK

Royal Society (1994). Disposal of radioactive wastes in deep repositories. Royal Society, London, UK

Steinberg E.P. and Glendenin L.E. (1956). Survey of radiochemical studies of the fission process. In Proceedings of the International Conference on the peaceful uses of atomic energy, Volume 7. Nuclear chemistry and effects of irradiation. United Nations, New York, USA.

Sanderson D.C.W., Cresswell A.J., Allyson J.D. and McConville P. (1997) Review of past nuclear accidents: source terms and recorded gamma-ray spectra. Report DOE/RAS/97.001, Department of the Environment, London, UK.

Stewart N.G. *et al* (1957). World-wide deposition of long-lived fission products from nuclear test explosions. Report MP/R2356, UK Atomic Energy Authority, Harwell, UK.

Swift D.J. (1990). The benthic fauna of Sellafield, Cumbria (north-east Irish Sea) (1990). *J. Mar Biol Assoc. - submitted*

Swift D.J. and Kershaw P.J. (1987). Bioturbation of contaminated sediments in the north-east Irish Sea. International Council for the exploration of the sea. Copenhagen, CM 1986/E:18. 12pp.

Tessier A., Campbell P.G.C. and Bisson M. (1979). Sequential extraction procedure for the speciation of particulate trace metals. *Anal. Chem.*, **51**, 844-851.

UNSCEAR (1977). Sources and effects of ionising radiation. United Nations Scientific Committee on the Effects of Atomic Radiation. United Nations, New York, USA.

UNSCEAR (1982). Sources and effects of ionising radiation. United Nations Scientific Committee on the Effects of Atomic Radiation. United Nations, New York, USA.

## Chapter 2

# **Review of techniques for the determination of pure beta emitters**

## 2 Review of techniques for the determination of pure beta emitters

### 2.1 Detection of beta-emitting radioisotopes

The measurement of a beta-emitting radioisotope may be performed either through the detection of the emitted beta particle (radiometric technique) or through direct measurement of the number of atoms of the specific radioisotope that are present in the sample (mass-spectrometric technique). In general, radioisotopes with relatively short half-lives and correspondingly high specific activity (activity per unit mass of the isotope in Bq/g) are best determined using a radiometric technique. Radioisotopes with long half-lives and low specific activity are best determined using a mass spectrometric technique. Of the radioisotopes considered in this study, only  $^{99}\text{Tc}$  ( $t_{1/2} = 2.13 \times 10^5$  y) is sufficiently long-lived to be measured at low level by mass-spectrometric techniques. Mass-spectrometric determination of these radioisotopes is discussed further in Chapter 3. Radiometric techniques were also considered for these radioisotopes, as well as for the other shorter-lived radioisotopes.

The decay energy of a pure beta-emitting radioisotope is shared between the emitted beta particle and an anti-neutrino. The beta particle emitted is not monoenergetic but may possess energies ranging from nearly the total decay energy ( $E_{\max}$ ) to near zero. Beta spectrometry is therefore of limited application in the qualitative determination of a mixture of beta-emitting radioisotopes. Qualitative detection and quantitative measurement of a pure beta emitter must therefore consist of a specific chemical separation of the element of interest followed by the measurement of the beta activity associated with that purified fraction. The specific chemical separations employed are reviewed further in Section 2.7. The detection systems used to measure the beta activity of final purified fractions are discussed in Section 2.2 and 2.3.

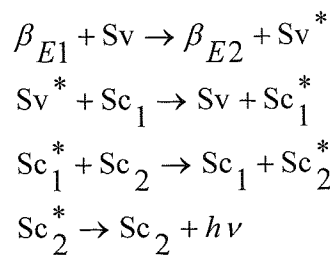
A wide range of detectors has been used for the determination of total beta activity. Detectors include Geiger-Müller tubes, ion chambers, solid anthracene scintillation detectors, surface barrier detectors (and the more recent passivated ion-implanted devices) and gas-flow proportional counters. However, one of the most versatile counting systems for the detection of beta-emitting radioisotopes is liquid scintillation counting

## 2.2 Liquid scintillation counting

### 2.2.1 *Physics of the scintillation process*

Liquid scintillation counting is suitable for the measurement of alpha, beta and some electron capture radioisotopes. Most modern counters incorporate a sample changing mechanism allowing the counter to be used continuously with limited operator interaction. The incorporation of an multi-channel analyser (MCA) allows spectrometric information to be recorded that can aid in the identification of the radioisotopes as well as permitting the deconvolution of signals from relatively simple mixtures of radioisotopes.

Central to the liquid scintillation counting technique is the scintillation vial and its contents. The scintillation vial contains the sample and a mixture, or cocktail, of organic compounds which enable energy associated with radioactive decay to be converted into light photons that are subsequently detected. Energy from radiation associated with the sample, construction material or background/cosmic radiation excites the scintillant solvent. This solvent molecule then interacts with an aromatic organic compound known as a primary scintillant. The excess energy is transferred to the primary scintillant molecule raising the molecule to an excited energy state and de-exciting the solvent molecule. The primary scintillant then de-excites to produce the ground state primary scintillant molecule and a photon of light with a wavelength between 350 and 400 nm. In some cocktail mixtures, however, the primary scintillant molecule de-excites by interaction with a secondary scintillant molecule. The excited secondary scintillator then de-excites with the emission of a photon of wavelength 400 - 430 nm. The use of a secondary scintillator causes a shift in emitted photon wavelength to one that is more efficiently detected by the photomultiplier tubes. Developments in photomultiplier technology have in general eliminated the need for the secondary scintillator. The process is summarised below for a beta particle.



Where  $\beta$  represents a beta particle of energy E1 or E2

Sv represents the solvent molecule

$\text{Sc}_1$  and  $\text{Sc}_2$  are the primary and secondary scintillant molecule respectively

$*$  represents an excited energy state

$h\nu$  represents the energy of a light photon of frequency  $\nu$

Not all of the energy associated with the beta particle is transferred to a single solvent molecule and multiple interactions are normal. The attenuated beta particle can continue through the solvent exciting many solvent molecules. For a given scintillant cocktail, the number of solvent molecules excited, and hence the final number of light photons produced, will increase with increasing beta particle energy.

The number of solvent molecules excited for a given beta energy depends on the solvent type. The radiolysis of a solvent leads to the formation of a range of species including ions and singlet and triplet excited state solvent molecules (as well as free radicals and molecular fragments). The energy deposited in the solvent leading to excitation/ionisation is also small compared to the energy of the ionising particle and is typically 4-6% of an electron's kinetic energy, 0.5-0.7% of an alpha particle's kinetic energy and 1.0% of a proton's kinetic energy. The remainder of the ionising particle energy is dissipated as heat (Horrocks, 1976). For polar solvents, such as water or methanol only ion pairs are produced, which do not participate in the scintillation process. However, for non-polar solvents such as xylene, a mixture of singlet and triplet excited states and very few ions are detected. It is also known that the recombination of ion pairs formed during radiolysis can lead to the secondary production of excited states and it has been suggested that even in non-polar solvents ion pair formation is significant, although all ion pairs formed recombine producing the excited state molecules. In polar solvents the ion pairs are stabilised by increased solvation of the ions and hence excited species are not formed (Thomas and Beck, 1980). It is for this reason that non-polar solvents are used in liquid scintillation cocktails. The ratio of singlet to triplet excited states also depends on the solvent and on the excitation source (alpha particles produce more triplet excited states than beta

particles).

Primary and secondary fluors are added to the solvent to convert energy from the excited solvent molecule to light photons. Solvent molecules are unsuitable by themselves as they have low photon emission probabilities, long fluorescence lifetimes (around 30ns, increasing the probability for quench) and emit photons at a wavelength unsuitable for detection by most liquid scintillation photomultiplier systems. As solvents are present at high concentrations there is also an increased probability of re-adsorption of any light photons emitted. Scintillator molecules have a much higher photon emission probability and much shorter fluorescence lifetimes (1-2 ns) and, as they are usually present at low concentrations, the probability of re-absorption of emitted photons is low (Horrocks, 1976). Voltz *et al* (1963) noted that energy transfers from one solvent molecule to the next, prior to the transfer of energy to the scintillator molecule, is via non-radiative processes (i.e. does not occur via emission of a photon from the solvent and readsorption and subsequent re-emission of a photon by a second solvent molecule). This transfer of energy between one solvent molecule and another is expected considering the much higher concentrations of solvent molecules compared to scintillator molecules. Horrocks (1976) also observed that the transfer of energy from solvent molecule to scintillator was non-radiative.

The total number of photons produced will depend on the initial energy of the beta particle. It is interesting to note that, below 300keV, the number of photons produced per unit energy is not constant but also depends on the total energy of the beta particle. Above 300keV the photons produced per unit energy is constant (Figure 2.1).

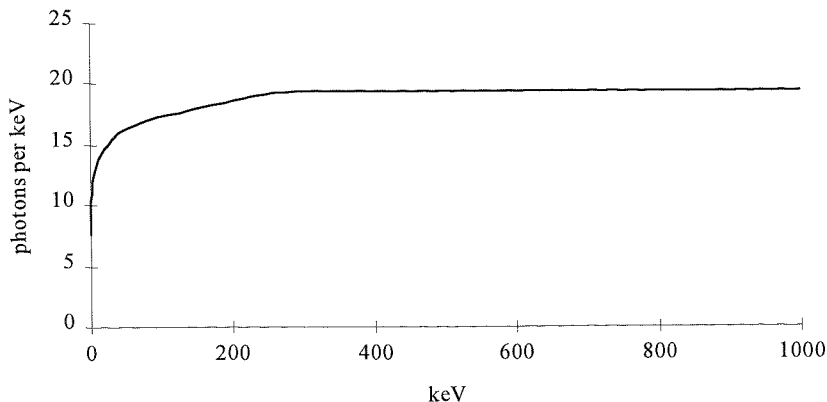


**Figure 2.1 : Photons produced per unit energy for a range of beta energies**

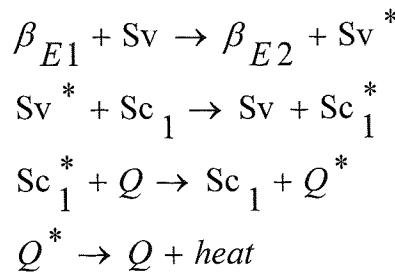
From Horrocks, 1976

### 2.2.2 Factors affecting the excitation process - Inhibition of the scintillation process

The detection of light photons produced from the interaction of ionising radiation with the scintillant cocktail can be adversely affected by the photons interacting with other compounds, contaminants etc. present prior to reaching the photomultiplier tubes. This reduction in efficiency of the detection system is known as **quench**. The effect of quench is to decrease the number of decay events that are registered by the photomultiplier tubes (decrease in counting efficiency) and to shift the energy spectrum of a nuclide to a lower energy region as fewer photons are registered for a given particle energy.

#### 2.2.2.1 Chemical quench

The chemical reactions that transfer the energy of the beta particle to produce a light photon can be inhibited. This is known as chemical quench. The excited solvent or primary scintillant molecule interacts with a molecule other than the secondary scintillant. The solvent or primary scintillant is de-excited and the second molecule is excited. This excited molecule then de-excites emitting the excess energy as heat instead of a light photon. No signal is therefore produced in the photomultiplier tubes and the event is not detected.



where Q is the quenching agent

A wide range of compounds can induce chemical quench. These include, amongst many others, dissolved oxygen, chlorinated organic compounds, acetone and water. The chemical quench process can be sub-divided as follows

- i. **Acid quenching.** Protonation of the primary or secondary scintillator modifies the excitation energy levels of the scintillator creating a mis-match for solvent- scintillator energy transfer.
- ii. **Concentration quenching.** The concentration of a component within the scintillator mixture is present at such a level as to interfere with the scintillation process.
- iii. **Dilution quenching.** Dilution of the sample with any molecule that does not participate in the scintillation process increases the effective distance between solvent molecules and reduces the efficient transfer of energy from the ionising radiation and the scintillant molecule.
- iv. **Dipole-dipole quenching.** Certain materials interact with the excited solvent molecule with subsequent transfer of energy via dipole-dipole interactions and dissipation of energy via non-radiative processes. Oxygen and nitromethane quench in this fashion.
- v. **Capture of secondary electrons.** Part of the excitation process involves the emission of secondary electrons by the solvent molecule after interaction with the ionising radiation. These secondary electrons can go on and excite further solvent molecules. Any molecule that captures these secondary electrons will effectively quench the scintillation process. Halogenated molecules quench effectively via this process.

Chemical quenching has a marked effect on the pulse height spectrum. As quenching of the sample increases the total number of observed events decreases as the counting efficiency drops. The pulse height spectrum shifts to lower energy channels as fewer photons are produced for a given keV of ionising radiation and the spectrum shifts towards lower energy. The extent of chemical quench for a given quantity of quenching agent depends on the cocktail being used (ter Wiel, 1992) and in particular the solvent.

Chemical quench due to dissolved oxygen can be removed by bubbling nitrogen through the sample. However, when using after-pulsing corrections (in time-resolved-LSC) a reduction rather than an increase in counting efficiency may be observed after purging of the O<sub>2</sub>.

In most other cases quenching is limited by sample purification prior to liquid scintillation measurement and by correction of the final measurement for any unavoidable quenching that is still occurring.

#### 2.2.2.2 *Colour / physical quench*

Another cause of quench occurs when the light photon is produced but is prevented from reaching the detector. The light photon is either absorbed by a molecule dissolved in the sample/cocktail mixture (colour quench) or is physically prevented from reaching the detector by an obstruction such as particulate matter suspended in the mixture (physical quench).

In colour quench, the quenching agent has an absorbance band that overlaps with the emission band of the scintillator. The light photons are absorbed and hence do not reach the photomultiplier tubes for detection. As scintillators usually emit in the blue region of the visible spectrum the greatest quenching is observed with red compounds. Colour quench is an absorbance process and therefore obeys Beer's law. Hence, the pathlength of the process (in this case the distance between the photon production site and the edge of the vial) is critical to the degree of absorbance observed. Colour quench therefore differs from chemical quench in that it is dependent on the vial size. In practice this results in broader pulse height spectra with a lower maximum energy as compared to a sample chemically quenched to the same counting efficiency.

In physical quenching the light photons produced are prevented from reaching the photomultiplier tubes by a physical barrier. Particulate matter seriously quenches the sample. Physical quench also occurs if the sample adsorbs onto the surface of the vial and is therefore not intimately mixed with the solvent. Any ionising radiation emitted cannot interact with the solvent under these conditions. Furthermore, if the adsorbed sample is in intimate contact with the scintillant, the counting efficiency will still be significantly reduced as only those radiations emitted towards the contents of the vial will excite the solvent molecule whereas those radiated towards the vial wall are lost.

#### 2.2.2.3 *Emulsions and micelle formation*

Micelle formation is necessary in dispersing aqueous samples uniformly throughout an organic solvent that is normally hydrophobic in nature. However, as the aqueous-to-organic ratio increases, the micelles formed will get larger. For low energy beta emitters such as tritium (with a maximum beta range of 6  $\mu\text{m}$ ) the majority of the beta decay energy may be deposited within the large micelles prior to the beta particle reaching the organic phase and hence the number of scintillation events is decreased. Typical beta particle ranges for a number of common radioisotopes are given in Table 2.1.

**Table 2.1 :  $E_{\max}$  and beta range for selected beta-emitting radioisotopes**

Nuclide	$E_{\max}$ keV	Maximum range (mm)
$^3\text{H}$	18.6	0.006
$^{14}\text{C}$	156	0.285
$^{35}\text{S}$	167	0.315
$^{45}\text{Ca}$	254	0.600
$^{32}\text{P}$	1709	7.8

#### 2.2.2.4 *Determination of sample counting efficiency*

Even following chemical separation and purification of an analyte the degree of quench may still vary from sample to sample although the range of quench should be narrow. The degree of quench associated with each sample and hence the counting efficiency of each sample may be determined using one of a range of techniques. The most direct way of determining the counting efficiency for a sample is to first count the sample, then to spike the sample with a

known amount of the analyte and finally to recount the sample. The increase in count rate coupled with the activity of the added spike can be used to calculate the counting efficiency and then to determine the activity of the analyte using the initial count-rate data. However, this technique requires two counts. For samples containing relatively high activities, the initial count rate of the sample may be used to determine the degree of quench using techniques such as the sample channels ratio to determine counting efficiency. However, this is not readily applicable to low-level environmental samples where insufficient counts are detected to permit such a correction procedure.

Other quench-correction procedures include the use of external standards which work by inducing Compton-derived events in the solvent which subsequently lead to scintillations. The apparent maximum ( $E_{\max}$ ) observed on the liquid scintillation Compton spectrum is dependent on the gamma photon energy ( $E_{\gamma}$ ) of the external standard and is given by the equation

$$E_{\max} = \frac{2E_{\gamma}^2}{2E_{\gamma} + 0.51MeV}$$

The intensity of the scintillations depends on, amongst other factors, the degree of sample quench. By positioning an external gamma source adjacent to the sample vial and measuring the effect of the radiation from the external source on the scintillation mixture a measure of quench which is independent of the sample activity may be made. In Wallac instruments the External Standard Spectral Quench Parameter, SQP(E), is determined. The spectrum of the external standard is stored in a 1024 channel MCA and the SQP(E) is described as the channel number which is the upper boundary to the spectrum containing 99.5% of the total counts of the spectrum. The SQP(E) value can then be used to determine the counting efficiency of the sample by comparison with standards of known counting efficiency and quench level.

### 2.2.3 *Factors affecting the scintillation process – Interference from non-beta derived scintillation processes*

#### 2.2.3.1 *Chemiluminescence*

Chemical quenching inhibits the production of photons by de-excitation of the solvent and/or scintillator molecules. However, it is possible for chemical reactions to occur which initiate

the excitation of solvent and scintillator molecules in the absence of ionising radiation. This is known as chemiluminescence. It is characterised by a number of properties as follows

- i. It is short lived. Chemiluminescence declines with time (typically 1-4 hours) and leaving samples in the dark following preparation can reduce the magnitude of the effect.
- ii. The number of photons produced for a chemiluminescence event is low and similar to a 10-20 keV beta emitter. The chemiluminescence peak therefore occurs at the low energy end of the liquid scintillation spectrum and only interferes with the determination of low energy beta nuclides such as tritium.
- iv. As with any chemical reaction, the chemiluminescence reaction is temperature dependent. Lowering the temperature inhibits the chemiluminescence reactions allowing beta measurements to be made. However, as the sample warms up the chemiluminescence reactions will begin again. Heating the samples to about 45°C increases the reaction rate and allows the chemiluminescence reactions to reach completion quickly before the sample is counted.
- v. Chemiluminescence reactions do not produce an isotropic burst of light. If the sample is monitored with two photomultiplier tubes counting in coincidence the chemiluminescence event will not trigger both photomultiplier tubes. However, chemiluminescence can give very high rates of photon production and it is possible for both photomultiplier tubes to be triggered simultaneously by two separate chemiluminescence events.
- vi. Chemiluminescence is more likely to occur in alkaline solutions. pH adjustment can be used to minimise the problem.

Chemiluminescence correction through counting electronics can be achieved using a number of techniques although in general it is better to modify the sample preparation technique to limit the chemiluminescence.

#### 2.2.3.2 *Photoluminescence*

Photoluminescence occurs when photo-initiated reactions excite the solvent molecules, which then increase the number of light photons produced. As the process is light-initiated photoluminescence can be reduced by leaving the vials in the dark (dark-adapting) for a few hours prior to counting.

## 2.3 Liquid scintillation counters

Most commercial scintillation counters consists of two photomultiplier tubes that detect photons emitted from the vial via the scintillation process. The associated electronics register both the number of counts detected within a specified time (related to the total activity of the sample) and also the intensity of each photon burst. The intensity of the burst is directly related to the energy of the beta particle that initiated the scintillation process. By incorporating a multichannel analyser (MCA) into the electronic circuitry, the number of events with a given intensity can be recorded separately allowing an energy spectrum to be derived.

In addition to the two photomultiplier tubes monitoring the sample vial, the Wallac 'Quantulus' has a further two photomultiplier tubes monitoring a chamber of scintillant gel (the guard chamber) directly above the sample chamber. These are set to count in anti-coincidence with the sample photomultiplier tubes. Any cosmic events that would normally trigger the sample photomultiplier tubes will also initiate a scintillation event in the guard chamber. When an event is registered in both sets of photomultiplier tubes it is regarded as a cosmic background event and subsequently rejected. In this way the Wallac 'Quantulus' liquid scintillation counter can differentiate between genuine decay events originating in the sample and cosmic background events originating outside the counter. For these reasons the observed background for the Quantulus counter is superior to that provided by the Packard 2250CA and Wallac 1410 counters.

Finally all liquid scintillation counters have associated lead shielding to reduce background derived from external radiation sources, sample changing mechanisms to permit the automatic counting of sample batches, and associated electronics and software to permit signal processing, data collection and manipulation.

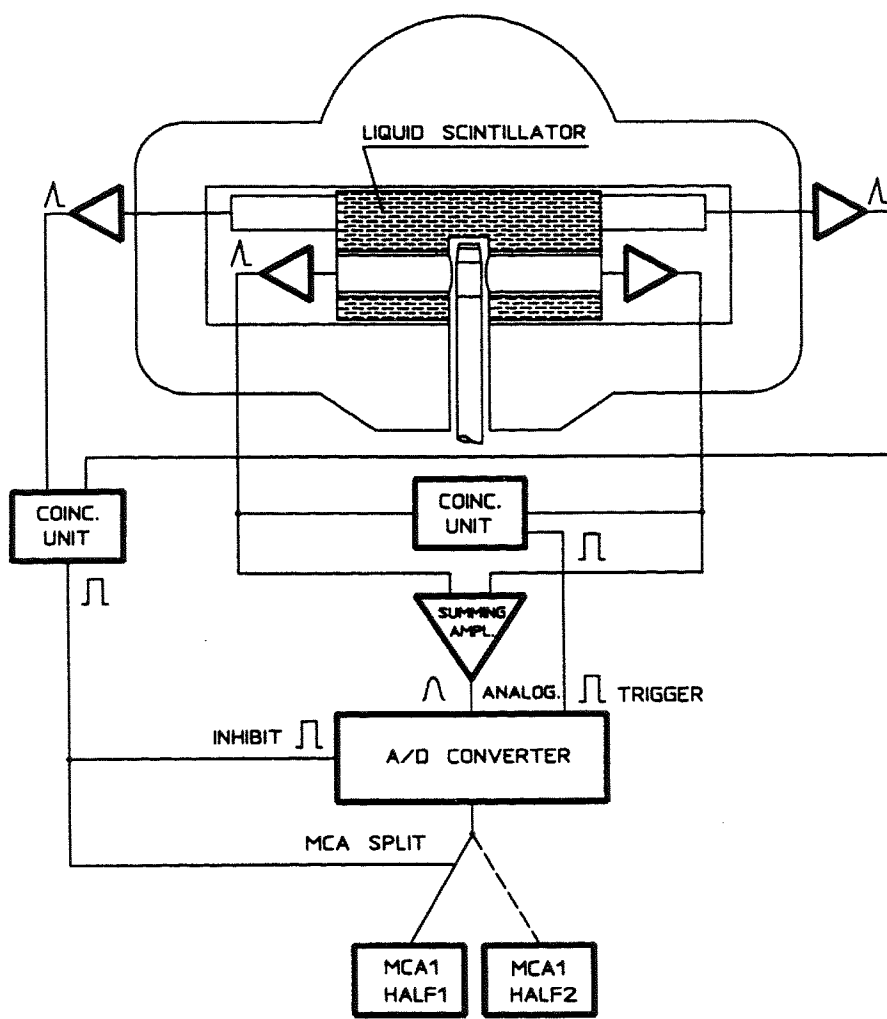


Figure 2.2 : Configuration of the Wallac 1220 'Quantulus' liquid scintillation counter (after Wallac, 1996)

## 2.4 Preparation of samples for liquid scintillation counting

With the exception of Cerenkov counting for high energy beta emitters (Section 2.5), all liquid scintillation counting techniques require that the purified beta emitter is intimately mixed with a liquid scintillation cocktail containing a solvent, co-solvent, primary fluor and, in many instances, a secondary fluor. In all cases, the solvent is usually an aromatic hydrocarbon such as benzene, toluene, linear alkyl benzenes (LABs) or di isopropyl naphthalene (DIPN). Source preparation therefore requires the mixing of the radioisotope being measured with the solvent. This is most readily achieved by preparing the radioisotope in a solution of an aromatic solvent often by extraction of the radioisotope into the aromatic solvent containing a suitable extractant. It is important that the extractant does not cause significant chemical quenching. An extreme of this approach is used in the low-level measurement of  $^{14}\text{C}$  where the stable carbon and  $^{14}\text{C}$  is chemically converted to benzene and used directly as the scintillant solvent. Extraction of the analyte into an organic solvent followed by mixing with liquid scintillation cocktails has also been widely used in the determination of  $^{222}\text{Rn}$  in aqueous samples where the radon is quantitatively extracted into toluene.

In most instances, the purified sample is present in an aqueous solution. Although the aqueous solution will not mix directly with the aromatic solvents, emulsifiers can be added to the liquid scintillation cocktail to permit direct intimate mixing of the aqueous and organic phases. Quenching of the samples will be significantly higher than that found for a purely aromatic system as water is an effective quenching agent. The scintillant will also have a limited capacity for the aqueous phase and once exceeded the counting efficiency will fall dramatically. The exact loading capacity will depend on the scintillant cocktail, the acidity and the dissolved salt content of the aqueous phase.

Solid samples may be counted in two ways by liquid scintillation counting. Precipitation of the analyte with an organic precipitant is often employed as a method for determining the chemical recovery of the analyte following separation chemistry. Many of these precipitates can be directly dissolved in the aromatic solvent of the liquid scintillation cocktail producing a homogeneous source with low chemical quench. Other precipitates will not readily dissolve in the cocktail. These must either be dissolved in an aqueous solution prior to mixing with the cocktail or can be suspended as a finely divided powder in the cocktail producing a

heterogeneous mixture. To ensure that the solid remains suspended it is important to form a gel in the scintillant. This is achieved by using a purpose-designed gel cocktail that forms a gel on mixing with water, or by adding silica to the cocktail. In either case the counting efficiency is lower than for a homogeneous sample.

Choice of vial is also an important consideration. Glass vials have elevated levels of natural isotopes such as  $^{40}\text{K}$  compared with polythene vials. In order to reduce the background still further, polythene vials were used throughout the study.

The use of plastic vials can lead to other problems. The liquid scintillation spectrum can be distorted by scintillant permeating into the wall of the vial. This is particularly a problem when using external standardisation for quench correction. The introduction of 'environmentally friendly' cocktails which employ low vapour pressure solvents has reduced this problem. However, when using xylene-based scintillants glass vials are often more appropriate.

## 2.5 Review of Cerenkov counting

### 2.5.1 *Introduction*

Cerenkov counting is a valuable technique for the determination of medium to high-energy beta emitters ( $> 300$  keV  $E_{\max}$ ) in solution using conventional liquid scintillation counters. The technique does not require scintillant allowing the sample to be recovered following counting and does not produce organic wastes that require a specific disposal procedure. As no scintillants are used, chemical quench is not significant, acidic samples are easily counted and backgrounds tend to be lower. Colour quench is still of importance. Counting efficiencies for Cerenkov counting are lower than for conventional liquid scintillation counting (e.g. for  $^{90}\text{Y}$  the counting efficiency drops from *Ca.* 100% with liquid scintillation counting to *Ca.* 40% with Cerenkov counting). Another potential benefit is that the low background obtained using Cerenkov counting results in a higher signal-to-background ratio than conventional liquid scintillation counting.

### 2.5.2 *Theory of Cerenkov radiation*

Cerenkov radiation is produced by a charged particle passing through a medium at a velocity greater than the speed of light in that medium. A good summary of Cerenkov radiation is given by Parker and Elrick (1970). As the charged particle passes through a dielectric medium, electronic polarisation is produced along the path of the charged particle. After the charged particle has passed the polarised molecules de-excite with the emission of electromagnetic radiation. The electromagnetic radiation produced is propagated with a phase velocity of  $c/n$  where  $c$  is the speed of light and  $n$  is the refractive index of the medium. If the velocity of the charged particle,  $v$ , is less than the velocity of the propagated electromagnetic radiation (i.e.  $v < c/n$ ) then the electromagnetic radiation will interfere destructively and no radiation is emitted.

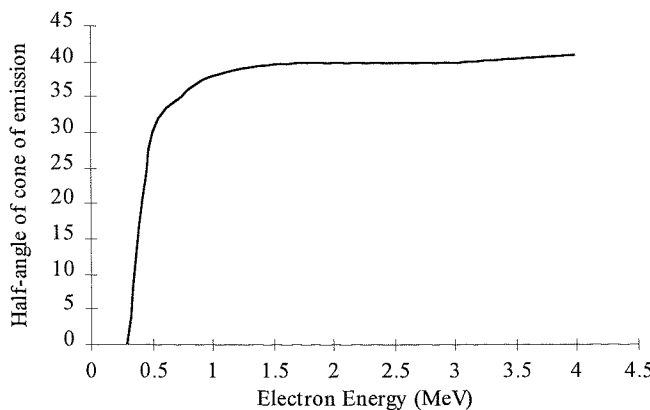


**Figure 2.3** Half-angle of cone of emission of Cerenkov light in water as a function of electron energy (after Parker and Elrick, 1970)

If  $v > c/n$  some constructive interference will occur in certain directions and a pulse of electromagnetic radiation is observed. Cerenkov radiation is therefore analogous to the sonic boom produced by aircraft travelling faster than the speed of sound. As with a sonic boom, the Cerenkov radiation is emitted in a cone with a half-angle,  $\phi$ . The half-angle is dependent on the velocity of the charged particle inducing the radiation and on the refractive index of the medium and is given by the equation  $\cos\phi = c/vn$ .

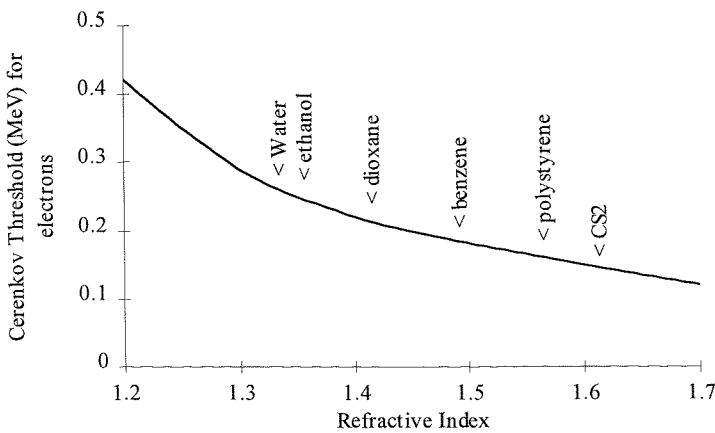


**Figure 2.4** Electron Threshold Energy for Cerenkov emission as a function of the refractive index of the medium. (After Parker and Elrick, 1970)

For a given medium it can therefore be seen that the charged particle must possess a certain minimum energy, or threshold energy, for Cerenkov radiation to be observed. The threshold can be calculated using the equation below. For practical purposes a threshold of 300 keV in water is normally assumed. In the equation 0.511 is the rest mass of the electron in MeV, and  $n$  is the refractive index of the medium.

$$E_{\min} = 0.511 \left[ \left( 1 - \frac{1}{n^2} \right)^{-0.5} - 1 \right] \text{MeV}$$

**Equation 1 - Calculation of threshold energy for production of Cerenkov radiation  
(after Kessler, 1989)**

A wide range of wavelengths are produced predominantly in the ultra-violet region, extending into the visible region but becoming negligible towards the infra-red region. The duration of the flash of light is very short (around 1ns) and the number of photons produced during the passage of the charged particle through the medium is lower than that encountered in liquid scintillation counting. For this reason the spectrum of a beta emitter appears at the low end of the energy spectrum, usually in the tritium region of a liquid scintillation counter. The number of photons produced ( $N_E$ ) is dependent on the energy ( $E$ ) of the beta particle entering the medium and is given by the equation below

$$N_E = c \int_E^{E_{\min}} \left( 1 - \frac{1}{\beta^2 n^2} \right) dx$$

**Equation 2-Calculation of the number of photons produced,  $N_E$ , for a given beta energy,  $E$ .**

### 2.5.3 Factors affecting Cerenkov counting efficiency

Only electrons with energies above the threshold energy will produce photons and the number of photons produced will depend on the actual energy of the electron. As a beta decay results in the production of beta particles (electrons) with a distribution of energies, only the proportion of beta articles in the distribution with energy above the threshold energy will result in observable Cerenkov radiation (see Table 2.2). As a consequence of this Cerenkov counting always results in lower counting efficiencies than conventional liquid scintillation counting as there is always a proportion of the beta spectrum that is below the threshold energy and

therefore does not contribute to the production of Cerenkov radiation. Counting efficiency is hence dependent on the beta decay energy of the nuclide.

**Table 2.2 : Average number of Cerenkov photons produced (300-700nm) per beta decay in water**

Radioisotope	Emax (MeV)	Photons per disintegration		% of $\beta$ -spectrum above Cerenkov threshold
		Mean	Maximum Energy	
$^{36}\text{Cl}$	0.71	7	40	60
$^{204}\text{Tl}$	0.77	5	47	53
$^{24}\text{Na}$	1.39	30	160	84
$^{32}\text{P}$	1.71	40	210	90

From Parker and Elrick, 1970

The production of Cerenkov radiation is influenced considerably by the refractive index of the medium and density of the solvent (which affects the 'stopping power' of the solvent). An increase in refractive index of 0.01 results in an increase in counting efficiency of less than 1% for  $^{40}\text{K}$  and  $^{144}\text{Ce}/^{144}\text{Pr}$  but an increase in efficiency of nearly 10% for  $^{36}\text{Cl}$  and  $^{204}\text{Tl}$  showing that the effect is more pronounced for beta emitters with energies nearer the threshold energy. A decrease in density of 7% results in an increase in efficiency of 10% for  $^{204}\text{Tl}$  but less than 1% for the high energy beta emitter,  $^{32}\text{P}$ . The decrease in density reduces the stopping power of the solvent and hence increases the path length of the beta particle in the medium, increasing the number of excitations that occur. Again this is more significant for low energy beta emitters.

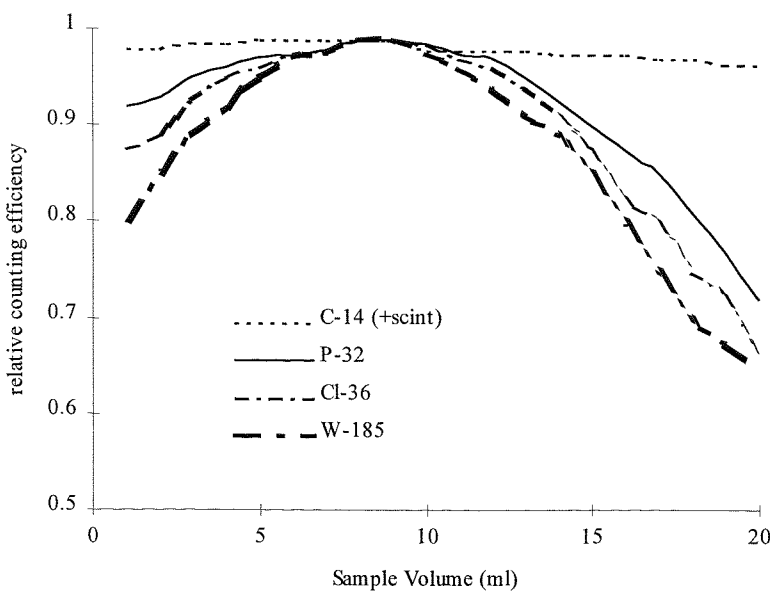


Figure 2.5-Effect of volume on Cerenkov counting efficiency (Ross, 1976)

The volume of the sample will affect the counting efficiency of the sample. A volume greater than 10ml has been found to give the maximum counting efficiency with efficiencies dropping by between 10% ( $^{90}\text{Sr}/^{90}\text{Y}$ ) and 22% ( $^{36}\text{Cl}$ ) on reducing the volume to 1ml (Kessler, 1989).

Once the Cerenkov radiation has been produced, its attenuation may limit the intensity reaching the photomultiplier and further reduce counting efficiencies. As shown earlier, the Cerenkov radiation is emitted directionally in a cone and hence coincidence circuitry may not efficiently detect Cerenkov events (c.f. scintillation events are isotropic and hence will trigger two photomultiplier tubes simultaneously). However, counting without coincidence will result in excessive backgrounds due to photomultiplier noise and chemiluminescence events.

The type of vial will affect the efficiency of Cerenkov measurement. As the majority of the emitted Cerenkov spectrum is in the ultra-violet region, significant absorption of Cerenkov radiation by the glass vial will occur. The use of polythene vials minimises this effect and increases counting efficiency. The diffusive nature of plastic vials also helps to overcome the directional nature of the Cerenkov radiation emission. The use of wavelength shifters which absorb the ultra-violet radiation and re-emit in the visible region have also been successfully used to overcome problems associated with the absorption of ultra-violet radiation in the glass

vials and photomultiplier envelope. The properties of some wavelength shifters are summarised in Table 2.3.

Table 2.3 - Wavelength Shifters used in Cerenkov counting

Shifter	Concentration	Effect on counting efficiency
2-naphthylamine-6,8-disulphonic acid, Na or K salt	100mg/litre	Doubled counting efficiency up to 2 MeV <sup>1</sup>
$\beta$ -methyl umbelliferone		Effect dependent on pH <sup>1</sup>
7-amino-1,3-naphthalene disulphonic acid	1000ppm	30-50% increase <sup>2</sup>
	5mM $E_{max} < 1$ MeV 2.5mM $E_{max} > 1$ MeV	not stated <sup>1</sup>
Esculin	5-1000mg/litre	50-70% increase in counting efficiency <sup>2</sup>
$\beta$ -naphthylamine	5-5000mg/litre	30-50% increase <sup>2</sup>
$\beta$ -naphtoic acid	5-1000mg/litre	10-30% increase <sup>2</sup>
p-terphenyl	500-1000mg/litre	10-30% increase <sup>2</sup>
naphthalene	5-1000mg/litre	-5-+5% increase <sup>2</sup>
Ca tungstate	100-1000mg/litre	-5-+5% increase <sup>2</sup>

Data from <sup>1</sup>Parker and Elrick, 1970

<sup>2</sup>Francois, 1973

The wavelength shifters improve counting efficiency considerably. However, as the wavelength shifter is dissolved in the solvent and acts in a similar manner to the secondary fluor in conventional liquid scintillant, the wavelength shifter can be subject to chemical quench and also prevents any recovery of the sample after counting. Hence a number of the advantages of Cerenkov counting are lost. One solution is to coat the surface of the photomultiplier tube with a thin layer of solid wavelength shifter such as lithium fluoride. This reduces the absorption of ultra-violet radiation by the glass envelope of the photomultiplier tube and its use does not affect the chemistry in the counting vial. However, this approach requires modification to counting equipment that is usually used for other purposes.

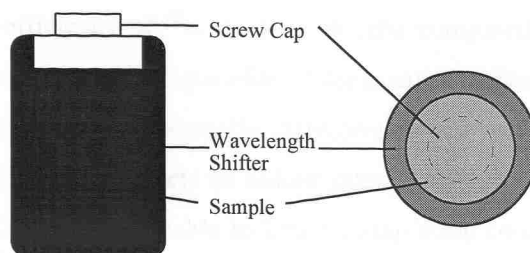


Figure 2.6 – Two-chamber vial proposed by Ross (1976) for Cerenkov counting

To overcome this Ross (1976) suggested the use of a two-chamber quartz vial. The inner chamber contained the sample whilst the outer chamber contained the wavelength shifter. As there was no mixing of the sample with the wavelength-shifter chemical quench could not occur and the sample was still recoverable after counting.

The effect of the two-chamber vial can be seen in Table 2.4. The inner sample chamber contained  $^{89}\text{Sr}$  in 0.01M HCl. The relative counting efficiency for  $^{89}\text{Sr}$  with various compounds in the outer compartment was determined. Strong chemical quenching agents in the inner sample chamber had no effect on the relative counting efficiency as Cerenkov radiation is not affected by chemical quench.

Table 2.4 : Relative counting efficiency of  $^{89}\text{Sr}$  in a two chamber vial.

Outer chamber contents	Concentration	Relative counting efficiency
water	100%	1.00
ethanol	95%	1.02
benzene	100%	1.06
toluene	100%	1.07
dimethyl-POPOP	0.7 g/litre in toluene	1.88
4-methyl-umbelliferone	0.5 g/litre in 75% ethanol	1.69
2-naphthol-3,6-disulphonic acid, Na salt	0.1 g/litre in water	1.59
$\beta$ -naphthol	0.1 g/litre in 50% ethanol	1.37
1-naphthylamine	0.1 g/litre in 50% ethanol	1.22

From Ross, 1976

Colour quench is of considerable importance in Cerenkov counting as many organic molecules absorb in the ultra-violet region. Colour quenching has proved of most concern when using Cerenkov counting in the measurement of biological materials. Francois (1973) noted a

decrease in counting efficiency of  $^{42}\text{K}$  in urine of 50% compared with  $^{42}\text{K}$  in water. Careful sample pre-treatment and chemical separation of the assayed radioisotope, although prohibitive in the biological sciences, is normally effective when using Cerenkov counting in radioanalytical chemistry. The effects of colour quenching can be corrected for by utilising quench correction techniques applicable to liquid scintillation counting although the technique of 'channels ratios' has been reported as the most successful correction technique (Ross, 1976).

#### *2.5.4 Application of Cerenkov counting*

Cerenkov counting has found a range of applications in biomedical studies. Measured nuclides have included  $^{90}\text{Sr}$  in urine,  $^{42}\text{K}$  in urine,  $^{24}\text{Na}$  in tissue media and  $^{86}\text{Rb}$  in plant ion transport studies. Cerenkov counting has also been used for the determination of  $^{32}\text{P}$  in a wide range of matrices.

$^{36}\text{Cl}$  (as chlorobenzene) has been determined using methyl salicylate as a medium. The methyl salicylate has a high refractive index and also exhibits wavelength shifting properties. A counting efficiency of 82% was measured compared to 28.4% for  $^{36}\text{Cl}$  in toluene alone (Wiebe and Ediss, 1976). However, the methyl salicylate was shown to be more resistant to chemical quench than a toluene-scintillant mixture.

In environmental monitoring, Cerenkov counting has found more limited application. Again the technique has mainly been applied to the determination of  $^{90}\text{Sr}/^{90}\text{Y}$  and  $^{32}\text{P}$ . Cerenkov counting provides a low background, non-destructive technique with counting efficiencies for  $^{90}\text{Y}$  around 45%.

$^{32}\text{P}$  has been determined in reactor effluents using Cerenkov counting (Baker et al, 1973). Following the removal of interfering ions on a mixed cation exchange resin/antimony chloride column and precipitation of  $^{35}\text{S}$  as barium sulphate, the  $^{32}\text{P}$  was precipitated as ammonium phosphomolybdate and then re-dissolved in 5M ammonium hydroxide prior to Cerenkov counting.

## 2.6 Comparison of liquid scintillation counting with non-radiometric techniques

For short-lived radioisotopes with correspondingly high specific activities, radiometric techniques offer the most sensitive means for quantification of the radioisotope. For long-lived radioisotopes, the specific activities of the isotopes are sufficiently low that the isotope can be detected with sufficient sensitivity using non-radiometric techniques. In order to obtain isotopic information most non-radiometric techniques rely on mass spectrometry. A wide range of mass spectrometric techniques has been developed that differ mainly in their method for ion production (Table 3.5).

**Table 3.5: Examples of mass spectrometric techniques that have been applied to measurement of long-lived radioisotopes**

Mass spectrometric technique	Acronym	Ion production	Sample introduced as
Thermal ionisation mass spectrometry	TIMS	Thermally (electrical heating of a filament supporting the sample)	Purified solid (loaded onto filament)
Inductively coupled plasma mass spectrometry	ICP-MS	Introduction of sample into a gas plasma	Solution Slurry Vapour (Laser ablation)
Secondary ion mass spectrometry	SIMS	Sputtering of secondary ions from the surface of a solid following impact by a primary ion (e.g. $O_2^+$ )	Solid
Resonance ionisation mass spectrometry	RIMS	Laser-induced specific ionisation of a separately atomised sample	Solid
Accelerator mass spectrometry	AMS	Tandem accelerator-produced particles	Purified solid

Of the techniques listed in Table 3.5 only ICP-MS and TIMS were readily available and hence considered further.

Of the isotopes studied in this project, only  $^{99}\text{Tc}$  has a sufficiently long half-life to be considered for measurement using a non-radiometric technique.

**Table 3.6 : Half-lives and specific activities for selected radionuclides**

Isotope	Half-life	Specific activity
	(Years)	Bq/g
<sup>55</sup> Fe	2.7	$8.9 \times 10^{13}$
<sup>63</sup> Ni	100.04	$2.1 \times 10^{12}$
<sup>90</sup> Sr	29.12	$5.1 \times 10^{12}$
<sup>99</sup> Tc	$2.13 \times 10^5$	$6.3 \times 10^8$

Determination of <sup>99</sup>Tc has been performed by a number of investigators using Thermal Ionisation Mass Spectrometry. TIMS relies on the precise measurement of the ratio of one isotope to another. <sup>99</sup>Tc will form a positive ion and hence could potentially be measured using the VG Sector 54 TIMS. However, there are no natural isotopes of Tc to ratio the <sup>99</sup>Tc to. One option is to spike the sample prior to chemical separation with a known quantity of a suitably long-lived isotope of Tc other than <sup>99</sup>Tc. The concentration of <sup>99</sup>Tc in the sample can then be determined using the technique of isotope dilution by measuring the ratio of <sup>99</sup>Tc to the second Tc isotope of known concentration. Two isotopes of Tc, <sup>97</sup>Tc ( $t_{1/2} = 2.6 \times 10^6$ y) and <sup>98</sup>Tc ( $t_{1/2} = 4.2 \times 10^6$ y), have sufficiently long half-lives to be suitable for use as a TIMS spike. Unfortunately, neither of these isotopes is readily available and so TIMS was not considered further for the determination of <sup>99</sup>Tc.

ICP-MS has found wider application in the routine analysis of long-lived radioisotopes. <sup>99</sup>Tc has been determined in a range of samples by ICP-MS (Tagami and Uchida, 1993; Ihsanullah and East, 1994; Yamamoto *et al*, 1994). Following chemical separation, the concentration of <sup>99</sup>Tc can be determined either by comparison with a calibration curve or by isotope dilution (*c.f.* TIMS). An isobaric interference from <sup>99</sup>Ru is observed and must be removed by chemically separating Ru from Tc. However, the limit of detection for <sup>99</sup>Tc using ICP-MS is only marginally superior to radiometric techniques. In addition, the developed chemical separation scheme for <sup>99</sup>Tc (see Chapter 4) was more easily integrated with liquid scintillation measurement of <sup>99</sup>Tc activity. ICP-MS was therefore not adopted in this study for <sup>99</sup>Tc determination.

**Table 3.7: Published mass-spectrometric techniques for the analysis of radioisotopes**

Mass spectrometric technique	Isotope	Typical detection limit pg/ml or ppt	Reference
SIMS	U isotopes in particles		Toole (1998)
RIMS	<sup>99</sup> Tc	0.0016 pg	Trautmann (1993)
	U and Pu		Donohue (1984)
AMS	<sup>14</sup> C		
	<sup>36</sup> Cl		Beasley (1992)
	<sup>63</sup> Ni		
	<sup>99</sup> Tc		
	<sup>129</sup> I		
Gore (1987)			
ICP-MS (pneumatic nebuliser)	<sup>90</sup> Sr	2 pg/ml <sup>a</sup>	Berryman (1997)
	<sup>93</sup> Zr	Not reported	Alonso (1994)
	<sup>99</sup> Tc	4 pg/ml	Ihsanullah (1994)
	<sup>129</sup> I	300 pg/ml	Brown (1988)
	<sup>226</sup> Ra	0.2 pg/ml	Hodge (1994)
	<sup>232</sup> Th		
	<sup>237</sup> Np	Ca. 0.01 pg/ml <sup>b</sup>	Yamamoto (1994)
TIMS	<sup>238</sup> U		
	<sup>239</sup> Pu, <sup>240</sup> Pu		
	Ra		Cohen (1991)
	<sup>235</sup> : <sup>238</sup> U		Taylor (1998)
	<sup>230</sup> : <sup>232</sup> Th		Edwards (1986/7)
	Pu		McCormick (1992)

<sup>a</sup>Using electrothermal vaporisation<sup>b</sup> with ultrasonic nebulisationpg = 1 x 10<sup>-12</sup>g

## 2.7 Review of chemical separation techniques employed prior to liquid scintillation counting

A wide range of radioanalytical separations has been developed for the separation of pure beta-emitting radioisotopes. In many cases, the techniques were developed for the analysis of reactor effluents or air filters used to sample nuclear weapon debris. In such cases the matrix is relatively simple and the chemical separation is optimised for the separation of radioisotopes from one another rather than from bulk matrix elements. In most cases the analysis of the specific radioisotope in an environmental matrix is more complex, requiring further method development (Chapters 4 & 5).

A summary of the published methods for Fe, Ni, Sr, and Tc isotopes is given below. Radioisotopes of each element with half-lives greater than 30 days are listed along with the main production route. Only neutron capture ( $n,\gamma$ ) and fission ( $n,f$ ) reactions are considered. For fission reactions, both thermal and fast neutron fission yields are listed. Thermal fission yields give an indication of likely production rates in nuclear reactors whilst fast neutron fission yields relate to detonation of nuclear weapons. In all cases the cumulative fission yield is quoted. For neutron activation, integrated thermal neutron cross sections for neutron energies between  $1 \times 10^{-5}$  and 10 eV are quoted. Fast neutron cross sections are not quoted, as they will be highly dependent on the neutron energy spectrum present during the detonation and the coincidence of fast neutron energies with resonance energies of the capturing nucleus.

### 2.7.1 Iron radioisotopes

#### Main production route : neutron capture of stable iron

Isotope	Half life	$\beta$ decay energy Emax keV (yield)	Parent isotope	Natural abundance	Thermal neutron cross section (barns)
$^{55}\text{Fe}$	2.70 y	e.c.	$^{54}\text{Fe}$	5.845 %	2.59
$^{59}\text{Fe}$	45.10 d	132 (1.3%) 275 (45.3%) 467 (53.1%)	$^{58}\text{Fe}$	0.282 %	1.27

e.c. – decay via electron capture

Iron-55 is produced along with  $^{59}\text{Fe}$  by neutron activation of stable Fe isotopes.  $^{55}\text{Fe}$  in low-level wastes has been determined following limited chemical purification via its x-ray

emission. Sensitive determination of  $^{55}\text{Fe}$  requires more rigorous chemical separation followed by liquid scintillation analysis. However, chemical separation is usually complicated by the large amounts of stable iron often present in the sample. Preconcentration of  $^{55}\text{Fe}$  has been achieved by precipitating  $\text{Fe}(\text{OH})_3$ . Although this step will effectively preconcentrate Fe and separate it from the alkali elements, many other radioisotopes will co-precipitate with the  $\text{Fe}(\text{OH})_3$ . If ammonia is used to precipitate the  $\text{Fe}(\text{OH})_3$  elements that form soluble amine complexes, such as Co and Ni, will remain in solution improving the degree of purification achieved in this step. Precipitation of a white ferriphosphate complex has also been used to purify Fe and provide a source suitable for liquid scintillation counting (Eakins and Lally, 1965). The ferriphosphate is prepared by dissolving  $\text{Fe}(\text{OH})_3$  in orthophosphoric acid and adding an alcoholic solution of 0.01M ammonium chloride. The compound thus formed has the reported stoichiometry of  $\text{NH}_4\text{H}_2[\text{Fe}(\text{PO}_4)_2]_2\cdot\text{H}_2\text{O}$ .

Purification of Fe has been performed using anion exchange chromatography (e.g. Baker *et al*, 1973). Fe is retained as the  $\text{FeCl}_4^-$  species in HCl concentrations greater than 6M and can either be eluted using dilute HCl or more rapidly using  $\text{HNO}_3$ . Extraction chromatography has been less widely used although methods based on Chelex 100 resin (König *et al*, 1995) and TRU® resin have been reported. Fe is readily purified from most other radioisotopes by extracting the iron chloro- complex from >6M HCl into a solvent such as di isopropyl ether, methyl isobutylketone or ethyl acetate. Extraction of Fe into di(2-ethylhexyl) phosphoric acid (HDEHP), diluted with toluene, has also been used to both separate Fe and produce a source suitable for liquid scintillation counting (Cosilito *et al*, 1968)

### 2.7.2 Nickel radioisotopes

#### Main production route : neutron capture of stable nickel

Isotope	Half life	$\beta$ decay energy	Parent isotope	Natural		Thermal neutron cross section (barns)
				$E_{\text{max}}$ keV (yield)	abundance	
$^{59}\text{Ni}$	$7.5 \times 10^4$ y	EC	$^{58}\text{Ni}$		68.3	4.64
$^{63}\text{Ni}$	100 y	66 (100 %)	$^{62}\text{Ni}$		3.59	14.25
$^{65}\text{Ni}$	2.5 h	655 (28.1%) 1021 (9.8%) 2137 (60.7%)	$^{64}\text{Ni}$		0.91	1.49

Nickel-63 is produced via the  $^{62}\text{Ni}(\text{n},\gamma)^{63}\text{Ni}$  reaction. Although  $^{62}\text{Ni}$  is only present in natural Ni at an abundance of 3.59%, the isotope has the highest neutron capture cross section of all the nickel isotopes and so activation of stable nickel will produce significant quantities of  $^{63}\text{Ni}$ .  $^{59}\text{Ni}$  will also be produced via the  $^{58}\text{Ni}(\text{n},\gamma)^{59}\text{Ni}$  reaction. However the neutron cross section for  $^{58}\text{Ni}$  is low and the ratio of  $^{59}\text{Ni}/^{63}\text{Ni}$  produced by thermal neutron irradiation of stainless steel is approximately 1:100 (Holm *et al*, 1990)

Dimethylglyoxime is by far the most commonly used complexing agent for nickel. The reagent is only slightly soluble in water and is usually dissolved in ethanol or acetone. However the sodium salt is more soluble in water and can be used instead. Palladium and bismuth (in the presence of chloride) will also form complexes, as will cobalt and copper, but to a lesser extent. Cobalt and copper interference is more significant if the sodium salt of dimethylglyoxime is used.  $\alpha$ -furildioxime has been used for complex formation with nickel. Cyclohexane-1,2-dionedioxime and cycloheptan-1,2-dionedioxime have also received attention for nickel determination by gravimetry as the compounds are water soluble and allow determination of smaller quantities of nickel. (Voter and Banks, 1949)

Testa *et al* (1991) took the separation of nickel a stage further by developing a method for preparing columns of dimethylglyoxime loaded onto a Microthene® support. This column was then used to extract nickel from solutions buffered at pH 8. Nickel was removed from the column using 0.1M HCl and recoveries (determined gravimetrically) were claimed to be 95-100%.

Ion-exchange purification can also be used to remove interfering radioisotopes from  $^{63}\text{Ni}$ . Nickel differs from other transition metals in not forming an anionic chloro-complex and hence is not retained on an anion exchange column in HCl media. By passing a sample in hydrochloric acid through an anion exchange column, most transition metals of significance are adsorbed, whereas nickel passes through the resin bed. Such an approach was adopted by Williams *et al* (1994) who used it to successfully decontaminate  $^{63}\text{Ni}$  from a number of other activation products, although a final tri-octylphosphine oxide (TOPO) extraction was required to remove all traces of chromium. The technique is useful in separating Ni from small quantities of Co that follow the Ni through the dimethylglyoxime column.

### 2.7.3 Strontium radioisotopes

#### Main production route : fission product

Radioisotope	Half-life	$\beta$ decay energy $E_{\max}$ keV (yield)	$^{235}\text{U}$ thermal fission yield	$^{235}\text{U}$ fast neutron fission yield	$^{239}\text{Pu}$ thermal fission yield	$^{239}\text{Pu}$ fast neutron fission yield
$^{85}\text{Sr}$	64.84 d	e.c. $\gamma$	$2.9 \times 10^{-10}$ %	-	$4.70 \times 10^{-9}$ %	$5.43 \times 10^{-9}$ %
$^{89}\text{Sr}$	50.5 d	1492 (100%)	4.77 %	4.39 %	1.68 %	1.69 %
$^{90}\text{Sr}$	29.12 y	546 (100%)	5.85 %	5.25 %	1.97 %	2.08 %

e.c. – decay via electron capture

$^{90}\text{Sr}$  is a major fission product that is usually concentrated by co-precipitation with calcium carbonate, oxalate (Doshi *et al*, 1968) or phosphate (from samples with high phosphate content such as milk or soils). Purification of the strontium from the calcium is achieved by selective precipitation of strontium nitrate through the addition of fuming nitric acid to aqueous solutions containing Sr. Barium and the associated fission product  $^{140}\text{Ba}$ , is separated from Sr by precipitating barium chromate at controlled pH. The  $^{90}\text{Y}$  daughter is removed by co-precipitation with iron hydroxide and the final source is counted periodically over about two weeks to monitor the  $^{90}\text{Y}$  in-growth (for example RADREM, 1989). A method has also been developed whereby fuming nitric acid is replaced by concentrated nitric acid (Bojonowski and Knapinska-Skiba, 1990). Water volumes are kept to a minimum and precipitates are washed with acetone to remove calcium.

Alternatively the  $^{90}\text{Sr}$  activity can be determined indirectly through the measurement of the  $^{90}\text{Y}$  daughter which is allowed to attain equilibrium. The  $^{90}\text{Y}$  fraction can then be purified and counted to determine the activity of the  $^{90}\text{Y}$ . This approach has been used in the determination of  $^{90}\text{Sr}$  in uranium fission products (Bajo and Tobler, 1996), reactor waste (Martin, 1987) and in grass and soil samples (Bajo and Keil, 1994). In all cases the  $^{90}\text{Y}$  was separated by solvent extraction into tributyl phosphate from nitric acid. The activity of  $^{90}\text{Sr}$  can then be calculated from the  $^{90}\text{Y}$  activity. This approach is useful if the presence of  $^{89}\text{Sr}$  is suspected, as this would interfere with the monitoring of  $^{90}\text{Y}$  in-growth in the  $^{90}\text{Sr}$  source. Final counting can be performed using a technique suitable for beta counting..

The separation of Ca and Sr has also been reported using zirconium molybdate (ORNL, 1956). Columns (10cm x 0.19cm<sup>2</sup>) of the material were prepared and 0.1M NH<sub>4</sub>Cl/0.005M HCl solutions containing the alkaline earth elements were loaded onto the columns. Ca was eluted

with 10 column volumes of 0.2M NH<sub>4</sub>Cl/0.005M HCl. Sr was eluted with 4 column volumes of 0.5M NH<sub>4</sub>Cl/0.005M HCl. Ba and Ra were eluted with 10 column volumes 1M NH<sub>4</sub>Cl/0.005M HCl and 5 column volumes of saturated NH<sub>4</sub>Cl/0.01M HCl respectively.

The use of macrocyclic ether extractants for the separation of radiostrontium has been reported (Kimura *et al*, 1979). Strontium was extracted into 0.012M dicyclohexyl 18-crown-6 in chloroform. Picrate was found to be the most effective counter-ion for the extraction

More recently the separation of Sr from Ca has been achieved using Sr-resin® resins supplied by Eichrom Industries. The resin, comprising of a crown ether (*tert*-butyl dicyclohexano-18-crown-6) supported on a polymeric macroporous resin (for example Amberlite™ XAD-7), selectively absorbs Sr without retaining the Ca. The resins have found many applications including the separation of <sup>90</sup>Sr from effluents and milk, although care must be taken as quantities of Ca can reduce the adsorption of Sr. It is interesting to note that the adsorption of Sr on the column is more seriously affected by the presence of K that must be removed prior to the sample being loaded onto the column (R Shaw, pers. comm.). Sr-resin® columns have been used for the separation of <sup>90</sup>Sr from up to 1 litre of milk samples (Jetter and Grob, 1994).

Cryptands as well as crown ethers have been used for the isolation of Sr from matrix elements, particularly Ca. 199 µmol of Cryptand C-222 on Chelite S resin adsorbed 90% Sr from a 100ml milk sample at pH 7 after 48 hours (Tait *et al*, 1995). Cs was retained to a limited degree but was easily removed by washing the resin. Sr was eluted with dilute nitric or hydrochloric acid.

#### 2.7.4 *Technetium radioisotopes*

##### Main production route : fission product

Radioisotope	Half-life	β decay energy E <sub>max</sub> keV (yield)	<sup>235</sup> U thermal fission yield	<sup>235</sup> U fast neutron fission yield	<sup>239</sup> Pu thermal fission yield	<sup>239</sup> Pu fast neutron fission yield
<sup>97</sup> Tc	2.60 x 10 <sup>6</sup> y	-	-	-	3.23 x 10 <sup>-9</sup> %	5.12 x 10 <sup>-9</sup> %
<sup>98</sup> Tc	4.20 x 10 <sup>6</sup> y	397 (100%)	6.13 x 10 <sup>-9</sup> %	1.6 x 10 <sup>-10</sup> %	2.0 x 10 <sup>-7</sup> %	3.4 x 10 <sup>-7</sup> %
<sup>99</sup> Tc	2.12 x 10 <sup>5</sup> y	294 (100%)	6.18 %	5.96 %	6.18 %	5.84 %

Pre-concentration of Tc from 1 - 100 litres of seawater has been achieved by co-precipitating the Tc(IV) on  $\text{Fe(OH)}_3$ . Tc(VII) must first be reduced to Tc(IV) by adding 0.7g/litre of  $\text{FeSO}_4 \cdot 7 \text{H}_2\text{O}$  to the acidified water (Holm, 1984). It is more usual to use  $\text{Fe(OH)}_3$  co-precipitation to remove contaminating radioisotopes whilst leaving the Tc(VII) in the supernate for further purification (for example Harvey *et al*, 1991).

Tc has been purified by co-precipitation on either rhenium sulphide (Harvey *et al*, 1991) or copper sulphide (Golchert and Sedlet, 1969) formed by adding thioacetamide to an acidic solution containing Tc and Re .

Final preparation of Tc sources is often achieved by co-precipitating the Tc on a precipitate of tetraphenyl arsonium perrhenate. This precipitate acts as a gravimetric yield monitor for Re (and hence Tc) and provides a source suitable for gas flow proportional counters, Geiger Müller tubes and liquid scintillation counting (the precipitate readily dissolves in scintillant). Harvey *et al* (1991) noted that co-precipitation of the Tc may not be quantitative below a certain concentration of tetraphenyl arsonium chloride (TPAC). 100% Tc was co-precipitated when only 30 mg of TPAC was present. However, 60 mg of TPAC was required to fully precipitate the Re (total of 10 mg Re present).

Carbonate co-precipitation has been used to remove contaminants such as the actinides, transition metals, lead, strontium and calcium from the Tc that remains in the supernate (Chu and Feldstein, 1984)

Chen *et al* (1990) used three 13 x 2.5 cm Dowex AG1-X4 (100-200 mesh) anion exchange resin columns running in parallel and conditioned with 0.5M sulphuric acid to extract Tc from 200 litre of acidified sea water. The columns were washed with 1M nitric acid and the Tc was striped from the columns with 10M nitric acid.

Harvey *et al* (1991) used anion exchange for a purification stage. A column of 1.5 ml of AG1-X8 (100-200 mesh) conditioned in 2M sodium hydroxide was used. A total of 100 ml of washings was passed through the column. The Tc and Re were eluted with sodium perchlorate reagent. It was noted that the Re eluted prior to the Tc and care was required to ensure that a sufficient volume of eluent had been passed through the column to completely elute both

elements. The perchlorate ions needed to be removed before precipitating the Re(Tc) as the tetraphenyl arsonium perrhenate. This was achieved by co-precipitation on rhenium sulphide.

Extraction of Tc from dilute sulphuric acid solutions into a 5% TOA-xylene mixture has been used to purify Tc (Golchert and Sedlet, 1969; Chen *et al*, 1990). Tc is back extracted into sodium hydroxide. Tc has also been extracted from nitric acid solutions using 30%TOA in xylene, although care must be taken as nitric acid concentrations above 4M lower the efficiency of the extraction (Hirano, 1989). Again the Tc was back-extracted into 5M sodium hydroxide.

TBP (Holm, 1984; Garcia-Leon, 1990) has been used to extract Tc from dilute sulphuric acid solutions. Formation of the tetraphenyl arsonium complex of Tc followed by solvent extraction into chloroform has also been used for Tc purification (Martin and Hylko, 1987)

The extraction of Tc as an amine complex can be achieved in two ways. The amine can be added to the aqueous phase to produce an amine complex, which can be extracted into an organic hydrocarbon. Alternatively, the amine can be dissolved in the organic phase, which is then used to extract Tc from the aqueous phase. The choice of method depends on the amine being used and its solubility in aqueous media. Generally the solubility of an amine decreases with molecular mass and in practice all amines containing more than six carbon atoms are regarded as insoluble (Morrison and Boyd, 1987). For quaternary amines all amines above trihexyl amine are insoluble.

Boyd and Larson (1956) investigated the extraction of Tc by a number of amines. A maximum distribution coefficient of 105 was noted using 0.3g cetyl dimethyl benzyl ammonium chloride (CDMBA) in 100 ml of chloroform. 5% TOA in benzene, 5% dimethyl octyl amine in benzene, Hyamine 10X and Hyamine 1622 exhibited distribution coefficients of 59.8, 53.1, 52.3 and 50 respectively (all extractions from 1N sulphuric acid). The distribution coefficients of Tc between a 5% TOA solution in various organic solvents and 1N sulphuric acid was also measured. The highest distribution coefficient was measured for 5% TOA in xylene (110.6). Distribution coefficients for benzene, trichloroethylene, carbon tetrachloride and chloroform were also measured (63.5, 52.2, 37.5 and 30.6 respectively).

Maeck *et al* (1961) studied the extraction of a wide range of elements including Tc and Re as quaternary propyl, butyl and hexyl amine complexes. The amine was added to the aqueous phase (except for the hexylamine, which was dissolved in methyl isobutyl ketone) and the aqueous phase mixed with methyl isobutyl ketone, which extracted any amine complex formed. It was noted that, in general, extraction efficiency increased with increasing molecular mass of the amine. Tc and Re were quantitatively extracted from sodium hydroxide (1 - 5N), sulphuric acid (1 - 5N) and hydrofluoric acid (1 - 5N) although the extraction of Re fell slightly in high HF concentrations. In the nitric acid system, extraction of Tc and Re fell with increasing nitric acid concentrations. In the hydrochloric acid system, Tc was quantitatively extracted over all acid concentrations. However, the extraction of the propylamine complex of Re fell with increasing acid concentration. It was proposed that the Tc and Re were extracted as species  $[(R_4N)^+ \cdot (Tc(Re)O_4)^-]$ .

## 2.8 References

Alonso J.I.G., Thoby-Schultzendorff D., Giovanonne B., Glatz J-P., Pagliosa G. and Koch L. (1994). Characterisation of spent nuclear fuel dissolver solutions and dissolution residues by inductively-coupled mass spectrometry. *J. Anal. Atom. Spec.*, **9**, 1209-1215.

Bajo S. and Keil R. (1994). Determination of <sup>90</sup>Sr in grass and soil. Report PSI Bericht Nr. 94-14, Paul Scherrer Institut, Villigen, Switzerland.

Bajo S. and Tobler L. (1996). Determination of <sup>90</sup>Sr in uranium fission products. Report PSI Bericht Nr. 94-14, Paul Scherrer Institut, Villigen, Switzerland.

Baker C.W., Sutton G.A. and Dutton J.W.R. (1973). Studies of liquid radioactive effluent discharged to the aquatic environment from CEGB nuclear power stations; the determination of the major beta-emitting isotopes. Symposium on the determination of radionuclides in environmental and biological materials, CEGB, Sudbury House, 2-3 April 1973.

Beasley T.M., Elmore D., Kubik P.W. and Sharma P. (1992). Chlorine-36 releases from the Savannah River site nuclear fuel reprocessing facilities. *Ground Water*, **30**, 539-543.

Berryman N. and Probst T. (1997). Rapid determination of <sup>90</sup>Sr by electrothermal vaporization-inductively coupled plasma mass spectrometry (ETV-ICP-MS). *Radiochim. Acta*, **76**, 191-195.

Bojonowski R. and Knapinska-Skiba D. (1990). Determination of low-level <sup>90</sup>Sr in environmental materials: a novel approach to the classical method. *J. Radioanalyt. Nucl. Chem., Articles*, **138** (2), 207-218.

Boyd G.E. and Larson Q.V. (1956) Solvent extraction of heptavalent technetium. In Oak Ridge National Laboratory report ORNL-2159. U.S. Atomic Energy Commission, USA.

<sup>30</sup>Brown R M, Long S E and Pickford C J (1988). The measurement of long lived radio nuclides by non radiometric methods. *The Science of the Total Environment*, **70**, 265-274.

Chen Q., Dahlgaard H., Hansen H.J.M. and Aarkrog A. (1990). Determination of <sup>99</sup>Tc in environmental samples by anion exchange and liquid-liquid extraction at controlled valency. *Anal. Chim. Acta* **228** 163-167.

Chu N.Y. and Feldstein J. (1984). Radiochemical determination of technetium-99. *Talanta*, **31** (10A), 809-813.

Cohen A.S. and O'Nions R.K. (1991). Precise determination of femtogram quantities of radium by thermal ionisation mass spectrometry. *Anal. Chem.*, **63**, 2705-2708.

Cosilito F.J., Cohen N. and Petrow H.G. (1968). Simultaneous determination of iron-55 and stable iron by liquid scintillation counting. *Anal Chem.*, **40** (1), 213-215.

Donohue D.L., Smith D.H., Young J.P., McKown H.S. and Pritchard C.A. (1984). Isotope analysis of uranium and plutonium mixtures by resonance ionisation mass spectrometry. *Anal. Chem.*, **56**, 379-381.

Doshi C.R. and Sreekumaran C. (1968). A simplified procedure for the estimation of strontium-90 in seawater. *Curr. Sci.*, **37**, 554-556.

Eakins J.D. and Lally D.A. (1965). The simultaneous determination of iron-55 and iron-59 in blood by liquid scintillation counting. AERE-R 4945, Harwell, UK.

Edwards R.L. Chen J.H. and Wasserburg G.J. (1986/7)  $^{238}\text{U}$ - $^{234}\text{U}$ - $^{230}\text{Th}$ - $^{232}\text{Th}$  systematics and the precise measurement of time over the past 500,000 years. *Earth Planet. Sci. Lett.*, **81**, 175-192

Francois B. (1973). Detection of hard  $\beta$ -emitting radionuclides in aqueous solutions using Cerenkov radiation : A review article. *Int. J. Nucl. Medicine and Biology*, **1**, 1-14.

Garcia-Leon M. (1990). Determination and levels of  $^{99}\text{Tc}$  in environmental and biological samples. *J. Radioanalytical and Nuclear Chemistry, Articles*, **138** (1) 171-179.

Golchert N.W. and Sedlet J. (1969). Radiochemical determination of technetium-99 in environmental water samples. *Anal. Chem.*, **41** (4), 669-671.

Gore H.E. (1987). Tandem accelerator mass spectrometry measurements of  $^{36}\text{Cl}$ ,  $^{129}\text{I}$  and osmium isotopes in diverse natural samples. *Phil. Trans. Roy. Soc. Lond.*, **A323**, 103-119.

Harvey B., Ibbett R.D., Williams K.J. and Lovett M.B. (1991) The determination of technetium-99 in environmental materials. Ministry of Agriculture, Fisheries and Foods. Aquatic Environmental Protection: Analytical methods number 8. Lowestoft, UK

Hirano S., Matsuba M. and Kamada H. (1989). The determination of  $^{99}\text{Tc}$  in marine algae. *Radioisotopes*, **38**, 186-189.

Hodge V F and Laing G A (1994). An evaluation of the inductively coupled plasma mass spectrometer for the determination of radium-226 in drinking water *Radiochimica Acta*, **64**, 211-215.

Holm E., Rioseco J. and Garcia-Leon M. (1984) Determination of  $^{99}\text{Tc}$  in environmental samples. *Nuclear Instruments and Methods in Physics Research*, **223**, 204-207.

Holm E, Oregioni B, Vas D, Pettersson H, Rioseco J and Nilsson U. (1990). Nickel-63: Radiochemical separation and measurement with an ion implanted silicon detector. *J. Radioanal. Nucl. Chem. Articles*, **138**, 111-118.

Horrocks D.L. (1976) The mechanism of the liquid scintillation process. In Noujaim A.A., Ediss C. and Weibe L.I. (eds) Liquid Scintillation, Science and Technology. Academic Press, New York, USA.

Ihsanullah and East B.W. (1994). Method for the determination of technetium-99 in environmental samples using inductively coupled plasma-mass spectrometry. *Radioact. Radiochem.*, **5**(2), 20-26.

Jetter H.W. and Grob B. (1994). Determination of radiostrontium in milk using an extraction chromatography. *Radioactivity and Radiochemistry*, **5** (3), 8-16.

Kessler M.J. (1989). Liquid scintillation analysis, Science and Technology. Packard Instruments Company, Meriden, Connecticut, USA

Kimura T., Iwashima K., Ishimoro T. and Hamada T. (1979). Separation of strontium-89 and -90 from calcium in milk with a macrocyclic polyether. *Anal. Chem.*, **51** (8), 1113-1116.

König W., Schupfner R. and Schüttelkopf H. (1995). A fast and very sensitive LSC procedure to determine Fe-55 in steel and concrete. *J. Radioanal. Nucl. Chem. Articles*, **193** (1), 119-125.

Maeck W.J., Booman G.L., Kussy M.E. and Rein J.E. (1961) Extraction of the elements as quaternary (propyl, butyl and hexyl) amine complexes. *Anal. Chem.*, **33**, (12), 1775-1780.

Martin J.E. (1987). Measurement of  $^{90}\text{Sr}$  in reactor wastes by Cerenkov counting of  $^{90}\text{Y}$ . *Appl. Radiat. Isot.*, **38** (11), 953-957.

Martin J.E. and Hylko J.M. (1987) Measurement of  $^{99}\text{Tc}$  in low-level radioactive waste from reactors using  $^{99\text{m}}\text{Tc}$  as a tracer. *Appl. Radiat. Isot.*, **38** (6), 447-450.

McCormick A. (1992). Thermal-ionisation mass spectrometry for small sample analysis of uranium and plutonium. *Appl. Radiat. Isot.*, **43**, 271-278.

Morrison R.T. and Boyd R.N. (1987) Organic Chemistry. 5th Edition. Allyn and Bacon Inc. Boston, USA.

ORNL (1956). Cation exchange properties of 'Zirconium molybdate' - separation of the alkaline earths. Chemistry Division semiannual progress report, period ending June 20, 1956. ORNL-2159, Oak Ridge National Laboratory, Oak Ridge, Tennessee, USA.

Parker, R.P. and Elrick R.H. (1970). Cerenkov counting as a means of assaying  $\beta$ -emitting radionuclides. In Bransome E.D. (ed.). The current status of liquid scintillation counting. Grune and Stratton, New York, USA.

RADREM (1989). Sampling and measurement of radionuclides in the environment. A report by the methodology sub-group to the Radioactivity Research and Environmental Monitoring Committee (RADREM). HMSO, London, UK.

Ross H.H. (1976). Theory and application of Cerenkov counting. In Noujaim A.A., Ediss C. and Weibe L.I. (eds), Liquid Scintillation : Science and Technology. Academic Press, New York, USA.

Tagami K. and Uchida S. (1993). Separation procedure for the determination of technetium-99 in soil by ICP-MS. *Radiochim. Acta*, **63**, 69-72.

Tait D., Wiechen A. and Haase G. (1995). Binding of Sr from milk by solid phase extraction with cryptand C222 sorbed on silica gel, cation exchange, chelating or adsorbent resins for simplified  $^{90}\text{Sr}$  analysis. *Sci. Total Env.*, **173/174**, 159-167.

Taylor R.N., Croudace I.W. and Warwick P.E. (1998). Optimised method for the measurement of Uranium by TIMS - *Chem Geol*, **144**, 73-80.

ter Wiel J. (1992) Effect of viscosity on quench characteristics of solvents for liquid scintillation counting. In Noakes J.E., Schonhoffer F. and Polach H.A. eds LSC 92. International Conference on Advances in Liquid Scintillation Spectrometry 1992. Radiocarbon, Department of Geosciences, University of Arizona, USA.

Testa C, Desideri D, Meli M.A., Roselli C.(1991). Extraction chromatography in radioecology. *Radioactivity and Radiochemistry*, **2** (4), 46-54.

Thomas J.K. and Beck G. (1980) Formation of excited states by the pulse radiolysis of liquid systems. In Peng C.T., Horrocks D.L. and Alpen E.L. (eds) Liquid Scintillation Counting-Recent Applications and Developments. Academic Press, New York, USA

Toole J., Adsley I., Hearn R., Wildner H., Montgomery N., Croudace I., Warwick P. & Taylor R. (1997). Status of analytical techniques for the measurement of uranium isotopic signatures. Workshop

on the status of measurement techniques for the identification of nuclear signatures, 25-27 February 1997, Geel Belgium. Report EUR 17313

Trautmann N. (1993). Ultratrace analysis of technetium. *Radiochim. Acta*, **63**, 37-43.

Vogel A. (1978). A textbook of quantitative inorganic analysis. Longman Group Ltd, London, UK

Voltz R., Laustriat G. and Coche A. (1963) *C.R. Acad. Sci., Paris*, **257**, 1473.

Voter R.C. and Banks C.V. (1949) Water soluble 1,2-Dioximes as analytical reagents. *Anal. Chem.*, **21** (11), 1320-1323.

Wallac (1996). Instrument manual; 1220 Quantulus ultra low level liquid scintillation spectrometer. Wallac Oy, Turku, Finland

Wiebe L.I. and Ediss C. (1976). Methyl salicylate as a medium for radioassay of  $^{36}\text{Cl}$  using a liquid scintillation spectrometer. In Noujaim A.A., Ediss C. and Wiebe L.I. (eds), Liquid Scintillation: Science and Technology. Academic Press, New York, USA.

Williams D.F., O'Kelly G.D. and Knauer J.B.. (1994). Flowsheet for the recovery and purification of  $^{63}\text{Ni}$ . *Radiochim. Acta*, **64**, 49-55.

Yamamoto M., Kofuji H., Tsumura A., Yamasaki S., Yuita K., Komamura M., Komura K. and Ueno K. (1994). Temporal feature of global fallout  $^{237}\text{Np}$  deposition in paddy field through the measurement of low-level  $^{237}\text{Np}$  by high resolution ICP-MS. *Radiochimica Acta*, **64**, 217-224.

## **Chapter 3**

### **Experimental**

#### **Development of source preparation and measurement techniques**

### 3 Development of source preparation and measurement techniques

#### 3.1 Stability of the Wallac 1220 Quantulus liquid scintillation counter

The performance and stability of the liquid scintillation counter was assessed throughout the project by routinely counting a  $^{14}\text{C}$  standard and blank sample that were supplied with the liquid scintillation counter. The two test sources were prepared in glass vials, purged with  $\text{N}_2$  and sealed to ensure that the sources were stable over long periods of time. The count rates observed for the two sources are plotted in Figure 3.1. The distribution of observed counts all lie within two standard deviations of the mean count rate.

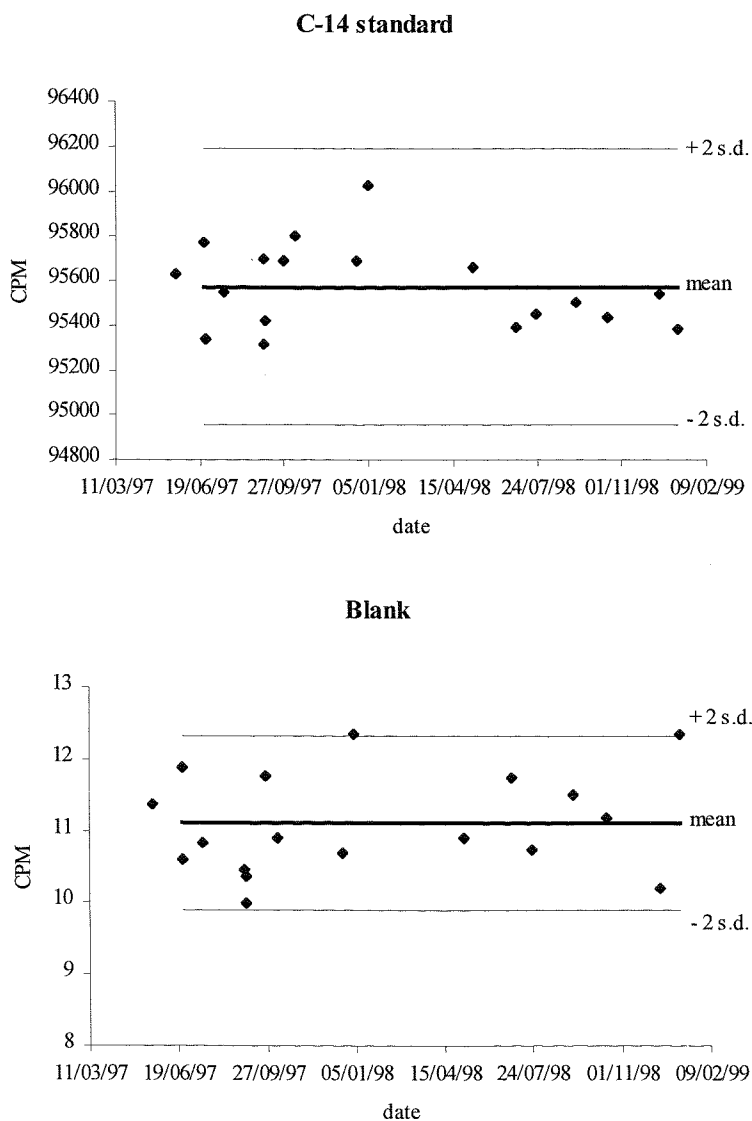


**Figure 3.1 : Scatter of measured standard and blank counts over the period of the study.**

### 3.2 Deconvolution of isotopes of the same element

The nature of the beta spectrum resulting from the continuous distribution of the decay energy between the beta particle and the antineutrino makes spectral deconvolution of all but simple binary mixtures of beta emitters highly imprecise. For radioisotopes of different elements, this limitation in deconvolution may be overcome by chemically isolating the radioisotopes of interest. However, for radioisotopes of the same element this is not applicable.

All the pure beta-emitters studied, with the exception of  $^{99}\text{Tc}$ , may be present in association with other radioisotopes of the same element. Strontium-90 will be accompanied by  $^{89}\text{Sr}$  ( $t_{1/2} = 50.5$  days). Deconvolution of mixtures of  $^{89}\text{Sr}$ ,  $^{90}\text{Sr}$  and the daughter  $^{90}\text{Y}$  may be achieved by making use of their varying half-lives and repeated counting. This has been discussed in Section 3.9.

Iron-59 ( $t_{1/2} = 45.10$  days) will be produced along with  $^{55}\text{Fe}$ . The presence of  $^{59}\text{Fe}$  may be readily determined using gamma spectrometry ( $E_{\gamma} = 1099$  keV [56.5%] and 1292 keV [43.2%]). If convenient the  $^{59}\text{Fe}$  may then be allowed to decay prior to  $^{55}\text{Fe}$  measurement. Alternatively, the liquid scintillation counter should be configured to distinguish between the  $^{59}\text{Fe}$  ( $E_{\beta\max} = 275$  keV [45.3%] and 467 keV [53.1%]) and the lower energy  $^{55}\text{Fe}$  with appropriate corrections being applied for the spill-over of  $^{59}\text{Fe}$  into the  $^{55}\text{Fe}$  energy window. The deconvolution of  $^{59}\text{Fe}$  from  $^{55}\text{Fe}$  was not considered as part of this study as any  $^{59}\text{Fe}$  originally present in the samples of interest had decayed prior to sample analysis. However, for waste characterisation, the potential for  $^{59}\text{Fe}$  to interfere with the  $^{55}\text{Fe}$  measurement must be taken into account.

Nickel-59 ( $t_{1/2} = 74$ , 950 years) is produced along with  $^{63}\text{Ni}$  by neutron activation of Ni. However, the typical activity ratio of  $^{63}\text{Ni}$ : $^{59}\text{Ni}$  has been estimated as 100:1 (Holm *et al*, 1990). Again, suitable windowing of the liquid scintillation counter and correction for spill-over of counts should be applied if the presence of  $^{59}\text{Ni}$  is suspected.

### 3.3 Optimisation of source preparation techniques for liquid scintillation counting

A number of source preparation techniques have been investigated as part of this study. These are :

1. Extracting the radioisotope into an organic solvent that is then mixed directly with the scintillant ( $^{99}\text{Tc}$ ).
2. Mixing an acidic solution containing the purified radioisotope directly with the scintillant ( $^{63}\text{Ni}$ , and the special case of  $^{55}\text{Fe}$  – see Section 3.6).
3. Precipitating the radioisotope with a stable carrier and counting the precipitate ( $^{63}\text{Ni}$ ,  $^{99}\text{Tc}$ ).

In addition, the counting of high-energy beta emitters may also be accomplished with minimal source preparation using the technique of Cerenkov counting. The application of Cerenkov counting to the measurement of  $^{90}\text{Sr}$  is discussed in Sections 3.8 & 3.9.

### 3.4 The extraction of a radioisotope into an organic solvent

Many non-halogenated organic solvents employed in solvent extraction will readily mix with liquid scintillant to produce a source that exhibits low quench. Such an approach is an integral part of a separation procedure. As such, the specific case of  $^{99}\text{Tc}$  will be discussed in detail in Chapter 4. In general, with careful choice of the organic solvent, quenching is significantly reduced in such systems and improved counting efficiencies compared to an aqueous-based system are achieved.

One drawback to extracting the analyte into the organic phase prior to mixing with scintillant is that, in many cases, it is difficult to determine the overall chemical recovery of the method including the final extraction stage. Although the final extraction procedure may be assumed to be 100% efficient, the nature of solvent extraction makes this assumption unreliable. For  $^{99}\text{Tc}$  this is overcome by using the gamma-emitting radioisotope  $^{99\text{m}}\text{Tc}$  that can be measured in the final source to determine the overall chemical recovery of the method. The  $^{99\text{m}}\text{Tc}$  is then allowed to decay prior to measurement of  $^{99}\text{Tc}$  by liquid scintillation counting, hence the  $^{99\text{m}}\text{Tc}$  added to the sample does not seriously interfere with the final  $^{99}\text{Tc}$  measurement.

The extension of this approach to other analytes is limited to those for which a technique is available to determine the overall chemical recovery of the method that includes the final extraction stage. This means that the approach of organic extraction for source preparation is limited to a small range of radioisotopes.

### 3.5 Measurement of acidic solutions by liquid scintillation analysis

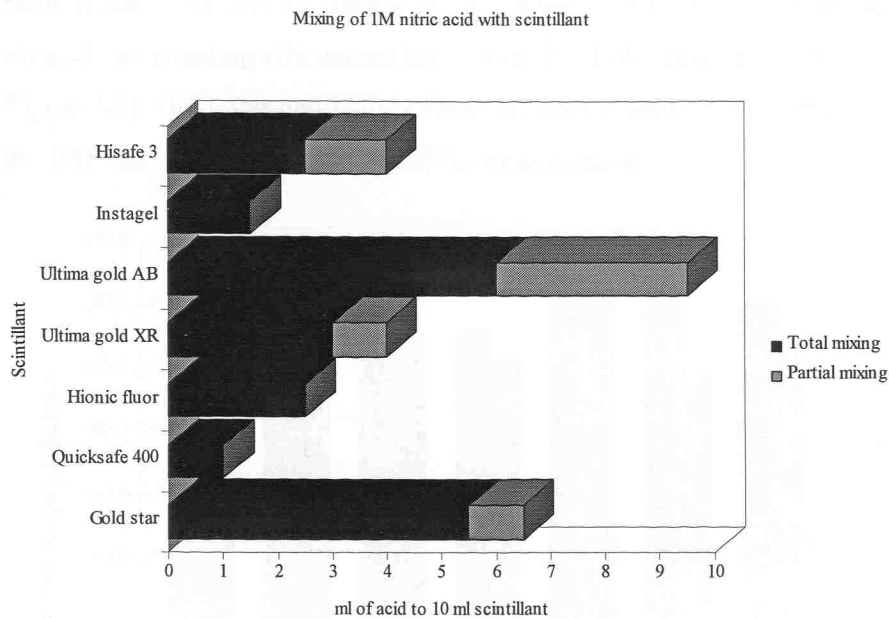
The chemical purification of  $^{63}\text{Ni}$  and  $^{55}\text{Fe}$  results in an acidic solution containing the purified radioisotope. This solution may be mixed with a commercially available liquid scintillant prior to liquid scintillation counting. The miscibility of commercially available scintillants varies widely and is dependent on the acid type and acid concentration. In general miscibility is improved with reducing acid strength and the final stages in the chemical purification of  $^{63}\text{Ni}$  are designed to limit the final acid strength for this reason.

#### 3.5.1 *Miscibility of scintillants with acid solutions*

A range of commercial scintillants was tested to study their miscibility with 1M  $\text{HNO}_3$  and 1M  $\text{HCl}$ . A known volume of the scintillant was shaken with increasing volumes of the acid. At first the acid and scintillant mixed completely to produce a homogenous, stable gel. However, as the acid volume was increased, the gel became less stable reaching a point where occluded bubbles, which did not dissipate on standing, were clearly visible. This condition is referred to as partial mixing. On further increasing the acid volume a white emulsion was formed that was unstable and not suitable for liquid scintillation counting. The volumes of acid resulting in these stages depends on the acid type and scintillant used (Figure 3.2 a and b).

The highest miscibility with acidic solutions was observed for Ultima Gold AB scintillant. This scintillant has been specifically designed to tolerate high acid loadings for simultaneous alpha / beta measurements in acidic solutions. However, the scintillant is expensive and its routine use is not financially justifiable. The second highest loadings were observed for Gold Star scintillant, a general-purpose scintillant suitable for routine use. Although the acid loadings are lower than for Ultima Gold AB they are still sufficiently high to be of use.

(a)



(b)

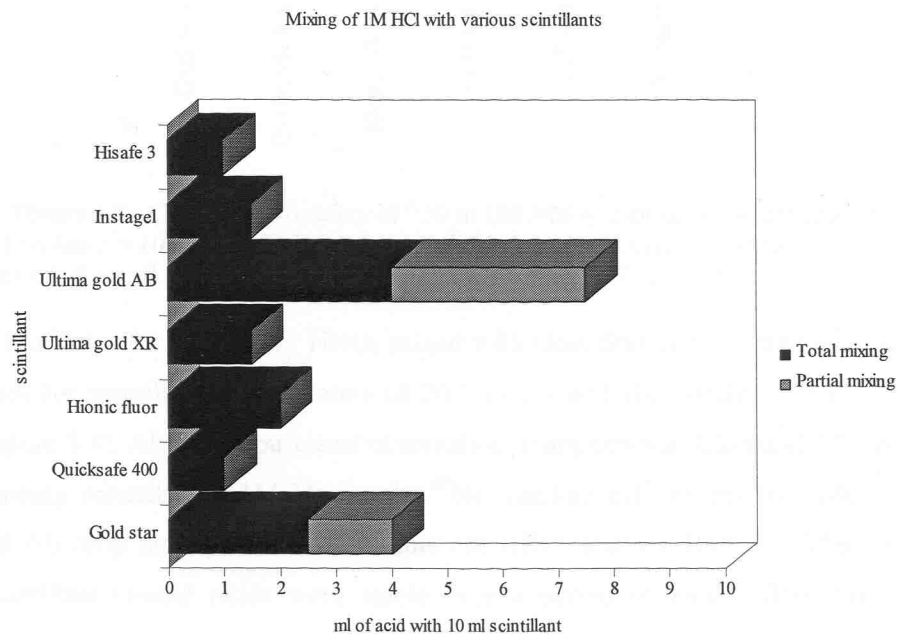


Figure 3.2 : Mixing characteristics of various commercial scintillants with

(a) 1M  $\text{HNO}_3$

(b) 1M  $\text{HCl}$

All assessments made at 22°C

Better miscibility is observed with 1M HNO<sub>3</sub> compared with 1M HCl. For a fixed mixing ratio of scintillant with acid, the counting efficiencies for <sup>63</sup>Ni in 1M HNO<sub>3</sub> vary only slightly with differing scintillants (Figure 3.3). Gold Star and Ultima Gold AB gave comparable counting efficiencies for <sup>63</sup>Ni at both the 19:1 and 5:1 scintillant-to-1M HNO<sub>3</sub> mixing ratios.

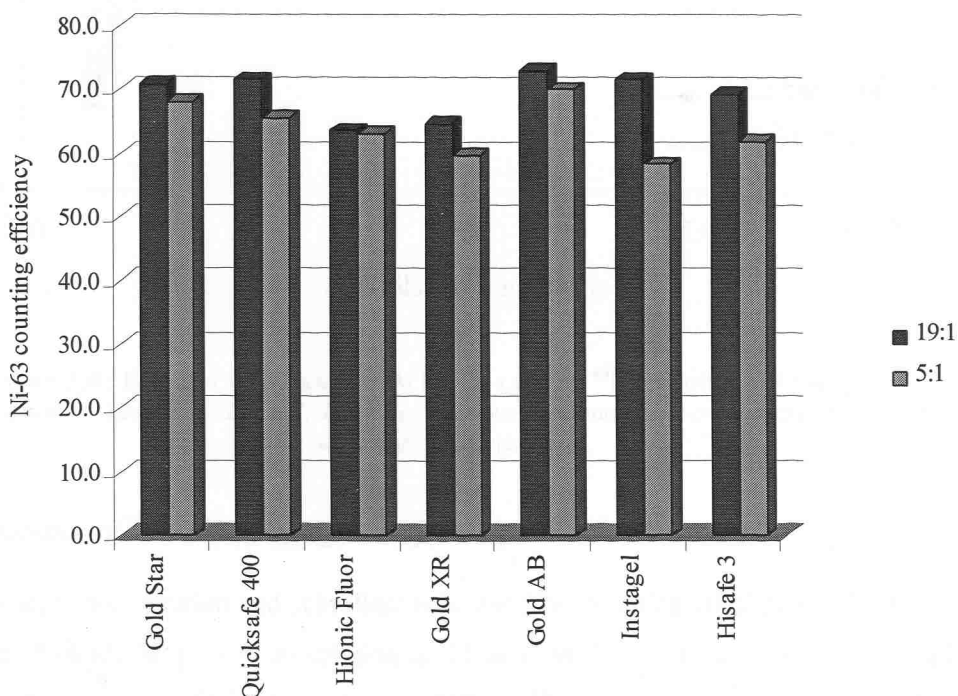


**Figure 3.3 : Counting efficiency of <sup>63</sup>Ni in 1M HNO<sub>3</sub> with different scintillants.**

*Total sample volume = 10ml in a 22ml polythene vial. Measurements were performed at two scintillant-to-acid ratios of 19:1 and 5:1. All measurements made on a Packard 2250CA liquid scintillation counter*

Counting efficiencies for <sup>63</sup>Ni in 1M HNO<sub>3</sub> mixed with Gold Star and Ultima Gold AB scintillants were constant for scintillant-to-acid ratios of 20:1 to 5:1 and then declined with increasing acid loadings (Figure 3.4). Although, on visual observation, it appears that Ultima Gold AB has a higher effective loading capacity for 1M HNO<sub>3</sub>, the <sup>63</sup>Ni counting efficiencies for both Gold Star and Ultima Gold AB drop rapidly at about the same 1M HNO<sub>3</sub> loading. Both scintillant types over the range of scintillant-to-acid ratios were stable over a period of eleven days following sample preparation. This suggests that there is no benefit in using the more expensive Ultima Gold AB for the measurement of <sup>63</sup>Ni.

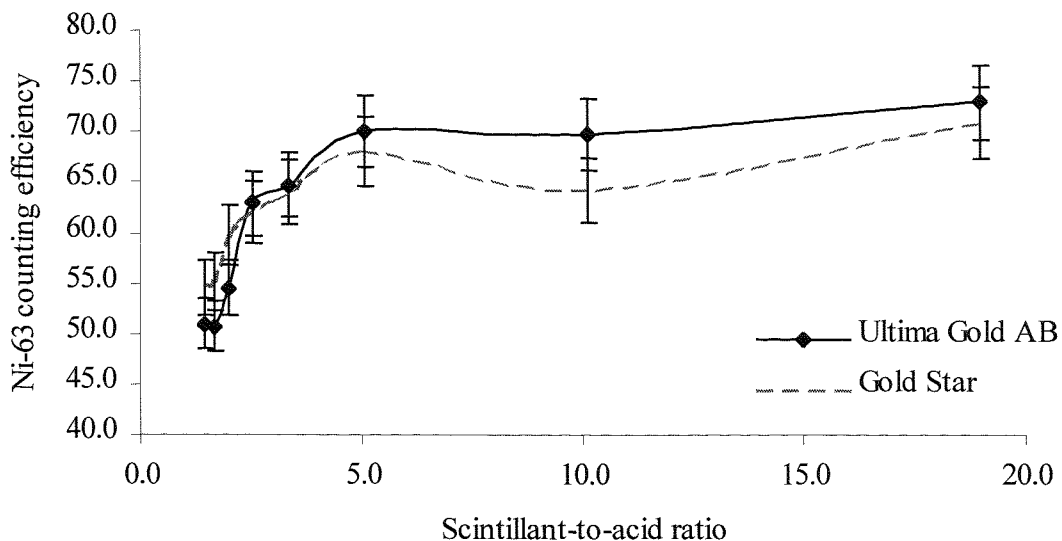


**Figure 3.4 : Effect of scintillant-to-1M HNO<sub>3</sub> ratio on <sup>63</sup>Ni counting efficiency.**

*Total sample volume = 10ml in a 22ml polythene vial. All measurements made on a Packard 2250CA liquid scintillation counter*

### 3.5.2 Dependence of <sup>63</sup>Ni counting efficiency on stable Ni mass

As well as the acid concentration and scintillant type, the <sup>63</sup>Ni counting efficiency will also depend on the amount of stable Ni present in solution and hence on the chemical recovery of stable Ni. Samples containing between 0.5 to 10mg Ni and 200 Bq <sup>63</sup>Ni were dissolved in 1ml 1M HCl and 2ml of water. 15ml Gold Star scintillant was added and the samples were counted on the Wallac 1220 Quantulus liquid scintillation counter.

The counting efficiency decreased as the quantity of stable Ni increased although the effect was limited (Figure 3.5). The small drop in counting efficiency was the result of an increase in sample quench which was apparent in the lower measured SQPE values. The measured SQPE quench index could therefore be used to determine the counting efficiency for each sample. The relationship between the SQPE and <sup>63</sup>Ni counting efficiency is given by the equation

$$E = 0.0077463(\text{SQPE})^2 - 11.701(\text{SQPE}) + 4487$$

where E = the counting efficiency for <sup>63</sup>Ni.

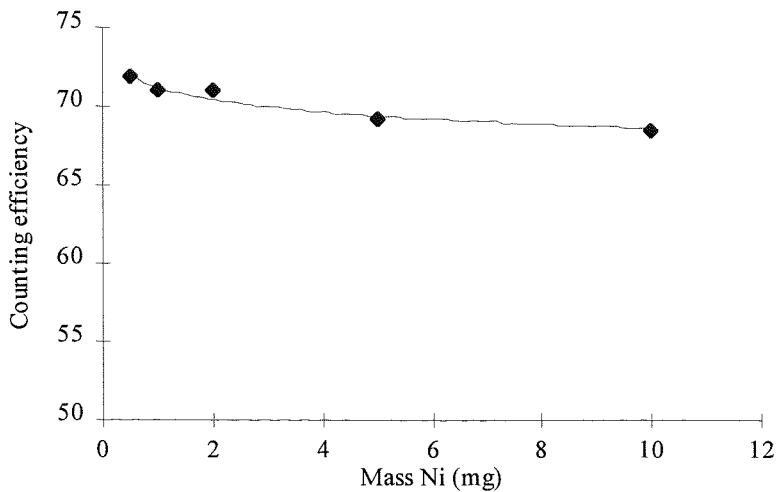


Figure 3.5 (a): Relationship between  $^{63}\text{Ni}$  counting efficiency and mass stable Ni

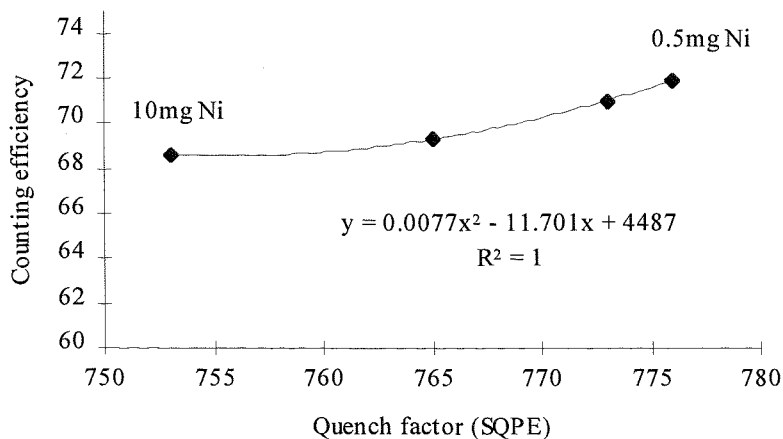


Figure 3.5 (b) : Relationship between  $^{63}\text{Ni}$  counting efficiency and SQPE value

### 3.6 Paper in *Radioact. Radiochem.*, 9(2), 19-25 (1998):

#### An Optimised Method for the Measurement of $^{55}\text{Fe}$ Using Liquid Scintillation Analysis.

P.E. Warwick<sup>1</sup>, I.W. Croudace<sup>1</sup> and M.E.D. Bains<sup>2</sup>

<sup>1</sup>School of Ocean & Earth Science, Southampton Oceanography Centre, European Way, Southampton, SO16 3NH

<sup>2</sup>AEA Technology, Weymouth, Dorset, DT2 8DH

##### 3.6.1 Introduction

Iron-55 is produced during nuclear weapons' detonation and nuclear power station operation. It has been estimated that a total of 700 PBq (i.e.  $10^{15}$  Bq) of  $^{55}\text{Fe}$  was released into the environment during weapons' testing (Hoang *et al*, 1968) with a further 5-6 TBq (i.e.  $10^{12}$  Bq) released as authorised discharge from BNFL Sellafield up to 1996. Iron-55 is produced via neutron activation of stable  $^{54}\text{Fe}$  (natural abundance = 5.8%) and is present in steel components and waste streams of nuclear reactors. Quantitative determination of the isotope is therefore important for waste disposal auditing purposes. Measurement of  $^{55}\text{Fe}$  has been achieved using low-energy gamma-ray spectrometry and gas-flow proportional counting (Cosilito *et al*, 1968) but the most common measurement technique is liquid scintillation counting.

Iron-55 ( $t_{1/2} = 2.7$  years; Browne and Firestone, 1986) decays via electron capture to  $^{55}\text{Mn}$  with the emission of Auger electrons and low-energy X-rays (5.89 keV, 16.2%). Both the K-Auger electron and the K-X ray emission are detected during the liquid scintillation measurement (Gibson and Marshall, 1972). In samples recently collected from operating nuclear reactor systems and effluent streams  $^{55}\text{Fe}$  is accompanied by the gamma emitter  $^{59}\text{Fe}$  ( $t_{1/2} = 44.5$  days). Iron-59 will interfere with the accurate determination of  $^{55}\text{Fe}$  by liquid scintillation counting and suitable corrections must be applied to correct for the spill-over of  $^{59}\text{Fe}$  counts into the  $^{55}\text{Fe}$  counting window. Methods for such a correction are discussed elsewhere (De Filippis, 1991). The low decay energy of  $^{55}\text{Fe}$  also makes it difficult to distinguish from chemiluminescence and care must be taken to eliminate this prior to counting by dark-adapting the scintillant mixture.

Sensitive measurement of  $^{55}\text{Fe}$  is highly dependent on sample preparation as the distinct yellow colour of Fe(III) is a very effective colour quenching agent. For example, the presence of only 20-mg of stable Fe in 1M HCl will result in a drop in counting efficiency to less than 1% (compared to 40% for an identical sample containing negligible stable Fe). A number of approaches have been adopted to reduce colour quenching from Fe(III). Solvent extraction of the Fe into di(2-ethylhexyl)phosphoric acid (Cosilito *et al*, 1968) resulted in severe quenching at Fe loadings greater

than 30 mg. Yonezawa *et al* (1985) extracted the Fe complex of 2,4-diphenyl-1,10 -phenanthroline into toluene containing diphenyloxazole. Cobalt was also co-extracted but was preferentially back-extracted with 0.005M EDTA. The Fe complex is brightly coloured and significant colour quench occurs even at quite low Fe concentrations ( $>10\text{-}\mu\text{g Fe}$ ). Colour quenching by Fe(III) can be largely overcome by reducing Fe(III) to Fe(II) using a suitable reductant. Konig *et al* (1995) used ascorbic acid to achieve this reduction. Counting efficiencies ranged from 26% (5 mg Fe loading) to 23% (100-mg loading). However, on standing for between 7 and 25 days the yellow colouration of Fe(III) returned. This may be restrictive when counting large numbers of samples or when counting for prolonged count times. Alternatively, for more stable sources, a colourless Fe-phosphate complex can be formed. Eakins and Brown (1965) precipitated Fe as a white ammonium ferriphosphate complex by adding an alcoholic solution of ammonium chloride to a solution of Fe in phosphoric acid. The precipitate was suspended in a gel and counted by liquid scintillation counting. This method was limited to an effective loading of 10-mg Fe. Although this approach overcame colour quenching, the technique required additional centrifugation stages prior to counting and was therefore more time-consuming.

Bains initially suggested dissolving a purified Fe fraction directly into dilute phosphoric acid to produce a colourless solution, which could be directly mixed with scintillant. Subsequent improvements in the mixing characteristics of scintillant cocktails with acids have meant that greater quantities of phosphoric acid solutions (and hence greater quantities of iron) may be added to scintillant. In this study phosphoric acid is used to dissolve the purified Fe fraction forming a colourless iron phosphate. This phosphoric acid solution is then mixed with scintillant producing a source suitable for liquid scintillation analysis. The scintillant type, volume and molarity of phosphoric acid and counting conditions are investigated and the minimum achievable limits of detection are determined.

### 3.6.2 Methodology

#### 3.6.2.1 Reagents

Phosphoric acid was supplied by Merck Ltd, Poole, Dorset. Instagel, Ultima Gold AB, Ultima Gold XR and Hionic Fluor were supplied by Packard UK Ltd, Pangbourne, Berkshire, UK. Quicksafe 400 was supplied by Zinsser Analytic, Maidenhead, Berkshire, UK. Gold Star scintillant was supplied by Meridian, Epsom, Surrey, UK. Iron-55, as a calibrated solution, was supplied by the National Physical Laboratory, Teddington, Middlesex, UK. Other reagents were supplied by Fisher Scientific, Loughborough, UK. All reagents used were analytical grade. Milli-Q® water was used throughout.

All measurements were made on a Wallac 1220 ‘Quantulus’ ultra low-level liquid scintillation counter.

### 3.6.2.2 Chemical separation of $^{55}\text{Fe}$ and LSA preparation

The pH of an acid leachate was adjusted to pH 5-6 with ammonia solution to precipitate  $\text{Fe(OH)}_3$ . The  $\text{Fe(OH)}_3$  precipitate was dissolved in 20 ml 8M HCl and transferred to a separating funnel. The Fe in the aqueous phase was extracted twice into 25 ml 3:1 mixture of ethyl acetate and butyl acetate. The organic layer was washed with 8M HCl and then the Fe was back-extracted into 6M  $\text{HNO}_3$ . The acid fraction was diluted to 10 ml and an aliquot was removed for stable Fe measurement using atomic absorption spectroscopy to determine the chemical yield of Fe. The remainder of the solution was evaporated to near dryness and the residue was dissolved in a few drops of 6M HCl. The HCl solution was evaporated again to near dryness producing a residue of iron (III) chloride. This residue was dissolved in the minimum amount of 2M  $\text{H}_3\text{PO}_4$ . Care was required not to allow the Fe fraction to completely evaporate to dryness prior to adding the  $\text{H}_3\text{PO}_4$  as prolonged heating converts the iron (III) chloride residue to the much more intractable oxide. The solution was transferred to a 20 ml polyethylene scintillation vial and scintillant was added. Iron-55 was then determined by liquid scintillation counting. Typical measurement parameters are shown in Table P1.

Table P1 : Liquid scintillation counting conditions (Wallac 1220 Quantulus counter)

Vial type	20 ml polyethylene vial
Count time	60 minutes
Optimised window (MCA 1.1)	1-200
PSA / PAC correction	Deactivated
Bias	Low

The capacity of various, commercially available, scintillants for phosphoric acid varies markedly. Mixing characteristics of various scintillants with 2M  $\text{H}_3\text{PO}_4$  have been determined and are shown in Figure P1. Ultima Gold AB (Packard) was chosen for subsequent studies as it exhibited the highest loading capacity for  $\text{H}_3\text{PO}_4$ .

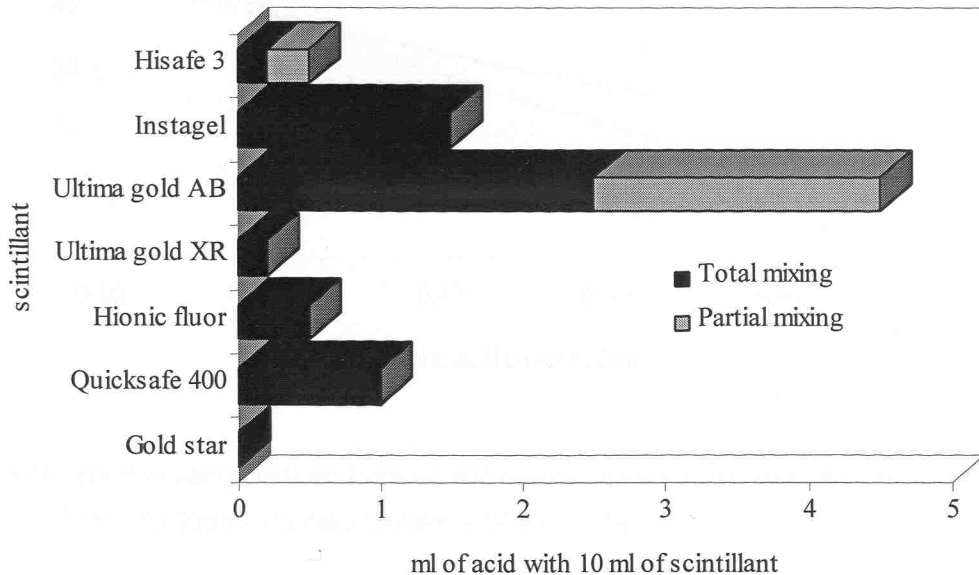


**Figure P1 : Mixing characteristics of various scintillants with 2M  $\text{H}_3\text{PO}_4$  at 22°C**

### 3.6.3 Discussion

For samples containing very little stable Fe, the  $^{55}\text{Fe}$  counting efficiency is dependent on the amount of phosphoric acid and the total aqueous volume present. The relationship between acid volume and counting efficiency for three acid concentrations is shown in Figure P2. In routine analysis 2M  $\text{H}_3\text{PO}_4$  is used to dissolve the chloride residue.

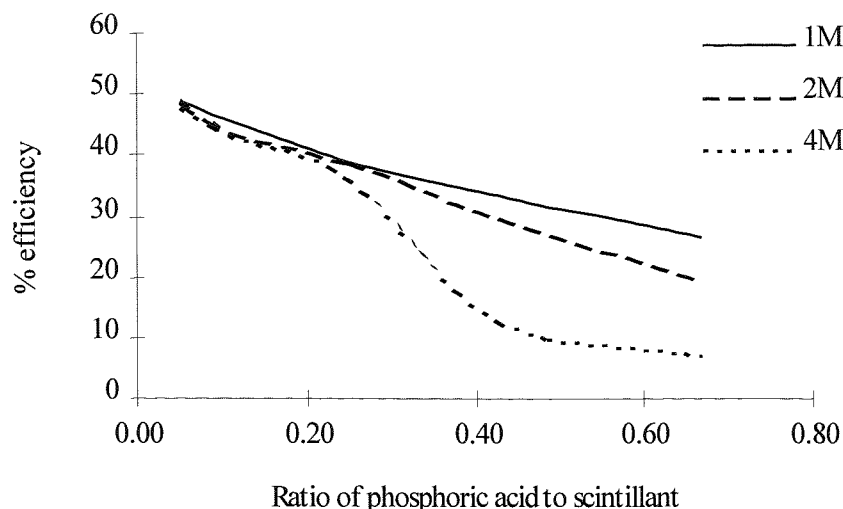


**Figure P2 : The effect of phosphoric acid volume and concentration on  $^{55}\text{Fe}$  counting efficiency**

(Note) Ultima Gold AB scintillant, total volume 10 ml

A maximum of 6 ml of 2M  $\text{H}_3\text{PO}_4$  can be added to 14 ml of scintillant to produce a source suitable for counting. It was found that approximately 300 $\mu\text{l}$  of 2M  $\text{H}_3\text{PO}_4$  is required to completely dissolve/decolourise 10-mg of Fe. This places an upper limit of 200 mg Fe which can be counted. The counting efficiency of the sample depends on the amount of Fe present and a typical relationship is shown in Figure P3. The efficiency rapidly drops as more Fe is added to the scintillant although even at a loading of 200 mg Fe the counting efficiency of 12% is acceptable. The fall in efficiency is due to rising quench resulting from the increase in Fe loading and an increase in the amount of  $\text{H}_3\text{PO}_4$  required to decolourise the Fe.

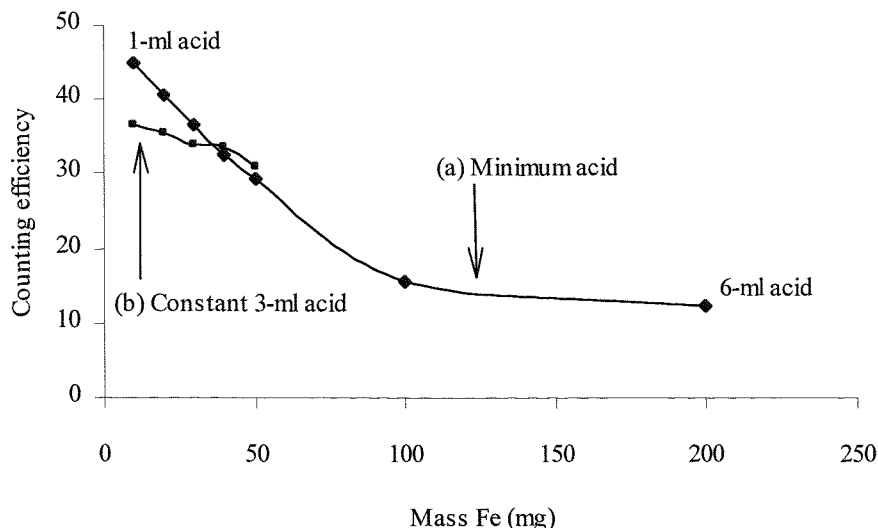


**Figure P3 : The effect of Fe loading on the  $^{55}\text{Fe}$  counting efficiency**

Curve (a)  $^{55}\text{Fe}$  counting efficiency vs Fe content. The minimum amount of 2M phosphoric acid was added to decolourise the sample. The fall in efficiency is a result of the Fe content and the added phosphoric acid. Curve (b) shows the effect of Fe mass on counting efficiency when a constant excess volume of 2M phosphoric acid (3ml) is used. The shallower gradient of this line compared to the first plot suggests that the phosphoric acid is the main factor controlling sample quench.

The increased loadings of Fe obtained in this study allow more sensitive measurement of  $^{55}\text{Fe}$  in samples with high Fe content such as soils and steel construction material. The limit of detection for  $^{55}\text{Fe}$  measurement is calculated from Equation 1 (derived from Currie, 1968).

$$L_D(\text{Bq/g}) = \frac{2.71 + 4.65\sqrt{C}}{t} \times \frac{100}{E} \times \frac{100}{R} \times \frac{1}{m} \quad [\text{Eqn. 1}]$$

where C represents background counts, t is the count time in seconds, E is the counting efficiency, R is the chemical recovery and m is the mass of sample analysed in grams. For a given count time and chemical recovery the limit of detection is governed by the mass of the sample analysed and the counting efficiency. Increasing the mass of the sample would be expected to lower the limit of detection. However, for samples containing iron as a major constituent, an increase in sample mass results in an increase in iron content of the final source leading to a reduction in counting efficiency. This effect is outweighed by the increase in sample mass being measured (Figure P4) and lower limits of detection are still achieved by analysing a greater mass of sample. The relationship between sample Fe content, maximum sample mass that may be analysed and the minimum achievable limit of detection are shown in Figures P5 and P6. All limits of detection are determined for the Wallac 1220 'Quantulus' with count times of 60 minutes.

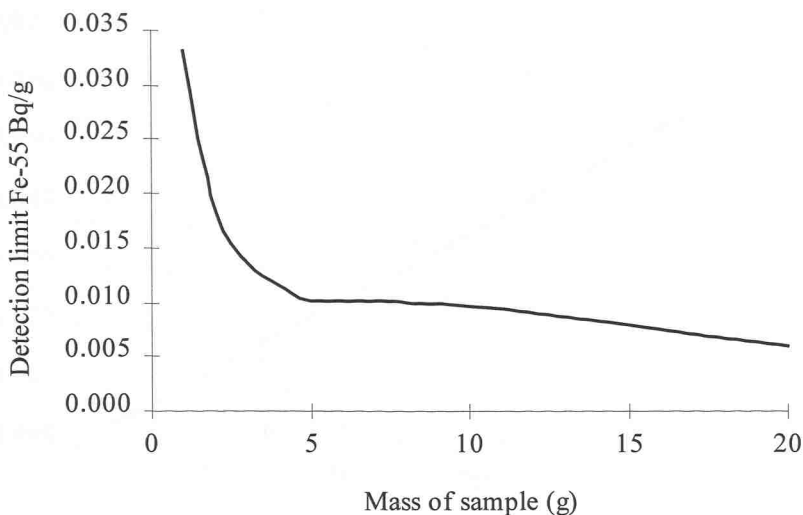


**Figure P4 :** The relationship between sample loading and  $^{55}\text{Fe}$  limit of detection (in Bq/g Fe) for a sample containing 10mg/g stable Fe

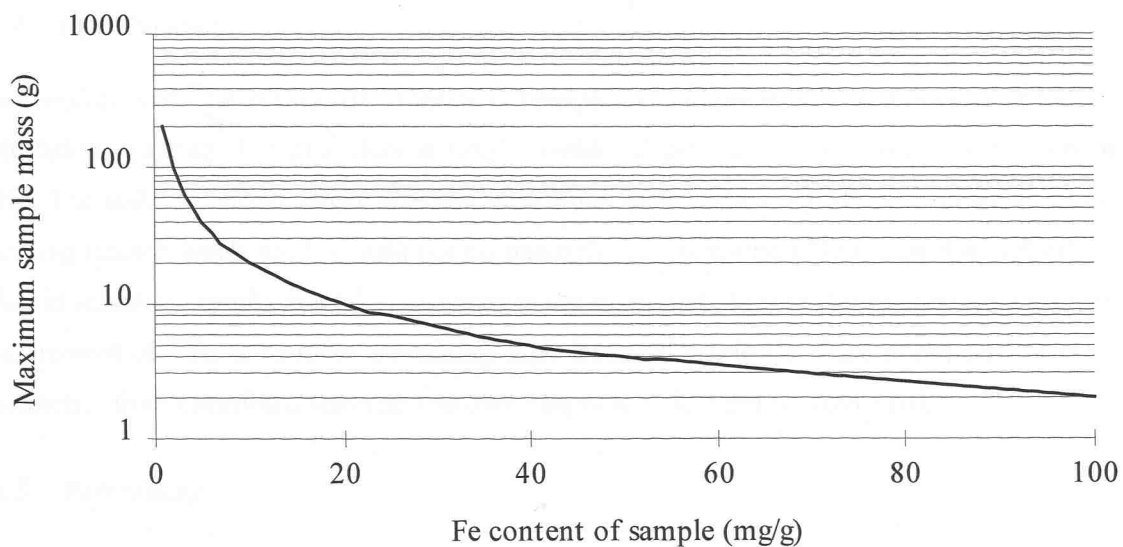


**Figure P5 :** The relationship between sample Fe content and the maximum sample mass which may be analysed

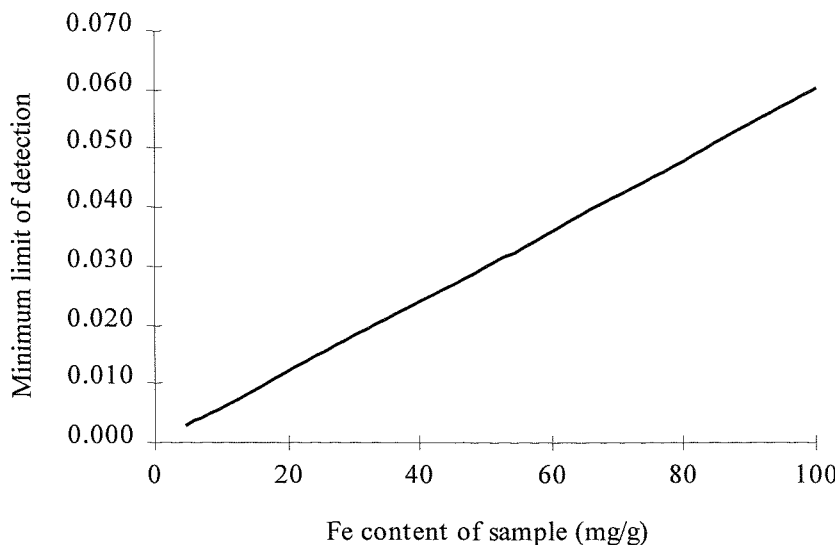


**Figure P6 : The relationship between sample Fe content and minimum achievable limit of detection in Bq/g (assuming that the maximum amount of sample permissible is analysed - see Figure 3.10)**

**(Note)** The minimum limit of detection shown above is theoretical and does not take into account the practical problems of analysing the very large maximum theoretical masses of samples

### 3.6.4 Conclusions

The dissolution of  $^{55}\text{Fe}$  as iron (III) chloride in phosphoric acid produces a source suitable for liquid scintillation counting. The procedure is simple, rapid and produces a colourless solution, which is stable. The stability allows larger numbers of samples to be dark-adapted and counted in batches. Resulting quench levels are low with correspondingly high counting efficiencies. Careful selection of liquid scintillant results in total Fe loadings in the scintillant of up to 200 mg permitting sensitive measurement of  $^{55}\text{Fe}$  in samples containing high levels of stable Fe. Care is required to prevent interference from chemiluminescence and dark-adaption of the sample is essential.

### 3.6.5 References

Cosilito F.J., Cohen N. and Petrow H.G. (1968). Simultaneous determination of iron-55 and stable iron by liquid scintillation counting. *Anal. Chem.*, **40** (1), 213-215.

Currie L.A. (1968). Limits of qualitative detection and quantitative determination. *Anal. Chem.*, **40** (3), 586-593.

De Filippis S. (1991).  $^{55}\text{Fe}$  and  $^{59}\text{Fe}$ : A qualitative comparison of four methods of liquid scintillation activity analysis. *Radioact. Radiochem.*, **2**(2), 14-21.

Eakins J.D. and Lally D.A. (1965). The simultaneous determination of iron-55 and iron-59 in blood by liquid scintillation counting. AERE-R 4945, Harwell, UK.

Gibson J.A.B. and Marshall M. (1972). The counting efficiency of  $^{55}\text{Fe}$  and other electron capture nuclides in liquid scintillator solutions. *Int. J. Appl. Radiat. Isot.*, **23**, 321-328.

Hoang C.T., Servant J. and Labeyrie J. (1968). Evaluation de la retombée mondiale du  $^{55}\text{Fe}$  à la suite des essais nucléaires dans l'atmosphère des années 1961 et 1962. *Health Phys.*, **15**, 323-332.

König W., Schupfner R. and Schüttelkopf H. (1995). A fast and very sensitive LSC procedure to determine Fe-55 in steel and concrete. *J. Radioanal. Nucl. Chem., Articles*, **193(1)**, 119-125.

Yonezawa C., Hoshi M. and Tachikawa E. (1985). Determination of specific activity of iron-55 by spectrophotometry and liquid scintillation counting with bathophenanthroline complex. *Anal. Chem.*, **57**, 2961-2965.

### 3.6.6 Addendum to Paper : An Optimised Method for the Measurement of $^{55}\text{Fe}$ Using Liquid Scintillation Analysis

#### 3.6.6.1 The relationship between $^{55}\text{Fe}$ counting efficiency and sample quench level (SQPE)

In the paper, relationships were found between the mass of stable Fe, the scintillant-to-phosphoric acid ratio and the  $^{55}\text{Fe}$  counting efficiencies. However, having optimised the method for routine measurement of  $^{55}\text{Fe}$  it is more useful to know the relationship between the  $^{55}\text{Fe}$  counting efficiency and the quench level of the sample as measured by the sample Spectral Quench Parameter (External) or SQPE value (Section 2.2.2.4). The quench level of each individual sample may then be determined at the start of the measurement and this can be used to calculate the  $^{55}\text{Fe}$  counting efficiency for that sample.

#### 3.6.6.2 Determination of sample SQPE

A solution of 200mg/ml Fe solution was prepared by dissolving an accurately weighed mass of  $\text{Fe}_2\text{O}_3$  (Johnson Matthey – Spectroscopic grade material) in 6M HCl and diluted with water to achieve the required concentration. 0.05, 0.10, 0.15, 0.20, 0.25, 0.50 and 1.0ml of this solution was pipetted into seven 50ml beakers along with 200Bq of  $^{55}\text{Fe}$  to give solutions of  $^{55}\text{Fe}$  containing 10, 20, 30, 40, 50, 100 and 200mg of stable Fe. The solutions were evaporated to incipient dryness and dissolved in the minimum of 2M  $\text{H}_3\text{PO}_4$  to produce a colourless solution. The solution was transferred along with 1ml of water washings to a 22ml polythene scintillation vial. 10ml of Ultima Gold AB scintillant was added and the samples were counted on a Wallac 1220 Quantulus liquid scintillation counter as described in Section 3.6.2.2. The SQPE and count rate were recorded for each sample and used to determine the relationship between the two parameters.

#### 3.6.6.3 Results & Discussion

Table 3.1 : Counting efficiency and quench levels for a range of Fe loadings

Mass of stable Fe	Volume of $\text{H}_3\text{PO}_4$ required	SQPE	Counting efficiency for $^{55}\text{Fe}$
10	1000	798.82	45.0
20	1500	780.44	40.5
30	2000	774.23	36.5
40	2500	759.91	32.4
50	2500	748.61	29.2
100	3500	687.29	15.5
200	3500	682.18	12.4

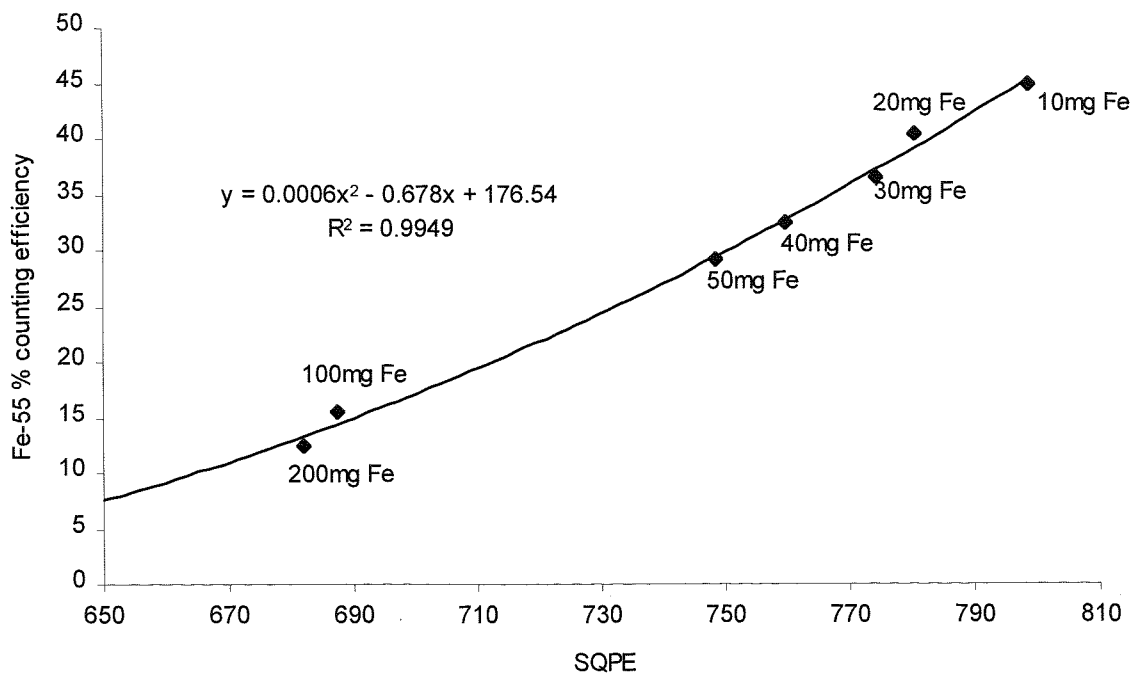


**Figure 3.6 : Relationship between <sup>55</sup>Fe counting efficiency and SQPE for the H<sub>3</sub>PO<sub>4</sub>-Ultima Gold AB counting system**

A fairly rapid decline in <sup>55</sup>Fe counting efficiency corresponds with decreasing SQPE value and this reflects the increase in stable Fe loading (Figure 3.6). The relationship between <sup>55</sup>Fe efficiency and SQPE is given by the equation

$$E = 0.000643(SQPE)^2 - 0.67799(SQPE) + 176.54$$

Where E is the percentage counting efficiency for <sup>55</sup>Fe.

Even at low SQPE values it is possible to measure <sup>55</sup>Fe, however for routine measurement SQPE values of < 680 would indicate that unacceptably high sample quench was occurring and that the measurement should be rejected.

## 3.7 Counting precipitates by liquid scintillation analysis

### 3.7.1 Introduction

Many radiochemical separations employ gravimetric analysis of a stable element following chemical purification to determine the chemical recovery of a radioisotope. It is desirable to count the precipitate produced in the gravimetric determination directly, without any further chemical treatment that may result in further loss of the analyte. Counting of solid samples by liquid scintillation counting may be achieved in two ways. An insoluble solid may be suspended in a liquid scintillation gel producing a heterogeneous mixture. The gel is formed either using a commercially available specialised cocktail (such as Optiphase MP scintillant) that will form a gel when mixed with water or alternatively by mixing the sample with fine silica flour prior to adding the scintillant. As the analyte is not intimately in contact with the scintillant cocktail, the counting efficiencies achieved in heterogeneous counting are generally lower than would normally be expected with homogeneous mixing of the sample and scintillant cocktail. In heterogeneous counting, it is critical that the sample is finely divided to prevent settling during counting.

Alternatively certain solids are soluble in the organic solvent base of scintillant cocktails and may dissolve to produce a homogeneous sample. Such sources tend to be more stable and give the highest counting efficiencies as there is no water or acid present to cause chemical quench. Compounds relevant to this study that may be used for gravimetric yield determination and which are soluble in commercial scintillant cocktails are shown in Table 3.2.

**Table 3.2: Compounds used for gravimetric determination of stable elements of interest**

Compound	Analyte	Empirical formula	Gravimetric factor
Nickel pyridine thiocyanate	$^{63}\text{Ni}$	$[\text{Ni}(\text{C}_5\text{H}_5\text{N})_4](\text{SCN})_2$	8.403
Strontium carbonate	$^{90}\text{Sr}$	$\text{SrCO}_3$	3.328
TPAR*(Re)	$^{99}\text{Tc}$ (Re proxy)	$(\text{C}_6\text{H}_5)_4\text{AsReO}_4$	3.402

\*Tetraphenyl arsonium perrhenate

With the exception of  $\text{SrCO}_3$ , the precipitates in Table 3.2 are based on an organic precipitant and are highly soluble in commercial scintillant cocktails. All of the precipitates are suitable for gravimetric determination of the stable analogue of the isotope of interest.  $\text{SrCO}_3$  is insoluble in scintillants but is readily dissolved in dilute acid prior to Cerenkov counting (Section 3.8).

### 3.7.2 Counting $^{63}\text{Ni}$ as the Ni-pyridine thiocyanate complex

Harvey and Sutton (1970) noted that Ni could be precipitated as a pale blue nickel pyridine thiocyanate. The precipitation of Ni as the pyridine thiocyanate complex produces a crystalline

precipitate with a gravimetric factor of 8.403. The high gravimetric factor means that the precipitate may be handled easily and weighed accurately even at low Ni spiking levels of 5mg. The precipitate, if oven-dried, is difficult to dissolve directly into commercially available, environmentally friendly liquid scintillation cocktails. This is overcome by first drying the Ni-pyridine thiocyanate in a vacuum dessicator and then slurring the precipitate with 1ml of water.

The counting efficiency for  $^{63}\text{Ni}$  was determined as 71% using an optimised window of 10-400. The counting efficiency did not vary with precipitate mass between 16 and 40 mg (Ni masses between 2-5mg) comparing well with other methods of source preparation (Table 3.3). The source was stable for a period of at least one week. The counting efficiency may also be determined by counting the Ni-pyridine thiocyanate in scintillant, spiking with a known amount of  $^{63}\text{Ni}$  and recounting. The difference in count rates can be used to determine the counting efficiency. It was found that this approach was suitable even though the  $^{63}\text{Ni}$  associated with the pyridine thiocyanate is in a different chemical form to the  $^{63}\text{Ni}$  spike. The limit of detection (as defined by Currie, 1968) with an instrument background of 2.0 cpm and a count time of 60 mins, is 13 mBq/sample.

**Table 3.3 : Comparison of LSC counting efficiencies for some Ni complexes**

Ni-complex	Counting efficiency (5mg Ni)
Ni-dimethylglyoxime	< 5%
Ni-pyridine thiocyanate	71 %
Ni-amine	~70 % <sup>1</sup>
Ni(II) in dilute HCl	69 % <sup>2</sup>

<sup>1</sup>Data from Kojima and Furukawa, 1985

<sup>2</sup>Ni in 1ml 1M HCl, 2ml water and 15ml Gold Star scintillant

All other data determined in this study

To improve the efficiency of transfer of precipitate, the filter membrane can be added to the cocktail. Membrane filters become translucent in scintillant cocktail and have little detrimental effect on the counting efficiency. Even with this pretreatment, the sample only slowly dissolves into scintillant and sufficient time must be allowed to permit total dissolution. To determine the rate of dissolution from the filter and the effect of the filter on counting efficiency, 12 samples were prepared containing 2mg Ni and 200 Bq of  $^{63}\text{Ni}$ . The Ni was precipitated as Ni pyridine thiocyanate using the procedure detailed above. The precipitate was filtered onto a previously weighed polycarbonate membrane filter, washed and dried in a vacuum dessicator overnight. The mass of the precipitate was determined and the chemical recovery calculated. A mean chemical recovery of 85% was obtained. Six samples and filters were then transferred directly into scintillation vials. 0.5ml of toluene was added and the samples thoroughly shaken. 10ml Gold Star scintillant was then added and the samples counted repeatedly over a period of 30 hours. The remaining six samples were removed from their filters and transferred into pre-weighed scintillation vials. The mass of

precipitate was weighed. A mean recovery of 57% was obtained showing the extent of losses incurred through the transfer of the precipitate from the filter membrane to the vial. 0.5ml of toluene was added along with 10ml of Gold Star scintillant and the samples were again counted repeatedly over a 30 hour period. All measurements were made using a Wallac 1220 Quantulus liquid scintillation counter. The mean count rate, corrected for chemical recovery was calculated at various times for all the samples. The mean counting efficiency for samples with and without filters for each time was calculated along with the standard deviation of the six measurements (Figure 3.7).

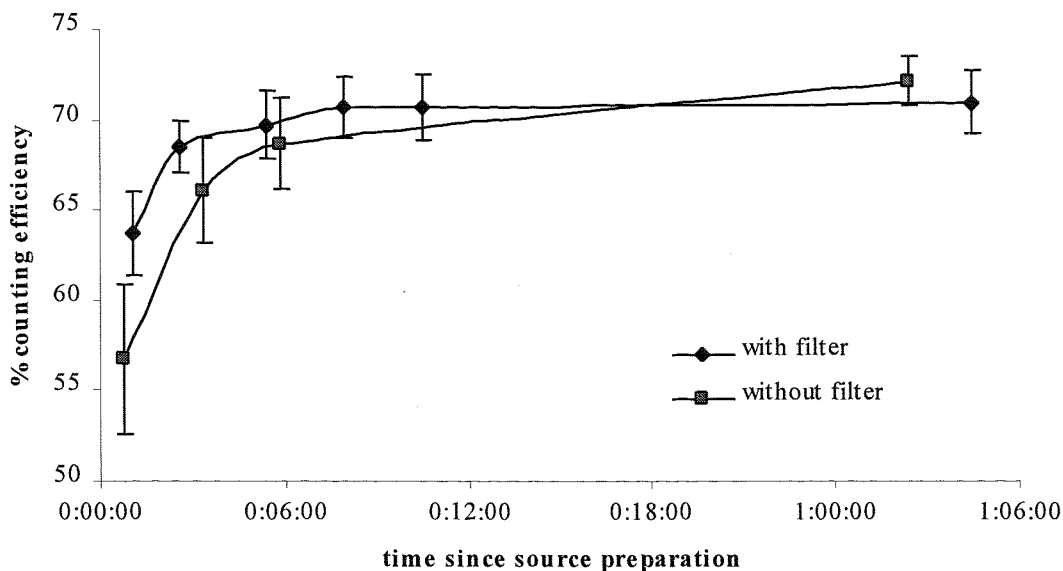
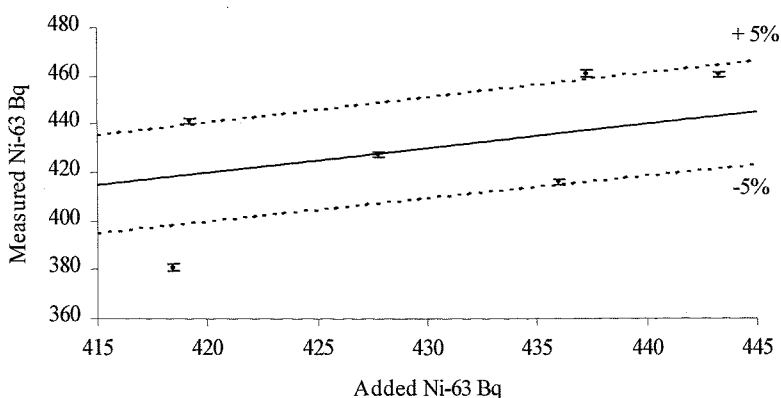


Figure 3.7 : Counting efficiency versus time (days:hours:minutes) for  $^{63}\text{Ni}$ -pyridine thiocyanate complex

Although the inclusion of the filter significantly improved the percentage of the sample that was transferred to the vial, the presence of the filter membrane had little effect on the overall counting efficiency. However, the dissolution of the complex into the scintillant was apparently slow and the time required for a stable solution to be formed was approximately 9 – 12 hours.

A set of test samples were prepared by spiking 10ml of dilute HCl with a known activity of  $^{63}\text{Ni}$  and 3mg of stable Ni. The pH of the solution was adjusted to pH 7 with ammonia solution. 0.5g of ammonium thiocyanate was added and the solution was heated to around 80°C, 1.5ml of pyridine was added and the mixture allowed to stand for 30 minutes. The pale blue precipitate that formed was filtered onto a 0.45  $\mu\text{m}$  polycarbonate membrane filter. The precipitate was washed and dried at 50°C overnight. The precipitate was carefully removed from the filter and transferred to a tared 20ml polythene scintillation vial. The scintillation vial was weighed to determine the mass of nickel pyridine thiocyanate. The precipitate was slurried in 1ml of water and 15ml Gold Star scintillant was added. The sample was then counted on the Wallac 1220 ‘Quantulus’ to determine  $^{63}\text{Ni}$  activity.

Chemical recovery, as determined by the mass of Ni pyridine thiocyanate, varied between 50 and 86%. Most of the losses occurred in transferring the precipitate from the membrane filter to the vial with some of the precipitate remaining entrained on the filter membrane. The calculated  $^{63}\text{Ni}$  activity varied markedly from the theoretical  $^{63}\text{Ni}$  added in an unsystematic manner (Figure 3.8). Spiking of the source and recounting showed that the quench levels in all the samples was similar and no solid precipitate was observed at the bottom of the vial. The samples were left to stand for one week and then recounted. No difference was observed in the count rates between the two count times, again suggesting that the precipitate had totally dissolved. The observed variability in count rate probably results in the incomplete drying of the sample or static build-up on the vial during weighing resulting in an imprecision in the measurement of the chemical yield. However, for certain applications, the variability in measured result is sufficiently low for the procedure to be of use.



**Figure 3.8 : Analysis of standards using Ni-pyridine thiocyanate as a gravimetric yield monitor**  
Error bars are at the  $2\sigma$  confidence level. The uncertainty in the  $^{63}\text{Ni}$  added activity is  $\pm 2\%$  2 s.d.

### 3.7.3 Counting of $^{99}\text{Tc}$ as the tetraphenyl arsonium perrhenate (TPAR) complex

Final preparation of Tc sources is often achieved by co-precipitating the Tc with a precipitate of tetraphenyl arsonium perrhenate. This precipitate acts as a gravimetric yield monitor for Re (and hence Tc) and provides a source suitable for gas flow proportional counters, Geiger-Müller tubes and liquid scintillation counting (the precipitate readily dissolves in scintillant). Harvey *et al* (1991) noted that co-precipitation of the Tc may not be quantitative below a certain concentration of tetraphenyl arsonium chloride (TPAC). Although 100% Tc was co-precipitated when only 30 mg of TPAC was present, 60 mg of TPAC was required to fully precipitate the Re (total of 10 mg Re present).

The counting efficiency of  $^{99}\text{Tc}$  by liquid scintillation counting is independent of the mass of tetraphenyl arsonium perrhenate in the range of 10–60mg. Typical counting efficiencies for  $^{99}\text{Tc}$  coprecipitated with tetraphenyl arsonium perrhenate on a Packard 2250CA counter, using 10ml of Instagel scintillant, is 95%. However, although Re has been widely employed as a yield monitor for  $^{99}\text{Tc}$ , the separation chemistry must be carefully selected and optimised to ensure that Re and Tc behave in an identical manner. Even then it is debatable whether Re is totally effective as a yield monitor.

### 3.7.4 Counting $^{99}\text{Tc}$ on TEVA<sup>®</sup> resin directly by liquid scintillation counting

Many recent radiochemical separations for  $^{99}\text{Tc}$  employ the extraction of Tc onto TEVA<sup>®</sup> resin as a procedure for purification of Tc from Ru (e.g. Bohnstedt *et al*, 1998). Elution of  $^{99}\text{Tc}$  from the TEVA<sup>®</sup> resin requires strong nitric acid that must then be removed by evaporation. Eichrom Industries (pers. comm.) had suggested that the TEVA<sup>®</sup> resin containing the  $^{99}\text{Tc}$  could be added directly to scintillant and this approach was investigated further.

Water must be used to transfer the TEVA<sup>®</sup> resin from the column to the liquid scintillation vial and this is likely to have the most effect on chemical quench. Four TEVA columns, each containing 0.4g of resin, were prepared and conditioned with water. Four 5ml water samples, each containing 2Bq of  $^{99}\text{Tc}$ , were prepared and transferred to the TEVA<sup>®</sup> columns. The columns were washed with 5ml of water and all eluents were collected and checked for  $^{99}\text{Tc}$  breakthrough. Each TEVA<sup>®</sup> resin sample was then transferred to a 22ml polythene vial with a measured volume of water. One TEVA<sup>®</sup> resin sample was transferred to the vial by cutting the column close to the top of the TEVA<sup>®</sup> resin bed and ejecting the resin with air. Gold Star scintillant was then added and the samples dark-adapted for one hour. Each sample was then counted on a Wallac 1220 Quantulus liquid scintillation counter to determine the counting efficiency.

**Table 3.4 : Counting efficiencies for  $^{99}\text{Tc}$  on TEVA<sup>®</sup> added directly to liquid scintillant**

Volume H <sub>2</sub> O	Volume Gold Star scintillant	Measured cpm (full window)	Dpm $^{99}\text{Tc}$ added	% counting efficiency	SQPE
0	10.0	103.4	118.4	87.3	768.2
1.0	9.0	101.1	118.0	85.6	749.6
1.5	8.5	108.1	118.0	91.6	742.6
2.0	8.0	104.2	118.3	88.1	737.4

The counting efficiency of  $^{99}\text{Tc}$  was not noticeably affected by the increasing water content of the sample even though the measured quench level of the sample fell slightly (Table 3.4). Counting

efficiencies were high although slightly lower than for other source preparation techniques such as TPAR precipitation (Section 3.7.3) and the TOA-xylene-scintillant mixture (Section 3.2). The mixture of TEVA® resin and scintillant is stable for considerable periods of time even though the resin (which is translucent in the scintillant) settles. This suggests that the Aliquat-336 extractant is desorbed from the supporting polymer and dissolved in the scintillant cocktail.

### 3.8 Optimisation of $^{90}\text{Sr}$ measurement by Cerenkov counting

#### 3.8.1 Effect of sample volume on Cerenkov counting efficiencies of $^{90}\text{Sr}/^{90}\text{Y}$

The Cerenkov counting efficiency will depend on the vial geometry, the volume of solution within the vial and to a lesser extent for  $^{90}\text{Y}$  on the refractive index of the solution. It was assumed that the refractive index of the solution will be constant for all samples and that this would be dependent on the reagents used to elute the Sr from the Sr-resin column. Hence only the vial geometry and volume of solution were considered in the optimisation of counting conditions.

A pure  $^{90}\text{Sr}$  standard was prepared by removing the  $^{90}\text{Y}$  daughter by co-precipitation with  $\text{Fe}(\text{OH})_3$ . The supernatant containing the  $^{90}\text{Sr}$  was diluted to a known volume with dilute  $\text{HNO}_3$ . Aliquots of this solution were transferred to six 22ml polythene vials (Meridian, Epsom, UK) and five 6ml polythene vials. The aliquots were diluted to a known volume using water. A further standard was prepared from an aliquot of the  $^{90}\text{Sr}$  standard mixed with 15ml Gold Star scintillant. Background samples containing no  $^{90}\text{Sr}$  were also prepared in an identical manner. Each sample was counted three times over a period of two weeks to measure the in-growth of  $^{90}\text{Y}$ . The count rate of each measurement was plotted against  $(1-e^{-\lambda t})$  where  $\lambda$  is the decay constant for  $^{90}\text{Y}$  and  $t$  is the interval between the initial  $^{90}\text{Y}$  separation and the time of measurement. The slope of the graph was calculated to determine the  $^{90}\text{Y}$  count rate at equilibrium and the intercept of the line at  $1-e^{-\lambda t} = 0$  was calculated to determine the  $^{90}\text{Sr}$  count rate at  $t = 0$ . The counting efficiency of  $^{90}\text{Y}$  and  $^{90}\text{Sr}$  for each sample was then calculated.

The Cerenkov counting efficiency for all samples was reasonably constant for  $^{90}\text{Sr}$  at 5% and showed no relationship with the vial geometry or sample volume. The counting efficiency for  $^{90}\text{Y}$  was dependent on the vial geometry and the sample volume. For small volumes up to 4ml the counting efficiency increased with increasing volume and was higher in the 6ml vial compared to the 22ml vial. The counting efficiency of  $^{90}\text{Y}$  did fall slightly as the volume approached 5ml in a 6ml vial. For volumes greater than 10ml in a 22ml vial the  $^{90}\text{Y}$  counting efficiency was reasonably constant (Figure 3.9).

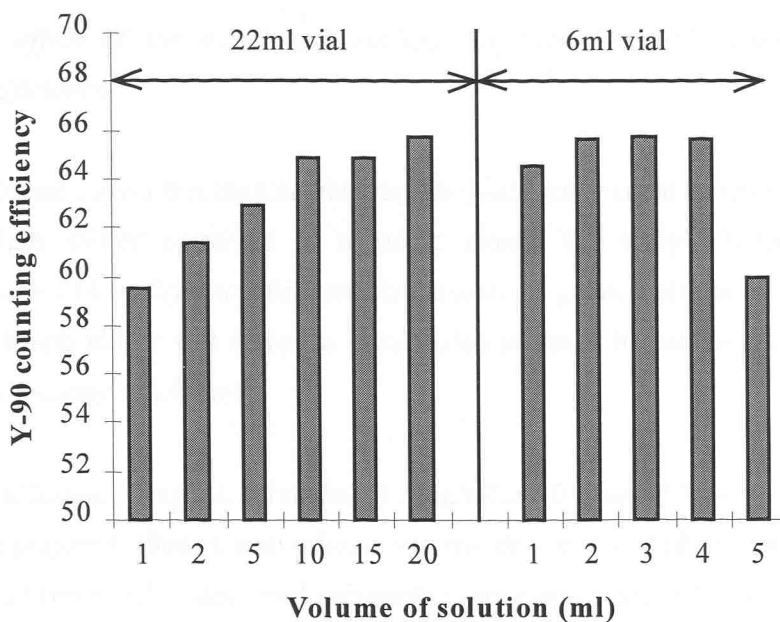


Figure 3.9 : The effect of sample volume and vial geometry on  $^{90}\text{Y}$  Cerenkov counting efficiency

Although counting efficiencies were found to increase with increasing volume in the 22ml vial background levels also increased and the corresponding figure of merit (FOM - defined as Efficiency<sup>2</sup>/background) decreased (Table 3.5).

Table 3.5 : The effect of sample volume and vial geometry on counting efficiency and background

Vial size (ml)	Volume of aqueous (ml)	$^{90}\text{Sr}$ efficiency	$^{90}\text{Y}$ efficiency	Bkg cpm	FOM
22	1	5.6	59.5	0.70	5093
	2	4.7	61.4	0.76	4961
	5	5.2	62.9	0.84	4705
	10	5.0	64.8	0.85	4966
	15	5.0	64.8	1.02	4138
	20	5.1	65.7	1.03	4205
6	1	4.6	64.5	0.62	6674
	2	4.9	65.6	0.66	6537
	3	5.0	65.8	0.64	6714
	4	5.0	65.6	0.67	6425
	5	5.8	59.9	0.77	4696
22	Std*	100	99.9	2.16	4627

\* Standard sample consisting of 0.1ml of  $^{90}\text{Sr}$  standard and 15ml Gold Star scintillant for comparison

### 3.6.2 The effect of the wavelength shifter, 7-hydroxy-4-methylcoumarin, on $^{90}\text{Y}$ Cerenkov counting efficiency

Ross (1976) had shown that the Cerenkov counting efficiency could be improved through the use of a wavelength shifter contained in a jacket around the sample (Chapter 2). 7-hydroxy-4-methylcoumarin (4-methyl-umbelliferone) had one of the greatest effects on the counting efficiency. This wavelength shifter was therefore investigated to see if its use would lead to an appreciable increase in counting efficiency.

Solutions of 2mg/ml, 1mg/ml, 0.5 mg/ml, 0.2 mg/ml and 0.1 mg/ml 7-hydroxy-4-methylcoumarin in water were prepared. 10ml of each solution was transferred to a 22ml polythene vial. 0.2ml of a pure  $^{90}\text{Sr}$  standard (prepared as described previously) was pipetted into a 6ml polythene vial and diluted to 3ml. The 6ml vial was then placed inside the 22ml vial resulting in the 6ml vial being surrounded with the wavelength shifter. Blank samples containing no  $^{90}\text{Sr}$  were prepared in an identical manner. A second set of standards were prepared using 0, 3, 6, 9 and 12ml of 0.5 mg/ml 7-hydroxy-4-methylcoumarin in the 22ml vial and 0.2ml of  $^{90}\text{Sr}$  standard diluted to 3ml in a 6ml vial. All samples were counted three times in a period of two weeks following  $^{90}\text{Y}$  separation and the  $^{90}\text{Sr}$  and  $^{90}\text{Y}$  counting efficiencies were calculated as described previously.

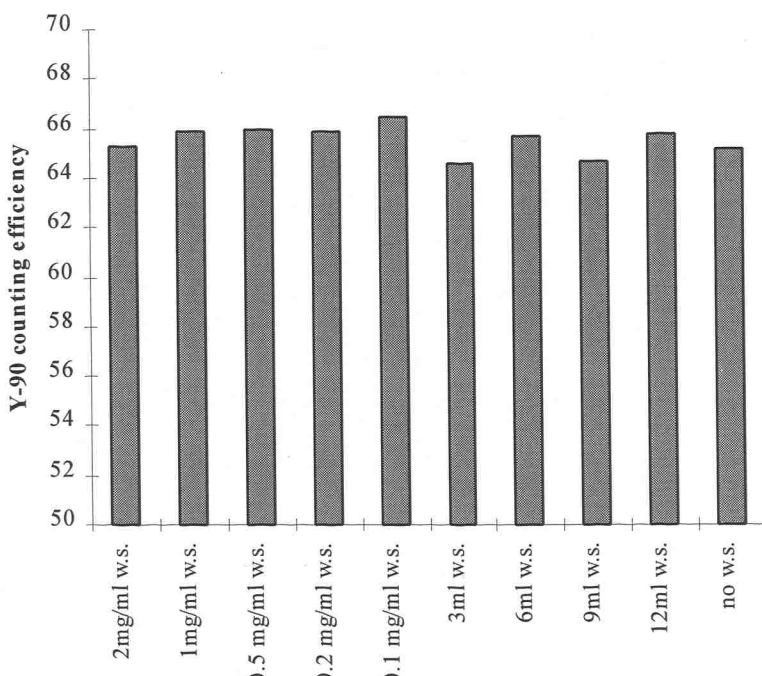


Figure 3.10 : Effect of the wavelength shifter 7-hydroxy-4-methylcoumarin on  $^{90}\text{Y}$  Cerenkov counting efficiency

Counting efficiencies for  $^{90}\text{Y}$  were not significantly affected by the presence of the wavelength shifter (Figure 3.10). The  $^{90}\text{Sr}$  counting efficiency was also unaffected. Background count rates were also similar for the samples ranging from 0.87 – 0.95 cpm (2mg/ml – 0.1 mg/ml wavelength shifter). The corresponding figures of merit were therefore also reasonably constant ranging from 4873-4372. Hence there appeared to be little advantage to the use of a wavelength shifter in the described technique. The lack of an increase in counting efficiency probably stems from the use of polythene vials instead of glass vials. As a high proportion of Cerenkov radiation is emitted in the UV region glass vials, which are effective at absorbing UV radiation, will have a significant adverse effect on the ultimate detection efficiency of the system. The use of a wavelength shifter, as described by Ross, overcame this by shifting the emitted light away from the UV region. In polythene vials this effect is non-existent hence the improvement in counting efficiency is not observed. This would also suggest that the envelope around modern photomultiplier tubes is not as an efficient absorber of UV radiation compared to the older photomultiplier envelopes.

### 3.9 Paper in preparation :

#### Simplified determination of $^{90}\text{Sr}$ activity and $^{90}\text{Sr}$ : $^{89}\text{Sr}$ ratios in low-level wastes using Cerenkov counting and mathematical deconvolution

P.E. Warwick<sup>1</sup>, I.W. Croudace<sup>1</sup>, C.J. Dale<sup>2</sup> and A.G. Howard<sup>3</sup>

<sup>1</sup>*School of Ocean & Earth Science, Southampton Oceanography Centre, European Way, Southampton, SO14 3ZH*

<sup>2</sup>*NNC Ltd, Winfrith Technology Centre, Winfrith, Dorchester, Dorset, DT2 8DH*

<sup>3</sup>*Dept. of Chemistry, University of Southampton, Southampton, SO17 1BJ*

##### 3.9.1 Abstract

The routine determination of  $^{90}\text{Sr}$  in fresh fission product wastes and environmental samples must necessarily involve an assay of the short-lived fission product  $^{89}\text{Sr}$ . The activity of  $^{89}\text{Sr}$  may significantly exceed that of  $^{90}\text{Sr}$  and any assessment of radiological risk must include  $^{89}\text{Sr}$ . The presence of significant levels of  $^{89}\text{Sr}$  may also interfere with the determination of  $^{90}\text{Sr}$  by in-growth of  $^{90}\text{Y}$ . This paper presents a straightforward method for determining both the  $^{90}\text{Sr}$  activity of a sample and the  $^{90}\text{Sr}$ : $^{89}\text{Sr}$  ratio. This is achieved by first chemically separating the Sr from the matrix elements. At this point the sample is counted as a solution using Cerenkov counting to provide  $^{89}\text{Sr}$ . After 10 days, when  $^{90}\text{Y}$  (from  $^{90}\text{Sr}$ ) has grown-in, another Cerenkov count is made which provides  $^{89}\text{Sr}$ + $^{90}\text{Y}$ . Windowing is not required, permitting the rapid set-up and calibration of the counter. A relationship between the two count-rates and the time between the two counts is used to calculate both  $^{90}\text{Sr}$  activity and isotope ratios. Derivation of the equations employed is described along with a discussion on the uncertainties associated with this approach.

##### 3.9.2 Introduction

Strontium-90 and  $^{89}\text{Sr}$  are both produced by thermal neutron fission of  $^{235}\text{U}$  and  $^{239}\text{Pu}$  and fast neutron fission of  $^{235}\text{U}$ ,  $^{238}\text{U}$  and  $^{239}\text{Pu}$  (Table P1).

**Table P1 : Cumulative percentage fission yields for  $^{89}\text{Sr}$  and  $^{90}\text{Sr}$**

Half life	Thermal neutrons			Fast neutrons		
	$^{235}\text{U}$	$^{238}\text{U}$	$^{239}\text{Pu}$	$^{235}\text{U}$	$^{238}\text{U}$	$^{239}\text{Pu}$
$^{89}\text{Sr}$	50.5 d	4.77	-	1.68	4.40	2.75
$^{90}\text{Sr}$	29.12 y	5.85	-	1.97	5.25	3.34

All data from JEF-PC, 1997

The measurement of  $^{90}\text{Sr}$  ( $t_{1/2} = 29.12$  y) in solid and liquid wastes is of considerable importance in estimating dose rates and fingerprinting of nuclear wastes. Strontium-89, with its much shorter half life of 50.5 days and a comparable fission yield to  $^{90}\text{Sr}$  will have a much higher activity than  $^{90}\text{Sr}$  in a mixture of fresh fission products. The  $^{89}\text{Sr}:\text{ }^{90}\text{Sr}$  activity ratio may approach 200:1 but it rapidly declines as the  $^{89}\text{Sr}$  decays and after one year the  $^{89}\text{Sr}:\text{ }^{90}\text{Sr}$  ratio will have fallen to near unity. The measurement of  $^{90}\text{Sr}:\text{ }^{89}\text{Sr}$  ratios therefore give an indication of the age of the fission waste being measured.

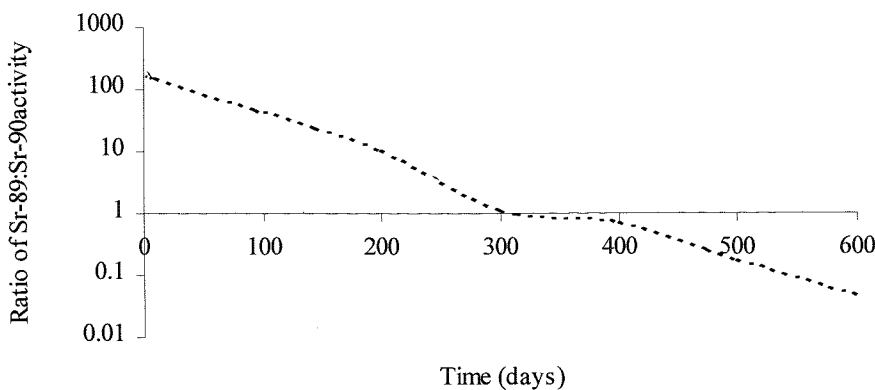


**Figure P1 : Change in  $^{89}\text{Sr}:\text{ }^{90}\text{Sr}$  ratio with time**

Both  $^{89}\text{Sr}$  and  $^{90}\text{Sr}$  are pure beta-emitting radioisotopes.  $^{90}\text{Sr}$  decays to the pure beta emitter  $^{90}\text{Y}$  ( $t_{1/2} = 2.67$  d). Although most separation chemistries for Sr separate the Sr from Y, time dependent ingrowth of  $^{90}\text{Y}$  is inevitable resulting in the Sr fraction always having a proportion of the  $^{90}\text{Y}$  daughter present. Therefore the purified Sr fraction consists of a complex mixture of  $^{89}\text{Sr}$ ,  $^{90}\text{Sr}$  and  $^{90}\text{Y}$ .

**Table P2 : Decay data for  $^{89}\text{Sr}$ ,  $^{90}\text{Sr}$  and  $^{90}\text{Y}$**

	Half life	Beta decay energy (MeV) (probability)
$^{89}\text{Sr}$	50.5 days	0.583 (0.0093%)
		1.492 (99.99%)
$^{90}\text{Sr}$	29.12 years	0.546 (100%)
$^{90}\text{Y}$ (daughter of $^{90}\text{Sr}$ )	2.67 days	0.523 (0.016%) 2.284 (99.98%)

*All data from JEF-PC, 1997*

The simultaneous determination of  $^{89}\text{Sr}$  and  $^{90}\text{Sr}$  can be achieved using a number of approaches. Randolph (1975) separated the  $^{90}\text{Y}$  from the Sr fraction and then counted the Sr fraction by Cerenkov counting. A window was set to discriminate the high-energy component of the ingrowing  $^{90}\text{Y}$  spectrum. Scintillant was then added and the sample was recounted on a liquid scintillation counter using two energy windows, one for  $^{90}\text{Sr} + ^{89}\text{Sr} + ^{90}\text{Y}$  and a second for  $^{89}\text{Sr}$  and  $^{90}\text{Y}$  alone. The scintillant-based count was used to determine the activity of  $^{90}\text{Sr}$  present, which was then used to correct the Cerenkov count and calculate the  $^{89}\text{Sr}$  activity present.

Buchtela and Tschurlovits (1975) did not separate the  $^{90}\text{Y}$  from the Sr fraction but counted the sample by Cerenkov counting with and without a wavelength shifter. The contribution from  $^{89}\text{Sr}$  and  $^{90}\text{Y}$  in the Cerenkov count could then be determined.

Dietz *et al* (1991) counted the purified Sr fraction, shortly after  $^{90}\text{Y}$  separation, on a liquid scintillation counter with two counting windows. Simultaneous equations were derived for the count-rates in these two windows, which could then be solved to give the  $^{89}\text{Sr}$  and  $^{90}\text{Sr}$  activities. It was assumed that the sample was counted within one day of  $^{90}\text{Y}$  separation and hence that the contribution from  $^{91}\text{Y}$  was negligible.

Kimura *et al* (1979) measured  $^{89}\text{Sr} + ^{90}\text{Sr} + ^{90}\text{Y}$  total activity on a low background beta counter following a two week equilibration period. The source was dissolved and the  $^{90}\text{Y}$  co-precipitated with  $\text{Fe}(\text{OH})_3$  which was counted to determine the  $^{90}\text{Y}$  (and hence  $^{90}\text{Sr}$ ) activity.  $^{89}\text{Sr}$  activity was then calculated from the two measurements by difference

If only the activity of  $^{90}\text{Sr}$  is required, the interference from  $^{89}\text{Sr}$  may be overcome by allowing the  $^{90}\text{Y}$  to achieve equilibrium with the  $^{90}\text{Sr}$ , chemically purifying and counting the  $^{90}\text{Y}$  using a technique such as liquid scintillation or gas flow proportional counting (Bajo and Keil, 1994). The presence of  $^{91}\text{Y}$  ( $t_{1/2} = 58.51$  days; thermal fission yield = 2.9%) in fresh fission product waste would seriously interfere with such an approach (Zhu *et al*, 1990) and would have to be corrected for (Bajo and Tobler, 1996).

The above techniques all require at least two counts and often require counting the sample under different conditions (with and without scintillant or wavelength shifter). Alternatively they employ windowing of the counter incurring further errors in the set-up and sample counting. An alternative simplified approach was therefore developed and optimised to reduce uncertainties inherent in the other techniques.

### 3.9.3 Methodology

The samples and standards must, as far as practical, be matrix-matched. To achieve this, the chemical separation of Sr must produce a final source of consistent composition for counting. Stable Sr (10mg) is routinely used for yield determination. Final measurement of the Sr is achieved using ICP-AES.  $^{85}\text{Sr}$  is not used as a yield monitor as it would interfere with the final Cerenkov measurement. Many methods have been reported for the effective purification of  $^{90}\text{Sr}$  including those based on the conventional precipitation of  $\text{Sr}(\text{NO}_3)_2$  with fuming nitric acid (e.g. Gregory, 1972; RADREM, 1989). However, this technique is relatively slow, difficult to scale-up for large sample throughput and potentially hazardous. A method was therefore developed (Warwick *et al*, 1998) whereby  $^{90}\text{Sr}$  was purified using the commercially available Sr resin (supplied by Hichrom, UK). The resin consists of 4,4'(5') bis(*tert*-butylcyclohexano)-18-crown-6 dissolved in octan-1-ol and supported on an inert Amberlite XAD-7 or Amberchrom CG71 support (Horwitz *et al*, 1991).  $^{90}\text{Sr}$  purification was achieved using a method described previously. A standard solution of  $^{90}\text{Sr}$  (in equilibrium with its  $^{90}\text{Y}$  daughter) was passed onto a 4 x 0.7cm Sr resin column in 8M  $\text{HNO}_3$ -0.5M  $\text{Al}(\text{NO}_3)_3$ . The column was washed with 8M  $\text{HNO}_3$  to remove all the  $^{90}\text{Y}$  and the  $^{90}\text{Sr}$  was eluted with water. The time of the last 8M  $\text{HNO}_3$  wash was recorded as  $t = 0$ . The purified  $^{90}\text{Sr}$  solution was then used to prepare a range of samples with differing  $^{90}\text{Sr}$  activity. Samples were also spiked with varying amounts of  $^{89}\text{Sr}$ . The final volume of each sample was adjusted to 10ml in a 22ml polythene scintillation vial giving a range of samples containing between 30 and 140 Bq of  $^{90}\text{Sr}$  and with  $^{90}\text{Sr}$ : $^{89}\text{Sr}$  ratios of 0.005 to 55. Samples were counted for 20 minutes directly following  $^{90}\text{Y}$  separation and again after 10 days on a Wallac 1220 ‘Quantulus’ low-level liquid scintillation counter. The two counts obtained were then used to calculate the  $^{90}\text{Sr}$ : $^{89}\text{Sr}$  ratio and  $^{90}\text{Sr}$  activities. The background count-rate was measured on 10ml 0.1M  $\text{HNO}_3$  as 0.97 cpm. The  $^{89}\text{Sr}$ ,  $^{90}\text{Sr}$  and  $^{90}\text{Y}$  counting efficiencies were measured as 38, 3.8 and 63% respectively.

### 3.9.4 Discussion

#### 3.9.4.1 Calculation of $^{90}\text{Sr}$ : $^{89}\text{Sr}$ ratios and $^{90}\text{Sr}$ activity

Cerenkov counting provides several advantages over other methods for the simultaneous determination of  $^{89}\text{Sr}$  and  $^{90}\text{Sr}$  (via  $^{90}\text{Y}$ ).

- It is more rapid than techniques based on a combined  $^{89}\text{Sr}$ ,  $^{90}\text{Sr}$  and  $^{90}\text{Y}$  measurement followed by the chemical separation of Y and separate measurement of  $^{90}\text{Y}$ .
- It is also not affected by the presence of  $^{91}\text{Y}$ .
- The use of Cerenkov-only counting of a single sample solution reduces the uncertainties of the measurement.

Some published techniques assume that the counting efficiency for  $^{90}\text{Sr}$  in Cerenkov counting is negligible. Although the counting efficiency for  $^{90}\text{Sr}$  by Cerenkov counting is low, it is not zero. Hence the count-rate determined by extrapolation of the in-growth curve to  $t=0$  originates from both  $^{89}\text{Sr}$  and  $^{90}\text{Sr}$ . For high levels of  $^{90}\text{Sr}$  and low levels of  $^{89}\text{Sr}$  this can lead to significant errors in the final activity calculation. Secondly, measured count-rates at intervals following separation of  $^{90}\text{Y}$  will not only represent the increase in activity due to  $^{90}\text{Y}$  in-growth, but will also include the decaying  $^{89}\text{Sr}$ . There will therefore be a deviation from the expected in-growth curve, the magnitude of which will depend on the ratio of  $^{89}\text{Sr}$  to  $^{90}\text{Sr}$  present in the original sample.

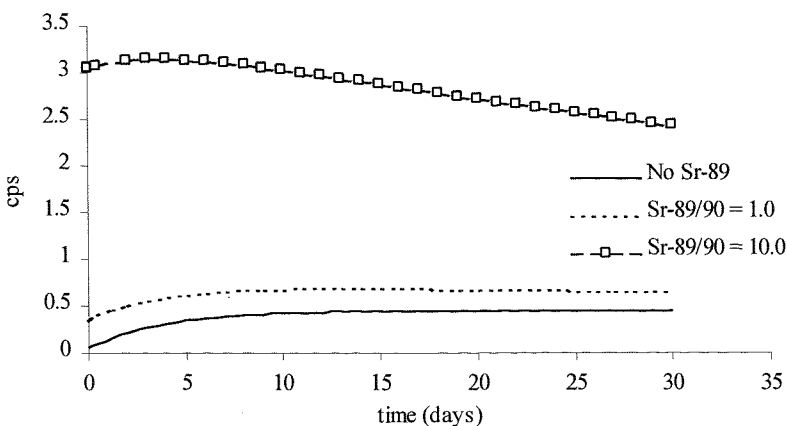


**Figure P2 : Variation in count-rate with time for samples containing  $^{90}\text{Sr}$  and  $^{89}\text{Sr}$ .**

$^{90}\text{Y}$  separated from  $^{90}\text{Sr}$  at  $t=0$ . Results calculated for 1Bq  $^{90}\text{Sr}$  mixed with variable quantities of  $^{89}\text{Sr}$ . Note that with no  $^{89}\text{Sr}$  present the curve rises exponentially reaching a maximum as  $^{90}\text{Y}$  attains equilibrium with the  $^{90}\text{Sr}$ . When  $^{89}\text{Sr}$  is introduced the curve rises, reaches a maximum and then starts to decline as the  $^{89}\text{Sr}$  decays. This decay would introduce significant errors in the calculated  $^{90}\text{Y}$  activity.

Although the presence of  $^{89}\text{Sr}$  adversely affects the calculation of  $^{90}\text{Sr}$  activity via  $^{90}\text{Y}$  in-growth, the deviation of observed counts from the expected in-growth curve for  $^{90}\text{Y}$  can be used to estimate the amount of  $^{89}\text{Sr}$  present in the sample and calculate a corrected  $^{90}\text{Sr}$  activity. By counting the sample twice over a period of two weeks by Cerenkov counting it is possible to determine both the  $^{89}/^{90}$  ratio and the  $^{90}\text{Sr}$  activity. It can be shown that the variation between two counts will be dependent on the time interval between the two counts and the time of  $^{90}\text{Y}$  separation and the ratio of  $^{89}\text{Sr}$  to  $^{90}\text{Sr}$ . The ratio of count-rates obtained at the two times can be compared against factors derived for known  $^{90}\text{Sr}$  activities and  $^{89}\text{Sr}$ : $^{90}\text{Sr}$  ratios and a best-fit analysis performed to obtain absolute values (Sutherland, 1988). Alternatively, simultaneous equations can be written for both the  $^{90}\text{Sr}$ : $^{89}\text{Sr}$  ratio and the  $^{90}\text{Sr}$  activity at both times and solved to give absolute values. Such simultaneous equations have been derived to calculate both the  $^{89}\text{Sr}$ : $^{90}\text{Sr}$  ratio and the  $^{90}\text{Sr}$  activity from two counts (Regan and Tyler, 1976) and multiple counts (Broadway and Guy, 1984). In this paper these equations are incorporated into a spreadsheet in order to perform the calculations readily. The spreadsheet also calculates the propagated uncertainties as well showing individual stage uncertainties.

One form of the equation is shown below

[eqn I]

$$\frac{A_{90}}{A_{89}} = \frac{(e^{-\lambda_2 t_1} \times E_{89}) - \frac{c_1}{c_2} (e^{-\lambda_2 t_2} \times E_{89})}{\frac{c_1}{c_2} [(1 - e^{-\lambda_1 t_2}) E_Y + E_{90}] - [(1 - e^{-\lambda_1 t_1}) E_Y + E_{90}]} \quad (1)$$

where      A =      Activity in Bq  
 $\lambda_1$  =      Decay constant for  $^{90}\text{Y}$   
 $\lambda_2$  =      Decay constant for  $^{89}\text{Sr}$   
 $E_{89/90/\text{Y}}$  =      Cerenkov counting efficiency for  $^{89}\text{Sr}$ ,  $^{90}\text{Sr}$  and  $^{90}\text{Y}$  respectively  
 $c_1$  and  $c_2$  =      count-rate at  $t_1$  and  $t_2$  (full window)

As windowing is not used, the total count-rate over a full energy range is recorded thereby improving the counting statistics of the measurement. Uncertainties are also minimised by counting twice using an identical counting regime.

Although two measurements at any interval following  $^{90}\text{Y}$  separation can be used, the deviation between count-rates observed with no  $^{89}\text{Sr}$  present and with  $^{89}\text{Sr}$  present are greatest when certain count times are chosen. To maximise the sensitivity of the technique for determining  $^{89}\text{Sr}$  and  $^{90}\text{Sr}$  it is desirable to count at these times. The maximum deviation in count-rates observed in the presence of  $^{89}\text{Sr}$  is observed when the samples are counted shortly after  $^{90}\text{Y}$  separation and then again after at least 10 days (Figure P3)

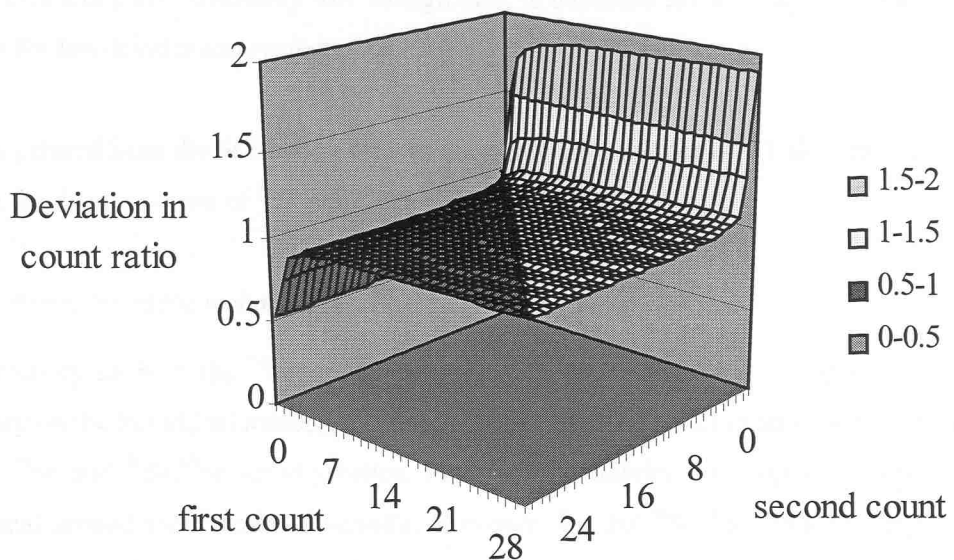


**Figure P3 : Difference between ratio of Sr-89/90 = 0 and Sr-89/90 = 0.1 for different measurement intervals.**

The theoretical Cerenkov count-rate for a sample containing no  $^{89}\text{Sr}$  ( $S_1$ ) and one with an 89/90 ratio of 0.1 ( $S_2$ ) were calculated at increasing intervals following  $^{90}\text{Y}$  separation. The ratios of count-rates at different times  $S_{1t=1}/S_{1t=2}$  and  $S_{2t=1}/S_{2t=2}$  were calculated for both samples. The ratio  $S_{1t=1}/S_{1t=2} \times S_{2t=2}/S_{2t=1}$  was then calculated and is plotted above. The plot shows the measurement times at which the greatest deviation in ratio occurs i.e. with measurements being performed straight after  $^{90}\text{Y}$  separation and at ten days following  $^{90}\text{Y}$  separation. If measurements are made at these two time intervals the greatest sensitivity for  $^{89}\text{Sr}$  determination is achieved.

The  $^{90}\text{Sr}$  activity may be determined using equation II

[eqn II]

$$A_{90} = (c_1 - \frac{k_2 c_2}{k_4}) \times \left( \frac{1}{k_1} - \frac{k_4}{k_2 k_3} \right)$$

where

$$k_1 = \left[ (1 - e^{-\lambda_1 t_1}) E_y + E_{90} \right]$$

$$k_2 = e^{-\lambda_2 t_1} \times E_{89}$$

and  $k_3$  and  $k_4$  are similar to  $k_1$  and  $k_2$  but for time  $t_2$

The mathematical technique, as described above, is equally applicable to conventional liquid scintillation counting or any other form of beta counting following substitution of the appropriate counting efficiencies. However, as  $^{90}\text{Sr}$  will count with a much higher counting efficiency by liquid scintillation counting, the deviations in count-rates caused by the  $^{89}\text{Sr}$  decay are less pronounced and the technique is therefore less sensitive to low levels of  $^{89}\text{Sr}$ . Cerenkov counting, with its low  $^{90}\text{Sr}$

counting efficiency and inherently low background, is therefore the most appropriate measurement technique for low-level measurements.

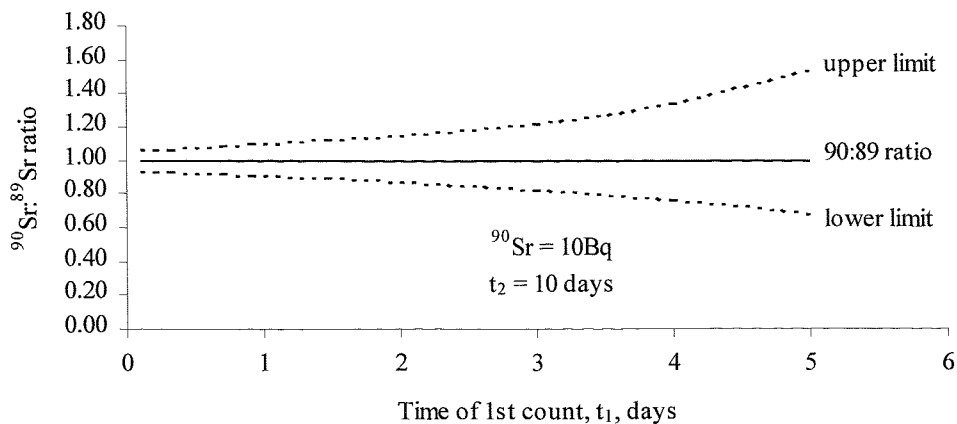
As Y is separated from the Sr fraction prior to counting, the presence of  $^{91}\text{Y}$  does not interfere in any way with the determination of  $^{89}\text{Sr}$  and  $^{90}\text{Sr}$ .

### 3.9.4.2 *Precision of the technique*

The uncertainty on both the  $^{90}\text{Sr}$  activity and  $^{90}\text{Sr}:\text{ }^{89}\text{Sr}$  ratio can be calculated by propagating the uncertainty on the individual measured counts. The calculations result in an upper and lower limit to both the  $^{90}\text{Sr}$  and  $^{90}\text{Sr}:\text{ }^{89}\text{Sr}$  activity ratios. For the  $^{90}\text{Sr}$  activity, the upper and lower limits are symmetrical around the calculated activity. However, for the  $^{90}\text{Sr}:\text{ }^{89}\text{Sr}$  ratio, the upper and lower limits are asymmetric around the calculated ratio.

The uncertainty on the  $^{90}\text{Sr}$  activity measurement is dependent on the  $^{90}\text{Sr}$  activity, the elapsed time between the two counts ( $\Delta t$ ) and the ratio of  $^{89}\text{Sr}$  to  $^{90}\text{Sr}$ . For short  $\Delta t$  the corresponding uncertainty is high. As  $\Delta t$  increases the uncertainty falls until for  $\Delta t$  greater than 10 days the uncertainty only slightly decreases with increasing time. The uncertainty of the  $^{90}\text{Sr}$  activity measurement also increases with decreasing  $^{90}\text{Sr}:\text{ }^{89}\text{Sr}$  ratio (Figures P4 and P5).

(a)



(b)

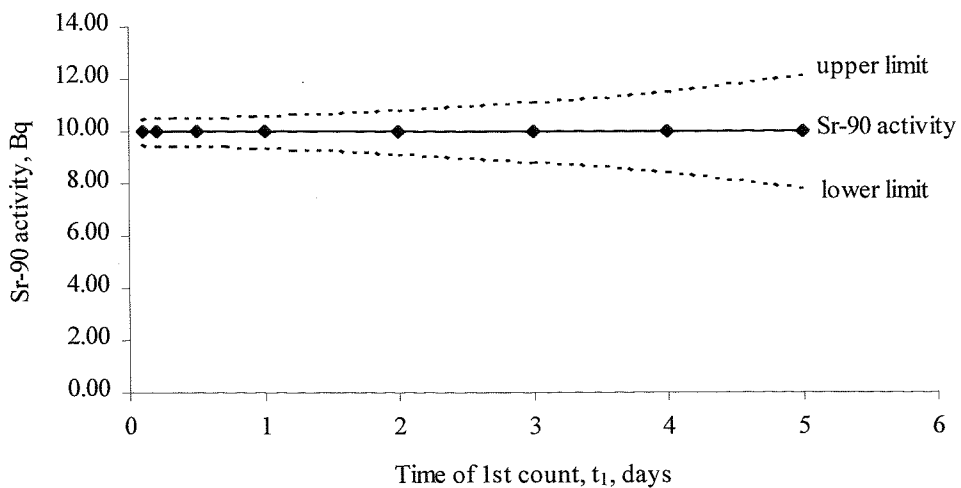


**Figure P4 : Dependence of uncertainty in (a)  $^{90}\text{Sr} : ^{89}\text{Sr}$  ratio and (b)  $^{90}\text{Sr}$  activity on the time of the 1<sup>st</sup> count,  $t_1$ .**

*In all cases the 2<sup>nd</sup> count is at  $t_2 = 10$  days. Count time 20 minutes.  $^{90}\text{Sr}$  activity = 10Bq*

The uncertainty on the  $^{90}\text{Sr} : ^{89}\text{Sr}$  ratio is dependent on the ratio present and follows a hyperbolic relationship. Ratios of between 0.5 and 10 can be measured with a relatively low uncertainty but errors increase sharply outside this range (Figure P5 b).

The uncertainty on the  $^{90}\text{Sr}$  activity increases as the ratio of  $^{90}\text{Sr} : ^{89}\text{Sr}$  decreases. The relative magnitude of this effect does not vary with  $^{90}\text{Sr}$  activity greater than 1 Bq. Below this activity the counting statistical uncertainty is significant compared to the uncertainty introduced by the presence of  $^{89}\text{Sr}$ . Hence the overall uncertainty is less dependent on the  $^{90}\text{Sr} : ^{89}\text{Sr}$  ratio (Figure P5 c).

The uncertainty on the  $^{90}\text{Sr} : {}^{89}\text{Sr}$  ratio is highly dependent on the activity of  $^{90}\text{Sr}$  present. For a given ratio, the uncertainty decreases with increasing activity as the counting statistical uncertainty decreases. The uncertainty increases significantly with increasing  $^{90}\text{Sr} : {}^{89}\text{Sr}$  ratio but this increase becomes smaller with increasing total activity.

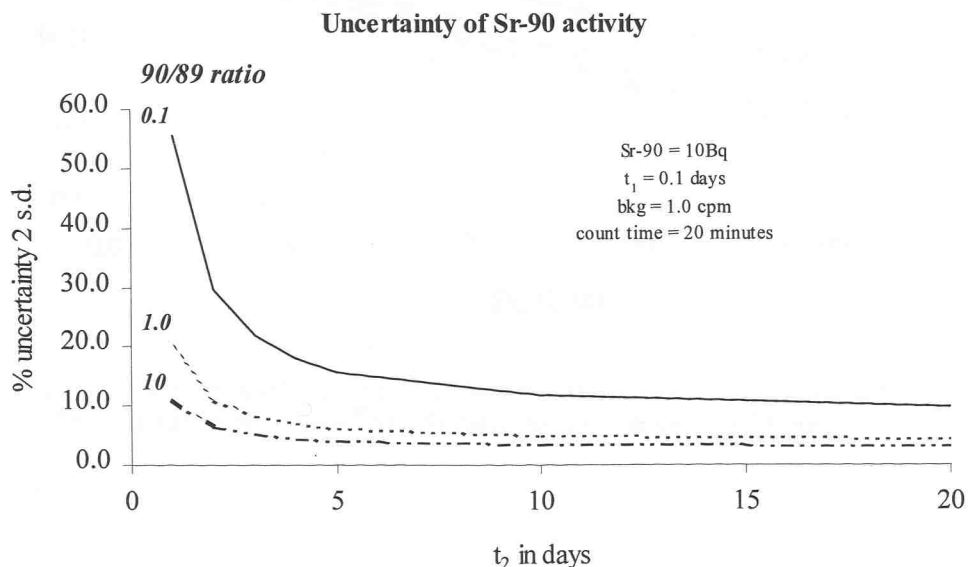


**Figure P5a : The variation of uncertainty in  $^{90}\text{Sr}$  activity with time of 2<sup>nd</sup> count,  $t_2$**

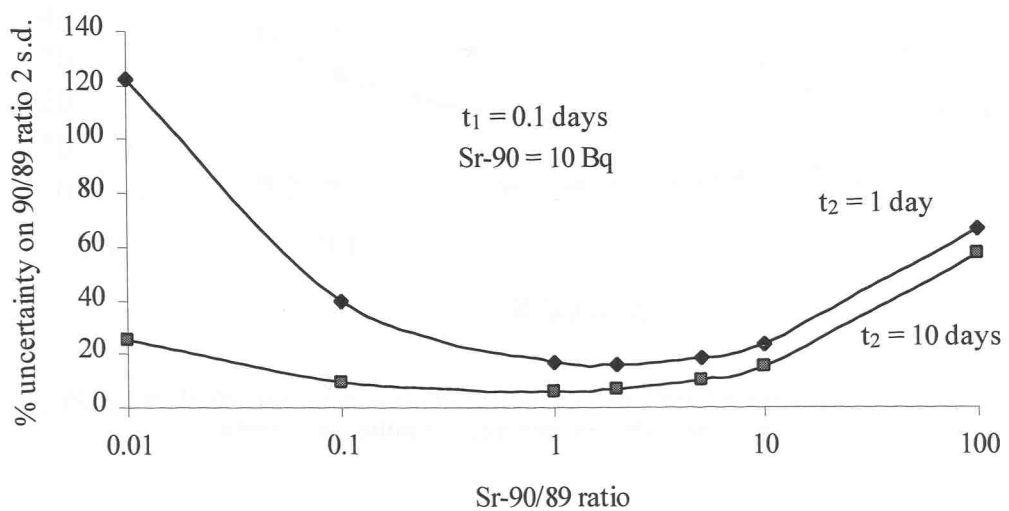


**Figure P5b : The dependence of uncertainty in  $^{90}\text{Sr} : {}^{89}\text{Sr}$  ratio (upper limit) with ratio and time of 2<sup>nd</sup> count,  $t_2$ .**

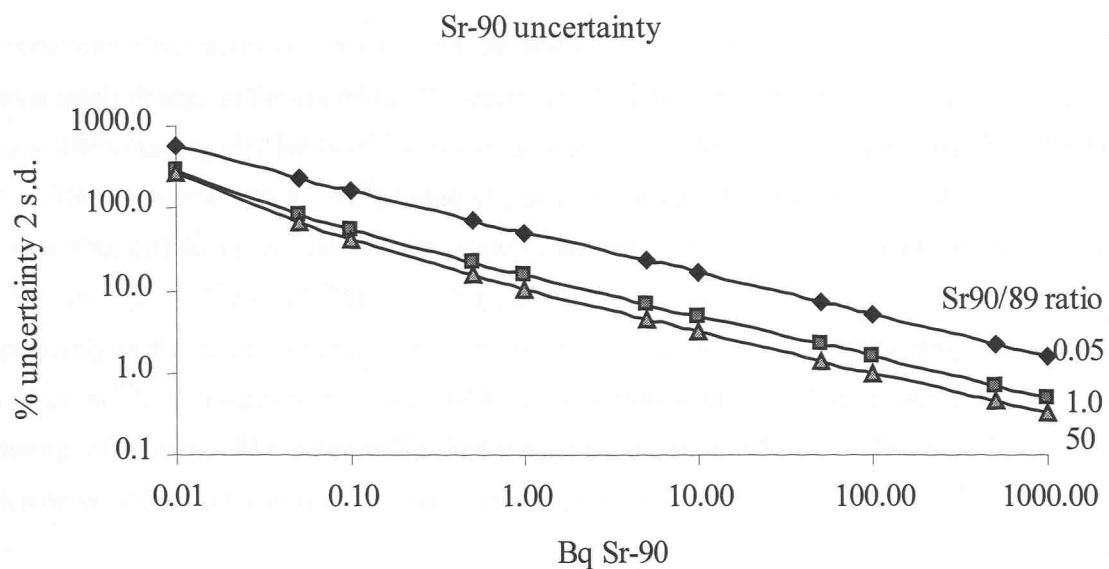


Figure P5c : The variation of uncertainty in  $^{90}\text{Sr}$  activity with the magnitude of the activity and the  $^{90}\text{Sr}:\text{ }^{89}\text{Sr}$  ratio All count times are 20 minutes

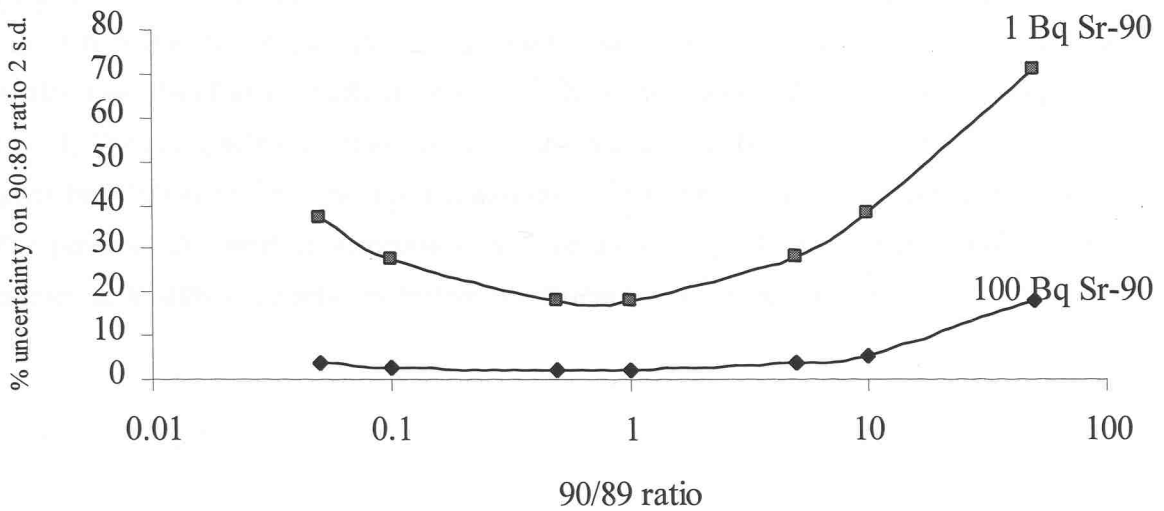
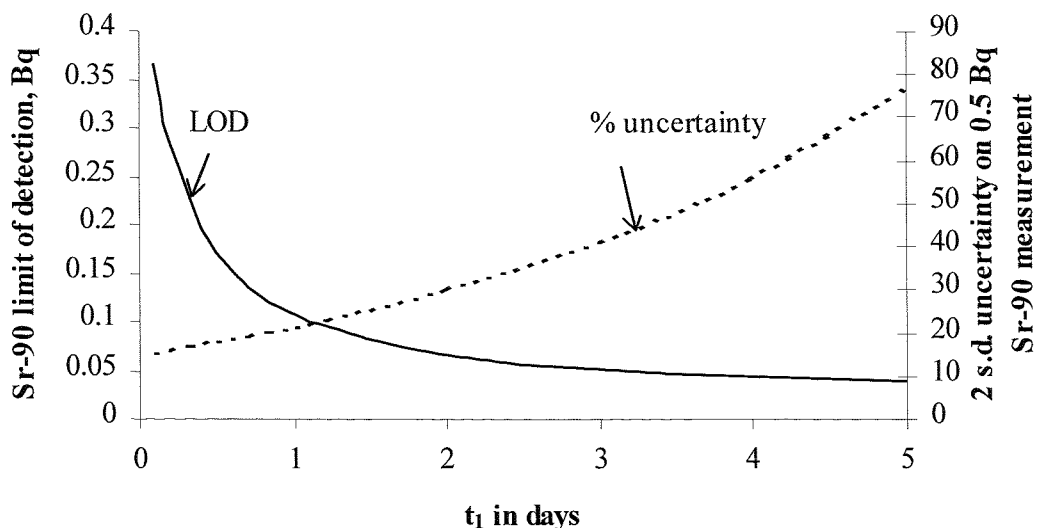


Figure P5d: The variation in the uncertainty of the  $^{90}\text{Sr}:\text{ }^{89}\text{Sr}$  ratio (upper limit) with the magnitude of the ratio and the  $^{90}\text{Sr}$  activity

The counting efficiencies are critical to the calculation of both the  $^{90}\text{Sr}$  activity and the  $^{90}\text{Sr}:\text{ }^{89}\text{Sr}$  ratio. Even a small change in the counting efficiencies can lead to significant errors in the final calculated values. The counting efficiency of  $^{90}\text{Y}$  is the most critical in the determination of the  $^{90}\text{Sr}:\text{ }^{89}\text{Sr}$  ratio. For a 10Bq Sr source with a  $^{90}\text{Sr}:\text{ }^{89}\text{Sr}$  ratio of 2 and counted for 100 minutes, a change of 10% in the  $^{90}\text{Y}$  counting efficiency results in a deviation of around 12% in the final value. By comparison a similar change in  $^{89}\text{Sr}$  and  $^{90}\text{Sr}$  counting efficiencies results in a deviation of 10% and 2% respectively in the final measured ratio. The relationship between the  $^{90}\text{Y}$  counting efficiency and deviation in  $^{90}\text{Sr}:\text{ }^{89}\text{Sr}$  ratio is quadratic and hence it is more pronounced at greater deviations of  $^{90}\text{Y}$  counting efficiency. The relationship between the variation of both  $^{89}\text{Sr}$  and  $^{90}\text{Sr}$  counting efficiencies and the deviation in the final calculated ratio is linear.

The  $^{90}\text{Y}$  counting efficiency is also critical in the calculation of  $^{90}\text{Sr}$  activity. Again a quadratic relationship is observed although the magnitude of the effect is slightly lower than for the  $^{90}\text{Sr}:\text{ }^{89}\text{Sr}$  ratio. A variation of 10% in the  $^{90}\text{Y}$  counting efficiency alters the calculated  $^{90}\text{Sr}$  activity by 10%. A similar variation in the  $^{90}\text{Sr}$  counting efficiency results in a variation on the  $^{90}\text{Sr}$  activity of only 0.1%. Variation of the  $^{89}\text{Sr}$  counting efficiency has no effect on the final  $^{90}\text{Sr}$  activity calculated.

The limit of detection for  $^{89}\text{Sr}$  and  $^{90}\text{Sr}$  will depend on the quantity of the other isotope present. If there is no  $^{89}\text{Sr}$  present then the limit of detection for  $^{90}\text{Sr}$  can be calculated assuming that the first count at  $t_1 = 0.1$  days must show a significant count above background. This gives a limit of detection (based on Currie, 1968) of 0.4 Bq for a 20 minute count and an instrument background of 1 cpm. If  $^{89}\text{Sr}$  is not being measured this limit of detection may be lowered by counting the sample slightly later following  $^{90}\text{Y}$  separation to allow more  $^{90}\text{Y}$  to grow in. If  $t_1$  is delayed to 0.5 days after  $^{90}\text{Y}$  separation, the limit of detection is reduced to 0.2 Bq. However, the overall uncertainty increases as the difference between the two count-rates at  $t_1$  and  $t_2$  becomes smaller.



**Figure P6 :** The effect of varying the time of the initial count,  $t_1$ , on the calculated limit of detection of  $^{90}\text{Sr}$  and the percentage uncertainty on the measurement of a 0.5 Bq  $^{90}\text{Sr}$  source. No  $^{89}\text{Sr}$  is present.  
Count times are 20 minutes,  $t_2$  is 10 days.

The measured  $^{90}\text{Sr}$  activity agreed well with the actual values over the range of  $^{90}\text{Sr} : ^{89}\text{Sr}$  ratios from 0.1 – 55. For ratio values below 0.1 the agreement between the measured and actual  $^{90}\text{Sr}$  activities were poorer although the results were still within the 2 s.d. uncertainty of 40%.

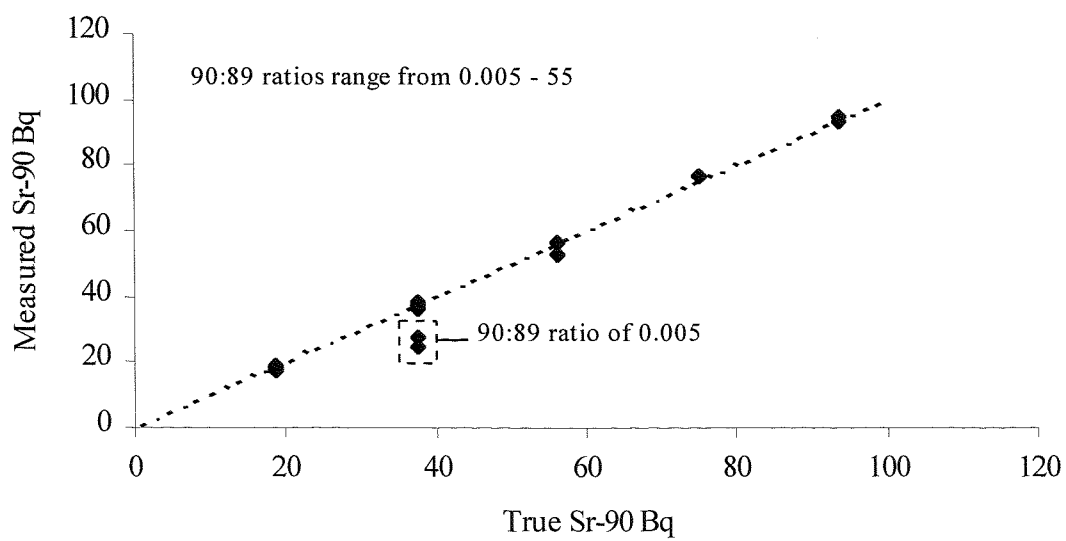


**Figure P7 :** Measured  $^{90}\text{Sr}$  activity versus actual activity for a range of samples. The  $^{90}\text{Sr} : ^{89}\text{Sr}$  ratio varies from 0.005 to 55.

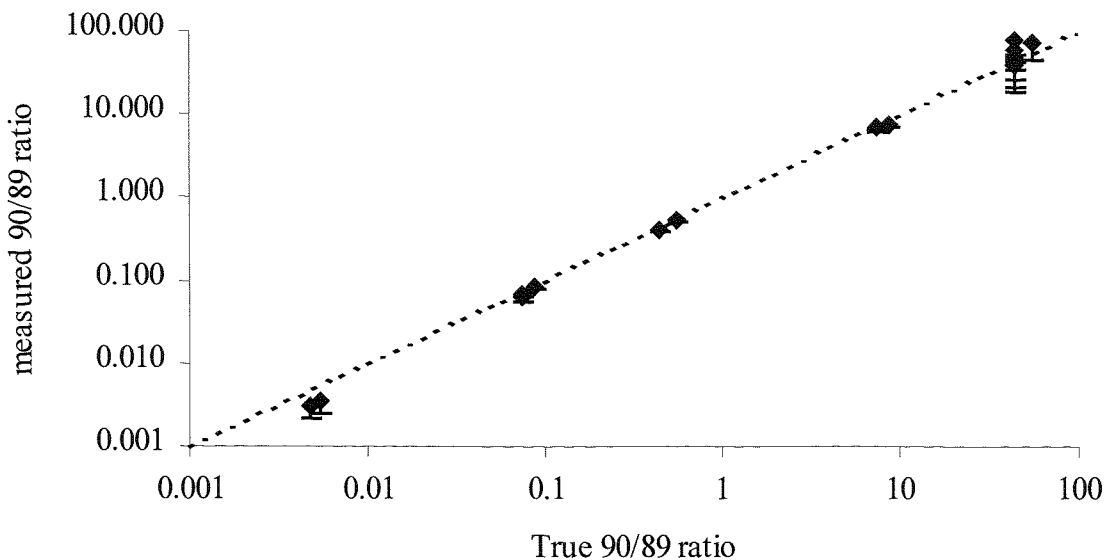


**Figure P8: Measured versus actual 90/89 Sr ratios**

Measured  $^{90}\text{Sr}$ : $^{89}\text{Sr}$  ratio values were also in good agreement with actual values over the range 0.005–10. The agreement of the measured value with the actual value appeared to be only slightly affected by the total  $^{90}\text{Sr}$  activity. Agreement was poor for samples with ratios over 50, but this is due to the large uncertainties in the measurement at this ratio. This is most probably due to the uncertainty in the counting efficiencies becoming more prominent in the overall measurement uncertainty. This may be overcome by constructing experimental calibration curves and normalising the measured/calculated values to these measured standards. However, even with such a normalisation procedure, the counting statistical uncertainties are still significant and accurate measurement of the  $^{90}\text{Sr}$ : $^{89}\text{Sr}$  ratio is not possible.

### 3.9.4.3 Testing the method

A standard sample was supplied blind to the first author by NNC Ltd. This was a certified solution containing  $^{90}\text{Sr}$ . The sample was analysed using the proposed method. The activity of  $^{90}\text{Sr}$  measured was in close agreement with the certified value (Table P3). No  $^{89}\text{Sr}$  was detected in the sample

**Table P3 : Measurement of standard  $^{90}\text{Sr}$  sample**

	Measured value	Certified value
$^{90}\text{Sr}$ Bq/litre	$25 \pm 3$	24

20ml of sample analysed. Chemical recovery 70.5%.

Uncertainties at the  $2\sigma$  confidence level

### 3.9.5 Conclusion

The method described provides a simple means to determine both the  $^{90}\text{Sr}$  activity and the  $^{90}\text{Sr}:\text{ }^{89}\text{Sr}$  ratio. The method has several advantages.

- It is more rapid than techniques based on a combined  $^{89}\text{Sr}$ ,  $^{90}\text{Sr}$  and  $^{90}\text{Y}$  measurement followed by the chemical separation of Y and separate measurement of  $^{90}\text{Y}$ .
- It is also not affected by the presence of  $^{91}\text{Y}$ .
- The use of Cerenkov-only counting of a single sample solution reduces the uncertainties of the measurement.
- Its limits of detection and measurement uncertainties have been assessed and found to be acceptable for the application in low-level waste analysis.
- It is suitable for the analysis of environmental samples under emergency conditions where levels of  $^{90}\text{Sr}$  and  $^{89}\text{Sr}$  in the local environment may be higher than the levels found routinely resulting from weapons' fallout and the Chernobyl incident.

### 3.9.6 Acknowledgements

This work has been supported by the Geosciences Advisory Unit, University of Southampton, AEA Technology, Harwell, UK and NNC Laboratories, Winfrith, UK (under Environment Agency contract NATCON\_147).

### 3.9.7 References

Bajo S. and Keil R. (1994). Determination of  $^{90}\text{Sr}$  in grass and soil. Report PSI Bericht Nr. 94-14, Paul Scherrer Institut, Villigen, Switzerland.

Bajo S. and Tobler L. (1996). Determination of  $^{90}\text{Sr}$  in uranium fission products. Report PSI Bericht Nr. 94-14, Paul Scherrer Institut, Villigen, Switzerland.

Broadway J.A. and Guy G.Y. (1983). Calculation of  $^{90}\text{Sr}$  and  $^{89}\text{Sr}$  concentrations in environmental samples using a generalised linear system. *Health Phys.*, **47**(3), 458-462.

Buchtela K. and Tschurlovits M. (1975). A new method for the determination of Sr-89, Sr-90 and Y-90 in aqueous solution with the aid of liquid scintillation counting. *Int. J. Appl. Radiat. Isot.*, **26**, 333-338.

Currie L.A. (1968). Limits of qualitative detection and quantitative determination. *Anal. Chem.*, **40** (3), 586-593.

Dietz M.L., Horwitz E.P., Nelson D.M. and Wahlgren M. An improved method for the determination of  $^{89}\text{Sr}$  and  $^{90}\text{Sr}$  in urine. *Health Phys.*, **61**(6), 871-877.

Gregory L.P. (1972). A simplified separation of strontium, radium and lead from environmental media by precipitation followed by fractional elution. *Anal. Chem.*, **44**, 2113-2115.

Horwitz E.P., Dietz M.L. and Fisher D.E. (1991). Separation and preconcentration of strontium from biological, environmental and nuclear waste samples by extraction chromatography using a crown ether. *Anal. Chem.*, **63**(5), 522-525.

Kimura T., Iwashima K., Ishimori T. and Hamada T. (1979). Separation of strontium-89 and -90 from calcium in milk with a macrocyclic ether. *Anal. Chem.*, **51**(8), 1113-1116.

Martin J.E. (1987). Measurement of  $^{90}\text{Sr}$  in reactor wastes by Cerenkov counting of  $^{90}\text{Y}$ . *Appl. Radiat. Isot.*, **38**(11), 953-957.

RADREM (1989). Sampling and measurement of radionuclides in the environment. A report by the methodology sub-group to the Radioactivity Research and Environmental Monitoring Committee (RADREM). HMSO, London, UK.

Randolph R.R. (1975) Determination of strontium-90 and strontium-89 by Cerenkov and liquid-scintillation counting. *Int J. Appl Radiat. Isot.*, **26**, 9-16

Regan J.G.T. and Tyler J.F.C. (1976). The determination of strontium-90 and strontium-89 in water without separation of strontium from calcium. *Analyst*, **101**, 32-38.

Sutherland J.K. (1988). A spreadsheet method for  $^{90}\text{Sr}$  and  $^{89}\text{Sr}$  interpretation. *Health Phys.*, **54**(1), 69-72.

Warwick P.E., Croudace I.W., Dale C.J. and Howard A.G. (1998). Extraction chromatographic techniques in the sequential separation of pure beta emitting radionuclides in low-level waste. Conference proceedings for the International workshop on the application of extraction chromatography in radionuclide measurement, Geel, Belgium

Zhu S., Ghods A., Veselsky J.C., Mirna A. and Schelenz R. (1990). Interference of  $^{91}\text{Y}$  with the rapid determination of  $^{90}\text{Sr}$  originating from the Chernobyl fallout debris. *Radiochim. Acta*, **51**, 195-198.

### 3.9.8 Derivation of equations

#### $^{90}\text{Sr}/^{89}\text{Sr}$ activity ratio

At a given time  $t_1$  following  $^{90}\text{Y}$  separation the measured activity of the Sr fraction will be a function of the initial  $^{90}\text{Sr}$  activity, the ingrown  $^{90}\text{Y}$  activity, the  $^{89}\text{Sr}$  activity and the respective counting efficiencies for each radioisotope.

$$cps_{t_1} = (A_{90} \times E_{90}) + [(1 - e^{-\lambda_1 t_1}) A_{90} E_y] + (e^{-\lambda_2 t_1} A_{89} E_{89}) \quad [\text{eqn 1}]$$

where  $A_{90}, A_{89}$  Activities of  $^{90}\text{Sr}$  and  $^{89}\text{Sr}$  at  $t=0$

$E_{90}, E_{89}$  and  $E_y$  Counting efficiencies of  $^{90}\text{Sr}$ ,  $^{89}\text{Sr}$  and  $^{90}\text{Y}$

$\lambda_1$  Decay constant for  $^{90}\text{Y}$

$\lambda_2$  Decay constant for  $^{89}\text{Sr}$

$$\begin{aligned} cps_{t_1} &= [(1 - e^{-\lambda_1 t_1}) E_y + E_{90}] A_{90} + (e^{-\lambda_2 t_1} \times E_{89}) A_{89} \\ &= k_1 A_{90} + k_2 A_{89} \end{aligned}$$

[eqn 2]

The ratio of count-rates at two different times  $t_1$  and  $t_2$  can be defined as follows

$$\frac{cps_1}{cps_2} = \frac{c_1}{c_2} = \frac{k_1 A_{90} + k_2 A_{89}}{k_3 A_{90} + k_4 A_{89}} \quad [\text{eqn 3}]$$

where  $k_3$  and  $k_4$  are similar to  $k_1$  and  $k_2$  but for  $t_2$

Rearranging equation 3 gives

$$\begin{aligned}
 \frac{c_1}{c_2} (k_3 A_{90} + k_4 A_{89}) &= k_1 A_{90} + k_2 A_{89} \\
 \left( \frac{c_1}{c_2} \right) k_3 A_{90} + \left( \frac{c_1}{c_2} \right) k_4 A_{89} &= k_1 A_{90} + k_2 A_{89} \\
 \frac{c_1}{c_2} k_3 A_{90} &= k_1 A_{90} + k_2 A_{89} - \frac{c_1}{c_2} k_4 A_{89} \\
 \frac{c_1}{c_2} k_3 A_{90} - k_1 A_{90} &= k_2 A_{89} - \frac{c_1}{c_2} k_4 A_{89} \\
 \left( \frac{c_1}{c_2} k_3 - k_1 \right) A_{90} &= \left( k_2 - \frac{c_1}{c_2} k_4 \right) A_{89} \\
 \frac{A_{90}}{A_{89}} &= \frac{k_2 - \frac{c_1}{c_2} k_4}{\frac{c_1}{c_2} k_3 - k_1}
 \end{aligned}$$

$$\frac{A_{90}}{A_{89}} = \frac{(e^{-\lambda_2 t_1} \times E_{89}) - \frac{c_1}{c_2} (e^{-\lambda_2 t_2} \times E_{89})}{\frac{c_1}{c_2} [(1 - e^{-\lambda_1 t_2}) E_Y + E_{90}] - [(1 - e^{-\lambda_1 t_1}) E_Y + E_{90}]} \quad [\text{eqn 4}]$$

<sup>90</sup>Sr activity

From equation 2

$$\begin{aligned}
 cps_{t_1} &= c_1 = k_1 A_{90} + k_2 A_{89} \\
 cps_{t_2} &= c_2 = k_3 A_{90} + k_4 A_{89} \quad [\text{eqn 5}]
 \end{aligned}$$

Hence

$$A_{89} = \frac{c_2}{k_4} - \frac{k_3}{k_4} A_{90} \quad [\text{eqn 6}]$$

Substituting equation 6 for  $A_{89}$  in eqn 5

$$c_1 = k_1 A_{90} + \frac{k_2 c_2}{k_4} - \frac{k_2 k_3}{k_4} A_{90}$$

$$c_1 - \frac{k_2 c_2}{k_4} = k_1 A_{90} - \frac{k_2 k_3}{k_4} A_{90}$$

Rearranging equation 7 gives  $A_{90}$

$$A_{90} = \left( c_1 - \frac{k_2 c_2}{k_4} \right) \times \left( \frac{1}{k_1} - \frac{k_4}{k_2 k_3} \right) \quad [\text{eqn 7}]$$

***Uncertainties on the  $^{89/90}\text{Sr}$  ratio and  $^{90}\text{Sr}$  activity***

It is assumed that the counting efficiencies for the individual isotopes are well characterised and hence the uncertainty is mainly derived from the counting statistical uncertainties  $\sigma c_1$  and  $\sigma c_2$ .

The main uncertainty in equation 4 derives from the counting statistical uncertainty on the ratio  $c_1/c_2$ . This uncertainty,  $\sigma R$ , on the ratio,  $R$  (equal to  $c_1/c_2$ ) is defined as

$$\frac{\sigma_R}{R} = \sqrt{\left(\frac{\sigma_{c_1}}{c_1}\right)^2 + \left(\frac{\sigma_{c_2}}{c_2}\right)^2} \quad [\text{eqn 8}]$$

where

$$\sigma_{c_1} = \sqrt{c_1} \quad [\text{eqn 9}]$$

At the 2 sigma confidence interval, the absolute uncertainty is therefore

$$2(\sigma_R) = 2 \times R \times \sqrt{\left(\frac{\sigma_{c_1}}{c_1}\right)^2 + \left(\frac{\sigma_{c_2}}{c_2}\right)^2} \quad [\text{eqn 10}]$$

Propagation of this uncertainty will place an upper and lower limit on the calculated  $^{90/89}\text{Sr}$  activity as follows.

Upper limit of ratio

$$\frac{A_{90}}{A_{89}}(\text{upper}) = \frac{(e^{-\lambda_2 t_1} \times E_{89}) - (R + 2\sigma_R)(e^{-\lambda_2 t_2} \times E_{89})}{(R + 2\sigma_R)[(1 - e^{-\lambda_1 t_2})E_Y + E_{90}] - [(1 - e^{-\lambda_1 t_1})E_Y + E_{90}]} \quad [\text{eqn 11}]$$

Lower limit of ratio

$$\frac{A_{90}}{A_{89}}(lower) = \frac{(e^{-\lambda_2 t_1} \times E_{89}) - (R - 2\sigma_R)(e^{-\lambda_2 t_2} \times E_{89})}{(R - 2\sigma_R)[(1 - e^{-\lambda_1 t_2})E_Y + E_{90}] - [(1 - e^{-\lambda_1 t_1})E_Y + E_{90}]} \quad [eqn\ 12]$$

Likewise an upper and lower uncertainty limit can be set on the calculated  $^{90}\text{Sr}$  activity by combining equations 7 and 9.

$$A_{90}(upper) = [(C_1 + 2\sigma_{C_1}) - \frac{k_2(C_2 - 2\sigma_{C_2})}{k_4}] \times (\frac{1}{k_1} - \frac{k_4}{k_2 k_3})$$

[eqn 13]

and

$$A_{90}(lower) = [(c_1 - 2\sigma_{C_1}) - \frac{k_2(c_2 + 2\sigma_{C_2})}{k_4}] \times (\frac{1}{k_1} - \frac{k_4}{k_2 k_3})$$

[eqn 14]

### 3.10 Conclusions

In all cases the chosen method for the measurement of the radioisotope of interest was liquid scintillation counting. In most cases the liquid scintillation counter offered the highest sensitivity of any technique. Counting efficiencies are in general very high compared to other radiometric techniques as the analyte is intimately mixed with the liquid scintillant ‘detector’ giving a  $4\pi$  counting geometry. The figure-of-merit obtainable was further increased by using the Wallac 1220 Quantulus ultra low-level liquid scintillation counter, which incorporates a range of features designed to significantly reduce background count rates. Although it is assumed that mass-spectrometric techniques would provide greater sensitivity for the long-lived radioisotopes, it was found in practice that the presence of isobaric interferences and operational difficulties meant that the available mass-spectrometric techniques of TIMS and ICP-MS gave no benefit in sensitivity compared with the Quantulus counter.

The sensitivity achievable using liquid scintillation counting is highly dependent on the source preparation technique employed. For  $^{89}\text{Sr}$  and  $^{90}\text{Sr}$ , the beta decay energy is sufficiently high to permit Cerenkov counting of the isotope. In this instance no scintillant is added resulting in no chemical quench and very low background count rates. Colour quench is still a concern and the final Sr fraction must be rendered colourless through chemical separation of the isotope. Deconvolution of the  $^{89}\text{Sr}$ ,  $^{90}\text{Sr}$  and  $^{90}\text{Y}$  present in the source was achieved by deriving simultaneous equations associated with two count rates measured at two time intervals following initial  $^{90}\text{Y}$  separation. The use of the wavelength shifter 4-methyl coumarin was not found to improve the counting efficiencies.

For  $^{55}\text{Fe}$ ,  $^{63}\text{Ni}$  and  $^{99}\text{Tc}$ , the beta decay energy was too low to permit Cerenkov counting. Methods were therefore developed to permit mixing of the purified isotope with commercial liquid scintillation cocktails. Extraction of the isotope into a non-quenching organic solvent was found to give the highest counting efficiencies and was adopted for the low-level measurement of  $^{99}\text{Tc}$ . However, difficulties in determining the chemical recovery following organic extraction meant that this approach was not suitable for the other radioisotopes of interest.

Precipitation of the radioisotope with a carrier was found in many cases to provide a source suitable for liquid scintillation counting. Ideally the precipitate was organic in nature and readily dissolved in the organic cocktail. Formation of a precipitate also permitted the determination of chemical yield gravimetrically. Precipitation of  $^{63}\text{Ni}$  as nickel pyridine thiocyanate and  $^{99}\text{Tc}$  as tetraphenyl arsonium perhenate (using Re as the carrier in the absence of a stable Tc isotope) produced source that readily mixed with commercial liquid scintillation cocktails. Although Ni pyridine thiocyanate gave

excellent counting characteristics, the counting efficiency was not significantly different to that found for  $^{63}\text{Ni}$  dissolved in a small volume of dilute HCl. In addition it was found that the precipitate was difficult to obtain in a dry state resulting in unacceptable uncertainties in the final yield determination. Although oven drying improved the reproducibility of the gravimetric yield determination it also resulted in a precipitate that was extremely difficult to dissolve totally in the scintillant increasing the measurement uncertainty. Co-precipitation of Tc with Re as the tetraphenyl arsonium perrhenate did provide good gravimetric yield data as well as a source that mixed readily with scintillant. However, Ru would not be separated during this precipitation and hence the organic extraction was still required to separate Ru from the Tc. In addition, the observed counting efficiency for the organic extract was higher than for the precipitate and hence the precipitate-based source preparation technique was not routinely used. However, direct mixing of  $^{99}\text{Tc}$  extracted onto TEVA resin was of considerable interest for certain applications where the ultimate limit of detection was not being sought.

For  $^{55}\text{Fe}$  and  $^{63}\text{Ni}$ , the radioisotope was dissolved in a small volume of mineral acid and mixed with a suitable liquid scintillant. Chemical recovery is determined by removing a small quantity of the purified sample, diluting it and measuring the stable Fe and Ni using ICP-AES. For  $^{63}\text{Ni}$ , the source was prepared from dilute HCl. For  $^{55}\text{Fe}$   $\text{H}_3\text{PO}_4$  was chosen to decolourise the Fe and minimise colour quenching in the sample. The  $^{55}\text{Fe}$  measurement was seriously affected by the quantity of stable Fe present in the sample. This effect was investigated fully and optimised conditions derived to maximise the sensitivity of  $^{55}\text{Fe}$  measurement in high-Fe samples.

### 3.11 References

Bohnstedt A., Langer-Lüer M., Stuhlfauth H. and Aumann D.C. (1998). Radiochemical characterisation of low- and medium-activity radioactive waste by destructive assay of long-lived alpha and beta emitting nuclides. In Odoj R., Baier J., Brennecke P. and Kühn K. (eds). Radioactive waste products 1997, Forschungszentrum Jülich GmbH, Germany.

Currie L.A. (1968). Limits of qualitative detection and quantitative determination. *Anal. Chem.*, **40** (3), 586-593.

Harvey B.R. and Sutton G.A. (1970). Liquid scintillation counting of nickel-63. *Int. J. Appl. Radiat. Isot.*, **21**, 519-523.

Holm E, Oregioni B, Vas D, Pettersson H, Rioseco J and Nilsson U. (1990). Nickel-63: Radiochemical separation and measurement with an ion implanted silicon detector. *J. Radioanal. Nucl. Chem. Articles*, **138**, 111-118.

Kojima S. and Furukawa M. (1985). Liquid scintillation counting of low activity  $^{63}\text{Ni}$ . *J. Radioanal. Nucl. Chem. Letters*, **95**(5), 323-330.

Ross H.H. (1976). Theory and application of Cerenkov counting. In Noujaim A.A., Ediss C. and Weibe L.I. (eds), Liquid Scintillation : Science and Technology. Academic Press, New York, USA.

## Chapter 4

# **Solvent extraction and Extraction chromatographic techniques**

## 4. Solvent extraction and extraction chromatographic techniques

### 4.1 Introduction

Many radiochemical separation techniques employ ion exchange chromatography to either preconcentrate and/or purify the analyte. Although ion exchange chromatography has found widespread application in many procedures, solvent extraction can, in numerous instances still offer a higher degree of specificity. In addition, the combination of an extractant and a solid support to produce a chromatographic material combines the specificity of solvent extraction with the improved separation efficiency and hence high decontamination factors offered by a chromatographic technique. The application of solvent extraction and extraction chromatography were therefore studied for the isolation and purification of pure beta emitting radioisotopes.

### 4.2 Definition of partition coefficient, distribution coefficient and $k'$

Separation of an element by solvent extraction relies on the partitioning of the analyte between two immiscible phases. In most cases one of the phases is aqueous whilst the other phase is either a pure organic liquid or extractant dissolved in an organic solvent. Ideally, separation is achieved through the quantitative extraction of one component into the organic layer whilst the second component remains in the aqueous phase. However, in reality, extraction may not be quantitative and the extracted component will partition between the two phases with only a certain percentage of the component being extracted. The percentage extracted will depend on the volumes of aqueous and organic phases. However, the degree of partitioning is defined by the **partition coefficient**,  $K_D$ .

$$K_D = \frac{[A]_{org}}{[A]_{aq}} \quad \text{at equilibrium}$$

where  $[A]_{org}$  and  $[A]_{aq}$  are the concentrations of the analyte in the organic and aqueous phases respectively at equilibrium. At low concentrations the partition coefficient is independent of the analyte concentration. However, at high concentrations, the organic phase may become saturated and reach a maximum loading. The maximum loading capacity of an extractant is therefore potentially another important parameter in assessing the suitability of an extractant in an analytical separation.

In extraction chromatography, the extractant is loaded onto an inert support which is then packed into columns to permit chromatographic separation. On loading a sample onto the column, the components will

partition between the mobile (solution) phase and the stationary (solid) phase. Chromatographic separation is achieved when the components of a mixture partition to differing degrees between the mobile and stationary phase. The degree of partitioning is defined as the ratio of a component on the solid phase to that in the mobile phase and is called the **distribution coefficient**,  $K_D$ . The distribution coefficient are determined experimentally by mixing a known mass of solid phase with a known mass of mobile phase containing the component being evaluated. The mixture is shaken to achieve equilibrium and the amount of the component in either the mobile or stationary phase is determined. The  $K_D$  is then calculated as follows

$$K_D = \frac{A_{\text{solid}} \times M_{\text{mobile}}}{A_{\text{mobile}} \times M_{\text{solid}}} \quad \text{at equilibrium}$$

where  $A_{\text{solid}}$  and  $A_{\text{mobile}}$  are the masses/activities of the analyte in the solid and mobile phases respectively and  $M_{\text{mobile}}$  and  $M_{\text{solid}}$  are the masses of mobile and solid phases respectively.

In much recent literature on extraction chromatographic materials, the parameter  $k'$  is used to indicate the magnitude of the affinity of the extractant for the analyte.  $k'$  is defined as the peak elution volume to free column volume ratio (Figure 4.1)

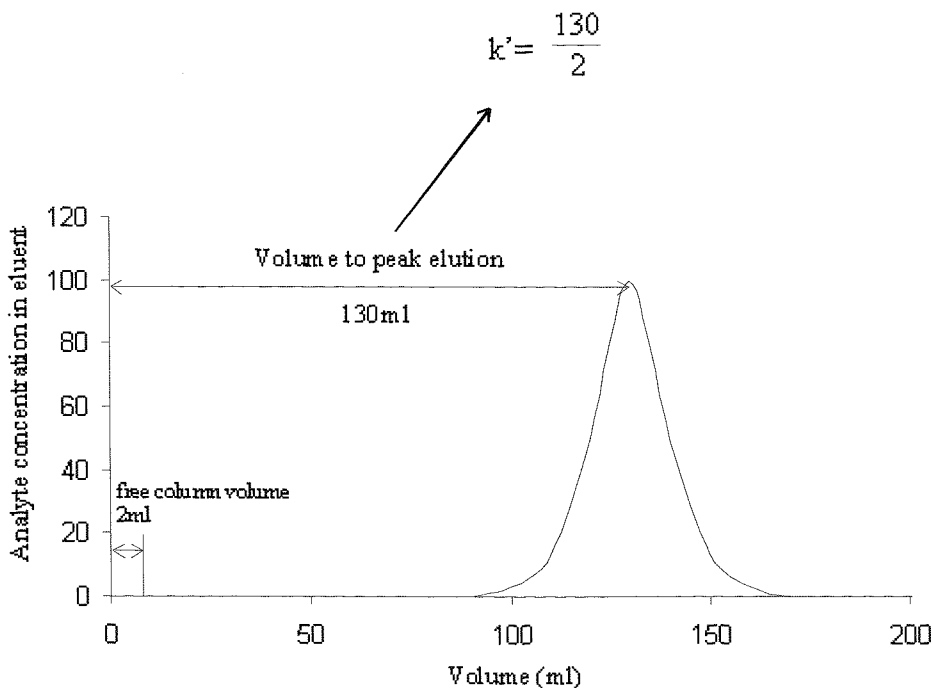


Figure 4.1 : Definition of  $k'$

## 4.3 Separation and purification of iron

### 4.3.1 Purification of $^{55}\text{Fe}$ by solvent extraction

Many metals including Fe may be extracted as protonated metal halo-complexes from strong acid solution. Singly charged complexes are preferentially extracted and higher extraction coefficients are noted for divalent and trivalent metal ions that form singly charged anionic halo- complexes. Fluoro complexes exhibit low extraction coefficients as the fluoride ion preferentially forms highly negatively charged complexes. Chloro-complexes are the most common complexes for practical extraction although bromo- and iodo-complexes have been used. Iron can be extracted from > 6M HCl into a number of solvents as the  $\text{FeCl}_4^-$  anion. Sb(V), As(III), Ga(III), Ge(IV), Au(III), Hg(II), Mo(VI), Nb(V), Pt(II), Po(II), Pa(V), Tl(III), Sc(III) are also extracted as chloro complexes. Sb(III), As(V), Co(II), In(III), Te(IV), Sn(II) and Sn(IV) are partially extracted. Between 15 and 30% of Sn is extracted from HCl into ethyl ether (Morrison and Freiser, 1962). Many oxygen-containing solvents have been employed. Ethers, such as diisopropyl ether (e.g. König *et al*, 1995) are commonly used for the extraction. Ethers are known to photochemically reduce Fe(III) to Fe(II) which is not extracted and hence the extraction into ether should be performed in subdued light (Vogel, 1978). Esters such as ethyl acetate and butyl acetate are also effective at extracting large quantities of Fe and have the benefit of low volatility. Esters are hydrolysed by strong HCl and mixtures must not be allowed to stand for too long during the separation.

### 4.3.2 Evaluation of three solvents for the extraction of $^{55}\text{Fe}$

Three solvents were investigated for their effectiveness at extracting iron. Ethyl acetate, diisobutyl ketone and di isopropyl ether were chosen as these solvents have been used routinely in the purification of  $^{55}\text{Fe}$ .

The distribution coefficient for Fe was determined for each solvent. Approximately 25mg of  $\text{Fe}_2\text{O}_3$  was dissolved in 50ml 6M HCl giving an iron standard of approximately 500 ppm. 5 ml of this solution was extracted with 10 ml of the solvent under investigation for approximately 5 minutes. The aqueous and organic fractions were allowed to separate and 1 ml of the aqueous phase was removed and diluted with 2% nitric acid prior to Fe measurement by atomic absorption spectrometry. The distribution coefficient of Fe from 6M HCl for each solvent was then calculated (Table 4.1). These values should be taken as a guide only as it has been shown that the observed distribution coefficient for the extraction of  $\text{FeCl}_4^-$  will depend on the amount of Fe present initially in the aqueous phase (Morrison and Freiser, 1962).

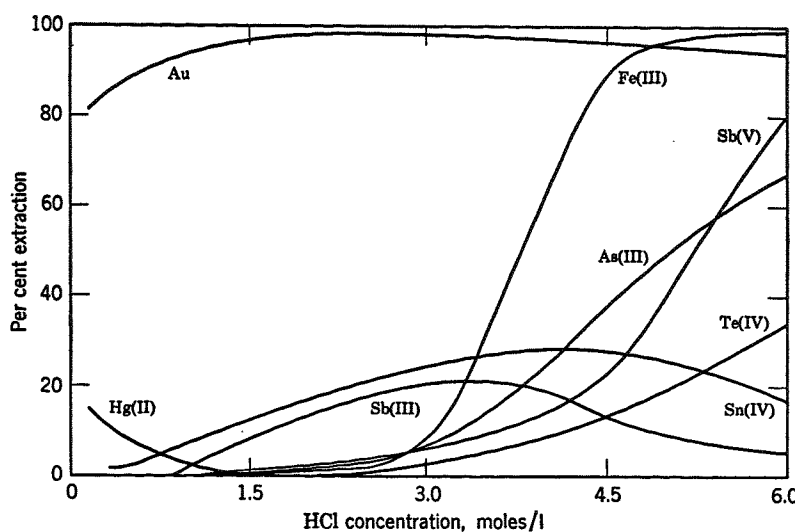


**Figure 4.2 : Effect of hydrochloric acid concentration on the extractability of chlorides by ethyl ether (Morrison and Freiser, 1962)**

The effective Fe loading capacity of each solvent was determined as follows. 5 ml of a 0.1g/ml Fe standard in 6M HCl was shaken with 5ml of the solvent for 5 minutes in a 50 ml separating funnel. The phases were allowed to separate and the aqueous phase run to waste. The organic phase was washed with 5ml 6M HCl to remove any acid occluded in the organic phase and adhering onto the funnel walls. The aqueous phase was run to waste and the organic phase was transferred to a clean separating funnel. The Fe in the organic phase was back-extracted from the organic phase into 2 x 5ml 1.6M nitric acid. 0.1ml of each nitric acid fraction was diluted to 10ml and the Fe concentration measured by atomic absorption spectrometry.

**Table 4.1 : Distribution coefficients and loading capacities of Fe for various solvents**

Solvent	Distribution coefficient	Effective loading capacity mg Fe/ml solvent
Ethyl acetate	65	95
Di isobutyl ketone	38	49
Di isopropyl ether	4	59

The highest distribution coefficients and highest effective loading capacity for Fe was observed when using ethyl acetate. During the routine separation of iron it was noted that the ethyl acetate was quite rapidly hydrolysed by the 6M HCl. Mixing ethyl acetate with butyl acetate, which is more slowly hydrolysed, reduced the rate of volume change. Butyl acetate alone was not used as the distribution coefficients for Fe are lower than for ethyl acetate. A ratio of two-thirds ethyl acetate to one-third butyl acetate was suggested by Bains and Warwick (1993). It should be noted that the effective loading capacity measured is not a true loading capacity as the solvent containing the Fe was washed with fresh 6M HCl, resulting in two

partitioning stages. However, the effective loading capacity represents more accurately the practical capacity of the solvent.

#### 4.3.3 Co-extraction of Sn with Fe

Morrison and Freiser (1962) noted that, along with the Fe, approximately 30% of Sn was also extracted into ethyl acetate from HCl solutions. However, extraction of Fe into di isopropyl ether has also been used to separate Fe from Sn during the radiochemical separation of Sn (Patten, 1989). These apparently contradictory observations possibly suggest that the efficiency of Sn extraction is dependent on the type of organic extractant used.

10 Bq of  $^{113}\text{Sn}$  was dissolved in 10ml of 6M HCl. This solution was shaken with 10ml of either 3:1 ethyl acetate/butyl acetate, di isobutyl ketone or di isopropyl ether for 5 minutes. The volumes of the aqueous and organic phases were measured and 5ml of the organic phase was removed and diluted to 20ml. The solution was left to stand for 24 hours to permit  $^{113}\text{In}$  to re-establish secular equilibrium with the  $^{113}\text{Sn}$  parent. The activity of  $^{113}\text{In}$  (and hence the activity of  $^{113}\text{Sn}$ ) in the organic phase was determined by gamma spectrometry.

The extent of Sn extraction from 6M HCl is dependent on the type of solvent used for the extraction. No Sn was extracted into di isopropyl ether whilst 8% and 38% of Sn was extracted into di isobutyl ketone and ethyl/butyl acetate respectively. This is in agreement with the observations made by both Morrison and Freiser (1962) and Patton and Penrose (1989). Diisopropyl ether is therefore a more appropriate choice of extractant if radio-tin is likely to be present in the samples.

#### 4.3.4 Extraction chromatographic techniques for the purification of $^{55}\text{Fe}$

Little has been published on the extraction chromatographic purification of  $^{55}\text{Fe}$ . One of the main limitations in the use of this technique is the requirement for large loading capacities necessary to accommodate the levels of stable Fe routinely found in samples. Konig *et al* (1995) used Chelex 100 resin to preconcentrate Fe from steel and concrete samples. The technique was not Fe-specific and solvent extraction was still required to purify the  $^{55}\text{Fe}$  prior to liquid scintillation counting. TRU® resin (supplied by Eichrom Industries) has also been employed for the isolation of  $^{55}\text{Fe}$ . Fe is retained from 8M HNO<sub>3</sub> and subsequently eluted with 2M HNO<sub>3</sub>. However, the maximum Fe loading for the procedure is limited to 3mg for a standard column containing 0.7g of resin. Silica-immobilised formylsalicylic acid was found to efficiently extract Fe

(Mahmoud and Soliman, 1997). Loading capacities of approximately 54 mg Fe per gram of resin were reported. However, the extractant was not specific to Fe and further purification of the  $^{55}\text{Fe}$  was required.

Initial attempts to load ethyl acetate onto an inert XAD-7 support were unsuccessful. Sufficient ethyl acetate was retained on the support to permit the initial extraction of 1 mg of Fe from 5ml of 6M HCl. Approximately 1 g of XAD-7 was slurried with 5ml of ethyl acetate. Approximately 50ml of 6M HCl was mixed with the slurry. The ethyl acetate-loaded XAD-7 was allowed to settle and the excess HCl was decanted off. The resulting mixture was used to prepare a 3 x 0.5 cm column. On passing 1mg of Fe in 5ml 6M HCl through the column a distinct yellow band was visible at the top of the column. However, this band of Fe passed rapidly through the column and breakthrough of Fe was noted after only 2ml of 6M HCl washings. The rapid elution of Fe from the column was explained by the relatively high solubility of ethyl acetate in 6M HCl and the hydrolytic degradation of the ethyl acetate. Both factors would result in a rapid decrease in the amount of ethyl acetate on the column and subsequent removal of the  $\text{FeCl}_4^-$  complex from the column.

Di isobutyl ketone (DIBK) loaded onto an inert XAD-7 support was also investigated. The solvent exhibited higher extraction coefficients for Fe compared to the more commonly used di isopropyl ether (DIPE). Although DIBK is more soluble in HCl than DIPE, the improved extraction coefficient makes the use of DIBK preferable to DIPE. 2g of Amberlite XAD-7 resin was slurried with 3.5ml of DIBK. The DIBK was added dropwise to the XAD-7 with constant stirring to produce a damp white solid. This solid was then slurried with 6M HCl again with dropwise addition of the HCl and constant stirring of the mixture. Too rapid an addition of HCl with insufficient stirring produced a hydrophobic solid that could not be used to prepare an extraction column. This method produced 4.5g of extraction material that was sufficient to prepare two columns of 5 x 0.7 cm (1.9ml column volume).

A standard was prepared containing 1mg Fe, 0.01mg rare earths, Ba, Co, Ni, U, Zr, Y, Th and Sn in 2ml of 6M HCl. The sample was loaded onto the column with dimensions of 5 x 0.7 cms (1.9ml column volume) and the column repeatedly washed with 2ml aliquots of 6M HCl. A total of 60ml of 6M HCl was passed through the column (equivalent to approximately 30 column volumes). The Fe was eluted with 3 x 2ml of deionised water. Each eluent fraction was diluted to 10ml with 2% nitric acid. The concentration of Fe was then determined using atomic absorption spectrometry. 100 (1 of each eluent fraction was diluted to 10ml with 2% nitric acid and the concentration of all other analytes was determined by ICP-MS.

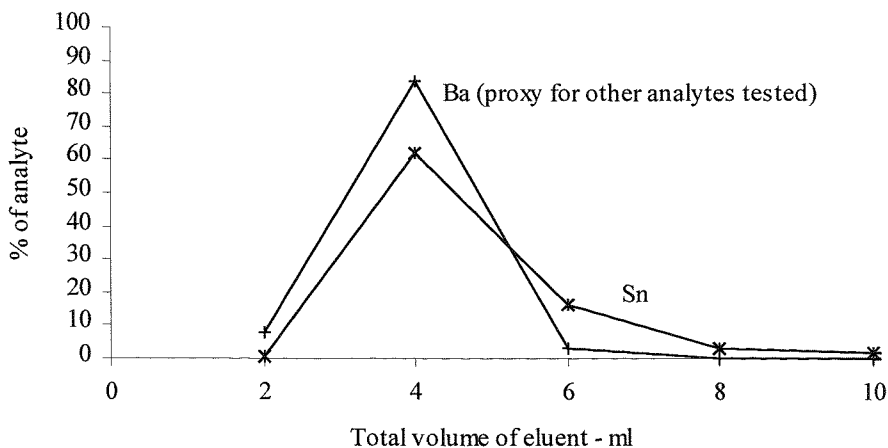


**Figure 4.3: Elution of potential contaminants with 6M HCl from a DIBK / XAD-7 column 5 x 0.7cm (1.9ml volume)**

All elements tested followed the elution pattern of Ba with the exception of Sn. Sn elution was slightly delayed although 100% of Sn was eluted in 10ml of 6M HCl.

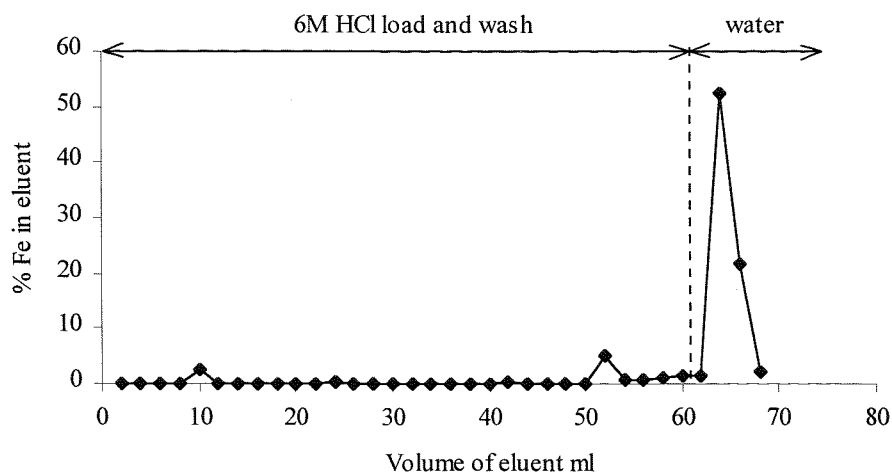


**Figure 4.4 : Retention and elution of 1mg Fe on a DIBK / XAD-7 column 5 x 0.7cm (1.9ml volume)**

#### 4.3.5 Maximum loading of Fe on the DIBK/XAD-7 column

One of the main limitations of any technique for the isolation of Fe is the maximum loading of Fe that the technique can tolerate. In general solvent extraction-based separations have higher Fe capacities than a column-based technique. A typical 5 x 0.7cm column has a column volume of 1.9ml of which approximately 1.5ml is DIBK. From the values in Table 4.1 the maximum Fe loading of the column is therefore 74 mg Fe. However, a solvent extraction-based technique using 20ml of undiluted DIBK would be capable of extracting 980 mg Fe. Therefore, although the DIBK column offers advantages in terms of improved

purification of Fe from other elements excessively large columns would be required for the separation of Fe from high Fe samples, such as soils and sediments, for which solvent extraction-based techniques are preferable.

## 4.4 Nickel-63

### 4.4.1 Isolation of Ni as the dimethylglyoxime complex

As noted in Chapter 2, isolation of Ni has normally been achieved by forming a Ni-dimethylglyoxime (DMG) complex and extracting the complex into chloroform. The complex is formed under alkaline conditions in the presence of ammonia. Citrate is often added to prevent precipitation of transition metals, such as Fe, that would normally hydrolyse at the alkaline pH employed. More recently, the isolation of Ni has been achieved by loading the dimethylglyoxime onto an inert support producing a material suitable for column chromatographic separations of Ni from other elements (Testa *et al*, 1991). The preparation and application of the dimethylglyoxime loaded onto an inert support was investigated further to evaluate its suitability for the current study.

### 4.4.2 Preparation of dimethylglyoxime-loaded onto XAD-7 and silica using three techniques

Dimethylglyoxime was loaded onto Amberlite XAD-7 and chromatographic grade silica using three techniques. The XAD-7 was ground and sized to 63-125 (m prior to further treatment. Evaporation of a solution of dimethylglyoxime onto XAD-7 has been generally used to prepare the chromatographi material. However, adsorption and precipitation of the DMG onto both XAD-7 and silica were investigated in an attempt to produce a more uniformly coated material.

#### *Adsorption*

0.25g of dimethylglyoxime was dissolved in 25ml of industrial methylated spirits. 2g of either silica or XAD-7 were slurried with this solution and the mixture was allowed to stand for 2 hours. The solid was isolated by filtration and dried in an oven overnight at 30°C.

#### *Precipitation*

0.25g of dimethylglyoxime was dissolved in a minimum of acetone (approximately 25ml). 2g of either silica or XAD-7 were slurried with the acetone and 125ml of water was added with continuous stirring to precipitate the dimethylglyoxime onto the solid. The mixture was filtered and dried in a vacuum dessicator overnight.

### Evaporation

0.25g of dimethylglyoxime was dissolved in 30ml of acetone. 2g of silica was slurried into the acetone and the mixture was allowed to stand with constant stirring whilst the acetone evaporated away. The solid was then dried further in a vacuum dessicator.

#### 4.4.3 Nickel loading and breakthrough on dimethylglyoxime-loaded resin

Columns were prepared from approximately 0.2g of DMG-based material produced using the techniques described above. The column dimensions were 2 cm long by 0.8cm internal diameter. Each column was conditioned using 0.14M ammonia solution. A 100 ml solution of ammonia was also prepared with a stable nickel concentration of 1 ppm. This was passed through the column in 10 ml fractions until a uniform red colouration throughout the extraction material was observed. The column was washed with 5 ml of deionised water and all the eluent was retained. The Ni complexed on the column was eluted with 8M HCl and diluted to 50ml with deionised water. It was noted that some of the dimethylglyoxime reagent had eluted from the column and had reacted with the excess Ni in the eluent forming a red precipitate. This was filtered off through a 0.45  $\mu\text{m}$  membrane filter and dissolved in 8M HCl. The final volume of this solution was adjusted to 50 ml with deionised water. Both fractions from each column were analysed by ICP-AES to determine the Ni concentration.

Table 4.2 : Ni loading capacities for a range of dimethylglyoxime based extraction columns

Support	Method for DMG loading	Mass used (g)	Mass Ni on column (mg)	Mass associated with DMG leached (mg)	Capacity mg Ni/g resin
Silica	Precipitation	0.2046	6.63	0.78	32.4
Silica	Adsorption	0.2152	6.06	0.51	28.2
XAD-7	Adsorption	0.1806	0.38	3.66	2.1
XAD-7	Evaporation	0.1827	4.97	1.27	27.2
Silica	Evaporation	0.1932	8.85	1.71	45.8
XAD-7	Precipitation / adsorption	0.2086	1.03	1.27	4.9
XAD-7	Evaporation	0.2028	2.28	1.24	11.2

The highest loading capacity was observed for silica loaded with dimethylglyoxime by evaporation. However, the flow rates through this column were slow in comparison with the XAD-7 based column and the later support was therefore used in preference.

#### 4.4.4 Elution profiles for Ni on a dimethylglyoxime-XAD-7 column

A 2 x 0.8 cm column was prepared using dimethylglyoxime loaded onto XAD-7 by evaporation. A solution containing 1% by volume of ammonia, 0.1 g of Ni and 0.8 kBq of  $^{63}\text{Ni}$  was loaded onto the DMG-XAD-7 column to produce a narrow loading band at the top of the column. A 1% ammonia solution was passed through the column in 5 ml fractions and the eluents were collected separately. Each eluent fraction was analysed separately by liquid scintillation counting and the results used to determine the break-through volume of the column. The experiments were repeated using a dimethylglyoxime-based column commercially available from Eichrom industries.

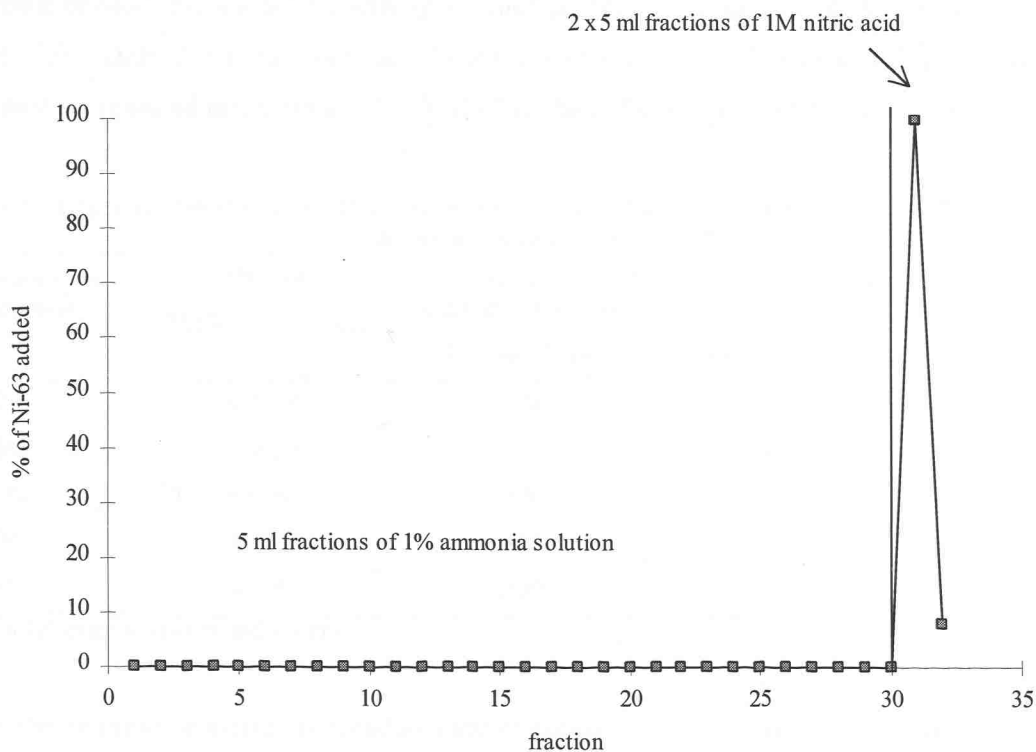


**Figure 4.5 : Retention and elution of Ni on a dimethylglyoxime-based resin column**

The elution profiles for both columns were identical (Figure 4.5 shows the elution profile for the commercial resin). No breakthrough of Ni was observed even after passing 150ml of ammonia solution through the column. This permits the column to be thoroughly washed to remove any potential contaminants prior to eluting the Ni with a dilute acid.

#### 4.4.5 Optimisation of conditions for the retention of nickel on DMG loaded XAD-7

The optimum ammonia concentrations for the reaction of nickel with DMG loaded XAD-7 was determined. It is known that in solution nickel will react with dimethylglyoxime in ammoniacal solutions. No information was available, however, on the optimum concentration of ammonia for the reaction to proceed. Solutions of 0.1%, 0.5%, 1.0%, 2.0% and 5.0% ammonia solutions (% v/v of 0.88 sp gr ammonia and water) were prepared containing a known activity of  $^{63}\text{Ni}$  (nominally 500Bq). 10 ml of each solution was equilibrated for two hours with XAD-7 loaded with dimethylglyoxime via adsorption. After two hours the XAD-7 was removed by filtration and the filtrate  $^{63}\text{Ni}$  activity was measured by liquid scintillation counting. The difference between the initial  $^{63}\text{Ni}$  activity and the  $^{63}\text{Ni}$  activity at equilibrium was used to determine the amount of  $^{63}\text{Ni}$  retained on the solid and hence a distribution coefficient could be calculated. All experiments were repeated using unmodified XAD-7 to check for any precipitation effects (Table 4.3).

**Table 4.3 : Effect of ammonia concentration on the uptake of Ni(II) by dimethylglyoxime/XAD-7 columns**  
Ammonia solution concentration\*

Ammonia solution concentration	Mass of DMG/XAD-7 solid	Activity of $^{63}\text{Ni}$ at start of experiment		Activity of $^{63}\text{Ni}$ at equilibrium	Distribution coefficient
		Bq/10ml filtrate	Bq/10ml filtrate		
0.2%	0.1039	424		4.31	9590
0.5%	0.0959	442		4.87	9460
1.0%	0.0962	440		5.08	9020
5.0%	0.1032	440		15.1	2740
10.0%	0.1063	449		28.4	1390

\*(% v/v of 0.88 sp gr ammonia and water)

Increasing the ammonia concentration reduces the retention of Ni. High distribution coefficients ( $> 9000$ ) were observed for ammonia solution concentrations below 1%. At 5% ammonia solution, the distribution coefficient declines rapidly.

#### 4.4.6 Extraction of interfering elements on dimethylglyoxime loaded resins

The uptake of a range of contaminating nuclides on XAD-7 loaded with dimethylglyoxime was investigated. The radioisotopes were dissolved in citrate solution to prevent precipitation of transition metals on adding ammonia solution. Ammonia solution was added to the buffer solution to produce a solution equivalent to 1% ammonia. The solution was split and one fraction was equilibrated with dimethylglyoxime loaded onto XAD-7 as described previously. The second fraction was equilibrated with untreated XAD-7 to provide a blank measurement. The solutions were equilibrated for 2 hours with constant mixing. The XAD-7 was removed by filtration through a Whatman GF/C filter and the amount of radionuclide present in the filtrate

was determined by gamma spectrometry. The amount of radionuclide present on the solid XAD-7 loaded with DMG was determined by the difference between the amount of radionuclide present in the filtrate of the DMG/XAD-7 material and the amount in the filtrate from the blank XAD-7 material. A distribution coefficient was then determined (Table 4.4).

**Table 4-4 : Distribution coefficients for different nuclides on DMG loaded XAD-7**

Radionuclide	Form	Distribution coefficient
<sup>241</sup> Am	Am(III)	2.2
<sup>133</sup> Ba	Ba(II)	2.3
<sup>109</sup> Cd	Cd(II)	< 1.0
<sup>139</sup> Ce	Ce(IV)	< 1.0
<sup>57</sup> Co	Co(II)	4.1
<sup>60</sup> Co	Co(II)	3.9
<sup>137</sup> Cs	Cs(I)	< 1.0
<sup>155</sup> Eu	Eu(II)	11.2
<sup>153</sup> Gd	Gd(III)	3.0
<sup>54</sup> Mn	Mn(II)	3.3
<sup>22</sup> Na	Na(I)	5.0
<sup>113</sup> Sn	Sn(IV)	6.4
<sup>85</sup> Sr	Sr(II)	< 1.0
<sup>88</sup> Y	Y(III)	4.2
<sup>65</sup> Zn	Zn(II)	< 1.0
<sup>63</sup> Ni	Ni(II)	9020

None of the possible interfering nuclides show significantly high distribution coefficients and would therefore be removed in washing solutions during the separation of nickel using a column prepared from a DMG loaded XAD-7. In any case many of these nuclides would precipitate out in the absence of the citrate buffer at these pH values and would therefore be removed via co-precipitation on iron hydroxide during the initial stages of analytical separation.

## 4.5 Strontium

### 4.5.1 Extraction of $^{90}\text{Sr}$ using Sr-resin

Strontium-90 was purified using a commercially available Sr resin (supplied by Hichrom, UK). The resin consists of 4,4'(5') bis(tert-butylcyclohexano)-18-crown-6 dissolved in octan-1-ol and supported on an inert Amberlite XAD-7 or Amberchrom CG71 support (Horwitz *et al*, 1991). The uptake of Sr from  $\text{HNO}_3$  solution increases with increasing  $\text{HNO}_3$  molarity (Figure 4.6). For example, Horwitz (1991) retained Sr from *Ca* 3M  $\text{HNO}_3$  whereas Ca was rapidly eluted. Breakthrough of Sr was observed after 13 free column volumes of 3M  $\text{HNO}_3$  had been passed through the column. Loading the Sr in 2M  $\text{HNO}_3$ -0.5M  $\text{Al}(\text{NO}_3)_3$  improved uptake of Sr with no breakthrough observed in 30 free column volumes. Possible problems include the uptake of Np, Pu and  $^{210}\text{Pb}$  on the Sr resin. These elements would seriously interfere with the  $^{90}\text{Sr}$  measurement and must be separated prior to the Sr being loaded onto the column.

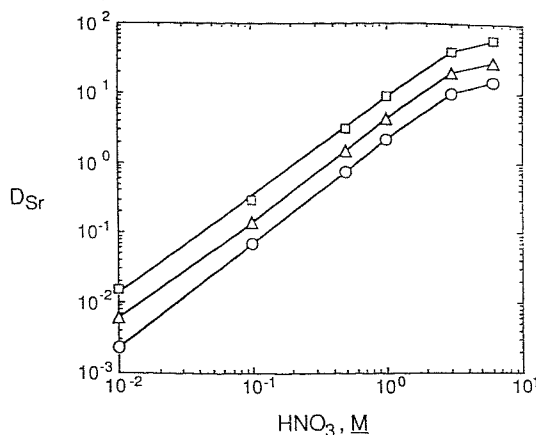


Figure 4.6 - Sr distribution between solutions of 4,4'(5') bis(tert-butylcyclohexano)-18-crown-6 in octanol-1-ol and nitric acid (T=25(C) (i) 0.1M (○) 0.2M (○) 0.4M (Reproduced from Horwitz *et al*, 1991)

Cobb (1994) showed that the uptake of Sr on Sr-resin® was seriously affected by the presence of potassium. To remove this interference, Sr may be precipitated as the oxalate at pH 3-4 along with the Ca in the sample solution (Figure 4.7). The Sr and Ca oxalates are then decomposed using a 3:1 mixture of nitric and perchloric acids. The resulting residue is then dissolved in 2M  $\text{HNO}_3$ -0.5M  $\text{Al}(\text{NO}_3)_3$  prior to loading on the Sr resin column.

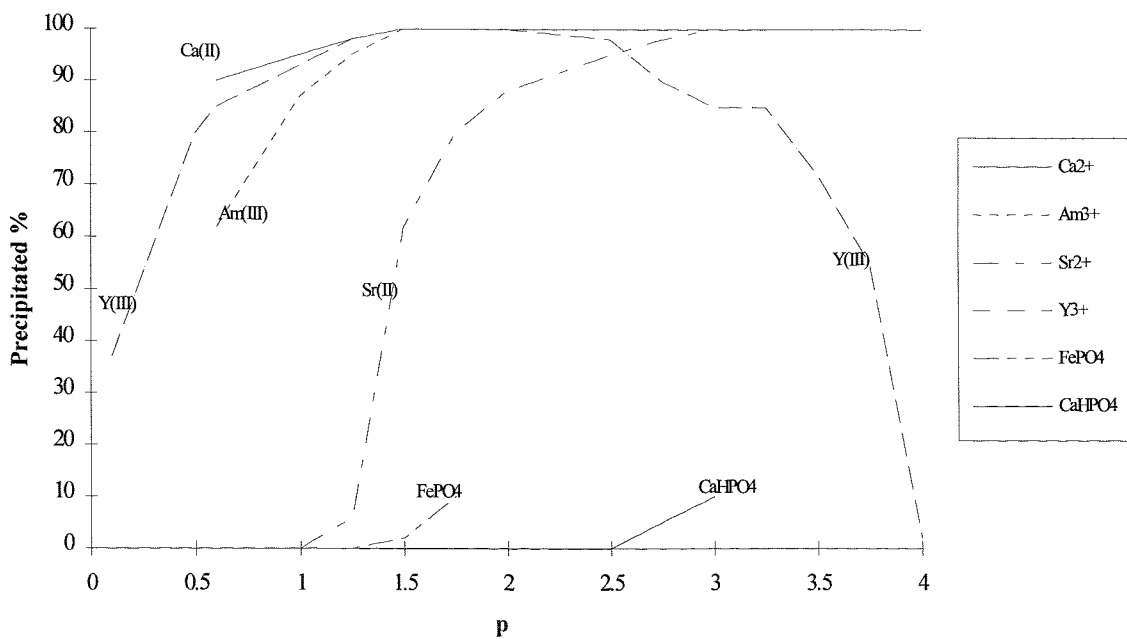


Fig 4.7 : pH dependence of metal oxalate precipitation (from Yamato, 1982)

#### 4.5.2 Adopted method for the purification of $^{90}\text{Sr}$

The waste fractions from the Ni purification chemistry were combined for separation of Sr. The pH of the solution was adjusted to pH 4.5 (the blue of bromocresol green indicator) with ammonia solution. 4% ammonium oxalate was added to precipitate strontium/calcium oxalate, which was isolated by centrifugation. The precipitate was dissolved in 5ml of concentrated  $\text{HNO}_3$  and transferred to a 20ml beaker. The solution was evaporated to dryness and the residue was dissolved in 3ml concentrated  $\text{HNO}_3$  and 1ml 70%  $\text{HClO}_4$ . This solution was evaporated to dryness to decompose oxalate and the residue was dissolved in 2ml 8M  $\text{HNO}_3$ -0.5M  $\text{Al}(\text{NO}_3)_3$ .

The  $\text{HNO}_3\text{-Al}(\text{NO}_3)_3$  solution was transferred to a 4 x 0.7cm Sr-resin<sup>®</sup> column previously conditioned with 8M  $\text{HNO}_3$ -0.5M  $\text{Al}(\text{NO}_3)_3$ . The beaker was washed with 2ml 8M  $\text{HNO}_3$ -0.5M  $\text{Al}(\text{NO}_3)_3$  and the washings were transferred to the column. The column was washed with 5ml 8M  $\text{HNO}_3$ -0.5M  $\text{Al}(\text{NO}_3)_3$  followed by 5ml 8M  $\text{HNO}_3$ . The Sr was then eluted with 10ml water into a tared 20ml polythene scintillation vial.

#### 4.6 Technetium-99

The development of an analytical technique for the separation of Tc from sediments has fallen into three parts

1. The study of the extraction of Tc into tri-n-octylamine (TnOA) and its application to Tc analysis in low-level waste
2. The incorporation of the Tc-TnOA extraction procedure into a chromatographic technique and the evaluation of this technique for routine separation
3. The development of a technique for the determination of Tc in environmental samples (Chapter 5).

The first two of these areas has been covered in detail through the preparation of two papers. The two papers are presented in turn in the following sections. The third paper on the analysis of  $^{99}\text{Tc}$  in environmental samples is reproduced in Chapter 5. It should be noted that this research has been performed with significant collaboration with other colleagues and where such collaboration has occurred the colleagues have been listed in the author list of the paper.

#### 4.7 Paper in *Radioactivity and Radiochemistry*, 7, 23 - 31 (1996):

### An Optimised Method for Technetium-99 Determination in Low Level Waste by Extraction Into Tri-n-octylamine

C J Dale<sup>1</sup>, P E Warwick<sup>2</sup> & I W Croudace<sup>2</sup>.

<sup>1</sup>NNC Ltd, Winfrith Technology Centre, Dorchester, Dorset, DT2 8DH

<sup>2</sup>School of Ocean & Earth Science, Southampton Oceanography Centre, European Way, Southampton,  
SO16 3NH

#### 4.7.1 Abstract

The paper describes the optimisation of the extraction of <sup>99</sup>Tc with tri-n-octylamine (TnOA) and its incorporation into a routine analytical method for the quantitative determination of <sup>99</sup>Tc in Low Level Waste (LLW). Extraction was found to be independent of TnOA concentration, sulphuric acid and hydrochloric acid concentrations and aqueous to organic ratios. The presence of nitric acid and nitrate anions significantly reduces the extraction efficiency. The incorporation of the extraction into an analytical scheme results in a technique capable of quantitatively separating Tc from a range of matrices and decontaminating the element from other commonly interfering radionuclides including <sup>106</sup>Ru.

#### 4.7.2 Introduction

Technetium, atomic number 43, was discovered in 1937 by Perrier and Segre. The element is not found in nature (except in minute quantities in uranium ore via the spontaneous fission of <sup>235</sup>U), but the radioisotope, <sup>99</sup>Tc, is produced by nuclear fission of <sup>235</sup>U (6 % fission yield). <sup>99</sup>Tc is, for all practical purposes, a pure beta emitter ( $E_{\max}$  295 keV) with a half-life of 213000 years (Browne and Firestone, 1986).

As a consequence of nuclear fuel reprocessing, <sup>99</sup>Tc is released into the environment in significant quantities. The radioisotope is also present in the environment from weapons testing in the 1950s and 1960s. <sup>99</sup>Tc is released into the marine environment where it is dispersed into the water column. However, Tc can be concentrated through uptake by marine biota and hence can enter the food chain (e.g. Schulte and Scoppa, 1987).

The determination of  $^{99}\text{Tc}$  in LLW is necessary in calculating repository inventories, especially considering its long half-life and probable abundance in the waste. However, the quantitative analysis of  $^{99}\text{Tc}$  in the diverse matrices present in LLW is problematic. The difficulties are compounded by the inevitable presence of other beta/gamma emitting radioisotopes which would interfere with the final measurement of the  $^{99}\text{Tc}$  beta activity by liquid scintillation counting if no separation was performed.

Tc as the pertechnetate anion ( $\text{TcO}_4^-$ ) can be isolated by extraction into a variety of organic solvents from acid media. Extraction of Tc from dilute sulphuric acid solutions into a 5% tri-n-octylamine (TnOA) in xylene mixture and back-extraction into sodium hydroxide solution has been used to purify Tc (Golchert and Sedlet, 1969 and Chen *et al*, 1990). Tc has also been extracted from nitric acid solutions using 30% TnOA in xylene, although the extraction efficiency is reduced at nitric acid concentrations above 4M (Hirano *et al*, 1989). Again the Tc was back-extracted into sodium hydroxide solution. Holm *et al* (1984) and Garcia-Leon (1990) used tributyl phosphate to extract Tc from dilute sulphuric acid solutions and Martin & Hylko (1987) extracted the tetraphenyl arsonium complex of Tc into chloroform.

Due to the high extraction efficiency of  $^{99}\text{Tc}$  into TnOA in xylene, the simplicity of the extraction technique and the good decontamination characteristics, this technique was chosen as the basis for the development of a rapid analytical method for quantifying  $^{99}\text{Tc}$  in LLW. In considering the use of yield monitors in the analysis it was found that no other radioisotope of Tc could be used as a yield monitor as all available radioisotopes of Tc, with the exception of  $^{99\text{m}}\text{Tc}$ , would interfere with the final measurement of  $^{99}\text{Tc}$  by liquid scintillation counting.  $^{99\text{m}}\text{Tc}$  was not used as a yield monitor due to the short half-life (6.02 hours) of the radioisotope which made its use uneconomic. To improve the Tc counting efficiency and shorten analysis time it was decided to mix the Tc in the TnOA/xylene phase directly with scintillant for counting and not to back-extract the Tc. The use of Re as a yield monitor was therefore also not possible. As no yield monitor was used it was necessary to develop the method so that > 95% recoveries were consistently achievable for the range of sample matrices being analysed.

#### 4.7.3 Methodology

##### 4.7.3.1 Reagents

Tri-n-octylamine and mixed xylenes were supplied by Aldrich Chemicals, Gillingham, Dorset, UK. Instagel, Ultima Gold and Ultima Gold AB scintillants were supplied by Packard Ltd, Pangbourne, Berks., UK. All other reagents were supplied by Fisher Scientific Ltd, Loughborough, Leics., UK.  $^{99}\text{Tc}$  was supplied as ammonium pertechnetate ( $473.6 \pm 7.1 \text{ kBq/g}$ ) in solution by Amersham International, Amersham, Berks.,

UK. The standard solution was diluted by mass to produce working solutions in the range of 4 - 10 kBq/g  $^{99}\text{Tc}$ .

#### 4.7.4 Extraction of Tc into tri-n-octylamine

The extraction of  $^{99}\text{Tc}$  was optimised by studying the effect of acid type, acid concentration, dissolved salt concentration, TnOA concentration and aqueous/organic ratios on the recovery of  $^{99}\text{Tc}$ .

##### 4.7.4.1 Effect of acid type and concentration

The extraction of Tc(VII) from hydrochloric acid, sulphuric acid and a mixture of nitric and sulphuric acids was studied. 10ml of the acid under investigation was spiked with a known activity of  $^{99}\text{Tc}$ . 5ml of 5% TnOA in xylene was added to the acid and the mixtures shaken for approximately 2 hours to ensure the extraction had attained equilibrium (although in practice it has been found that complete extraction of  $^{99}\text{Tc}$  is obtained after only 2 minutes). The mixtures were allowed to separate and 1ml of the organic layer was transferred to a polythene scintillation vial. 15ml of Instagel scintillant was added to the vial and the contents thoroughly mixed. The samples were counted on a Packard 2250CA liquid scintillation analyser to determine the amount of  $^{99}\text{Tc}$  extracted into the organic layer. The counting efficiency was determined by adding a spike of  $^{99}\text{Tc}$  to the sample in the scintillation vial and recounting. The difference in the two count rates due to the addition of the second spike was used to determine the counting efficiency. This assumed that the addition of the second spike had a negligible effect on the quench level of the sample and hence the associated counting efficiency. The results are shown in Figures P1-4.

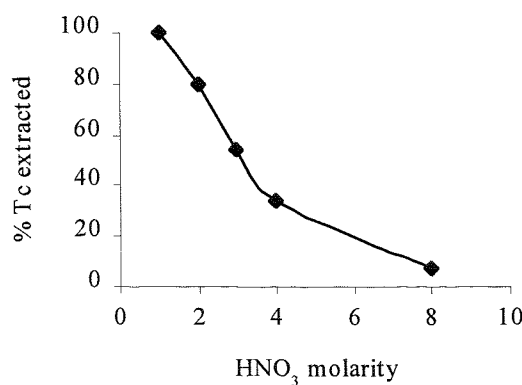


**Figure P1 : The effect of nitric acid molarity on the extraction of Tc(VII) into TnOA from nitric acid**

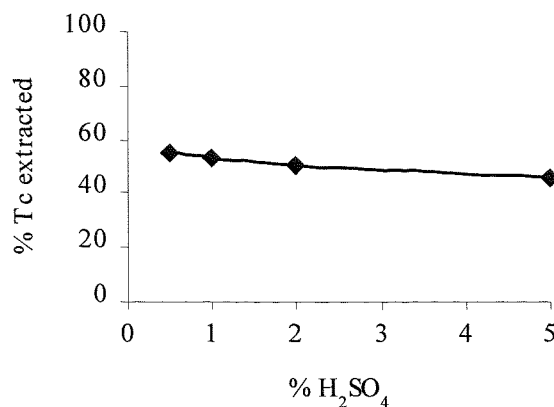


**Figure P2 : The effect of varying the % sulphuric acid on the extraction of Tc(VII) into TnOA from 3M nitric / sulphuric acids**

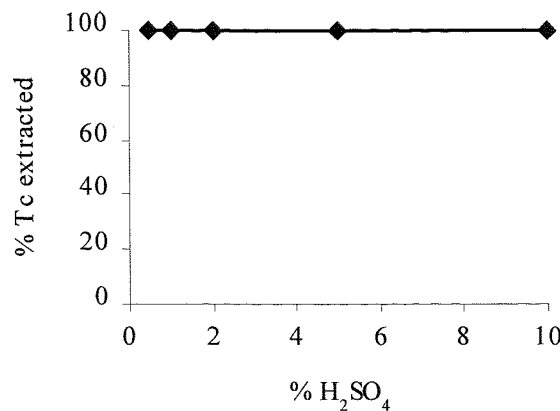


**Figure P3 : The effect of % sulphuric acid on the extraction of Tc(VII) into TnOA from sulphuric acid**

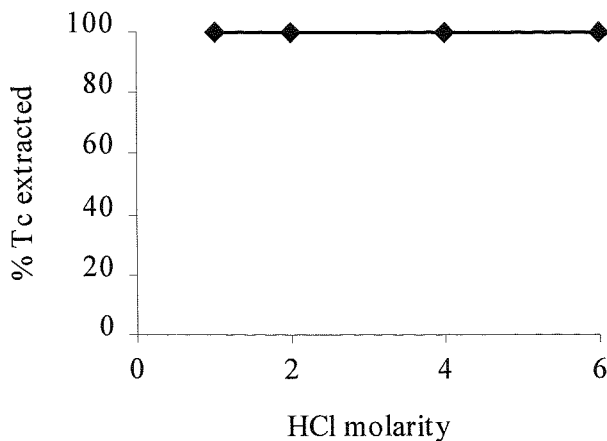


**Figure P4 : The effect of hydrochloric acid molarity on the extraction of Tc(VII) into TnOA from hydrochloric acid**

#### 4.7.4.2 The effect of TnOA volume and concentration on Tc(VII) extraction

To investigate the effect of TnOA volume on extraction, 7 samples were prepared by spiking 10ml of 1% sulphuric acid with a known activity of  $^{99}\text{Tc}$ . 50 $\mu\text{l}$  of 30% hydrogen peroxide was added to each sample to stabilise the Tc(VII) oxidation state. A range of volumes of 5% TnOA in xylene, ranging from 1 ml to 10ml, were added to the vials and the contents were equilibrated for approximately two hours with thorough mixing. The phases in the vial were allowed to separate and 1ml (0.5ml in the 1ml total sample) of the xylene phase was transferred to a 20ml scintillation vial. 10ml of Instagel scintillant was added to each sample and the samples were counted on the Packard 2250CA liquid scintillation analyser to determine the amount of extracted Tc. Counting efficiency was determined by spiking the sample with  $^{99}\text{Tc}$  and recounting.

In the second experiment, six samples were prepared by spiking 10ml of 1% sulphuric acid with  $^{99}\text{Tc}$  as pertechnetate. 50 $\mu\text{l}$  of 30% hydrogen peroxide and 5ml of TnOA in xylene were added. The concentration of TnOA was varied between 0.5% and 10%. The mixtures were allowed to equilibrate for approximately 2 hours and then allowed to stand. 1ml of the TnOA/xylene phase was transferred to a scintillation vial, 10ml of Instagel scintillant was added and the sample counted on the Packard 2250CA liquid scintillation analyser. Counting efficiency was determined by spiking the sample with a known amount of  $^{99}\text{Tc}$  and recounting. The results of the two investigations are shown in Figures P5 and P6.

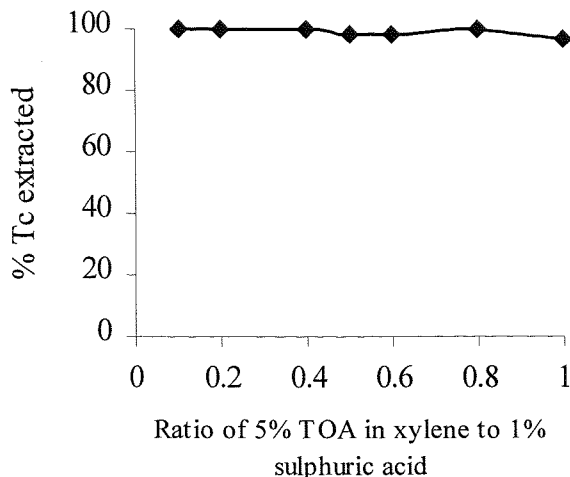


**Figure P5 : The effect of aqueous / organic ratios on the extraction of Tc(VII) into TnOA**

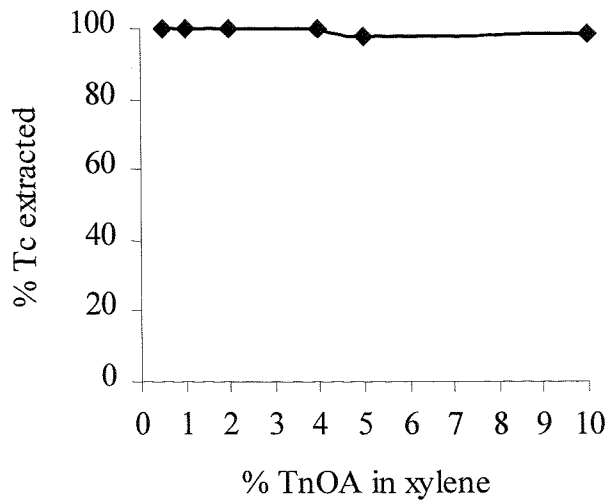


**Figure P6 : The effect of TnOA concentration on the extraction of Tc(VII) in TnOA**

#### 4.7.4.3 The effect of dissolved salt concentration on Tc(VII) extraction

10ml of 1M, 2M and 4M solutions of ammonium chloride and ammonium nitrate were prepared and spiked with a known activity of  $^{99}\text{Tc}$ . Each sample was acidified with 0.5ml of concentrated sulphuric acid and 50l of 30% hydrogen peroxide was added. 5ml of 5% v/v TnOA in xylene was added and the mixtures allowed to equilibrate with constant mixing for 2 hours. The phases were allowed to separate and 1ml of the

TnOA/xylene phase and 10ml of Instagel scintillant was transferred to a 20ml scintillation vial for counting to determine the amount of  $^{99}\text{Tc}$  extracted.

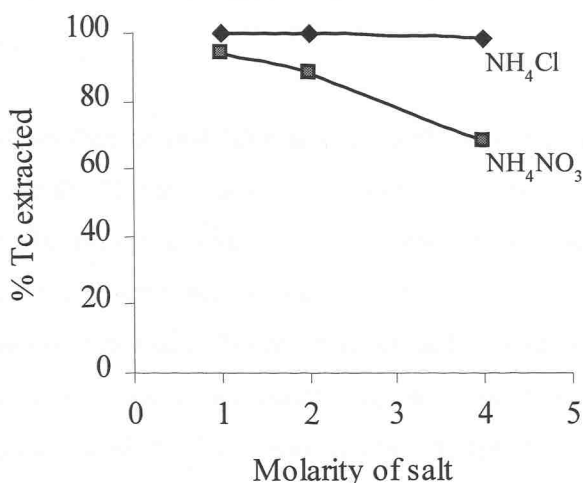


Figure P7 : The effect of dissolved salts on the extraction of Tc(VII) into TnOA

#### 4.7.4.4 Determination of $^{99}\text{Tc}$ liquid scintillation counting efficiency

In all measurements, the liquid scintillation counting efficiency of  $^{99}\text{Tc}$  in the sample/scintillant mixture is determined by spiking the sample after initial counting with a known activity of  $^{99}\text{Tc}$  and recounting the sample. The increase in count rate is used to determine the counting efficiency. However, the  $^{99}\text{Tc}$  in the sample is associated with the organic xylene phase prior to addition of the scintillant whereas the spike is added as an aqueous solution. This may lead to a variation in counting efficiency between the  $^{99}\text{Tc}$  associated with the sample and that associated with the spike.

To check the validity of this approach to counting efficiency determination 5ml of 2M sulphuric acid was spiked with a known activity of  $^{99}\text{Tc}$ . The solution was extracted twice with 5ml of 5% TnOA in xylene. The two extracts were combined and 1ml of the organic phase was mixed with 15ml of Ultima Gold. 1ml of the aqueous phase was mixed with 15ml of Ultima Gold AB (which shows superior mixing characteristics with acidic solutions). This was counted to show that more than 99% of  $^{99}\text{Tc}$  had extracted into the organic phase. The organic phase was then counted and the counting efficiency assuming 100% extraction was determined. The organic phase was then spiked with a known activity of  $^{99}\text{Tc}$  in aqueous solution and recounted. A second counting efficiency based on the increase in count rate after spiking was determined. The counting efficiency for  $^{99}\text{Tc}$  associated with the organic extraction was calculated as  $101 \pm 4\%$ . Spiking of the sample gave a counting efficiency of  $98 \pm 3\%$ . This confirmed that spiking was a suitable method for determining counting efficiency of the sample.

#### 4.7.5 Method for the determination of $^{99}\text{Tc}$

The optimised extraction procedure described above was incorporated into an analytical scheme for the quantification of  $^{99}\text{Tc}$  in LLW.

Between 5 - 20g of sample (depending on matrix) is leached with nitric, hydrochloric, or a mixture of both acids. The sample is filtered and the filtrate diluted to a known volume with deionised water. An aliquot of the dilution is mixed with 0.5ml conc. nitric acid, 3 drops of 30% hydrogen peroxide and 0.5ml of 10mg/ml Fe (as iron chloride) in a 50ml centrifuge tube. The sample is heated on a water bath at around 50°C for 5 minutes. The sample is diluted to 30ml with deionised water and 5ml of 0.88 S.G. ammonia solution is added. The sample is centrifuged, the supernatant (containing the Tc) is decanted into a clean stoppered tube and 1.5ml of 1.84 S.G. sulphuric acid is added. 5ml of 5% v/v TnOA in xylene is added, the stopper replaced and the sample spin mixed for 2 minutes. The two phases are allowed to separate and the upper organic phase is transferred to a labelled sample container. A further 5ml of TnOA in xylene is added to the aqueous phase and the extraction repeated. The organic phase from the second extraction is combined with the first extract. A known volume (typically 1ml, although up to 10ml will mix with the scintillant) of the organic extract is mixed with 10ml of Ultima Gold or equivalent scintillant and the sample counted using liquid scintillation analysis. After counting the sample is spiked with a known activity of  $^{99}\text{Tc}$  (in no more than 0.1ml of standard solution) and recounted to determine the counting efficiency.

#### 4.7.6 Decontamination factors for interfering radionuclides

Decontamination factors were determined by spiking a blank sample with a known activity of the radioisotope under investigation. The sample was then analysed using the method described above and the amount of radionuclide in the final Tc fraction was determined. The following radionuclides (at specified activities) did not give a count rate above instrument background and therefore would not interfere with  $^{99}\text{Tc}$  measurements at a limit of detection of 0.1Bq/ml of leachate. The radionuclides investigated were  $^{45}\text{Ca}$  (1300Bq),  $^{55}\text{Fe}$  (7800Bq),  $^{60}\text{Co}$  (8400Bq),  $^{90}\text{Sr}$ (13100Bq),  $^{125}\text{Sb}$  (5000Bq),  $^{129}\text{I}$  (4340Bq),  $^{133}\text{Ba}$  (10600Bq),  $^{137}\text{Cs}$  (8400Bq),  $^{144}\text{Ce}$ (3200Bq),  $^{232}\text{U}$  (350Bq),  $^{239}\text{Pu}$  (2970Bq),  $^{243}\text{Am}$  (209Bq).

#### 4.7.7 Typical recoveries for a variety of sample matrices

A range of sample types, spiked previously with  $^{99}\text{Tc}$ , were analysed using the above technique. Typical recoveries of Tc are given in Table P1.

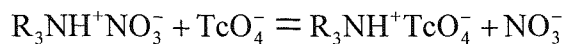
Table P1 : Typical recoveries of  $^{99}\text{Tc}$  for a range of matrices

Matrix	Mass/volume analysed	Recovery $^{99}\text{Tc}$
Sediment	11g	55%, 59%
Nitric Acid spiked	5ml	99%
Tissues/Paper	17g	102%
Tissues	12g	100%
Paper/Tissues	4g	102%
Mop strands/string	10g	99%
Plastic/rubber	10g	102%
Plastic gloves/overshoes	5g	104%
Acidified effluent	5ml	94%
Glass	32g	87%
Rock/cement	1g	90 - 104% (n=9)

Method uncertainties were estimated to be approximately 5%, which accounts for the observed recoveries greater than 100%.

#### 4.7.8 Discussion

It has been shown that the extraction of  $^{99}\text{Tc}$  from solutions of sulphuric and hydrochloric acid of various concentrations is quantitative. However, the presence of nitric acid significantly reduces the extraction efficiency. This is probably due to the ion-pair formation of the protonated tri-n-octylamine with the nitrate ion and subsequent competition for ion pair formation with pertechnetate and not to a change in the degree of protonation of the amine group. This is confirmed by the reduced extraction of pertechnetate in the presence of ammonium nitrate at constant acid concentration. The competition between nitrate and pertechnetate is represented in the equation below.



Dissolved ammonium chloride has no significant effect on  $^{99}\text{Tc}$  extraction. The ratio of acid to organic phase and TnOA concentration also has no significant effect on the extraction efficiency of  $^{99}\text{Tc}$ .

Counting efficiencies for the samples analysed ranged from 96-98% (counting window 2-295 keV) dropping to around 90% when the lower limit of the counting window was increased to exclude chemiluminescence (counting window 8-295 keV). No significant variation in efficiency was noted between different scintillant

types and between 10ml and 15ml of scintillant mixed with 1ml of organic sample. The choice of scintillant type for each experiment was determined mainly by availability of the scintillants at the two laboratories.

Using the method described above quantitative and rapid separations of  $^{99}\text{Tc}$  from a range of leachates having low dissolved solids was achieved. Leachates containing high dissolved solid contents (such as sediment) gave reduced recoveries of  $^{99}\text{Tc}$ . The sediments (moistened with conc. ammonia solution) were gradually heated to 400°C in a muffle furnace after spiking, and it is possible that the low recoveries were due to volatilisation of the  $^{99}\text{Tc}$ . It has been found that the inclusion of a carbonate precipitation prior to solvent extraction may also improve the recoveries of  $^{99}\text{Tc}$  by removing the significant quantities of calcium associated with sediments that may interfere with the solvent extraction stages. A modified version of the method, including the carbonate precipitation was used to analyse a water sample in the 1995 National Physical Laboratory Intercomparison exercise. A measured value of  $43 \pm 4$  Bq/kg was found, compared with the NPL reported value of  $40.1 \pm 0.5$  Bq/kg (Jerome *et al*, 1995). This was considered a satisfactory agreement considering the low levels of  $^{99}\text{Tc}$  present.

Interference from a range of radionuclides has been found to be negligible. The behaviour of  $^{106}\text{Ru}$  in this separation has not been tested directly, although samples containing  $^{106}\text{Ru}$  have been analysed and no evidence for interference has been observed.

The method described above has been accredited by the National Measurement Accreditation Service (NAMAS) at the Taywood laboratories and is routinely used in the analysis of LLW.

#### 4.7.9 Acknowledgements

This work was part-funded under HMIP contract PECD 7/9/609. The authors would like to thank Dr A G Howard, Dept of Chemistry, University of Southampton for helpful comments on the manuscript.

#### 4.7.10 References

Browne E. and Firestone R.B. (1986). Table of radioactive isotopes. John Wiley, New York.

Chen Q., Dahlgaard H., Hansen H.J.M. and Aarkrog A. (1990). Determination of  $^{99}\text{Tc}$  in environmental samples by anion exchange and liquid-liquid extraction at controlled valency. *Analyt. Chim. Acta*, **228**, 163-167.

Garcia-Leon M. (1990). Determination and levels of  $^{99}\text{Tc}$  in environmental and biological samples. *J. Radioanalyst. Nucl. Chem. Articles*, **138** (1), 171-179.

Golchert N.W. and Sedlet J. (1969). Radiochemical determination of technetium-99 in environmental water samples. *Anal. Chem.*, **41** (4), 669-671.

Hirano S., Matsuba M. and Kamada H. (1989). The determination of  $^{99}\text{Tc}$  in marine algae. *Radioisotopes*, **38**, 186-189.

Holm E., Rioseco J. and Garcia-Leon M. (1984) Determination of  $^{99}\text{Tc}$  in environmental samples. *Nuclear Instruments and Methods in Physics Research*, **223**, 204-207.

Jerome S.M. Allen D.R., Dean J.C.J., Keightley J.D., Perkin E.M.E and Woods M.J. (1995) Environmental Radioactivity Intercomparison 1995. NPL report RSA(EXT)60, National Physical Laboratory, Teddington, Middlesex, UK.

Martin J.E. and Hylko J.M. (1987) Measurement of  $^{99}\text{Tc}$  in low-level radioactive waste from reactors using  $^{99\text{m}}\text{Tc}$  as a tracer. *Appl. Radiat. Isot.*, **38** (6), 447-450.

Schulte E.H. and Scoppa P. (1987). Sources and behavior of technetium in the environment. *Sci. Total Environ.*, **64**, 163-179.

*4.7.11 Addendum to paper :*

**An Optimised Method for Technetium-99 Determination in Low Level Waste by Extraction Into Tri-n-octylamine**

Following the publication of this paper in *Radioactivity and Radiochemistry*, we were notified that the original NPL value for  $^{99}\text{Tc}$  in the intercomparison standard was incorrectly quoted by NPL. The true value for the standard was given as 44 Bq/kg showing far better agreement with the value of 43 Bq/kg measured in this study. A amendment was subsequently published in *Radioactivity and Radiochemistry*.

#### 4.8 Paper - In preparation :

### Solid-Phase Extraction of Technetium-Amine Complexes onto C<sub>18</sub>-Silica and its application to the isolation of <sup>99</sup>Tc

P E Warwick<sup>1</sup>, I W Croudace<sup>1</sup>, A G Howard<sup>2</sup> & J A Caborn<sup>1</sup>

<sup>1</sup>*School of Ocean & Earth Science, Southampton Oceanography Centre, European Way, Southampton, SO16 3NH*

<sup>2</sup>*Dept. of Chemistry, University of Southampton, Southampton, SO14 1BJ*

#### 4.8.1 Abstract

The extraction of Tc tripentylamine complexes onto C<sub>18</sub>-silica solid-phase extraction columns is described and evaluated for the determination of <sup>99</sup>Tc in the presence of other isotopes. The Tc-amine complex is quantitatively extracted from sulphuric acid on a C<sub>18</sub>-silica extraction column and can be recovered from the column by elution with dilute alkali. A clean separation of Tc from all likely contaminants was achieved using the solid-phase extraction columns. The use of C<sub>18</sub>-silica solid-phase extraction columns is a viable and attractive alternative to the use of organic solvents in the isolation of <sup>99</sup>Tc.

#### 4.8.2 Introduction

Technetium-99 is a major fission product (approximately 6% fission yield) which is routinely discharged to the environment in the authorised discharges from nuclear facilities. The determination of <sup>99</sup>Tc in liquid effluents and solid waste is therefore an important part of statutory monitoring programmes.

A number of methods have been published for the determination of technetium (Tc) isotopes in which the element is separated from an aqueous solution by solvent extraction of a pertechnetate-(tertiary amine) ion-pair complex (Chen *et al*, 1990; Golchert and Sedlet, 1969; Hirano *et al*, 1989). Dale *et al* (1996) have shown that the extraction of Tc into tri-n-octylamine is quantitative from sulphuric and hydrochloric acids over a range of concentrations, but not from nitric acid solutions. The extraction of Tc from sulphuric and hydrochloric acids was found to be independent of the amine concentration in the organic solvent and the relative proportions of aqueous and organic phases. The solvent extraction of Tc into tri-n-octylamine allows rapid separation of the element and effective decontamination from interfering radioisotopes. However,

solvent extraction has a number of disadvantages as the technique is relatively labour intensive and produces significant quantities of organic waste that requires controlled disposal.

A novel approach to avoiding solvent extraction is to form an organic complex with Tc that can be subsequently extracted onto a commercially available C<sub>18</sub> silica cartridge. The aim of this study was to develop a technique for the pre-concentration of the Tc-amine complex by solid-phase extraction thereby avoiding the use of organic solvents and making the separation more suitable for the routine analysis of <sup>99</sup>Tc in large sample batches.

Although tri-n-octylamine (TnOA) has been extensively used in the isolation of Tc, it is immiscible with water. Lower tertiary amines are sufficiently soluble in the aqueous solution containing the Tc and form ion-pair complexes that are readily extractable into an organic phase. Maeck *et al* (1961) investigated the extraction of a range of elements, including Tc, as ion-pair complexes with more water-soluble tertiary amines (propyl-, butyl- and hexyl-amines). This describes the development of a solid-phase extraction procedure based upon the use of these smaller tertiary amine ion-pair agents

#### *4.8.3 Experimental and Results*

##### *4.8.3.1 Reagents*

Unless otherwise stated, all reagents were of analytical grade or equivalent. Tributylamine and tripentylamine (general laboratory grade) were supplied by Aldrich Chemicals Ltd, Gillingham, Dorset. The Isolute<sup>TM</sup> C<sub>18</sub> columns (500mg C<sub>18</sub>-silica with a loading of 18.6% C<sub>18</sub>) were supplied by Jones Chromatography, Hengoed, Mid-Glamorgan. <sup>99</sup>Tc (as ammonium pertechnetate) was supplied by Amersham International Plc (Buckinghamshire, UK). Instagel( scintillant was supplied by Packard UK, (Pangbourne, Berks, UK). Gold Star scintillant was supplied by Meridian (Epsom, Surrey, UK). All other reagents were supplied by Fisher Scientific (Loughborough, Leics, UK).

##### *4.8.3.2 Mixing of tributylamine and tripentylamine with 2M sulphuric acid*

A preliminary study was carried out to investigate the mixing of the amines with 2M sulphuric acid. Sulphuric acid was chosen as previous studies (Dale *et al*, 1996) had shown that Tc-amine extraction efficiencies from this medium were high. 10ml of 2M sulphuric acid was transferred to a glass vial and a known volume of the tertiary amine was added. The mixture was shaken and checked for any evidence of separation. This was repeated with increasing volumes of amine until the sulphuric acid became saturated and the excess amine separated out.

Up to 400 $\mu$ l of tripentylamine and 7000 $\mu$ l of tributylamine were found to dissolve in 10ml of sulphuric acid.

#### 4.8.3.3 Extraction of the butyl- and pentyl-amine complexes of Tc

The extractability of the Tc-amine complexes formed with tributylamine and tripentylamine was determined by measuring the percentage of the Tc-amine complex that extracted into xylene. The effect of amine concentration on the extractability of the complex was studied.

10ml 2M sulphuric acid was spiked with a known activity of  $^{99}\text{Tc}$  (nominally 500Bq; 0.015 $\mu\text{Ci}$ ). The samples were then mixed with a given volume of either tributylamine or tripentylamine. 50 $\mu\text{l}$  of 30% hydrogen peroxide was added to each sample to ensure that the Tc was present as the pertechnetate anion. 5ml of xylene (mixed isomer) was added to each sample and the contents were mixed for 2 hours on a slowly rotating wheel to attain equilibrium. The phases were allowed to separate and 1ml of the xylene was transferred to a clean 20ml scintillation vial. 10ml of Instagel<sup>TM</sup> scintillant was added to each vial, the contents were thoroughly mixed and the samples were counted on a Packard 2250CA liquid scintillation counter. The counting efficiency was determined by spiking one of the samples with a known amount of  $^{99}\text{Tc}$  and the sample was recounted. Sample quench over the range of samples was constant.

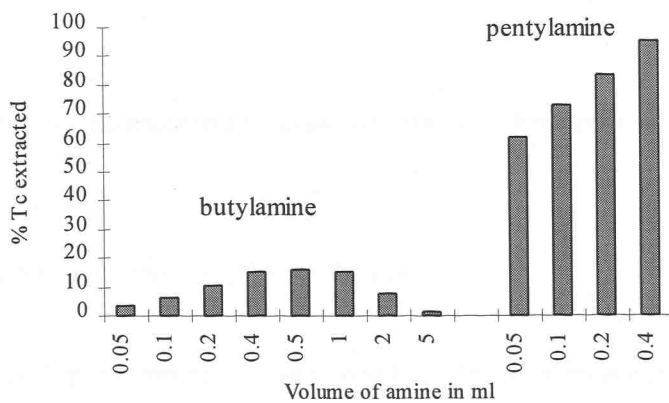


**Figure P1 : Effect of amine type and volume (ml) in 10ml of sulphuric acid on the extraction of Tc-amine into xylene**

Although the tributylamine mixes more readily with 2M sulphuric acid, the tripentylamine complex of Tc is extracted more efficiently into xylene (Figure P1). Tripentylamine was therefore used for all subsequent experiments.

#### 4.8.3.4 Solvent extraction of $^{99}\text{Tc}$ amine complexes

9.6ml of nitric, hydrochloric or nitric acids at various concentrations were spiked with a known amount of  $^{99\text{m}}\text{Tc}$  tracer. The mixture was spiked with 400 $\mu\text{l}$  of amine and the solution was thoroughly mixed. 10ml of xylene was added and the mixture was shaken for 1 hour. The two phases were allowed to separate and the amount of  $^{99\text{m}}\text{Tc}$  remaining in the aqueous phase was determined using a high purity germanium gamma spectrometry system.

Although sulphuric acid was chosen for this study, it is apparent (Figure P2) that extraction of the Tc-tripentylamine complex should be practical from dilute HCl (up to 4M) and to a lesser extent from dilute  $\text{HNO}_3$ .

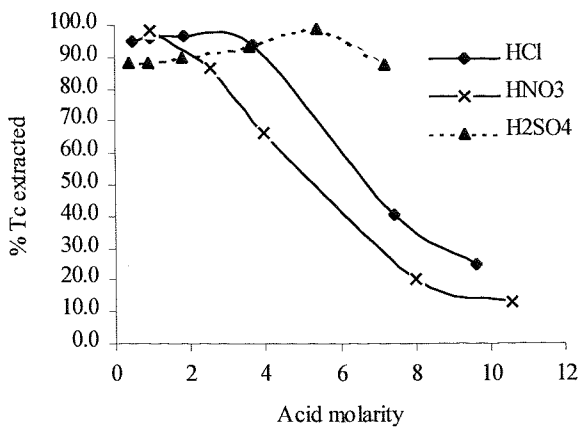
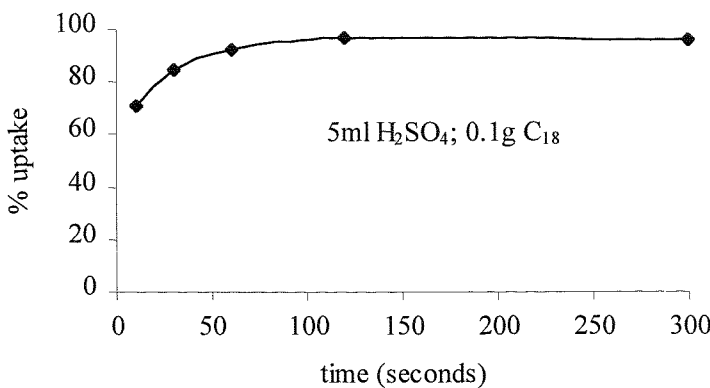


Figure P2 : Extraction of Tc-tripentylamine ion-pair complex from various acid types/molarities

#### 4.8.3.5 Uptake of the Tc-Tripentylamine complex on $\text{C}_{18}$ -silica

The rate of uptake of the Tc-tripentylamine complex onto  $\text{C}_{18}$ -silica was determined by spiking a solution of 4% tripentylamine in 2M sulphuric acid with a known amount of  $^{99\text{m}}\text{Tc}$  and shaking 10ml of this solution with 0.1g of  $\text{C}_{18}$ -silica. After a set time, the mixture was filtered through a 0.2  $\mu\text{m}$  PTFE filter and the amount of  $^{99\text{m}}\text{Tc}$  present in the aqueous phase was determined by gamma spectrometry. The rate of uptake was found to be fast with 70% of  $^{99\text{m}}\text{Tc}$  being extracted after only 10 seconds and 100% of the  $^{99\text{m}}\text{Tc}$  being removed from the aqueous phase after 60 seconds (Figure P3). The extraction kinetics were therefore not a limiting factor in the use of this procedure.



**Figure P3 : Rate of uptake of the Tc-tripentylamine ion-pair complex on C<sub>18</sub> silica**

Isolation of the <sup>99</sup>Tc-tripentylamine complex on a C<sub>18</sub> silica column was investigated. 10ml of 2M sulphuric acid was spiked with 400μl of tripentylamine and a known activity (approximately 500Bq; 0.015μCi) of <sup>99</sup>Tc. This solution was loaded onto an Isolute<sup>TM</sup> C<sub>18</sub> column which had previously been conditioned with 10ml 2M sulphuric acid mixed with 400μl of tripentylamine. The eluent obtained during the loading process was retained. The column was washed with nine 5ml fractions of 2M sulphuric acid (a total of 45ml 2M sulphuric acid passing through the column). Each fraction of eluent was retained separately and 1ml of each fraction was mixed with 15ml Instagel<sup>TM</sup> scintillant and counted on a Packard 2250CA liquid scintillation counter. The counting efficiency was determined by spiking one of the samples with a known activity of <sup>99</sup>Tc and recounting the sample. These measurements were used to determine the amount of <sup>99</sup>Tc lost during the washing stages (Figure P4a).

In a second experiment the above procedure was repeated. However, this time the column was washed with seven 10ml fractions of sulphuric acid containing 400μl of tripentylamine. Again each eluent fraction was retained separately and the <sup>99</sup>Tc activity determined by mixing 1ml of each fraction with 15ml of Gold Star scintillant. No breakthrough of <sup>99</sup>Tc was observed in any of the fractions.

In a third experiment, 10ml of 2M sulphuric acid was mixed with 400μl of tripentylamine and 500Bq (nominally 0.015μCi) of <sup>99</sup>Tc. The mixture was loaded onto an Isolute<sup>TM</sup> C<sub>18</sub> column. The column was washed with four portions of 10ml of 2M sulphuric acid containing 400μl of tripentylamine. 1ml of each fraction was mixed with 15ml of Instagel scintillant and counted using liquid scintillation analysis. Four 10ml fractions of 1M ammonia solution were also passed through the column to remove the Tc extracted on the column. Both fractions were evaporated to incipient dryness at around 50°C. The residue was dissolved in 1ml of 2M sulphuric acid and mixed with 15ml of Gold Star scintillant. The <sup>99</sup>Tc activity in the two fractions was determined by liquid scintillation analysis. Counting efficiency was determined as described previously.

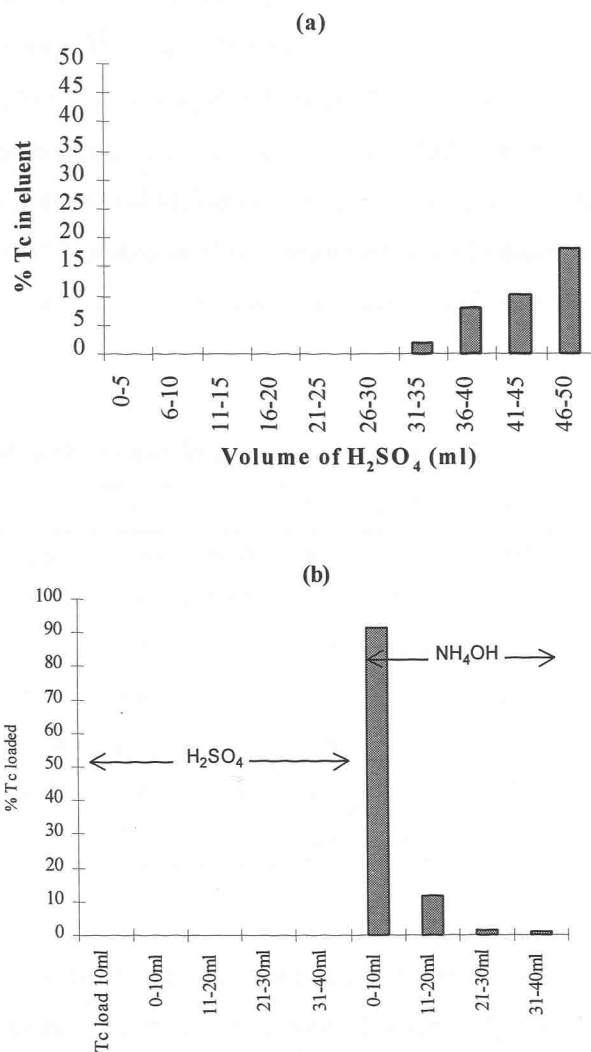


**Figure P4 :**  $^{99}\text{Tc}$  breakthrough from a  $\text{C}_{18}$  column loaded with  $^{99}\text{Tc}$ -tripentylamine after washing with (a) 2M sulphuric acid and (b) 2M sulphuric acid containing tripentylamine followed by 1M ammonia  
*Column dimensions 1 x 0.5 cm Isolute  $\text{C}_{18}$ -silica. Columns contained 500mg  $\text{C}_{18}$ -silica with a loading of 18.6%  $\text{C}_{18}$*

The Tc extracted on the  $\text{C}_{18}$  column is slowly removed by successive additions of 2M sulphuric acid to the column (Figure P4a). This is probably due to the slow leaching of tripentylamine from the column. The addition of tripentylamine to the sulphuric acid prevents this gradual elution and in excess of 80ml of washings can be passed through the column without breakthrough of the Tc (Figure P4b). The Tc can be eluted from the column using a dilute alkali such as 1M ammonia solution that de-protonates the tertiary amine destroying the ion-pair complex. The concentration of ammonia had a negligible effect on the rate of Tc elution.

#### 4.8.3.6 Decontamination of $^{99}\text{Tc}$ from interfering radioisotopes using the $\text{C}_{18}$ column

A mixture of gamma emitting radioisotopes consisting of  $^{241}\text{Am}$ ,  $^{109}\text{Cd}$ ,  $^{139}\text{Ce}$ ,  $^{57}\text{Co}$ ,  $^{60}\text{Co}$ ,  $^{137}\text{Cs}$ ,  $^{203}\text{Hg}$ ,  $^{54}\text{Mn}$ ,  $^{113}\text{Sn}$ ,  $^{85}\text{Sr}$  and  $^{88}\text{Y}$  was dissolved in 10ml of 2M  $\text{H}_2\text{SO}_4$  containing 400 $\mu\text{l}$  tripentylamine. The mixed gamma

solution, commercially available as a calibration solution, is suitable for representing most metal groups found in nuclear waste streams. The solution was transferred to a C<sub>18</sub> column that had previously been conditioned with 10ml of H<sub>2</sub>SO<sub>4</sub> containing 400µl tripentylamine. The eluent from this loading was retained and measured by gamma spectrometry on a Canberra Nuclear HPGe well detector. The column was washed with 5ml portions of the sulphuric acid/tripentylamine mixture and each fraction counted on the gamma spectrometry system. This was repeated until no gamma emitting isotopes were detected in the eluent. The percentage of each isotope in the eluent compared to the load solution was calculated and results are shown in Table P1.

**Table P1 : Elution of selected radiosiotopes from a C<sub>18</sub> column with 2M H<sub>2</sub>SO<sub>4</sub>-4% tripentylamine**

	Volume	<sup>241</sup> Am	<sup>109</sup> Cd	<sup>139</sup> Ce	<sup>57</sup> Co	<sup>60</sup> Co	<sup>137</sup> Cs	<sup>203</sup> Hg	<sup>54</sup> Mn	<sup>113</sup> Sn	<sup>85</sup> Sr	<sup>88</sup> Y
E1(load)	10ml	96.60	81.01	96.58	96.48	96.51	96.23	1.97	96.49	87.82	96.03	96.55
E2	5ml	3.40	18.09	3.42	3.52	3.49	3.77	2.04	3.50	10.57	3.97	3.45
E3	5ml	n.d.	0.31	n.d.	n.d.	n.d.	n.d.	80.66	0.01	0.45	n.d.	n.d.
E4	5ml	n.d.	0.25	n.d.	n.d.	n.d.	n.d.	11.95	n.d.	0.31	n.d.	n.d.
E5	5ml	n.d.	0.34	n.d.	n.d.	n.d.	n.d.	1.97	n.d.	0.54	n.d.	n.d.
E6	5ml	n.d.	n.d.	n.d.	n.d.	n.d.	n.d.	0.70	n.d.	n.d.	n.d.	n.d.
E7	5ml	n.d.	n.d.	n.d.	n.d.	n.d.	n.d.	0.70	n.d.	0.31	n.d.	n.d.

n.d. not detected

Complete removal of the majority of contaminants is achieved after only 10ml of washings. <sup>109</sup>Cd and <sup>113</sup>Sn tailed through the column more than the other isotopes but were effectively removed after a total of 20ml solution had passed through the column. Only <sup>203</sup>Hg was retained to some extent on the column, with the first 15ml of washings only containing 4% of the total activity. However, after 40ml of washings only 0.7% of the original <sup>203</sup>Hg was eluted.

#### 4.8.3.7 Separation of Ru from Tc using a C<sub>18</sub> column

The determination of <sup>99</sup>Tc by LSC is complicated by the presence of the beta emitting isotope <sup>106</sup>Ru. The presence of stable <sup>99</sup>Ru also interferes isobarically with the measurement of <sup>99</sup>Tc by ICP-MS. It was therefore necessary to study the behaviour of Ru on the C<sub>18</sub> column. 1mg of Ru (VIII) standard was added to 10ml of 2M sulphuric acid containing 400µl of tripentylamine. The solution was transferred to a C<sub>18</sub> column which had previously been conditioned with 2M sulphuric acid containing 400µl of tripentylamine. The column was washed with five 10ml aliquots of 2M H<sub>2</sub>SO<sub>4</sub>/amine followed by one 10ml aliquot of 1M NH<sub>4</sub>OH. Each of the fractions was diluted with 2% nitric acid and Ru was determined by ICP-MS. The brown colour of the Ru standard was visibly removed from the column during the loading phase and first

two washes. The remaining fractions were colourless in appearance. This was confirmed by the ICP-MS measurements.

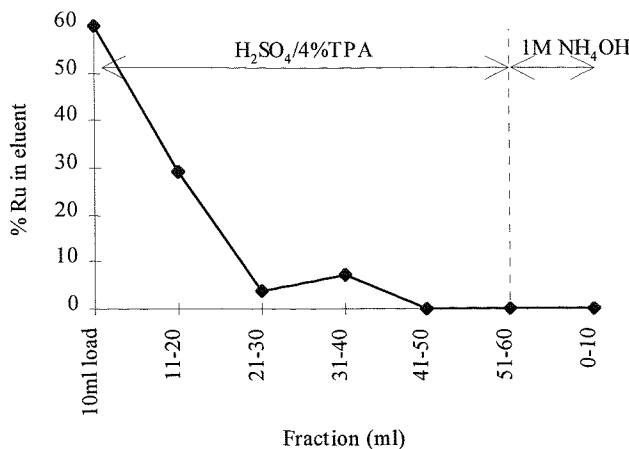


**Figure P5: Removal of Ru from a C<sub>18</sub> column (column dimensions as in Figure P4)**

#### 4.8.4 Comparison of the C<sub>18</sub>-silica based separation with other chromatographic techniques

Preconcentration of Tc may be achieved using anion exchange chromatography. Tc is retained under a wide range of conditions and can only be eluted from the column using concentrated nitric acid or a solution of thiourea. Although anion exchange chromatography has been widely used for the preconcentration of Tc, Ru will follow Tc and will interfere with both radiometric (via <sup>106</sup>Ru) and mass spectrometric (via stable <sup>99</sup>Ru) measurement of <sup>99</sup>Tc.

TEVA resin, supplied by Eichrom Industries, has been shown to quantitatively extract Tc from aqueous solution (Horwitz *et al*, 1995) and has been used in a method for <sup>99</sup>Tc analysis in effluents (Banavali *et al*, 1995) and environmental samples (Butterworth *et al*, 1995). Tc is retained from dilute nitric and hydrochloric acid with many other interfering radionuclides including Ru being rapidly eluted. Large sample volumes may be passed through the column without breakthrough of Tc making the column ideal for the analysis of river waters and drinking waters. Compared with the C18-silica based separation described above, TEVA resin also has the advantage that it does not require the addition of an organic compound to the load and wash solutions and hence does not produce such a complex waste. Both TEVA and C18 silica may be mixed directly with liquid scintillation cocktails producing sources suitable for counting by liquid scintillation counting with similar counting efficiencies for <sup>99</sup>Tc. However, strong nitric acid is required to elute the Tc and subsequent evaporation of this eluent may lead to losses of volatile pertechnic acid. Evaporation of the ammonia eluent from the C<sub>18</sub>-silica column is less likely to result in the loss of Tc

especially if the temperature of this evaporation is carefully controlled. The cost of the TEVA resin is also a disadvantage in the commercial analysis of large numbers of samples.

#### *4.8.5 Conclusions*

The formation of a tripentylamine complex of Tc in aqueous solution and subsequent extraction of the complex onto a C<sub>18</sub> column has many advantages over the conventional solvent extraction of Tc into a mixture of tri-n-octylamine in xylene. The C<sub>18</sub> column quantitatively extracts Tc from a 2M sulphuric acid solution containing tripentylamine. The column can then be washed thoroughly with the sulphuric acid/tripentylamine mixture to remove contaminating radioisotopes including Ru. Elution of the Tc can then be effected using a dilute alkali. If ammonia is used to elute the Tc this eluent can be evaporated to dryness and the residue containing the Tc can be dissolved in 2M nitric acid prior to ICP-MS determination of the Tc. Alternatively the Tc can be measured by liquid scintillation analysis.

The described extraction chromatographic technique does not produce organic solvent waste and the column and washings can be disposed of safely. Additionally, the separation is less labour-intensive than solvent extraction and a number of columns can be operated simultaneously. The technique takes longer than the solvent extraction technique for single sample analysis and where a rapid turnaround of results is required the solvent extraction technique still has advantages. It is proposed that the C<sub>18</sub> column technique detailed above could replace the frequently used solvent extraction stage for the determination of Tc in many sample matrices.

#### *4.8.6 Acknowledgements*

The authors would like to thank Dr R Carpenter, Analytical Services Group, AEA Technology, Harwell for supporting this study.

#### 4.8.7 References

Banavali A.D., Raimondi J.M., Moreno E.M. and McCurdy D.E. (1995) The determination of technetium-99 in low-level radioactive waste. *Radioact. Radiochem.*, , 6(3), 26-35

Butterworth J.C., Livens F.R. and Makinson P.R. (1995). Development of a method for the determination of low levels of technetium-99. *Sci. Total Env.*, 173/174, 293-300

Chen Q., Dahlgaard H., Hansen H.J.M. & Aarkrog A. (1990) Determination of  $^{99}\text{Tc}$  in environmental samples by anion exchange and liquid-liquid extraction at controlled valency. *Anal. Chim. Acta*, 228, 163 - 167.

Dale C.J., Warwick P.E., & Croudace I.W. (1996). An optimised method for Technetium-99 determination in low level waste by extraction into tri-n-octylamine. *Radioact. Radiochem*, 7, 23 - 31.

Goldchurt N.W., & Sedlet J. (1969) Radiochemical determination of technetium-99 in environmental water samples. *Anal. Chem*, 41 669 - 671.

Hirano S., Matsuba M. and Kamada H. (1989). The determination of  $^{99}\text{Tc}$  in marine algae. *Radioisotopes*, 38, 186-189.

Horwitz E.P., Dietz M.L. Chiarizia R., Diamond H., Maxwell S.L. and Nelson M.R. (1995) Separation and preconcentration of actinides by extraction chromatography using a supported liquid anion exchanger: application to the characterisation of high-level nuclear waste solutions.. *Anal. Chim. Acta*, , 310, 63-78.

Maeck W.J., Booman G.L., Kussy M.E. & Rein J.E. (1961). Extraction of the elements as Quaternary Propyl, Butyl and Hexyl amine complexes. *Anal. Chem*, 33 1775 - 1750.

#### 4.9 Use of TEVA resin for the purification of Tc

TEVA resin has become widely used for the extraction-chromatographic separation of  $^{99}\text{Tc}$ . TEVA resin consists of the amine-based extractant Aliquat-336 adsorbed onto an inert polyacrylamide support. Under highly acidic conditions, TEVA will extract tetravalent actinides as well as Tc. However, under weakly acidic conditions the distribution coefficient for the actinides drops rapidly whilst the distribution coefficient for Tc rises. Re is adsorbed along with Tc making it a suitable yield monitor for Tc under these separation conditions (Butterworth *et al*, 1995). As well as efficiently extracting Tc from a range of solution types, TEVA resin shows no uptake of Ru. Good separation factors for Tc and Ru are therefore obtained.

Tc is also retained under alkaline conditions and hence can be used to separate Tc from the alkaline supernatant resulting from the precipitation of Fe as  $\text{Fe}(\text{OH})_3$ . Distribution coefficients were determined for ammonia concentrations ranging from 0.01% to 5% (percentage of 0.88 Sp.Gr. ammonia mixed with water). pH values ranged from 8.8 to 11.8. 10ml of the ammonia solution was spiked with 2,000 Bq of  $^{99\text{m}}\text{Tc}$  and shaken with 0.1g of TEVA resin for one hour. The samples were filtered through a Whatman 540 filter and the activity in the aqueous fraction measured by gamma spectrometry. The activity associated with the resin was then calculated and used to determine the distribution coefficient. In all cases the distribution coefficient was calculated as greater than 40,000.

Ni and Sr will also be present in this alkaline supernatant but will not be retained on the TEVA column. Ni and Sr may then be subsequently separated from the column raffinate using techniques described in Sections 4.4 and 4.5.

Elution of Tc is somewhat more problematic. Nitric acid is the most common eluent with acid strengths greater than 8M being required (Butterworth *et al*, 1995). However, for low-level analysis using ICP-MS and for liquid scintillation counting, the nitric acid must be evaporated. This potentially could lead to losses of Tc by volatilisation and care is required during such an evaporation stage. Alternatively, TEVA resin may be mixed directly with liquid scintillation cocktail prior to counting.

## 4.10 Conclusions to Chapter 4

Solvent extraction techniques have been identified that are suitable for the separation of  $^{55}\text{Fe}$ ,  $^{63}\text{Ni}$  and  $^{99}\text{Tc}$ . Iron-55 may be effectively extracted as its chloro-complex from HCl at concentrations  $>6\text{M}$ . The Fe is extracted as the ion pair  $\text{H}^+\text{FeCl}_4^-$ . A range of oxygen-containing solvents including ethers, esters and ketones has been used in the extraction of Fe. Of the three solvents investigated, ethyl acetate shows the highest partition coefficient and loading capacity although the solvent also shows the highest extraction of Sn. If extraction of Sn must be avoided, di isopropyl ether is more suitable although the partition coefficient for Fe is significantly lower.

Nickel-63 was readily extracted by dimethylglyoxime, which forms an extractable chelate under ammoniacal conditions. Potential interferences included Pd and possibly Co, which also form dimethylglyoxime complexes. Technetium-99 may be effectively extracted into trioctylamine from a range of acidic solutions. The mechanism of extraction is an ion pair formation with the Tc being extracted by the protonated amine as the pertechnetate anion.

In all cases, the solvent extraction techniques identified could be adapted into an extraction chromatographic technique. Extraction chromatographic separations in general provided a far better alternative to solvent extraction with easier processing of larger sample batches and improved separation of the analyte from interferences. The use of extraction chromatography compared to solvent extraction also reduced the volumes of organic solvents used and eliminated the requirement for specific disposal routes. An extraction chromatographic technique using a commercially available extractant was also studied for  $^{90}\text{Sr}$ .

Routine application of extraction chromatography for  $^{55}\text{Fe}$  separation was limited to samples of low Fe content. For ferrous and environmental samples, and in particular sediment, where Fe contents are relatively high, the loading capacity of the extraction chromatographic material was restrictive with prohibitively large columns being required to permit extraction of all the Fe present. In such instances, solvent extraction, with its higher loading capacities, was the preferred method of separation.

Extraction chromatographic separation of  $^{99}\text{Tc}$  was readily achieved by using both the  $\text{C}_{18}$  silica approach of extracting the Tc-amine complex from aqueous solution and also by using the commercially available TEVA resin. However, solvent extraction of  $^{99}\text{Tc}$  into trioctylamine was the preferred option in the current study as the extraction procedure produces an organic solution of  $^{99}\text{Tc}$  that readily mixes with scintillant prior to liquid scintillation counting.

#### 4.11 References

Butterworth J.C., Livens F.R. and Makinson P.R. (1995). Development of a method for the determination of low levels of technetium-99. *Sci. Total Env.*, **173/174**, 293-300

Horwitz E.P., Dietz M.L. and Fisher D.E. (1991). Separation and preconcentration of strontium from biological, environmental and nuclear waste samples by extraction chromatography using a crown ether. *Anal. Chem.*, **63**, 522-525.

Testa C, Desideri D, Meli M.A., Roselli C.(1991). Extraction chromatography in radioecology. *Radioact. Radiochem.*, **2(4)**, 46-54.

## Chapter 5

# **Sequential separation of beta emitters**

## 5 Sequential separation of beta emitters

### 5.1 Introduction

Having optimised the purification and measurement techniques for individual pure beta-emitting radioisotopes it was necessary to combine these techniques to produce a scheme for the sequential separation of  $^{55}\text{Fe}$ ,  $^{63}\text{Ni}$ ,  $^{90}\text{Sr}$  and  $^{99}\text{Tc}$  from all other contaminating radioisotopes and from each other. Such a separation scheme should also isolate the radioisotopes from the bulk sample matrix. Such a sequential separation scheme permits the analysis of all four isotopes in materials where there is a limited sample size available for analysis or in samples where the levels of the isotopes are low hence allowing more of the sample to be allocated for a given analysis. In both instances there is insufficient material to perform four separate analyses. Sequential separation schemes also permit the analysis of the four isotopes in a more cost efficient manner improving analytical turn-round times and reducing the amount of hands-on time required from the analyst.

The sequential separation schemes developed fall into two categories

1. Schemes for the separation of  $^{55}\text{Fe}$ ,  $^{63}\text{Ni}$ ,  $^{90}\text{Sr}$  and  $^{99}\text{Tc}$  from relatively simple matrices such as low-level waste leachate and liquid effluents.
2. Analysis of  $^{55}\text{Fe}$ ,  $^{63}\text{Ni}$ ,  $^{90}\text{Sr}$  and  $^{99}\text{Tc}$  in environmental samples mainly sediments.

The first of these categories is discussed in a paper (submitted to a conference on the application of extraction chromatography held in Geel, Belgium in November 1998). Although suitable for a wide range of low-level waste characterisation applications, the sample treatment prior to chemical separation was not suitable for environmental samples such as sediments. The development of the sequential separation scheme for environmental samples is therefore discussed separately in Section 5.3. Finally it was found that the analysis of  $^{99}\text{Tc}$  in environmental samples required quite specific sample pretreatment and was best performed on a separate sub-sample. The analysis of  $^{99}\text{Tc}$  in environmental samples is therefore described separately in the form of a paper published in *Analytica Chimica Acta* in 1999 (Section 5.4).

## 5.2 Extraction chromatography techniques in the sequential separation of pure beta-emitting radioisotopes in low-level waste

Based on a paper presented at the International workshop on the application of extraction chromatography in radionuclide measurement, Geel, Belgium, November 1998.

### 5.2.1 *Abstract*

The determination of radioisotopes decaying by pure beta emission and electron capture such as  $^{55}\text{Fe}$ ,  $^{63}\text{Ni}$ ,  $^{90}\text{Sr}$  and  $^{99}\text{Tc}$  is an important requirement of many comprehensive waste monitoring programmes. Unlike alpha and gamma spectrometry, no effective spectrometric technique is available for the identification of beta-emitting radioisotopes as the decay energy is distributed between the beta particle and anti-neutrino. Identification of any pure beta emitters present must necessarily be a qualitative assessment of beta energy following an element-specific chemical separation.

This paper describes the sequential separation and assay of pure beta-emitting radioisotopes employing extraction chromatographic-based techniques. The application of extraction chromatography to replace conventional solvent extraction-based techniques has permitted rapid sequential separation of the nuclides of interest with improved decontamination factors and a significant reduction in reagent volumes, particularly organic solvents.

### 5.2.2 *Introduction*

Iron-55,  $^{63}\text{Ni}$ ,  $^{90}\text{Sr}$  and  $^{99}\text{Tc}$  are produced in significant quantities during routine reactor operations and are therefore potentially present in low-level solid and liquid effluent wastes. The qualitative detection and quantitative determination of these radioisotopes is hindered by the lack of any appreciable gamma emissions. Positive identification and determination of these nuclides therefore relies on a combination of element-specific chemistries and beta energy windowing. Many chemical separation techniques have been developed based on solvent extraction and ion exchange chromatography. However, the techniques employing extraction chromatography combine the selectivity of specific solvent extraction systems with the practical benefits afforded by a column-based separation technique. In addition, the use of extraction chromatography results in improved separation efficiencies of the analyte from other radioisotopes and a significant reduction in the volume of waste organic solvents generated.

The application of extraction chromatography to the determination of pure beta emitters is not novel. Nickel-63 has been routinely separated on a dimethylglyoxime based column (Testa *et al*, 1991), <sup>90</sup>Sr on a commercially available crown-ether extraction column (Sr resin –Horwitz *et al*, 1991) and <sup>99</sup>Tc on a quaternary amine-based extraction column (TEVA resin – Bohnstedt *et al*, 1998). Although Fe has been separated on TRU resin (Bohnstedt *et al*, 1998) and trioctylamine-based resins (Testa *et al*, 1991), working capacities are low (around 4-5mg) and many routine determinations of <sup>55</sup>Fe still rely heavily on the use of solvent extraction. This paper describes an extraction chromatographic separation of <sup>55</sup>Fe based on di-isobutyl ketone (DIBK) and discusses a sequential separation of <sup>55</sup>Fe, <sup>63</sup>Ni, <sup>90</sup>Sr and <sup>99</sup>Tc using extraction chromatographic based techniques.

### 5.2.3 *Methodology*

#### *Reagents*

All reagents used were analytical grade. Anion exchange resin (quaternary amine type, 100-200 mesh; 8% cross linked), TEVA resin, Ni specific resin and Sr specific resin were supplied by Hichrom Industries, UK. Gold Star scintillant and polythene vials were supplied by Meridian, Epsom, UK. Ultima Gold AB scintillant was supplied by Packard UK Ltd, Pangbourne, UK. All other reagents were supplied by Aldrich Chemicals, Gillingham, Dorset, UK

#### *Column preparation*

All columns used in this study were 5 x 0.7cms I.D. The chromatographic materials employed in this study are summarised in Table 5.1. All chromatographic materials were slurried in the loading medium and transferred to the column.

**Table 5.1 : Extraction chromatographic materials**

Analyte	Extractant	Support	Preparation	Capacity <sup>(a)</sup>
Fe	Di isobutyl ketone (DIBK)	Amberlite XAD-7	2g of DIBK slurried with 2g XAD7	70mg max.
Ni	Dimethylglyoxime (DMG)	Amberlite XAD-7	1.5g DMG dissolved in acetone. 4g of XAD-7 added and mixture warmed with constant stirring to evaporate the acetone	2 mg working (Eichrom 1998)
Sr	Tert-butyl dicyclohexano-18-crown-6	Amberlite XAD-7	Commercially available (Sr-resin®)	5 –6 mg working (Eichrom 1998) 24 mg max.
Tc	Aliphatic quaternary amine	Amberlite XAD-7	Commercially available (TEVA resin)	12 mg <sup>(b)</sup>

<sup>a</sup>maximum capacity of a standard 2ml of resin material for stable analogue of the analyte<sup>b</sup>determined for Pu only(Eichrom, 1998)

### Sample preparation

The sample (usually a tissue swab, although a range of samples including concrete and metalwork may be analysed) is placed in a wide mouth flask and the sample oxidised by wet oxidation with  $\text{HNO}_3$  and  $\text{H}_2\text{O}_2$ . If  $^{99}\text{Tc}$  is being determined wet oxidation is not appropriate. In this case the sample is acid leached without prior treatment or, for organic-rich samples, moistened with ammonia and then ignited in a muffle furnace gradually ramping the temperature from 200°C to 550°C. The residue is dissolved in a suitable mineral acid and reserved for chemical analysis

### Sequential separation utilising extraction chromatography

A summary of the sequential separation is shown in Figure 5.1. 1mg Ni, 2mg Sr and, for low Fe samples, 1mg Fe are added to each sample as carriers and chemical yield monitors.  $^{99\text{m}}\text{Tc}$  is also added as a yield monitor for  $^{99}\text{Tc}$ . Chemical recoveries of Fe, Ni and Sr were determined by measuring an aliquot of the sample before and after separation using atomic absorption spectrometry (AAS).

### 5.2.4 Sample counting

Measurements of beta activity were performed using a Wallac 1220 ‘Quantulus’ low-level liquid scintillation counter.  $^{55}\text{Fe}$  was dissolved in a minimum of 2M  $\text{H}_3\text{PO}_4$ , to produce a colourless solution, and transferred to a 22ml polythene liquid scintillation vial. Ultima Gold AB scintillant was added as this scintillant showed the highest capacity for  $\text{H}_3\text{PO}_4$  of a range of scintillants tested. Up to 200mg of stable Fe could be loaded into the scintillant in this way (Warwick *et al*, 1998). The purified  $^{63}\text{Ni}$  fraction was dissolved in dilute HCl and transferred to a scintillation vial with water. The dilute acid sample was then mixed with Gold Star scintillant. The eluent from the Sr resin column containing  $^{90}\text{Sr}$  was collected directly into a scintillation vial. The vial was then counted repeatedly by Cerenkov counting over a two-week period to monitor the in-growth of the  $^{90}\text{Y}$  daughter. The TEVA resin, quantitatively containing the  $^{99}\text{Tc}$  and  $^{99\text{m}}\text{Tc}$  yield monitor, was transferred into a plastic 22ml vial with 1ml of Milli-Q water. 18ml of Gold Star scintillant was then added and the sample counted on a HPGe gamma spectrometry system to determine the recovery of  $^{99\text{m}}\text{Tc}$ . The sample was then left for one week to allow the  $^{99\text{m}}\text{Tc}$  to decay before determining the  $^{99}\text{Tc}$  activity on the liquid scintillation counter (Wigley *et al*, 1999). The counting conditions for each nuclide are summarised in Table 5.2. All samples were dark-adapted prior to liquid scintillation counting.

**Table 5.2 : Counting conditions for the Wallac 1220 ‘Quantulus’ liquid scintillation counter**

	$^{55}\text{Fe}$	$^{63}\text{Ni}$	$^{90}\text{Sr}$	$^{99}\text{Tc}$
			( $^{90}\text{Y}$ daughter)	
Sample description	2M $\text{H}_3\text{PO}_4$ + Ultima Gold AB	Dil HCl + Gold Star	Dil $\text{HNO}_3$ No scintillant	TEVA resin + Gold Star
Window	1-200	10-400	1-1024	125-647
Background	1.7 cpm	4.8 cpm	0.9 cpm	2.4 cpm
Efficiency	15-45%	70%	65%	90%
Counting bias	Low	Low	Low	High
PSA/PAC		Disabled		
Count time	60 mins	60 mins	60 mins	60 mins
Limit of detection	0.03*	0.03	0.02	0.02
	(Bq/sample)			

PSA – pulse shape analysis; PAC – pulse amplitude comparison

Limits of detection ( $L_D$ ) calculated as defined by (Currie, 1968).

\* $^{55}\text{Fe}$   $L_D$  will depend on the Fe content of the sample – (see Warwick *et al*, 1998)

### 5.2.5 Discussion

#### i) Iron-55

The DIBK/XAD-7 column provided a highly selective method for  $^{55}\text{Fe}$  separation.  $^{55}\text{Fe}$  was effectively separated from all contaminating radioisotopes including Sn (known to partially follow Fe during conventional solvent extraction). As relatively small volumes of DIBK were present in the column the loading capacity was correspondingly lower than for solvent extraction. For a 5 x 0.7cm column the maximum loading is approximately 70mg. This is sufficient for most effluents and low-level wastes but would be unacceptably low in the separation of Fe from certain ferrous wastes.

#### ii) Technetium-99

The TEVA column quantitatively retains Tc from alkaline solutions permitting direct loading of the ammoniacal supernatant without any evaporation stages. Elution of Tc from the TEVA column is difficult, requiring 8-16M  $\text{HNO}_3$ , which must subsequently be removed by evaporation (Butterworth *et al*, 1995). This has been simplified by mixing the TEVA resin directly with the liquid scintillant. Recoveries of 80-100% are readily obtainable. The extractant appears to dissolve in the liquid scintillant producing a stable, homogenous mixture for counting. The resin support becomes effectively translucent in the scintillant cocktail and has little effect on the observed counting efficiency.

#### iii) Nickel-63

The load and first wash solutions from the TEVA column are passed directly onto the Ni column. The two columns may be run in a stacked configuration further reducing the overall analytical time. The addition of ammonium citrate maintains any traces of other transition metals in solution. The Ni column is washed thoroughly with 1% ammonia solution prior to elution of the Ni with 6M HCl. The Ni-dimethylglyoxime complex is soluble in excess ammonia hence ammonia concentrations must not exceed 1%. Co forms a soluble dimethylglyoxime complex and, if present in high quantities,  $^{60}\text{Co}$  is found in the purified  $^{63}\text{Ni}$  fraction. The inclusion of the anion exchange stage significantly improves the decontamination of  $^{60}\text{Co}$  from the  $^{63}\text{Ni}$ . Co is effectively retained on the anion exchange resin from 9M HCl as the  $\text{CoCl}_4^-$  complex whilst Ni passes through the column as a cationic species. The presence of dimethylglyoxime in the solution will prevent Co from being effectively adsorbed and the complexant must first be destroyed with *aqua regia*.

#### iv) Strontium-90

The purification of  $^{90}\text{Sr}$  using the Sr resin offers considerable benefits in terms of safety and

time over the conventional fractional precipitation of nitrates from fuming nitric acid. Potassium is known to compete with Sr uptake on the resin. Precipitation of Sr as the oxalate removes K and prevents subsequent interference on the Sr column. The precipitation of the oxalate also effects preconcentration of the Sr from the bulk solution. In this study the oxalate was destroyed with a 3:1 mixture of nitric and perchloric acids although other investigators have not included this step, instead simply dissolving the oxalate into the loading solution. The addition of  $\text{Al}(\text{NO}_3)_3$  to the loading medium increases the  $\text{NO}_3^-$  concentration and improves Sr uptake on the resin (Horwitz *et al.* 1991).

### 5.2.6 *Conclusions*

The introduction of a sequential separation scheme for the determination of  $^{55}\text{Fe}$ ,  $^{63}\text{Ni}$ ,  $^{90}\text{Sr}$  and  $^{99}\text{Tc}$  has reduced the analysis time and has permitted the determination of all the radioisotopes on a single small sample. Chemical recoveries were marginally lower than those found for individual element separation although the recoveries were still satisfactory. In practice the sequential separation technique has reduced the amount of analyst time spent on a measurement and permits the analysis of a greater number of samples. Incorporation of extraction chromatography has also removed the need for hazardous acids and environmentally unfriendly solvents.

### 5.2.7 *Acknowledgements*

This study has been supported by the Geosciences Advisory Unit, Southampton Oceanography Centre, Southampton, UK and the NNC Laboratories, Winfrith, UK (under Environment Agency contract NATCON\_147).

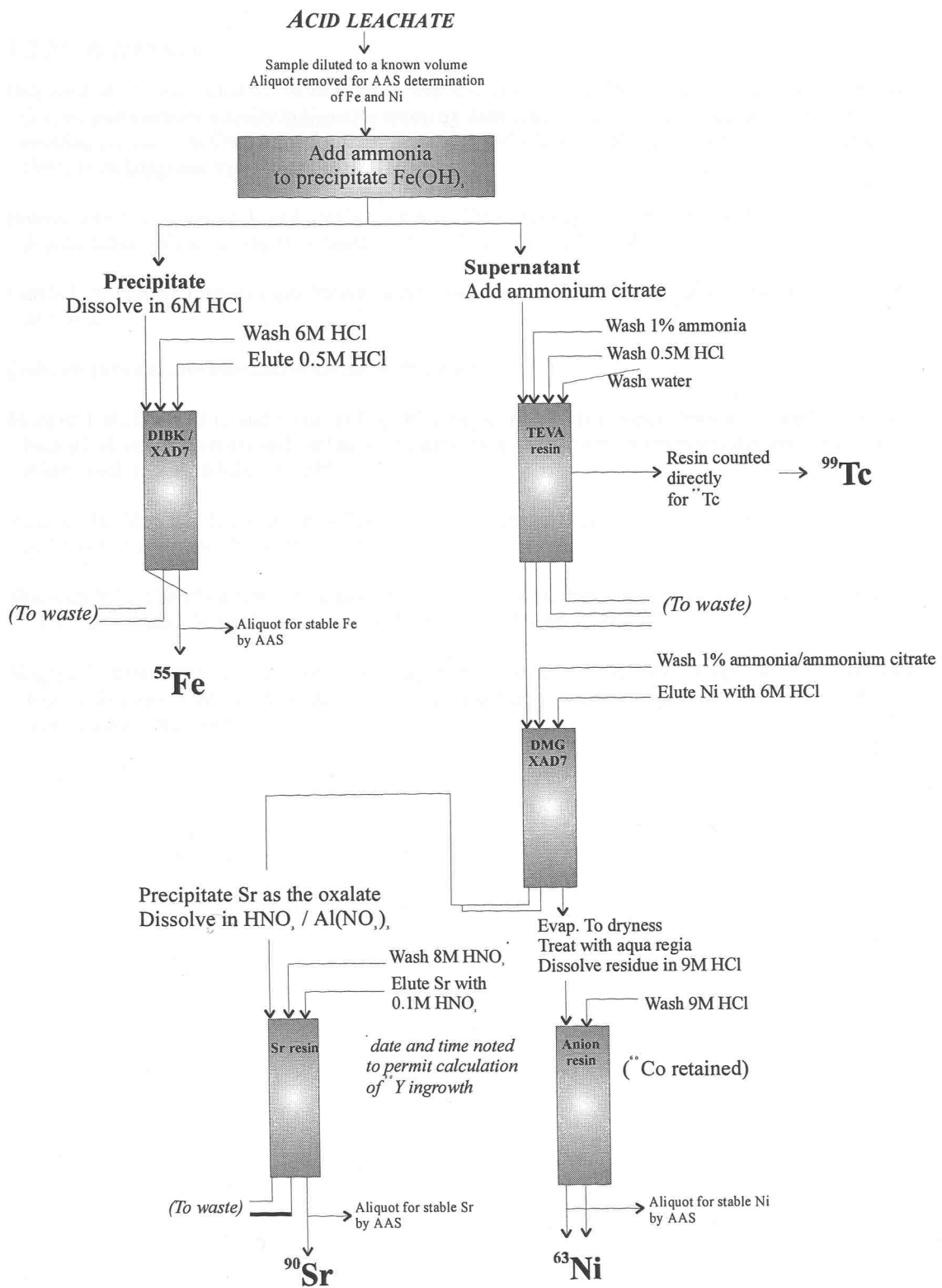


**Figure 5.1 : Summary of the sequential separation scheme as used for low-level waste analysis**

### 5.2.8 References

Bohnstedt A., Langer-Lüer M., Stuhlfauth H. and Aumann D.C. (1998). Radiochemical characterisation of low- and medium-activity radioactive waste by destructive assay of long-lived alpha and beta emitting nuclides. In Odoj R., Baier J., Brennecke P. and Kühn K. (eds). Radioactive waste products 1997, Forschungszentrum Jülich GmbH, Germany.

Butterworth J.C., Livens F.R. and Makinson P.R. (1995). Development of a method for the determination of low-levels of technetium-99. *Sci. Tot. Env.*, **173-174**, 293-300.

Currie L.A. (1968). Limits of qualitative detection and quantitative determination. *Anal. Chem.*, **40** (3), 586-593.

Eichrom personal communication and sales literature

Horwitz E.P., Dietz M.L. and Fisher D.E. (1991). Separation and preconcentration of strontium from biological, environmental and nuclear waste samples by extraction chromatography using a crown ether. *Anal. Chem.*, **63**(5), 522-525.

Testa C, Desideri D, Meli M.A., Roselli C.(1991). Extraction chromatography in radioecology. *Radioact. Radiochem.*, **2** (4), 46-54.

Warwick P.E., Croudace I.W. and Bains M.E.D. (1998). An Optimised Method for the Measurement of <sup>55</sup>Fe Using Liquid Scintillation Analysis. *Radioact. Radiochem.*, **9**(2), 19-25.

Wigley F., Warwick P. E., Croudace I.W., Caborn J., Sanchez A.L. (1998). An optimised method for the routine determination of technetium-99 in environmental samples by liquid scintillation counting – *Anal. Chim. Acta*, **380**, 73-82..

### 5.3 Sequential separation of $^{55}\text{Fe}$ , $^{63}\text{Ni}$ , $^{90}\text{Sr}$ and $^{99}\text{Tc}$ from sediments

#### 5.3.1 *Introduction*

The separation scheme derived for low-level radioactive wastes (Section 5.2) is not suitable for the analysis of sediments without some modification. Firstly, the concentration of stable Fe in sediments is too high to permit purification of Fe by an extraction chromatographic method. A solvent extraction-based procedure with a high stable Fe loading capacity was therefore adopted. Secondly, the sample preparation stage required careful optimisation to avoid the loss of volatile  $^{99}\text{Tc}$ . The final separation of  $^{99}\text{Tc}$  on TEVA resin is still an option although higher counting efficiencies and lower limits of detection are achieved by extracting the  $^{99}\text{Tc}$  into tri octylamine in xylene and then mixing the organic extract directly with scintillant. The modified procedure is discussed below. The separation and analysis of  $^{99}\text{Tc}$  is discussed separately in Section 5.4.

#### 5.3.2 *Proposed separation scheme*

##### 5.3.2.1 *Sample preparation*

An aliquot of the sediment sample was weighed and ignited at 550°C. The ignited sample was spiked with stable Ni and Sr and the sample was acid leached with 40ml of *aqua regia* at 50 °C overnight. The sample was centrifuged and the supernatant was transferred to a 150ml beaker. The residue was then leached with a fresh 40ml portion of *aqua regia* for 2 hours. The sample was centrifuged and the supernatant combined with the first leachate. The solution was evaporated to approximately 10ml and diluted to 50ml with water. 1ml of this solution was removed and diluted to 10ml for stable Fe determination by ICP-AES. The remaining solution was transferred to a beaker with water washings.

##### 5.3.2.2 *Initial separation by iron (III) hydroxide scavenging*

The pH of the leachate was adjusted to between 5 – 7 with 0.88 S.G. ammonia resulting in the precipitation of  $\text{Fe(OH)}_3$ . The precipitate was isolated by centrifugation and the supernatant was retained for  $^{63}\text{Ni}$  and  $^{90}\text{Sr}$  analysis. The  $\text{Fe(OH)}_3$  precipitate was dissolved in the minimum of 6M HCl. and the Fe reprecipitated by the addition of ammonia. The mixture was centrifuged and the supernatant was combined with the previous supernatant for  $^{63}\text{Ni}$  and  $^{90}\text{Sr}$  analysis. The precipitate was retained for  $^{55}\text{Fe}$  analysis.

### 5.3.2.3 *Purification of $^{55}\text{Fe}$*

The  $\text{Fe}(\text{OH})_3$  precipitate was evaporated to dryness and the residue was dissolved in 20ml 6M HCl. The solution was transferred to a 100ml separating funnel and 10ml of 2:1 ethyl acetate and butyl acetate were added. The mixture was shaken for approximately 1 minute to extract the Fe into the organic layer. The aqueous and organic layers were allowed to separate and the aqueous layer was transferred to a clean separating funnel. The aqueous fraction was extracted with a second 10ml of ethyl acetate and butyl acetate and the two organic phases were combined.

The organic fraction containing the Fe was washed with 10ml of 6M HCl and the aqueous fraction discarded. The Fe was then back-extracted into 2 x 10ml of 1M  $\text{HNO}_3$ . The  $\text{HNO}_3$  fraction was evaporated to dryness and the residue was dissolved in 8M HCl. The 8M HCl solution was loaded onto a 4 x 0.7cm Eichrom 1X8 anion exchange column previously conditioned with 8M HCl. The column was washed with 2 x 5ml of 9M HCl followed by 5ml of 6M HCl. Fe was then eluted with 10ml of 7.2M  $\text{HNO}_3$ . The  $\text{HNO}_3$  fraction was diluted to a 50ml and 1ml was removed and diluted to 10ml for measurement of stable Fe by ICP-AES. The remainder of the sample was evaporated to dryness prior to preparation of the liquid scintillation source.

### 5.3.2.4 *Purification of $^{63}\text{Ni}$ and $^{90}\text{Sr}$*

The supernatant following the  $\text{Fe}(\text{OH})_3$  precipitation contained both  $^{63}\text{Ni}$  and  $^{90}\text{Sr}$  along with  $^{60}\text{Co}$  and  $^{137}\text{Cs}$ . The solution was evaporated to dryness and dissolved in 20ml of 0.05M citric acid. The pH of the solution was adjusted to pH 8 using ammonia solution and loaded onto a 4 x 0.7cm dimethylglyoxime column previously conditioned with 1% ammonia solution (1ml of 0.88 Sp. Gr. ammonia diluted to 100ml). A distinct red band immediately formed at the top of the column. The column was washed with 20ml 1% ammonia solution. The load and wash solutions were retained for Sr analysis. Ni was eluted from the column with 6M HCl. 1mg of Co carrier was added to the eluent and the eluent was evaporated to dryness. The residue was dissolved in 2ml 9M HCl and loaded onto a 4 x 0.7 cm anion exchange column. The column was washed with 10ml 9M HCl and the load and wash solutions were diluted to 20ml. 1ml of the solution was removed and diluted to 10ml for stable Ni analysis by ICP-AES. The remainder of the solution was evaporated to dryness prior to measurement of  $^{63}\text{Ni}$  by liquid scintillation counting.

The load and washings from the DMG column were diluted to approximately 50ml with Milli-Q water. A few drops of bromocresol green indicator solution were added and the pH of the solution was adjusted to between pH 4 and 5 (sky blue colour of bromocresol green) with 2M HCl and 1% ammonia solution. 5ml of 4% ammonium oxalate solution was added to precipitate Ca and Sr as oxalates. The solution was centrifuged and the precipitate washed with Milli-Q water. The precipitate was dissolved in 3ml conc. HNO<sub>3</sub> and transferred to a 50ml beaker with a further 2ml conc. HNO<sub>3</sub>. 1ml of 40% HClO<sub>4</sub> was added and the solution was evaporated to dryness. The residue was dissolved in 5ml 8M HNO<sub>3</sub>-0.5M Al(NO<sub>3</sub>)<sub>3</sub> and transferred to a 3 x 0.7 cm Sr resin column. The column was washed with 10ml 8M HNO<sub>3</sub>-0.5M Al(NO<sub>3</sub>)<sub>3</sub> and 10ml 8M HNO<sub>3</sub>. Sr was eluted directly into a 22ml polythene vial with 10ml Milli-Q water. The sample was counted three times by Cerenkov counting. 0.1ml of the solution was then removed and diluted to 10ml with 2% HNO<sub>3</sub>. Stable Sr was then measured using ICP-AES.

#### *5.3.2.5 Preparation of sources for liquid scintillation analysis*

The optimisation of sample preparation techniques prior to liquid scintillation analysis have been discussed in Chapter 3. The following techniques were adopted for routine application.

The purified Fe residue (Section 5.3.2.3) was dissolved in a minimum of 6M HCl and carefully evaporated to incipient dryness on a warm hotplate (approximately 50°C surface temperature). The residue was then dissolved in 1ml 2M H<sub>3</sub>PO<sub>4</sub> and transferred to a 22ml polythene scintillation vial with 2ml of Milli-Q water. 15ml Ultima Gold AB scintillant were added and the sample shaken and stored in the dark for 24 hours before counting.

The Ni residue (Section 5.3.2.4) was dissolved in 1ml 1.2M HCl and transferred to a 22ml polythene scintillation vial with 2ml water. 15ml Gold Star scintillant were added and the samples stored in the dark for 24 hours prior to liquid scintillation counting.

All samples were counted on a Wallac 1220 ‘Quantulus’ low-level liquid scintillation counter (Chapter 2). Background samples were prepared by mixing the appropriate amount of acid with the scintillant such that the resulting source was of a similar composition to that of the unknown sources. In addition the stability and performance of the counter were checked

frequently by counting commercially prepared  $^3\text{H}$ ,  $^{14}\text{C}$  and blank samples (see Section 3.1). Optimisation of counting conditions has been discussed previously (Chapter 3) and are summarised below (Table 5.3).

**Table 5.3 : Summary of counting conditions used in the determination of beta emitters in sediments**

	$^{55}\text{Fe}$	$^{63}\text{Ni}$	$^{90}\text{Sr}$ ( $^{90}\text{Y}$ daughter)
Composition of final source	2M $\text{H}_3\text{PO}_4$ + Ultima Gold AB	Dil HCl + Gold Star	Dil $\text{HNO}_3$ No scintillant
Window	1-200	10-400	1-1024
Background	1.7 cpm	4.8 cpm	0.9 cpm
Efficiency	15-45%	70%	65%
Counting bias	Low	Low	Low
Count time	240 mins	240 mins	120 mins

### 5.3.3 Discussion of the sequential separation of $^{55}\text{Fe}$ , $^{63}\text{Ni}$ and $^{90}\text{Sr}$

#### 5.3.3.1 Use of yield monitors

Losses of the analyte during radiochemical separations are probable although the extent of such losses is minimised through careful optimisation of the method. Even after optimisation it is necessary to monitor the chemical recovery of the analyte following purification. This may be achieved in a number of ways.

- Optimise the method as thoroughly as possible and assume that the chemical recovery is consistently 100%
- Analyse samples of known analyte concentration to determine typical losses during the chemical separation. An average chemical recovery may then be calculated and this value applied to subsequent analyses.
- Add a known amount of a stable element that will act as an analogue to the analyte e.g. stable strontium for  $^{90}\text{Sr}$  or stable nickel for  $^{63}\text{Ni}$ . The recovery of the stable element may then be determined following purification and the chemical recovery applied to correct for analyte loss.

- Add a known amount of another isotope of the analyte e.g.  $^{99m}\text{Tc}$  for  $^{99}\text{Tc}$ . The recovery of the added radioisotope may be measured following purification and the chemical recovery applied to the analyte.

Options 1 and 2 are not desirable. Chemical recovery will vary depending on the sample matrix and great care is required to ensure that the standard matrix is closely matched to that of the unknown sample. This is not always practically possible. Even when the standard and sample matrices are identical, the chemical recovery will vary depending on the exact conditions employed during the analysis. Variations in the efficiency of transfer of the sample from beaker to beaker or the specific dimensions of a separation column will all affect the final chemical recovery. Although every effort is made to reproduce the separation conditions for all samples, variations in chemical recovery from sample to sample still occur and it is preferable to determine the specific recovery for each sample.

Options 3 and 4 permit the determination of chemical recovery for each individual sample. For this recovery to be determined accurately it is important that the yield monitor is added as soon as possible before any analytical operation is performed. It is also vital that the element is added in the same chemical form and oxidation state as the analyte to ensure that the two species will behave in a similar manner during the chemical separation. In some circumstances, there is sufficient element present in the sample so as to permit its use for chemical yield determination. This is true of Fe in sediments. The stable Fe content of the sample may be determined both prior to and following chemical separation and the chemical recovery calculated. This may then be used to correct the measured  $^{55}\text{Fe}$  activity for losses during purification. In most instances the concentration of the stable element is too low and additional element must be added. One benefit of this approach is that the presence of the stable element acts as a 'carrier' for the radioisotope being determined and reduces losses through surface adsorption effects. The chemical recovery of the carrier may be determined using a number of techniques including atomic absorption spectrometry, ICP-AES, ICP-MS, colourimetry or gravimetrically by precipitating both the carrier and analyte. This final approach is the most convenient and often also provides a source that is suitable for counting. For radioisotopes with no stable analogue it may be possible to use another element whose chemistry is identical to the analyte under the specified separation conditions. Such an approach has been employed in the analysis of technetium using rhenium as a yield monitor (Harvey, 1991).

The addition of another radioisotope of the analyte is often used as a yield monitor as it permits the determination of chemical recovery using radiometric techniques. This approach is also useful for radioisotopes with no stable analogue such as promethium and technetium. However, the added radioisotope may interfere with the final measurement of the analyte and such interference must be corrected for. If the radioisotope that is being used as a yield monitor has a short half-life compared to the analyte the source should be left to allow the yield monitor to decay following its measurement before attempting to measure the analyte. This is the case with the analysis of  $^{99}\text{Tc}$  where  $^{99\text{m}}\text{Tc}$  ( $t_{1/2} = 6.04$  hours) is used as the yield monitor.

**Table 5.4 : Yield monitors used in this study**

Analyte	Yield monitor	Method for measurement of yield monitor
$^{55}\text{Fe}$	Stable iron (inherent to the sample)	AAS / ICP-AES
$^{63}\text{Ni}$	Stable nickel	AAS / ICP-AES
$^{90}\text{Sr}$	Stable strontium	Grav (as $\text{SrCO}_3$ )/ICP-AES
$^{99}\text{Tc}$	$^{99\text{m}}\text{Tc}$	Gamma spectrometry

Grav. = gravimetric

### 5.3.3.2 *Sediment ignition*

Chemical separation of radioisotopes from sediments is complicated by the presence of organic humic and fulvic acids that can complex isotopes and hinder an otherwise routine separation. Samples are therefore normally ignited prior to any chemical separation being attempted. Radioisotopes that form volatile species such as  $^{99}\text{Tc}$ ,  $^{106}\text{Ru}$  and  $^{129}\text{I}$  may be lost during the ignition and precautions must be taken to limit this loss. Other radioisotopes may form refractory oxides on ignition and will subsequently be difficult to dissolve. However, no significant losses of Fe, Ni and Sr were observed at ashing temperatures of 550°C (Bock, 1979). Significant losses of even non-volatile elements have been reported and attributed to spray formation. All samples were therefore dried at 110°C to remove water and limit the potential for spattering during sample ignition.

### 5.3.3.3 Sample attack / dissolution

Sample dissolution was a crucial part of the analytical scheme. Although techniques that are appropriate to one analyte may be developed fairly readily, a single dissolution technique for all the analytes of interest is more demanding. Specific problems exist for technetium as the element can form volatile species that may be lost during this dissolution stage. For this reason Tc is discussed separately. Sample dissolution for all other analytes was achieved using an *aqua regia* attack.  $^{55}\text{Fe}$ ,  $^{63}\text{Ni}$  and  $^{90}\text{Sr}$  are readily dissolved using this approach.

### 5.3.3.4 Efficiency of *aqua regia* attack

The radioisotopes  $^{55}\text{Fe}$ ,  $^{63}\text{Ni}$  and  $^{90}\text{Sr}$  are readily leached as they are most likely associated with iron oxy-hydroxides ( $^{55}\text{Fe}$  and  $^{63}\text{Ni}$ ) and fine particulate clays ( $^{90}\text{Sr}$ ) that are readily attacked by acid solution. However, the stable elements of these isotopes present in the sediment may not be totally dissolved as the element will most likely be associated with various, more intractable, mineral phases. The degree of stable element leaching following the *aqua regia* attack is important as it will determine the chemical composition of the solution presented for chemistry and may introduce quantities of an element that has also been added for determination of chemical yield.

The leaching efficiency was determined by measuring the chemical composition of three dried sediments (collected from the Ravenglass saltmarsh) by X-ray fluorescence spectrometry. Two grams of each sediment were then digested with 40ml of *aqua regia* overnight at 50°C with constant stirring. The mixture was centrifuged and the residue was attacked with a fresh 40ml portion of *aqua regia* for 2 hours. The sample was filtered and washed with Milli-Q water before drying at 110°C overnight. The residue was weighed, ground and the chemical composition was determined using X-ray fluorescence analysis.

**Table 5.5 : Milligrams of element leached from 2g of sediment**

	Si	Ti	Al	Fe	Mn	Mg	Ca	Na	K	P	S	Rb	Sr	Pb	Zn	Ni
Sed 1	109	1.3	28	47	1.7	21	28	15	7.6	-	2.6	0.009	0.021	0.005	0.013	0.009
Sed 2	93	1.1	31	56	1.6	25	24	20	8.6	0.6	2.2	0.009	0.022	0.004	0.035	0.014
Sed 3	93	1.1	31	53	2.4	22	17	17	8.1	0.6	2.7	0.009	0.015	0.005	0.023	0.010

**Table 5.6 : Percentage of element leached from a marine sediment with *aqua regia***

	Si	Ti	Al	Fe	Mn	Mg	Ca	Na	K	P	S	Rb	Sr	Pb	Zn	Ni
Sed 1	15	15	24	76	87	77	90	45	18		88	21	41	55	58	68
Sed 2	13	12	23	77	86	78	89	54	18	28	89	18	42	52	77	76
Sed 3	13	13	25	79	91	77	85	50	18	32	91	20	34	60	74	75

Samples leached twice with 40ml *aqua regia* at 50°C

The amount of minerogenic/authigenic Ni and Sr leached from 2g of sediment are low (maximum of 14µg and 22µg respectively) and would not add significantly to the carrier introduced for yield determination. The mass of Fe leached is high at approximately 50mg. This represents approximately 77% of the total Fe present in the sample. The remaining Fe was intractable. Mn was leached to a greater extent (up to 90%) presumably reflecting a larger proportion of Mn associated with the readily soluble oxy-hydroxides and smaller proportion of minerogenic Mn. Only 14% of Si was leached but this represented approximately 100mg of Si. During routine analysis, a white solid often formed on the surface of the solution. SEM-EDS analysis of this solid confirmed that it was Si-based and that no other elements of interest were carried with the solid.

#### 5.3.3.5 Chemical separation

The precipitation stage effectively separates the radioisotopes into two groups; those which co-precipitate with the Fe(OH)<sub>3</sub> and those that remain in the supernatant. Those elements that co-precipitate with the Fe(OH)<sub>3</sub> include Sn(II+IV), Zr(IV), Y(III), lanthanides such as Pm(III) and Sm(III) and actinides including Th(IV), U(IV+VI), Np(V) and Pu(III+IV). If NaOH is used to adjust the pH Ni and Co will also follow the Fe(OH)<sub>3</sub>. However, both form soluble amine complexes and hence remain in the supernatant when ammonia is used for the pH adjustment. The use of NaOH will prevent the precipitation of Sn and Al as under highly alkaline conditions these elements form soluble stannates and aluminates respectively. Technetium as Tc(IV) will follow the Fe(OH)<sub>3</sub> but if oxidised to Tc(VII), the Tc will also remain in the supernatant. Strontium and Cs will not follow the Fe(OH)<sub>3</sub> precipitate. However due to the gelatinous consistency of Fe(OH)<sub>3</sub> the precipitate may contain occluded Cs, Ni, Sr and Tc. This contamination was limited by dissolving the Fe(OH)<sub>3</sub> precipitate in dilute acid and re-precipitating the Fe(OH)<sub>3</sub> using ammonia solution.

Solvent extraction of the Fe from 6M HCl into ethyl/butyl acetate or diisopropyl ether effectively separates the Fe from these other contaminants. Sn is also partially extracted into ethyl acetate but is not extracted into diisopropyl ether.

Following this purification, an alpha peak was evident in the liquid scintillation spectrum along with a low energy peak in the  $^{55}\text{Fe}$  region. The spectrum was indicative of Pu with associated  $^{241}\text{Pu}$  ( $E_{\text{max}} = 20$  keV) appearing in the  $^{55}\text{Fe}$  energy region. An anion exchange purification stage was therefore included to remove any traces of Pu following the Fe chemistry. This did not remove the alpha emitter from the Fe fraction. The alpha emitter was found to autodeposit on an Ag disc from HCl solutions confirming that the alpha activity observed was derived from natural Po. Po is known to extract into diisopropyl ether from HCl solutions. In addition Po is retained on an anion exchange resin from HCl as the  $\text{PoCl}_6^{2-}$  species ( $k_D = >10^3$ ; Korkisch, 1989) and, unlike Pu, would be eluted along with Fe in 7.2M HNO<sub>3</sub>. Although present in the Fe fraction,  $^{210}\text{Po}$  does not interfere with the  $^{55}\text{Fe}$  energy region and no further purification was necessary.

Retention of Ni on the dimethylglyoxime column was observable through the formation of a distinct crimson-red band at the top of the column. Spiking with 10mg Ni resulted in a very broad red band that gradually bled through the column and into the waste. This loss of Ni was easily overcome by reducing the quantity of Ni spike to 2mg. Addition of citric acid to the load solution improved retention of Ni on the column whilst ensuring that other transition metals were retained in solution. Co forms a soluble dimethylglyoxime complex. The yellow complex was observed to wash slowly through the column if Co was spiked into the load solution. The formation of the Co-dimethylglyoxime complex reduced the dimethylglyoxime available for Ni complexation lowering the loading capacity of the column. To avoid such a loss in loading capacity, Co was not added as a carrier prior to the dimethylglyoxime column. However, traces of  $^{60}\text{Co}$  were still detectable in the Ni fraction following elution from the dimethylglyoxime column. The Ni fraction was therefore dissolved in 9M HCl and passed through an anion exchange column. Co is moderately retained as  $\text{CoCl}_4^-$  ( $k_D = 40$ ; Korkish, 1989) whilst the Ni does not form an anionic chloro complex and hence passes through the column (Korkish, 1989). Retention of Co on the anion exchange column was reduced by the presence of dimethylglyoxime in the 9M HCl load solution. The Ni eluent from the dimethylglyoxime column was therefore evaporated to dryness and the residue was treated with *aqua regia* to destroy any dimethylglyoxime.

Sr was isolated from the load and wash solutions of the dimethylglyoxime column. The use of a commercially-available crown ether-based extraction chromatographic material, Sr-Resin, for purification of  $^{89}\text{Sr}$  and  $^{90}\text{Sr}$  has been widely reported. Potassium reportedly interferes with the retention of Sr on the column and must be separated prior to the column purification. Precipitation of Sr (along with Ca) as the oxalate achieves this separation. The pH of the solution is adjusted to 4 –5 with ammonia solution (the blue of bromocresol green indicator) and 4% ammonium oxalate is added. For samples low in Ca, approximately 10mg of Ca must be added to give sufficient precipitate to handle. In some instances, more ammonium oxalate must be added before precipitation commences. This suggests that the initial oxalate added may complex other elements in solution and further oxalate is required to achieve the critical concentration required to initiate precipitation. The Ca/Sr oxalate is dissolved in 8M  $\text{HNO}_3$ . This solution may be loaded directly onto the Sr-resin column although it is possible that the retention of Sr may be reduced by the presence of oxalate. The oxalate was therefore decomposed using a 3:1 mixture of  $\text{HNO}_3:\text{HClO}_4$ . The use of an excess  $\text{HNO}_3$  along with  $\text{HClO}_4$  ensures that the oxidation proceeded in a safe controlled manner. The resulting residue was dissolved in a mixture of 8M  $\text{HNO}_3$ -0.5M  $\text{Al}(\text{NO}_3)_3$  and loaded onto the Sr-resin column. The addition of  $\text{Al}(\text{NO}_3)_3$  to the load solution has been reported to improve the uptake of Sr on the column. Following sample loading, the column is washed with 8M  $\text{HNO}_3$  to remove any residual  $\text{Al}(\text{NO}_3)_3$  before the Sr is eluted with water directly into a polythene vial ready for Cerenkov counting.

#### 5.3.3.6 *Recoveries of Fe, Ni and Sr*

The chemical recovery of Fe was dependent on the amount of stable Fe present and hence on the amount of sample analysed. For 2g sediment samples containing approximately 50mg of Fe the mean chemical recovery was 85% (69-94%; n=14). For a 5g sediment sample containing 125mg Fe the mean recovery was only slightly lower at 79% (53-84%; n=15).

The mean chemical recovery of Ni was 77% (62-92%; n=31) for a spiking level of 2mg Ni. Reduction of the Ni spike to 1mg led to an apparent reduction on chemical recovery with a mean recovery of 66% (49-81%; n=8).

Initially, sediment samples were spiked with 10mg of Sr to permit the gravimetric

determination of chemical recovery. Chemical recoveries at this spiking level were however, low with a mean recovery of 45% (34-66%; n=28). Similar recoveries were also observed for acid blank samples spiked with 10mg Sr. A reduction in the amount of Sr spike to 2mg resulted in no significant increase in Sr recovery with a mean recovery of 48% (32-70%; n=7). However, this meant that the chemical recovery had to be determined using either atomic absorption spectrometry or ICP-AES. One very low recovery was observed for a carbonate-rich sediment (IAEA-367) that gave a chemical recovery of 14%. Although the columns can tolerate and effectively separate a certain level of Ca, very high Ca loadings will also reduce the retention of Sr on the column.

#### *5.3.3.7 Decontamination of other radioisotopes*

Gamma spectrometric measurement of all purified fractions did not detect the presence of any other radioisotopes above about 0.1Bq in the sample. Inspection of the liquid scintillation beta spectra also showed that the purified fraction was not contaminated, with the exception of the Fe fraction that contained traces of  $^{210}\text{Po}$  (Section 5.3.3.5).

#### *5.3.3.8 Re-use of Sr resin column*

The use of Sr-resin columns permits the rapid and efficient separation of Sr and Ca and removes the need for conventional selective nitrate precipitation with fuming  $\text{HNO}_3$ . However, the widespread use of Sr-resin in routine separation has been hindered by the high cost of the resin material. There has therefore been some interest in reusing columns to reduce the cost per analysis. Re-use of chromatographic material is normally not recommended as there is a potential risk of sample cross-contamination as well as a reduction in the loading capacity and distribution coefficient following repeated re-use of the material. For re-use to be viable, it must be possible to efficiently elute the analyte and any potential interference from columns so that traces of the analyte/interferent are not transferred to the next sample. In addition the performance of the chromatographic material must not be significantly compromised.

In order to evaluate the potential for Sr-resin to be recycled, a series of 3 x 0.7cm columns were prepared and conditioned with 8M  $\text{HNO}_3$ -0.5M  $\text{Al}(\text{NO}_3)_3$ . The columns were loaded with the purified Sr fraction of a Ravenglass sediment and the columns were washed and eluted as described in Section 5.3.2.4. The columns were then washed with 20ml of water and reconditioned with 10ml 8M  $\text{HNO}_3$ -0.5M  $\text{Al}(\text{NO}_3)_3$ . A fresh Sr fraction was then loaded and

the procedure repeated. This cycle of load-wash-elute-recycle was repeated four times. Within each cycle one column was chosen for evaluation. This column was loaded with an inactive solution of 10mg Sr in 8M HNO<sub>3</sub>-0.5M Al(NO<sub>3</sub>)<sub>3</sub>. The column was washed and eluted as described previously with the column being finally eluted with 10ml water into a polythene scintillation vial.. The sample was counted three times in a ten-day period to determine the level of <sup>90</sup>Sr activity contamination originating from previous samples processed on the column. 0.1ml of the solution was also diluted to 10ml with 2% nitric acid and the stable Sr recovery was determined by ICP-AES.

In all cases no <sup>90</sup>Sr activity was detected in the blank samples. This indicates that for the levels of <sup>90</sup>Sr activity found in the sediment samples, cross-contamination between samples resulting from the recycling of the Sr-resin was insignificant. The chemical recoveries of Sr dropped slightly with continuing re-use of the Sr-resin. This may be associated with the relatively high Sr loadings of 10mg resulting in the columns being saturated with Sr. Hence even a slight reduction in column loading capacity during repeated recycling results in an observable decrease in Sr recovery.

**Table 5.7 : Effect of Sr-resin recycling on the percentage chemical recovery of Sr**

	Col 1	Col 2	Col 3	Col 4	Col 5	Col 6	Col 7	Col 8
<b>Cycle 1</b>	65	62	41	45	43	46	53	40
<b>Cycle 2</b>	<b>60</b>	66	44	46	42	42	47	41
<b>Cycle 3</b>	38	54	39	42	45	42	<b>50</b>	38
<b>Cycle 4</b>	34	41	40	<b>43</b>	43	44	45	36

*Italicised values in boxes refer to blank samples. All other values are for purified Sr fractions from a Ravenglass sediment.*

*10mg Sr loading throughout assuming a 100% recovery for sediment samples following initial chemistries*

## 5.4 Paper published in *Analytica Chimica Acta*, 380, 73-82, 1999.

### An Optimised method for the routine determination of Technetium-99 in Environmental Samples by Liquid Scintillation Counting

Wigley F<sup>1</sup>., Warwick P. E<sup>1</sup>., Croudace I.W<sup>1</sup>., Caborn J<sup>1,2</sup>., Sanchez A. L<sup>2</sup>.

<sup>1</sup>*School of Ocean and Earth Science, Southampton Oceanography Centre, Empress Dock, Southampton SO14 3ZH. Tel. 01703 592780. Fax. 01703 596450.*

<sup>2</sup>*Institute of Terrestrial Ecology, Merlewood Research Station, Grange-Over-Sands, Cumbria.*

#### 5.4.1 Abstract

A method has been developed for the routine determination of <sup>99</sup>Tc in a range of environmental matrices using <sup>99m</sup>Tc ( $t_{1/2} = 6.06$  hours) as an internal yield monitor. Samples are ignited stepwise to 550°C and the <sup>99</sup>Tc is extracted from the ignited residue with 8M nitric acid. Many contaminants are co-precipitated with Fe(OH)<sub>3</sub> and the Tc in the supernatant is pre-concentrated and further purified using anion exchange chromatography. Final separation of Tc from Ru is achieved by extraction of Tc into 5% tri-n-octylamine in xylene from 2M sulphuric acid. The xylene fraction is then mixed directly with a commercial liquid scintillant cocktail. The chemical yield is determined through the measurement of <sup>99m</sup>Tc by gamma spectrometry and the <sup>99</sup>Tc activity is measured using liquid scintillation counting after a further two weeks to allow decay of the <sup>99m</sup>Tc activity. Typical recoveries for this method are in the order of 70 -95%. The method has a detection limit of 1.7 Bq kg<sup>-1</sup> based on a two-hour count time and a 10g sample size. The chemical separation for twenty-four samples of sediment or marine biota can be completed by one analyst in a working week. A further week is required to allow the samples to decay before determination.

#### 5.4.2 Introduction

Technetium-99 ( $t_{1/2} = 2.2 \times 10^5$  years) is a fission product of <sup>235</sup>U with approximately a 6% yield. Tc only exists naturally in minute quantities at 0.25 – 0.31 parts per trillion in pitchblende arising from spontaneous fission Kenna *et al*, 1964). Most <sup>99</sup>Tc in the environment is derived from the discharge of fission waste products from nuclear fuel reprocessing plants and from

weapons' fallout. The total input of  $^{99}\text{Tc}$  to the environment from weapons' fallout is estimated at 140 TBq (Aarkrog *et al*, 1986), while discharges to the marine environment from Sellafield reprocessing plant have been estimated at 1220 TBq from 1954 to 1996 (BNFL, 1983-1997; Gray *et al*, 1995) There have been significant increases in inputs of  $^{99}\text{Tc}$  into the Irish Sea since the commissioning of the Enhanced Actinide Removal Plant (EARP) in 1994 (Leonard *et al*, 1997) and subsequent treating of stockpiled Medium Active Concentrate (MAC) waste. Discharges from EARP in 1995 were 180 TBq with a reduction to 150 TBq in 1996 (BNFL, 1983-1997).

The aim of this study was to develop an effective and robust method for  $^{99}\text{Tc}$  determination particularly suited to measurement of the isotope in sediments and marine biota. The low concentrations in many environmental samples, the volatility of Tc, Tc speciation and spectral interferences from yield monitors all cause potential difficulties.

### 5.4.3 *Methodology*

#### 5.4.3.1 *Instrumentation*

Determination of  $^{99}\text{Tc}$  was made using a using a Wallac 1220 Quantulus<sup>TM</sup> Ultra Low Level Liquid Scintillation Counter. Liquid Scintillation Counting (LSC) was chosen in preference to Inductively Coupled Plasma – Mass Spectrometry (ICP-MS). The benefits of LSC for routine determination of  $^{99}\text{Tc}$  include cost effectiveness and limits of detection which are to comparable with ICP-MS. Gas flow proportional counting and anthracene screen counting were not considered to be sensitive enough.

Technetium-99m was measured using a Canberra well-type high purity germanium (HPGe) gamma ray spectrometer. The spectral deconvolution program Fitzpeaks (JF Computing, Stanton in the Vale, UK.) was used to analyse gamma spectra.

#### 5.4.3.2 *Reagents*

Analytical reagents and deionised water were used throughout this study. Tri-n-octylamine and mixed xylenes were supplied by Aldrich Chemicals. Instagel<sup>TM</sup> and Ultima Gold AB<sup>TM</sup> liquid scintillation cocktails were supplied by Packard UK Ltd, Pangborne, U.K. GoldStar and Ecosafe liquid scintillation cocktails were supplied by Meridian, Epsom, U.K. All other reagents were supplied by Fisher Scientific Ltd, Loughbrough, U.K. Technetium-99 was

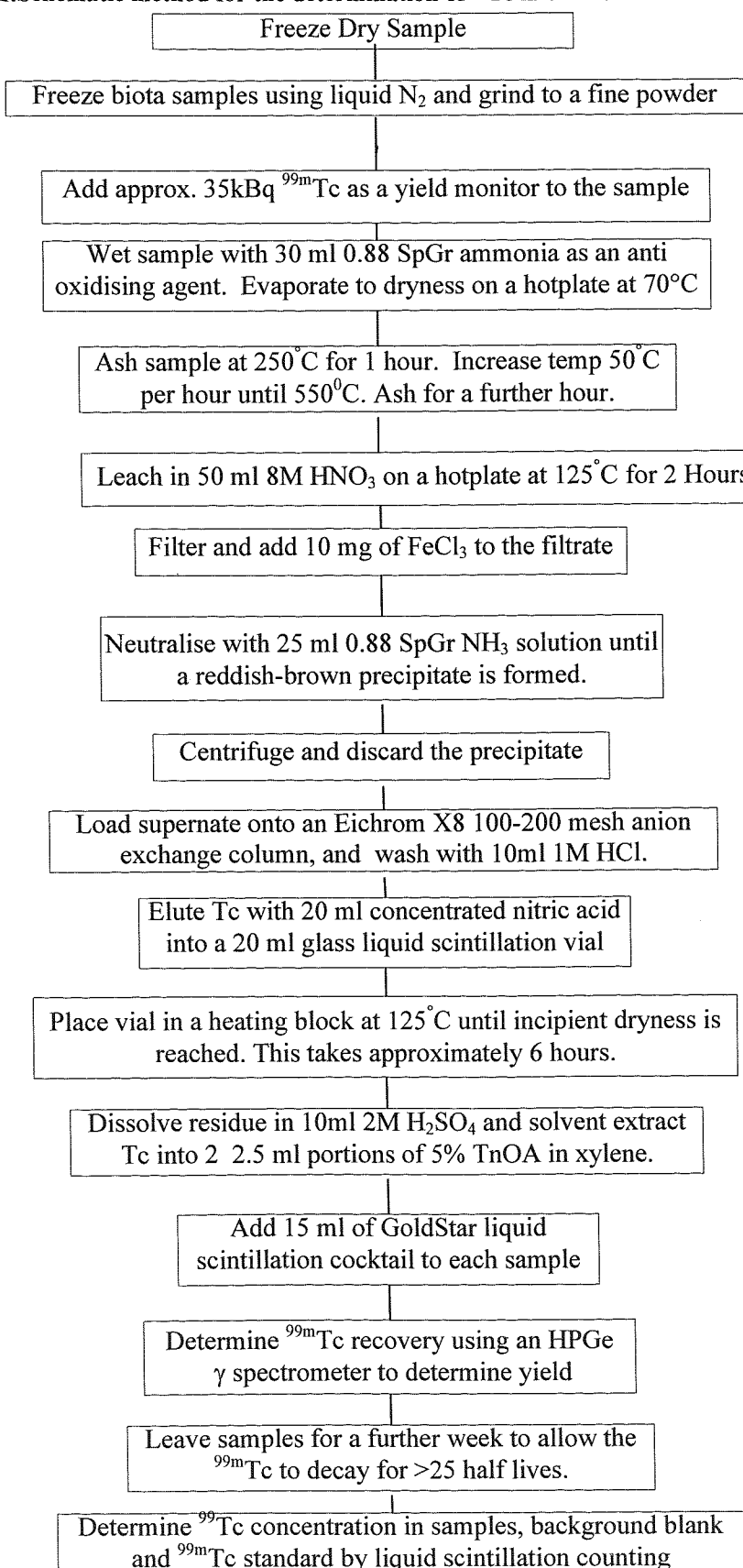
supplied as sodium pertechnetate by the National Physical Laboratory (NPL), and  $^{99m}\text{Tc}$  as Na pertechnetate was generously supplied by Southampton General Hospital.

#### 5.4.3.3 *Method Summary*

A schematic summary of the method used for the determination of  $^{99}\text{Tc}$  in environmental samples is shown in Figure 5.2. The method can be divided into sample preparation, acid leaching, decontamination and determination stages.

#### 5.4.3.4 *Yield Determination*

The  $^{99m}\text{Tc}$  yield monitor was counted using a well-type (HPGe)  $\gamma$  ray spectrometer using the 140 keV emission line. As  $^{99m}\text{Tc}$  decays to  $^{99}\text{Tc}$ , the decay of the yield monitor will contribute to the activity of  $^{99}\text{Tc}$  in the sample. The contributed activity is small with a 100 kBq  $^{99m}\text{Tc}$  spike decaying to 0.3 kBq of  $^{99}\text{Tc}$  daughter. The concentration of  $^{99}\text{Tc}$  produced by the decay of  $^{99m}\text{Tc}$  in each sample is calculated after correction for the background count.

**Figure P1.**Schematic method for the determination of  $^{99m}$ Tc in environmental samples.

### 5.4.4 Discussion

The different stages in the analytical procedure were investigated in order to determine the optimum conditions for the separation, purification and measurement of  $^{99}\text{Tc}$  (*i.e.* where losses of Tc are minimised and contaminants are effectively separated from  $^{99}\text{Tc}$ ). The loss of Tc at each of the following stages was determined using a  $^{99\text{m}}\text{Tc}$  spike: (1) sample preparation and ashing; (2) leaching; (3) separation chemistry. Optimisation of  $^{99}\text{Tc}$  recovery was tested by using homogenised seaweed, lobster and sediment samples in the ashing and leaching stages. Testing of the reproducibility of the method was made using an in-house reference material. Determination was made on each sub-sample to assess the effectiveness of extraction of  $^{99}\text{Tc}$  from the sample matrix. This is because the yield monitor cannot be relied on to act as a faithful comparison until all matrix-bound Tc is in solution.

#### 5.4.4.1 Choice of Yield Monitor

A number of different isotopes of Tc, and stable Re, have been used as yield monitors for Tc analysis (Table P1). As Re could not be relied upon to faithfully follow the Tc separation chemistry, a Tc isotope other than  $^{99}\text{Tc}$  was required. Technetium-99m was chosen due to its availability and its readily measurable gamma emission. The short half life of  $^{99\text{m}}\text{Tc}$  (6.06 hours) also means that the isotope may be allowed to decay prior to the measurement of the  $^{99}\text{Tc}$ .

**Table P1. Potential tracer elements for determination of recovery of  $^{99}\text{Tc}$ .**

Tracer	Half Life	Determination method	Disadvantages	Reference
$^{95\text{m}}\text{Tc}$	60 days	$\gamma$ spectrometry	Spectral interference / separate determination method required / availability	Goldchert & Sedlet, 1969 Kaye <i>et al</i> , 1982
$^{97}\text{Tc}$	$2.6 \times 10^6$ years	ICP-MS	availability / high cost	
$^{97\text{m}}\text{Tc}$	91 days	$\gamma$ spectrometry	Spectral interference / separate determination method required / availability	Kaye <i>et al</i> , 1982
$^{99\text{m}}\text{Tc}$	6.06 hours	$\gamma$ spectrometry	Spectral interference / separate determination method required / short half life	Chen <i>et al</i> , 1994 Holm <i>et al</i> , 1984 Martin & Hylko, 1987
Re	Stable	ICP-MS, ICP-AES Gravimetric analysis	Spectral interference / separate determination method required / differing chemistry	Harvey <i>et al</i> , 1991 Matsuoka <i>et al</i> , 1990

#### 5.4.4.2 Sample preparation

Biota and sediment samples are first freeze-dried and then ground to a fine powder. It was found that the distribution of  $^{99}\text{Tc}$  in samples, particularly seaweeds, was heterogeneous. Many seaweeds proved difficult to grind when simply dried. A fine powdered sample was readily obtained however; by first freezing the samples in liquid nitrogen, prior to grinding. Samples with a more delicate tissue structure, such as lobster (*Homarus gammarus*) and are easily ground without prior freezing.

#### 5.4.4.3 Ashing Conditions

Some previous methods have suggested that loss of Tc may occur on ashing due to the volatilisation of technetium anhydride ( $\text{Tc}_2\text{O}_7$ ); the product of dehydrating pertechnic acid ( $\text{HTcO}_4$ ) on heating (Harvey *et al*, 1991). Pertechnic acid is formed by the oxidation of Tc in the presence of organic acids. The addition of ammonia to the sample prior to ashing neutralises the free acidic sites on complex organic molecules to inhibit the formation of

HTcO<sub>4</sub> (Harvey *et al*, 1991; Foti *et al*, 1972). Hydrochloric acid has also been used to prevent the volatilisation of Tc by reducing Tc to its less volatile +4 oxidation state (Harvey *et al*, 1991).

Some controversy exists over the optimum ashing temperature for Tc determination. Losses of more than 50% have been observed at temperatures greater than 500°C (Harvey *et al*, 1991) while ashing temperatures of up to 600°C (Garcia Leon, 1990) and 750°C (Holm *et al*, 1984; Tagami & Uchida, 1993) have been used with no apparent losses of <sup>99</sup>Tc.

#### **a) Effect of temperature and wetting agents on Tc loss during ashing**

Ammonia and HCl were tested for their efficiency at reducing the loss of Tc, in samples of marine biota and sediments. In addition 2% SnCl<sub>2</sub> was investigated as the compound is widely used as a reducing agent. Approximately 10g of sample was taken and spiked with <sup>99m</sup>Tc. Samples were then wetted with either concentrated hydrochloric acid, 2% tin (II) chloride in hydrochloric acid, or 0.88 Specific Gravity (Sp.Gr.) ammonia. A control sample spiked with <sup>99m</sup>Tc and which had no other pre-treatment was also ignited. The samples were dried on a hotplate at 125°C and the initial <sup>99m</sup>Tc activity determined using an HPGe  $\gamma$  spectrometer. The samples were then heated in a furnace ramped at 50°C per hour to temperatures between 450°C and 900°C. Samples were heated to temperatures between 450°C and 550°C in a furnace with an internal capacity of 80 litres. Samples ignited to 750°C and 900°C were heated in a tube furnace. The <sup>99m</sup>Tc activity was again determined and any loss of <sup>99m</sup>Tc due to volatilisation was calculated (Figure 5.3a).

**Figure P2 a. Loss of  $^{99m}\text{Tc}$  during ashing.** Results are on triplicate measurements of sediment and marine biota samples spiked with  $^{99m}\text{Tc}$ . All samples were ignited in a ramped furnace from 250°C with an increase of 50°C per hour. Error bars at  $2\sigma$ .

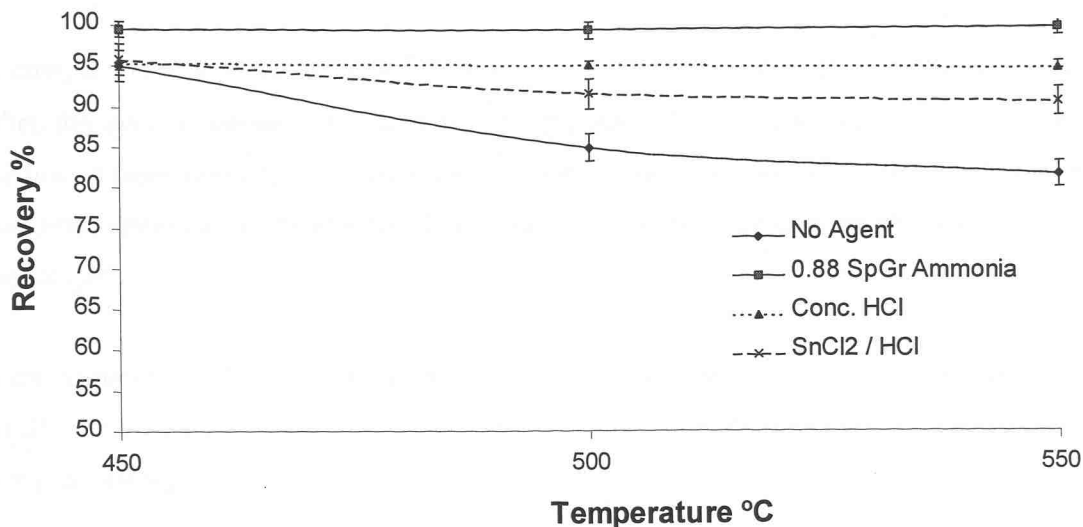
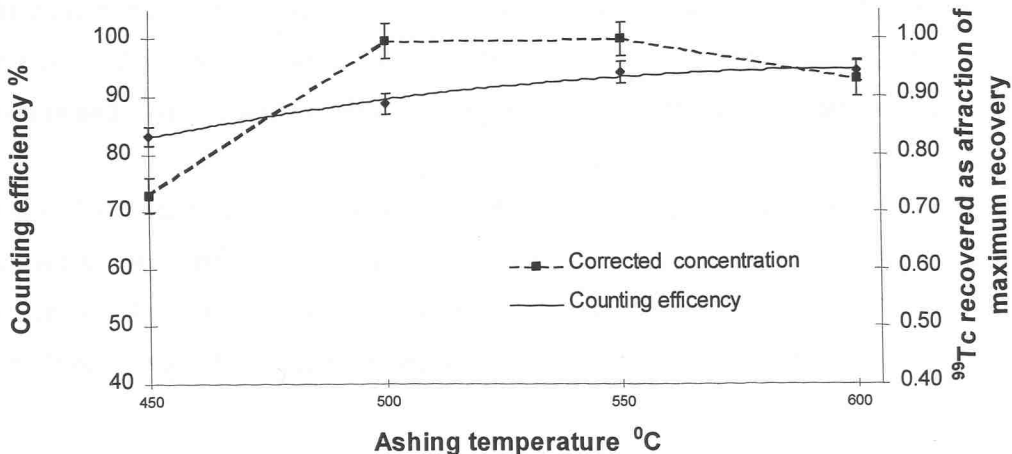


**Figure P2 b. Counting efficiency and loss of  $^{99}\text{Tc}$  through separation chemistry as a function of ashing temperature.** Homogeneous lobster samples were ashed to 450°C, 500°C, 550°C and 600°C. The remainder of the determination was made using identical conditions, the samples measured by liquid scintillation counting and the final concentrations shown as a percentage of the maximum recovery at 550°C. Measurement was also made of the counting efficiency. Error bars at  $2\sigma$ .



For sediments, seaweed and lobster samples there was no appreciable loss of Tc at temperatures up to 550°C when ammonia was added prior to ignition. Samples pre-treated with SnCl<sub>2</sub> or HCl showed losses of over 5%, while the greatest losses were observed from samples which had no pre-treatment (Figure P2 a).

A comparison was made between <sup>99</sup>Tc recoveries when the sample ignition was ramped and when the ignition temperature was static. Ashing times of four hours were used. At 450°C, the lowest temperature tested, recoveries were substantially reduced, 47% (HCl pre-treatment) and 39% (ammonia pre-treatment). This is due to incomplete destruction of organic acids in the sample.

Some variation in the optimum ashing conditions was observed when using furnaces with smaller internal capacities and a constant supply of air to the samples was necessary to allow complete ashing.

#### **b) Effect of ashing temperature on counting efficiency during LSC**

The counting efficiency and apparent <sup>99</sup>Tc concentration were determined for a range of ashing temperatures (Figure P2 b).

It was found that ashing at less than 500°C resulted in incomplete oxidation and subsequent high quenching in the final sample during liquid scintillation analysis. This was especially true in pigmented samples such as lobsters (*Homarus gammarus*) and red seaweed (*Chondrus crispus*). The counting efficiency increases with increase in ashing temperature as more of the compounds that cause quenching are oxidised at higher ashing temperatures (Figure P2 b)

Unoxidised black carbonaceous residues were found to act as a sorbent for Tc and reduced the chemical recovery of Tc during the leaching process. The highest chemical recovery after correction for counting efficiency is at 550°C. The low chemical recovery at 450°C is the result of incomplete ashing resulting in a poor leaching of the sample.

#### 5.4.4.4 Leaching

##### a) Acid type

The effectiveness of several different leaching agents was tested on seaweed, lobster and sediment samples and the comparative recoveries determined (Figure P3 a). Nitric acid (8 M) showed the highest recovery of  $^{99}\text{Tc}$  from 'in-house' seaweed, sediment and lobster reference samples. HCl was less efficient at leaching Tc than  $\text{HNO}_3$ . This can be explained by the partial reduction of Tc(VII) to Tc(IV) in HCl at concentrations greater than 4 M (Pruett, 1981; Watanabe & Hashimoto, 1995). Recovery of  $^{99}\text{Tc}$  when leaching with diluted *aqua regia* or 8M HCl + 3%  $\text{H}_2\text{O}_2$  is also lower than that recovered with 8M  $\text{HNO}_3$ . The reasons for this are unclear but may also be due to loss of Tc through reduction.

**Figure P3 a. Total  $^{99}\text{Tc}$  leached from the sample matrix, using different leaching agents, as a percentage of the total recovered with nitric acid.**

All samples were heated at 125°C for 2 hours. Error bars at  $2\sigma$ .

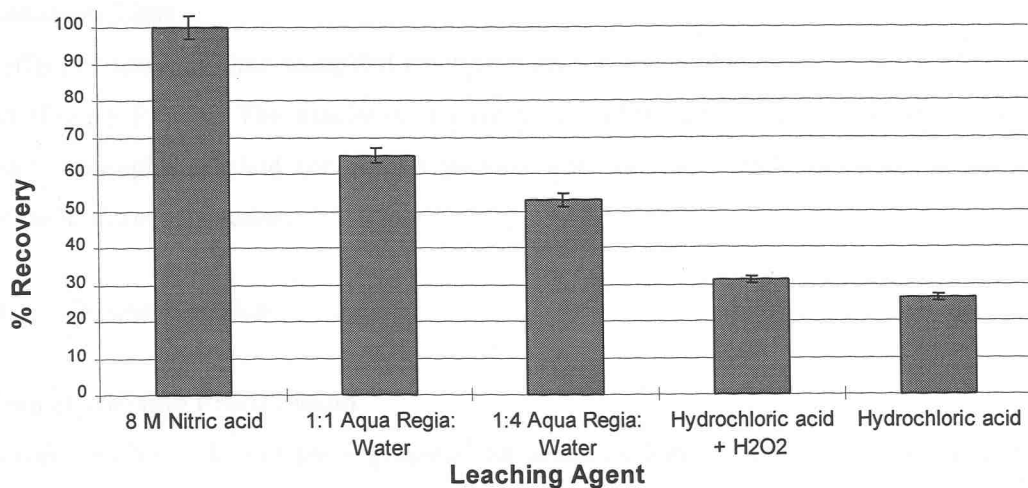
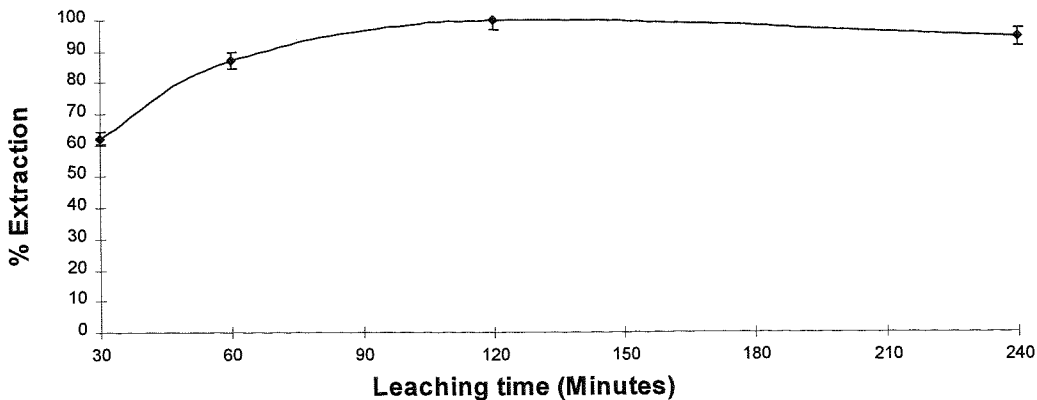


**Figure P3 b. Effect of leaching time on recovery of  $^{99}\text{Tc}$  from sample matrices.**

Homogenous samples were leached for 30 minutes, 60 minutes, 120 minutes and 240 minutes on a hotplate at 125°C in 8 M nitric acid. The remainder of the determination was carried out under identical conditions. Error bars at  $2\sigma$ .



### b) Leaching Time

The effect of leaching time using 8M nitric acid on a hotplate at a temperature of 125°C was tested (Figure P3 b). The maximum recovery was observed in samples leached for 120 minutes. Samples leached for shorter periods were not thoroughly attacked by the acid resulting in lower recoveries.

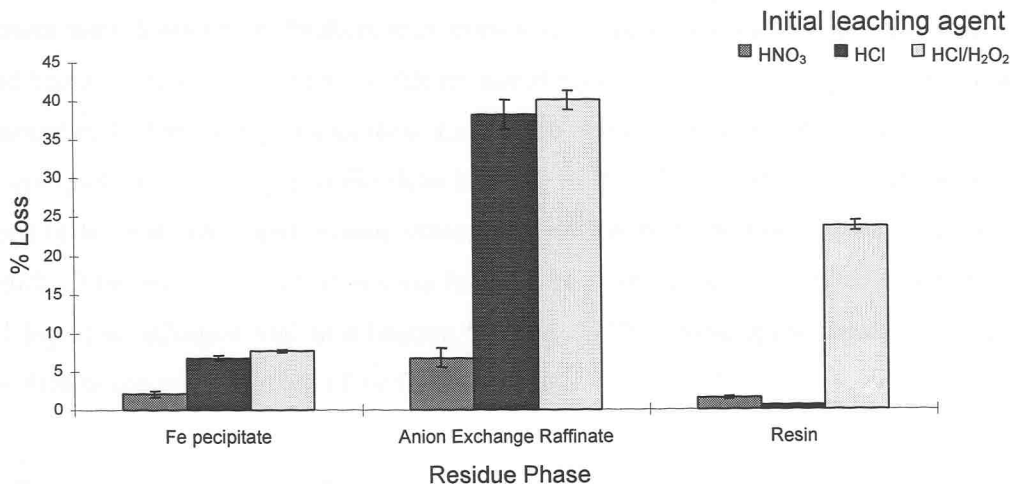
#### 5.4.4.5 Decontamination

##### a) Iron Hydroxide Precipitation

Following leaching, the sample is prepared for anion exchange chromatography. The initial step is to remove possible contaminants (such as transition metals, actinides and lanthanides). However alkali and alkaline earth metals ( $^{90}\text{Sr}$ ,  $^{137}\text{Cs}$ ), Re(VII), Ru (VIII) and Tc(VII) are not precipitated. If ammonia is used to neutralise the solution cobalt and nickel are also retained in solution as amine complexes.

Losses of  $^{99}\text{Tc}$  to the iron hydroxide precipitate after neutralisation with ammonia are lower when 8M nitric acid is used as a leaching agent (Figure 5.5). This further supports the notion that some of the Tc is reduced to insoluble Tc (IV) in HCl solutions. The small quantity of Tc lost to the iron hydroxide precipitate from nitrate solutions is most likely to be occluded Tc (VII).

**Figure P4 Loss of  $^{99m}\text{Tc}$  yield monitor to residue phases with different leaching agents. Error bars at  $2\sigma$ .**



### b) Anion Exchange Chromatography

Analytical grade anion exchange resin 1X8 (100-200) mesh (Eichrom) was used both for decontamination and concentration of the sample. Technetium is retained on the anion exchange column from alkaline solution. Alkali and alkaline earth metals and divalent transition metals pass through the column into the raffinate separating most of the main contaminants including  $^{60}\text{Co}$ ,  $^{63}\text{Ni}$ ,  $^{90}\text{Sr}$  and  $^{137}\text{Cs}$  from Tc. The anion exchange column also separates Tc from Ca, which would interfere with the solvent extraction separation.

The solutions containing ammonium nitrate, formed by the neutralisation of nitric acid with ammonia, were found to give substantially lower losses of Tc to the raffinate than from ammonia solutions containing ammonium chloride (Figure P4). This is expected, as the  $K_D$  for Tc in alkaline nitrate media on anion exchange resin is higher than in the corresponding chloride media (Korkisch, 1989). When solutions are loaded in chloride media with  $\text{H}_2\text{O}_2$  present from the leaching process, retention of  $^{99}\text{Tc}$  on the resin after elution of Tc are higher than if  $\text{H}_2\text{O}_2$  is not used (Figure P4)

### c) Solvent extraction

The Tc is eluted from the anion exchange resin column with concentrated nitric acid, evaporated and dissolved in 2M sulphuric acid for solvent extraction. Some workers noted that potential losses of Tc could occur during this evaporation step. The loss of Tc is increased by

the presence of chloride (Dixon *et al*, 1997), and the smallest loss is achieved by evaporation at temperatures less than 80°C.

This study found that the geometry of the container had a significant effect on Tc losses. Losses were higher from beakers than from glass scintillation vials. The vials were narrower and had a restriction at the top, which enhanced refluxing of the solution thereby reducing the amount of Tc lost during evaporation. Loss of Tc occurred if the sample in the vial was heated to complete dryness. Due to the short half life of the  $^{99m}$ Tc yield monitor evaporation times need to be minimised and a compromise between recovery and rate of evaporation must be struck. The optimum conditions were found to be evaporation of 20 ml of solution from a 20 ml liquid scintillation vial in a heating block at 125°C taking approximately 6 hours. This resulted in the loss of 5-10% of Tc from solution.

Ruthenium-106 is not quantitatively separated from  $^{99}$ Tc by anion exchange chromatography (Maeck *et al*, 1961) and further purification of the sample is required. This is achieved by solvent extraction of  $^{99}$ Tc from 2M sulphuric acid into 5% tri-n-octylamine (TnOA) in xylene (Dale *et al*, 1996). Ruthenium-106 is retained in the aqueous phase. The organic phase may then be mixed directly with commercial scintillation cocktails. As no aqueous phase is then present to contribute to quench, counting efficiencies are higher than if an aqueous solution is mixed directly with the scintillant.

**Table P2 a. Extraction of contaminants into tertiary amines in xylene from 2M sulphuric acid**  
[After Maeck *et al*, 1961]

Element	Extraction into tertiary amines
Tc, Re, Au, Ta.	Quantitative extraction
Mo, W, Ag, Cd.	Partial extraction
Ru, Mn, Fe, Cr, Ni, Co, U, Np, Pu, Am, Be, Na.	No extraction

**Table P2 b. Activities of abundant radioisotopes before and after decontamination.**

Sample Type	Potential interferent	Bq in original Sample	Bq after decontamination	Decontamination factor
Seaweed	$^{137}\text{Cs}$	16	<0.016	> 1000
	$^{241}\text{Am}$	11	<0.015	> 730
	$^{106}\text{Ru}/^{106}\text{Rh}$	5.6	<2	> 3
Sediment	$^{137}\text{Cs}$	12540	<0.017	> 740000
	$^{241}\text{Am}$	24673	<0.014	> 1760000
	$^{106}\text{Ru}/^{106}\text{Rh}$	8.4	<2	>5

#### d) Decontamination factors

The effectiveness of the method for decontamination of radioisotopes in marine biota and sediment samples was determined for some abundant radioisotopes by measuring their activities before and after decontamination chemistry (Table 5.9b).  $^{137}\text{Cs}$ ,  $^{241}\text{Am}$  and  $^{106}\text{Ru}$  were chosen as all are usually present in environmental samples and may produce an interference when determination is made by liquid scintillation counting.

The absence of  $^{137}\text{Cs}$ ,  $^{241}\text{Am}$  and  $^{106}\text{Ru}$  in the  $\gamma$  spectra of the final liquid scintillation source coupled with the absence of any high energy  $\beta$  emitting isotopes in the liquid scintillation spectra, indicates effective removal of any potential interferants.

The distribution coefficients for Ru between 5% tri-iso octylamine (TiOA) in xylene and 0.5 M  $\text{H}_2\text{SO}_4$  are as low as  $1.7 \times 10^{-3}$  (Chen *et al*, 1990).

## e) Chemical recovery

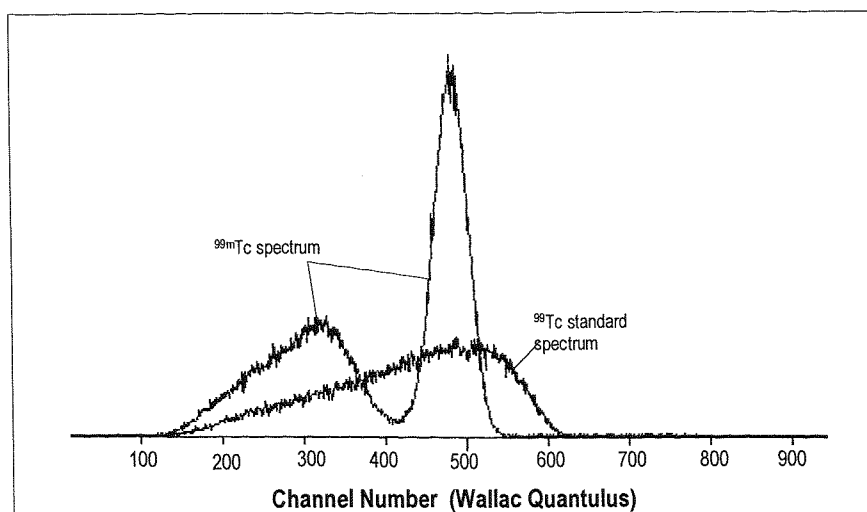
**Table P3.** Typical recoveries of  $^{99m}\text{Tc}$  after separation chemistry

Sample	Mean Recovery	Recovery Range %	n
Method blank	93%	88 - 97	9
Ravenglass sediments	81%	74 - 92	60
<i>Ascophyllum nodosum</i>	74%	70 - 79	36
<i>Chondrus crispus</i>	79%	72 - 85	24
Lobster	75%	72 - 78	16
All types	85%	70 - 95	170

Typical chemical recoveries for the method vary between 70% to 95% with a mean of 85% (Table P3). Variation depends mainly on the differing sample matrix, with better recoveries generally observed for samples with lower organic carbon content.

#### 5.4.4.6 Liquid Scintillation Counting

Liquid scintillation counting was used to measure the activity of  $^{99}\text{Tc}$  in the samples, with di-isopropyl-naphthalene based scintillation cocktails giving the best limits of detection. However it was found that  $^{99m}\text{Tc}$  produced a significant interference if it had not decayed (Figure P5).

**Figure P5.** Interference of  $^{99m}\text{Tc}$  on a  $^{99}\text{Tc}$  spectrum.

A  $^{99m}\text{Tc}$  standard counted immediately after the determination of the yield monitor has an activity of 5800 dpm and gives a count of 1100 cpm, whilst the activity from a typical  $^{99}\text{Tc}$  sample is 700 cpm. An interference at such a high level would mean that a reliable determination of low level environmental samples would not be possible, if the  $^{99m}\text{Tc}$  yield monitor is not allowed to decay first. A period of seven days ( $> 25$  half-lives) from the determination of the yield monitor was found to be sufficient. This means that the minimum length of time required for the determination of  $^{99}\text{Tc}$  is two weeks.

#### 5.4.4.7 Method statistics and reference materials

Method blanks were run through the separation procedure to determine the detection limit ( $L_D$ ) (Currie, 1968). For a count time of 120 minutes, a counting efficiency of 90%, a sample weight of 10g and a chemical recovery of 85%, the method has a detection limit of  $1.7 \text{ Bq kg}^{-1}$ . Reductions could also be made in  $L_D$  with an increase in the sample size or a longer count time.

#### Accuracy and precision of the method

As no international environmental reference materials exist for Tc, it was necessary to test the method using a material prepared as a preliminary reference samples at the Scottish Universities Research and Reactor Centre (SURRC). All activities of these samples determined using this method fall within preliminary working ranges established at “Technetium 1998” (8-9 April 1998, at a conference held at Southampton Oceanography Centre - McCartney, 1998) (Table P4).

**Table P4. Measured activities of preliminary reference materials.**

Sample	Sample activity $\text{Bq kg}^{-1}$ Measured	$1\sigma$	Working Range $\text{Bq kg}^{-1}$ Reported *
A	5.3	2	1.8 – 5.3
B	36.7	2	37 – 88
C	4233	70	3000 – 4700
D	16441	1050	13000 – 23000
E	142383	6200	102000 - 172000

\*Preliminary working values presented at Technetium 1998 McCartney (1998)

### 5.4.5 *Conclusions*

1. A method has been developed to determine  $^{99}\text{Tc}$  in a variety of environmental matrices including seaweed, lobster and sediments, using  $^{99\text{m}}\text{Tc}$  as the yield monitor.  $\text{Tc-99m}$  was found to be the most suitable yield monitor.
2. 0.88 SG ammonia was found to effectively reduce the loss of  $^{99}\text{Tc}$  through volatilisation during ashing.
3. The optimum ashing condition was to gradually increase the temperature from 250°C to 550°C at 50°C increments per hour as it minimises losses of Tc.
4. Optimum leaching was found to be with 8M nitric acid heated for two hours on a hotplate at 125°C.
5. Initial concentration and decontamination of  $^{99}\text{Tc}$  was using an iron hydroxide precipitation, anion exchange using Eichrom X8 (100–200) mesh anion exchange resin, and removal of ruthenium by solvent extraction of Tc into 5% TnOA in xylene.
6. The yield monitor is determined using a HPGe  $\gamma$ -ray spectrometer. Recoveries are typically in the range of 75% -95%.
7. Determination of  $^{99}\text{Tc}$  is made after a further week following the  $^{99\text{m}}\text{Tc}$  decay. The method has a limit of detection of 1.7 Bq kg<sup>-1</sup> assuming a 10g sample size and a 2 hour count time.

### 5.4.6 *Acknowledgements*

The authors would like to thank Dr R Carpenter, AEA Technology, Harwell, UK for partial support of this project. The project was jointly funded by the Geosciences Advisory Unit, Southampton Oceanography Centre, AEA Technology, Harwell and the Institute of Terrestrial Ecology, Merlewood. Reference samples and data were provided by Dr M. McCartney SURRC, East Kilbride. Dr N. Fleming, Nuclear Medicine, Southampton General Hospital generously provided  $^{99\text{m}}\text{Tc}$ .

### 5.4.7 Reference

Aarkrog A., Dahlgaard H., Hellstadius L., Holm E., Mattsson S. & Rioseco J. In “Technetium in nature” Eds. Desmet and Myttenaere. (1986) 69 - 78 Elsevier. Science, London, UK.

Beals D.M. & Hayes D.W. Technetium-99, Iodine-129 and tritium in the wastes of the Savannah River Site. *Sci. Total. Environ.* **173** (1996) 101 – 115.

BNFL. Annual report on the radioactive discharges and monitoring of the environment. Directorate of Health, Safety & Environmental Protection. (1983 – 1995) BNFL. Warrington.

Chen Q., Dahlgaard H., & Nielsen S.P. Determination of  $^{99}\text{Tc}$  in sea-water at ultra low levels. *Anal. Chim. Acta*, **285** (1994) 177 - 180.

Chen Q., Dahlgaard H., Hansen H.J.M. & Aarkrog A. Determination of  $^{99}\text{Tc}$  in environmental samples by anion exchange and liquid-liquid extraction at controlled valency. *Anal. Chim. Acta*, **228** (1990) 163 – 167.

Currie L.A. Limits for qualitative detection and quantitative determination: Application to radiochemistry. *Anal. Chem.*, **40** (1968) 586 - 593.

Dale C.J., Warwick P.E., & Croudace I.W. An optimised method for Technetium-99 determination in low level waste by extraction into tri-n-octylamine. *Radioactivity and Radiochemistry*, **7** (1996) 23 - 31.

Dixon P., Curtis D.B., Musgrove J., Roensh F., Roach F. & Rokop D. Analysis of naturally produced Technetium and Plutonium in Geologic materials. *Anal. Chem.*, **69** (1997) 1692 - 1699.

Foti S., Delucchi E., & Akamian V. Determination of picogram amounts of technetium in environmental samples by Neutron Activation Analysis. *Anal. Chim. Acta*, **60** (1972) 269 - 276.

Garcia Leòn M. Determination and levels of  $^{99}\text{Tc}$  in environmental and biological samples. *J. Radioanal. Nucl. Chem.*, **138** (1990) 171 - 179.

Goldchurt N.W., & Sedlet J. Radiochemical determination of technetium-99 in environmental water samples. *Anal. Chem.*, **41** (1969) 669 - 671.

Gray J., Jones S. R. & Smith A. D. Discharges to the environment from the Sellafield Site, 1951 – 1992. *J. Environ. Radioactivity*, **2** (1995) 23 – 40.

Harvey B.R., Ibbett R.D., Williams K.J., & Lovett M.B. The determination of technetium-99 in environmental materials. MAFF Directorate of Fisheries research: Aquatic Environmental Protection: Analytical Methods, **8** (1991) 1 - 22.

Holm E., Rioseco J., & García Leòn M. Determination of  $^{99}\text{Tc}$  in environmental samples. *Nuclear Instruments and Methods in Physics research*, **233** (1984) 204 - 207.

Kaye J.H., Merrill J.A., Kinnson R.R., Rapis M.S., & Bailou N.E. Radiochemical determination of technetium-99. *Anal. Chem.*, **54** (1982) 1154 - 1163.

Kenna B.T. & Kuroda P.K. Technetium in nature. *J. Inorg. Nucl. Chem.*, **26** (1964) 493 - 499.  
Korkish J. Handbook of ion exchange resins: Their application to inorganic analytical chemistry.  
(1989) *CRC Press. Boca Raton, Fla, USA.*

Leonard K.S., McCubbin D., Brown J., Bonfield R.A. & Brooks T. A summary report of the distributions of  $^{99}\text{Tc}$  in UK coastal waters. *Radioprotection – Colloques*, **32** (1997) 109 – 114.

Maeck W.J., Booman G.L., Kussy M.E. & Rein J.E. Extraction of the elements as Quaternary Propyl, Butyl and Hexyl amine complexes. *Anal. Chem.*, **33** (1961) 1775 - 1750.

Martin J.E. & Hylko J.M. Measurement of  $^{99}\text{Tc}$  in low level radioactive waste from reactors, using  $^{99\text{m}}\text{Tc}$  as a tracer. *J. Appl. Radiat. Isot.*, **38** (1987) 447 - 450.

Matsuoka N., Umatat T., Okamura M., Monoshima N., & Takashima Y. Determination of  $^{99}\text{Tc}$  from the aspect of environmental radioactivity. *J. Radioanalytical and Nuclear Chemistry*, **140** (1990) 73 - 78.

McCartney M. Personal communication. (1997) Paper presented at Tc1998 at the Southampton Oceanography Centre.

Pruett D.J., The solvent extraction behaviour of Technetium. Part II the hydrochoric acid – Tri-n-butyl phosphate system. *Radiochim Acta*, **29**. (1981) 107 – 111.

Tagami K. & Uchida S. Separation procedure for the determination of Technetium-99 in soil by ICP-MS. *Radiochim. Acta*, **63** (1993) 69 - 72.

Watanabe S. & Hashimoto K. Solvent extraction of technetium in urine with TBP. *J. Radioanal. Nucl. Chem.*, **201** (1995) 361 - 370.

## 5.5 Conclusions

Sequential separation of  $^{55}\text{Fe}$ ,  $^{63}\text{Ni}$ ,  $^{90}\text{Sr}$  and  $^{99}\text{Tc}$  from low-level wastes is readily achievable using extraction chromatographic techniques. Commercially available Sr-resin and TEVA® resin were the most appropriate materials for the purification of  $^{90}\text{Sr}$  and  $^{99}\text{Tc}$  respectively whilst diisobutylketone and dimethylglyoxime-based materials were prepared and characterised for the purification of  $^{55}\text{Fe}$  and  $^{63}\text{Ni}$  respectively. Good separation and decontamination factors for all isotopes were observed. Chromatographic separation resulted in a significant reduction in organic solvents wastes arising and permitted rapid analysis of larger batch sizes compared with solvent extraction-based techniques. The combination of separate extraction chromatographic techniques into a single sequential separation scheme resulted in a reduction in analysis time whilst permitting the determination of a series of isotopes on samples of limited size.

Modification of the sequential separation scheme for sediment analysis was required. Chemical recovery of  $^{63}\text{Ni}$  and  $^{90}\text{Sr}$  was determined through the addition of stable Ni and Sr with the measurement of these stable elements in the purified fraction by ICP-AES. Iron-55 recovery was determined by measuring the stable Fe content of the sample before and after purification. Recovery of  $^{99}\text{Tc}$  was determined through the addition of  $^{99\text{m}}\text{Tc}$  yield monitor. Relatively low loading capacities of the diisobutylketone chromatographic material meant that it was unsuitable for the purification of high-Fe samples such as sediments and a solvent-extraction based separation scheme was therefore adopted. However, for  $^{63}\text{Ni}$  and  $^{90}\text{Sr}$ , the extraction chromatographic separation was still suitable for routine application and a sequential separation scheme for  $^{55}\text{Fe}$ ,  $^{63}\text{Ni}$  and  $^{90}\text{Sr}$  was developed.

The determination of  $^{99}\text{Tc}$  was not included in the sequential separation scheme as special precautions during the drying, ashing and leaching stages were required that were specific to  $^{99}\text{Tc}$  and probably not as suitable for the other radioisotopes.  $^{99}\text{Tc}$  analysis was therefore performed on a separate aliquot of sample. Conditions for the ashing and leaching of sediments prior to  $^{99}\text{Tc}$  separation were optimised. Preconcentration of  $^{99}\text{Tc}$  from the sediment leachate (following an  $\text{Fe}(\text{OH})_3$  scavenge) was achieved using anion exchange chromatography and final purification of  $^{99}\text{Tc}$  was achieved by extraction into tri octylamine in xylene. TEVA® resin could be used for this final purification stage. However, elution of  $^{99}\text{Tc}$  from TEVA® resin requires strong  $\text{HNO}_3$  that would have to be evaporated off prior to liquid scintillation

counting. This would add a further stage to the separation with the potential for loss of the  $^{99}\text{Tc}$ . TEVA® resin can be added directly to scintillant but for low-level environmental  $^{99}\text{Tc}$  analysis, where limits of detection are often approached the TOA-xylene-scintillant mixture provided the most suitable source for liquid scintillation counting.

For all isotopes chemical recoveries were consistently high although over-spiking of the sample with Sr led to some samples with lower than expected recoveries. The final purified fraction for all isotopes contained no other contaminating radioisotopes with the exception of  $^{55}\text{Fe}$ , which contained traces of  $^{210}\text{Po}$ . This contamination did not affect the  $^{55}\text{Fe}$  determination by liquid scintillation counting.

Re-use of the Sr-resin® was investigated and found to be viable for the sample type and activity levels tested.

## 5.6 References

Bock R. (1979). A handbook of decomposition methods in analytical chemistry. Blackie Group, Glasgow, UK.

Harvey B., Ibbett R.D., Williams K.J. and Lovett M.B. (1991) The determination of technetium-99 in environmental materials. Ministry of Agriculture, Fisheries and Foods. Aquatic Environmental Protection: Analytical methods number 8. Lowestoft, UK

Korkisch J. (1989). Handbook of ion exchange resin: their application to inorganic analytical chemistry. CRC Press, Boca Raton, USA

## Chapter 6

# **A study of beta emitters in a saltmarsh environment**

## 6. A study of beta emitters in a saltmarsh

### 6.1. Introduction

#### 6.1.1. Sources of anthropogenic radioactivity in the Irish Sea area

Fission products, activation products and actinides in the Irish Sea are derived from three main sources. Global nuclear weapons' fallout and radioactivity from the Chernobyl accident in 1986 both contributed to the inventory of radioisotopes in global waters including the Irish Sea. However, the main source of anthropogenic radioactivity in the area is the BNFL nuclear fuel-reprocessing site at Sellafield.

The BNFL Sellafield site (formerly known as Windscale) is located on the West Cumbrian coast and is one of four sites operated by BNFL in the UK. Work commenced at the site on the reprocessing of irradiated nuclear fuel to meet the UK programme for nuclear weapons development that required kilogram quantities of plutonium for the Cold War. Originally the site consisted of two air cooled reactors for Pu production, known as the Windscale piles, nuclear fuel reprocessing plants designed for the recovery of Pu and ancillary operations in support of the reactors and reprocessing operations. The Windscale piles were shut down in October 1957 following a fire in one of the piles, which resulted in the uncontrolled release of  $10^{15}$  Bq of fission products (mainly  $^3\text{H}$  and  $^{131}\text{I}$ , but also other fission products and  $^{210}\text{Po}$ ) to the local environment (Crick and Linsley, 1984). In 1956 the first of four Magnox-type reactors was brought on-line. All of these reactors are still in operation. In addition, a prototype Advanced Gas-cooled reactor became fully operational in 1963 and continued operation until 1981.

Although originally designed to isolate valuable Pu for the nuclear weapons' programme, the reprocessing plant at Sellafield was also used to isolate Pu for the UK fast breeder programme, as well as to recover and recycle the  $^{235}\text{U}$  that remained following fuel irradiation (now the main function of the site). A review of the reprocessing operations at Sellafield has been published (Gray *et al*, 1995) and is summarised here.

Fuel from the Windscale pile reactors was stored under water in open fuel ponds. Between 1960 and 1985, Magnox fuel was stored under water in closed fuel ponds (B30). Since 1985 the irradiated fuel has been stored in an enclosed pond which is located in the Fuel Handling Building, B311. Following storage, fuel was originally transferred to a Pu separation plant (B204) and subsequently on to the Pu purification plant (B209S). Both plants commenced operation in 1952 with the Pu purification plant ceasing operation in 1954. Pu purification

was transferred to a new plant, B203, which operated between 1954 and 1987. In 1964 a new integrated separation and purification plant, B205, was commissioned and B204 reverted to the recovery of Pu from residues. Swarf from the pile reactors' fuel was stored in a dry condition in the 'silos', B41. Between 1963 and 1990 Magnox swarf was stored under water in building B38. Since 1990, this swarf has been treated in the new encapsulation and storage facility.

Following the commissioning of the prototype AGR, the primary separation plant, B204, was modified to handle oxide fuel. The modified plant commenced reprocessing operations in 1969 but ceased operation in 1973 following a non-routine release of  $^{106}\text{Ru}$ . Since 1973, oxide fuel was stored on site until the Thermal Oxide Reprocessing plant, THORP, began handling fuel in 1988.

#### *6.1.2. Atmospheric and Liquid Discharges from Sellafield*

Reprocessing operations at Sellafield can be summarised as follows. Fuel from the Magnox and more recently PWR reactors is stored for a period to permit the decay of short-lived fission products. The fuel is then sheared and the fuel dissolved in 6-11M  $\text{HNO}_3$ . The hulls do not dissolve and are isolated for waste treatment and subsequent disposal. The uranium, plutonium and fission products are then segregated using a process known as the PUREX process. In this process the  $\text{HNO}_3$  concentration is reduced to 3-4M and U(VI) and Pu(IV) are extracted into tributylphosphate (TBP) diluted with kerosene. Pu is then reduced to Pu(III) and back-extracted into  $\text{HNO}_3$ . Reduction of Pu can be achieved through the addition of U(IV). U(IV) and U(VI) both remain in the organic phase and are subsequently back-extracted with dilute  $\text{HNO}_3$ . U and Pu are then further purified using additional TBP extraction cycles.

During the shearing and dissolution stages of the operation significant quantities of the volatile radioisotopes such as  $^3\text{H}$  and  $^{131}\text{I}$  are liberated from the fuel rods. The vent gases from this process, containing the volatile radioisotopes, are passed through a series of filters before being released into the environment through stacks. Once discharged into the atmosphere, the volatile radioisotopes are rapidly dispersed by prevailing winds with some subsequent deposition occurring through the radioisotopes being carried on precipitation. In addition to the radioactivity released during reprocessing operations, airborne releases have also routinely occurred from the Windscale piles, the Magnox and AGR reactors, the vitrification plants and the open fuel storage ponds. Authorised releases have also occurred from so-called 'approved places' namely R & D laboratories located on the site. Releases from the Windscale pile

stacks has included activity released by burst cartridges, approximately 20 kg of irradiated particulate uranium oxide originating from corroding cartridges lodged in outlet air ducts and volatile fission products released during the 1957 fire. Due to the range of sources for airborne release of radioactivity, the associated range of discharge stack heights and the variable weather conditions prevalent at a given discharge event it is difficult to generalise on the dispersion of the airborne discharge.

Liquid wastes from the reprocessing operation are discharged to the Irish Sea via a pipeline that extends 2.5 km beyond high water. Significant radioactive effluent discharges commenced in 1952 although relatively small levels of radioactivity were discharged in 1951. The majority of the radioactive liquid effluent discharged from the Sellafield site originates from the reprocessing operations on the site and the purge waters from the fuel storage ponds. Since 1988 discharges have also arisen from the THORP fuel receipt and storage area.

Additional smaller discharges arise from surface drainage water, laundry effluent and sewage. Discharges from the reprocessing operations originate from medium active liquors mainly produced during the purification of Pu and U. Liquors from the Pu purification plants, B209S and B203 were originally transferred to a holding tank to permit the decay of short-lived radioisotopes and then discharged to sea. The integrated separation and purification plant, B205, employed a concentration procedure to reduce the volume of the medium active liquor and hence permit its storage for longer periods. However, the increased throughput of fuel for reprocessing resulted in activities in the liquor increasing to a level where it was no longer viable to continue discharges. Levels of actinides discharged were reduced using a flocculation/precipitation treatment from the mid-1970s until 1980 when effluents from B205 were stored until the Enhanced Actinide Removal Plant was commissioned in 1994. All liquid effluents from B205 are now treated in EARP prior to discharge to sea.

Purge waters from fuel storage ponds were originally discharged to sea without any treatment. Temporary (unspecified) measures were introduced in the late 1970s to reduce the levels of radioactivity in the purge waters and in 1985 the Site Ion- eXchange Effluent Plant (SIXEP) commenced operation. SIXEP employs an array of sand filters and clinoptilolite ion exchangers to remove many of the fission products from the purge waters prior to sea discharge. Levels of  $^{90}\text{Sr}$ ,  $^{134}\text{Cs}$  and  $^{137}\text{Cs}$  in the liquid discharge have therefore dropped significantly since 1985.

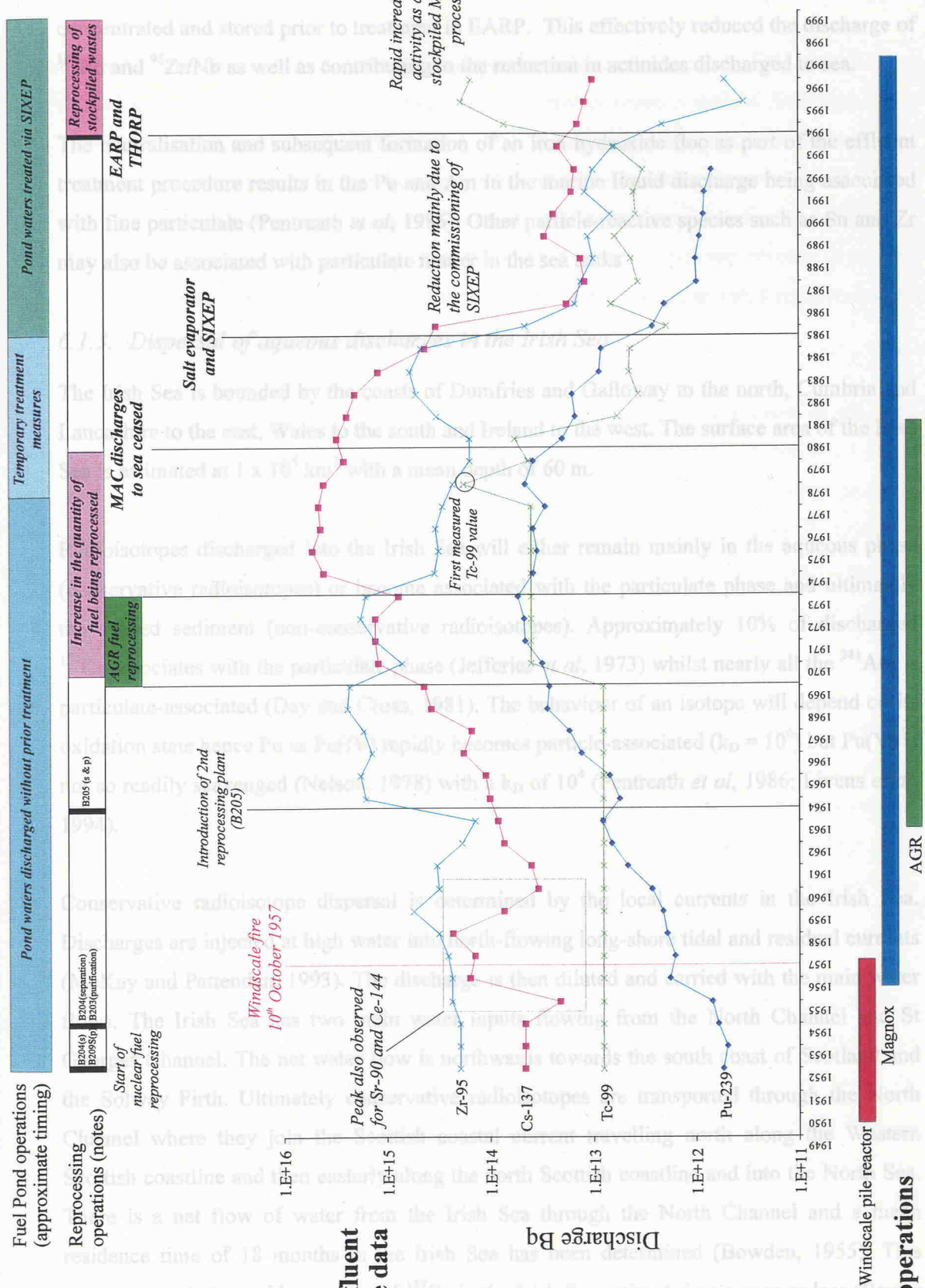


Figure 6.1: Site operations and radionuclide discharge patterns for the Sellafield site

The introduction of the salt evaporator in 1985 permitted salt-bearing liquors to be concentrated and stored prior to treatment in EARP. This effectively reduced the discharge of  $^{106}\text{Ru}$  and  $^{95}\text{Zr}/\text{Nb}$  as well as contributing to the reduction in actinides discharged to sea.

The neutralisation and subsequent formation of an iron hydroxide floc as part of the effluent treatment procedure results in the Pu and Am in the marine liquid discharge being associated with fine particulate (Pentreath *et al*, 1986). Other particle-reactive species such as Sn and Zr may also be associated with particulate matter in the sea tanks

#### *6.1.3. Dispersal of aqueous discharges in the Irish Sea*

The Irish Sea is bounded by the coasts of Dumfries and Galloway to the north, Cumbria and Lancashire to the east, Wales to the south and Ireland to the west. The surface area of the Irish Sea is estimated at  $1 \times 10^5 \text{ km}^2$  with a mean depth of 60 m.

Radioisotopes discharged into the Irish Sea will either remain mainly in the aqueous phase (conservative radioisotopes) or become associated with the particulate phase and ultimately the seabed sediment (non-conservative radioisotopes). Approximately 10% of discharged  $^{137}\text{Cs}$  associates with the particulate phase (Jefferies *et al*, 1973) whilst nearly all the  $^{241}\text{Am}$  is particulate-associated (Day and Cross, 1981). The behaviour of an isotope will depend on its oxidation state hence Pu as Pu(IV) rapidly becomes particle-associated ( $k_D = 10^6$ ) but Pu(V) is not so readily scavenged (Nelson, 1978) with a  $k_D$  of  $10^4$  (Pentreath *et al*, 1986; Livens *et al*, 1994).

Conservative radioisotope dispersal is determined by the local currents in the Irish Sea. Discharges are injected at high water into north-flowing long-shore tidal and residual currents (McKay and Pattenden, 1993). The discharge is then diluted and carried with the main water flows. The Irish Sea has two main water inputs flowing from the North Channel and St Georges Channel. The net water flow is northwards towards the south coast of Scotland and the Solway Firth. Ultimately conservative radioisotopes are transported through the North Channel where they join the Scottish coastal current travelling north along the Western Scottish coastline and then easterly along the north Scottish coastline and into the North Sea. There is a net flow of water from the Irish Sea through the North Channel and a mean residence time of 18 months in the Irish Sea has been determined (Bowden, 1955). This compares with the residence time of  $^{137}\text{Cs}$  in the Irish Sea estimated as a year or less (Baxter *et al*, 1979). Some recirculation of radioactivity occurs southward both along the Cumbrian

coastline and down the Eastern coast of Northern Ireland. However little radioactivity appears to be transported through St Georges Channel and into the English Channel.

Following transport into the North Sea, conservative radioisotopes such as  $^{99}\text{Tc}$  and  $^{137}\text{Cs}$  are carried across the North Sea to the Scandinavian coastline where Sellafield discharge signal combines with the discharge signal from the La Hague reprocessing plant in France. The discharge is then carried northward along the Scandinavian coastline into the Arctic Ocean where the contaminated water divides (Figure 6.2). One fraction is carried eastward into the Barents Sea. However, the majority of the discharge is carried westward towards Greenland and subsequently down the eastern coastline of Canada and the USA at which point the signal has been rendered undetectable through dilution.

Particle-associated radioisotopes are far less mobile. A significant proportion of the non-conservative radioisotopes discharged into the Irish Sea are scavenged and deposited in the mud belt lying off the Cumbrian coastline. Subsequent redistribution of these radioisotopes is dependent on the resuspension and subsequent transport of these sediments. Following a significant reduction in the activity discharged by Sellafield it has been estimated that the dominant mechanism for supply of radioisotopes to the Solway Coast is via the transport of contaminated sediments (MacKenzie *et al*, 1987; McDonald *et al*, 1990).

Determination of radioisotope depth profiles in sediment core samples has been used to determine a discharge chronology for the particular radioisotope (e.g. Kershaw *et al*, 1990). The use of Irish seabed sediments in this manner is not appropriate due to low sedimentation rates of between 0.02 and 0.08 cm/yr and significant levels of bioturbation (Kershaw *et al*, 1983; Kershaw, 1986; Kershaw *et al*, 1988). Likewise intertidal sediments often experience significant post-depositional mixing again destroying any chronological record.

Saltmarsh sediments are more suitable as they exhibit high sedimentation rates of the order of a few cm/yr and are less prone to post-depositional mixing. Saltmarsh sediments were therefore chosen for this study. A number of suitable saltmarshes are located along the Cumbrian and South West Scotland coastlines. Of these, the Ravenglass saltmarsh at the mouth of the Esk estuary has been widely studied as it is only 10km south of Sellafield and has received relatively high activities of the Sellafield discharge. This saltmarsh was therefore chosen for further investigation.

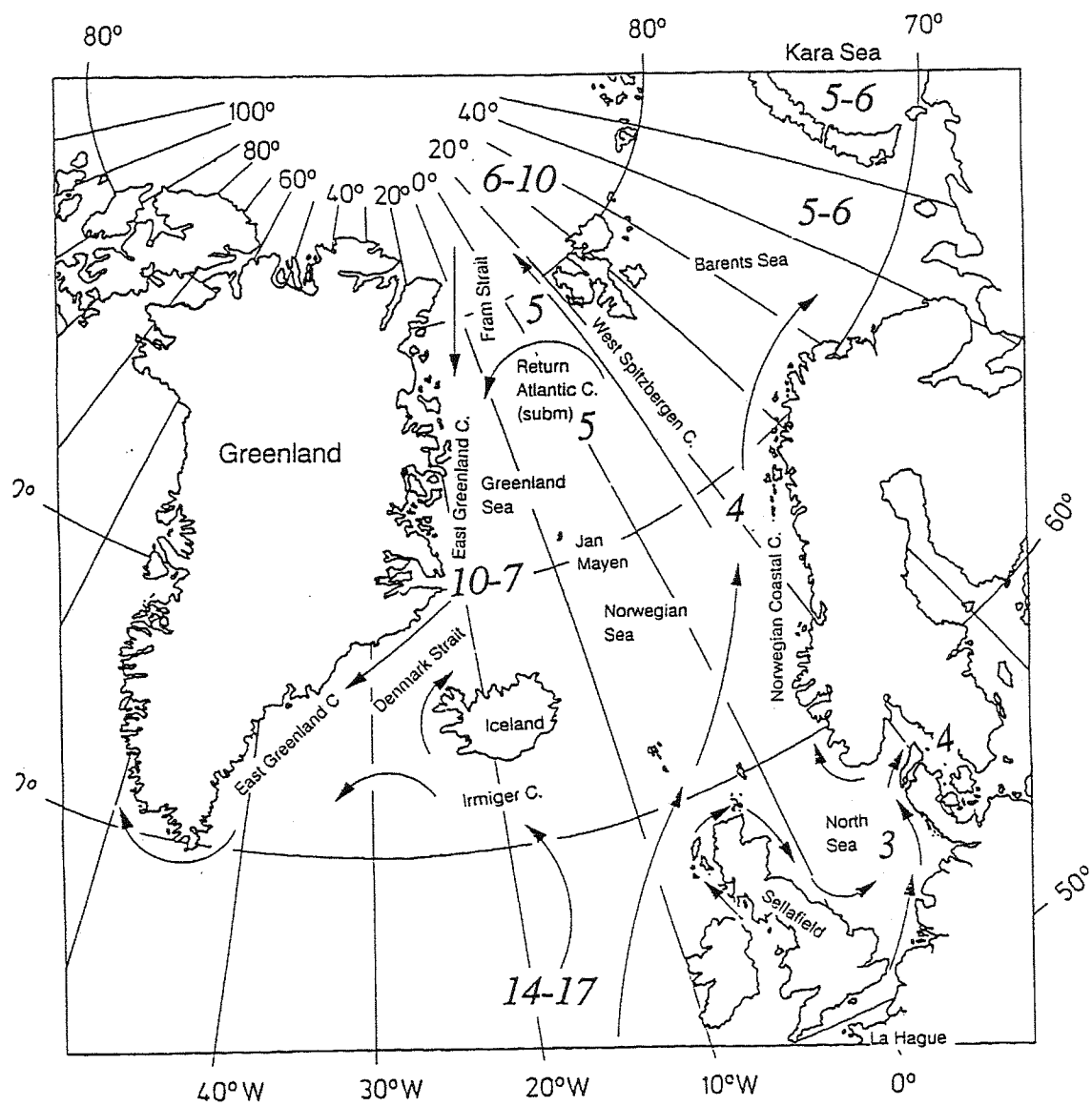


**Figure 6.2 : Dispersal of Sellafield and La Hague discharge**  
(numbers are transit times in years - afetr Dahlgaard, 1995)

## 6.2. Methodology

022. Sun

The saltwater  
The core was  
sampling point  
tube, which  
approximate  
differences 53° N

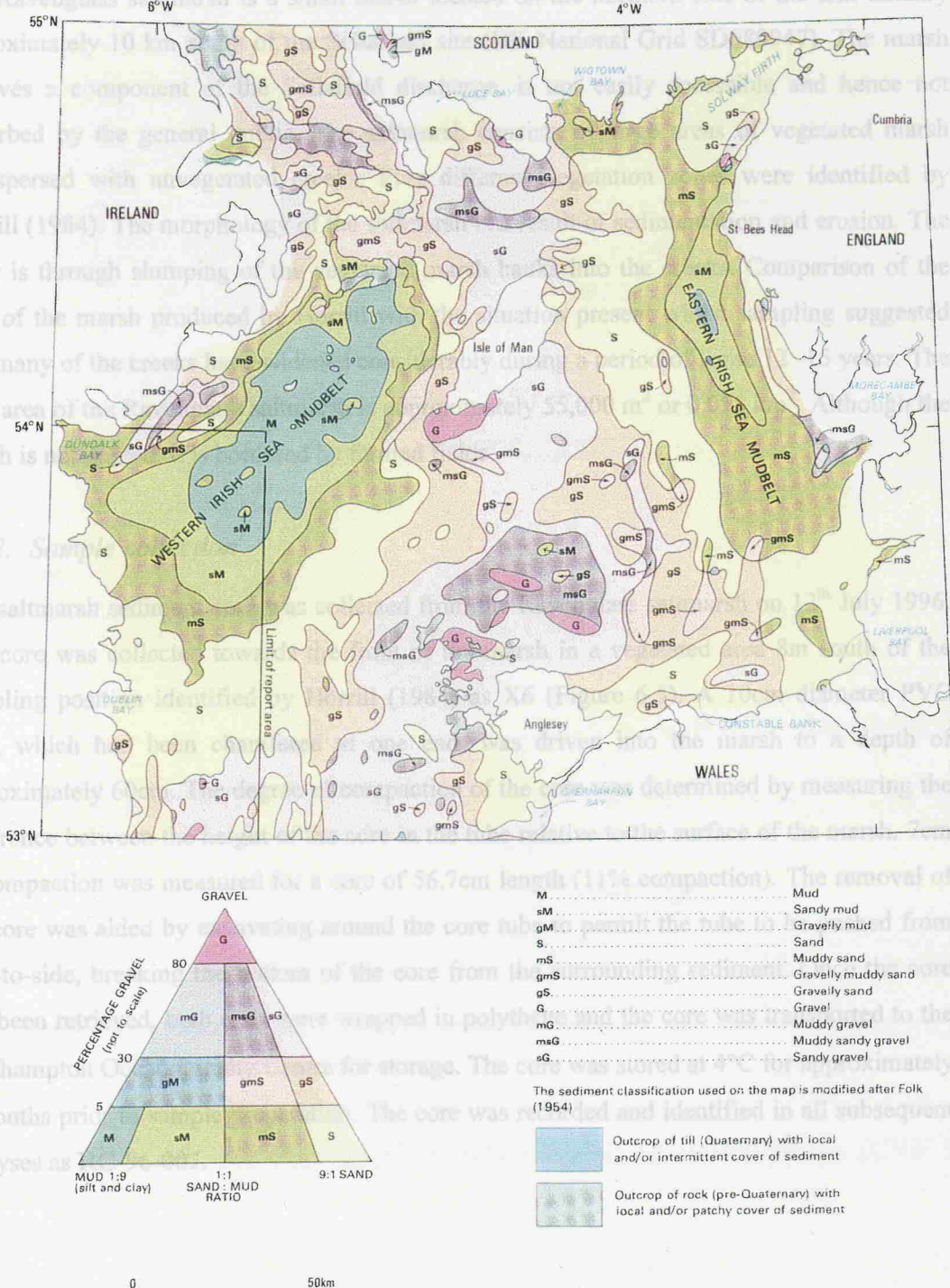


**Figure 6.3 : Irish sea - seabed sediment map  
(after Jackson *et al*, 1995)**

## 6.2. Methodology

### 6.2.1. *The Ravenglass Saltmarsh sampling site*

The Ravenglass saltmarsh is a small marsh located on the northern side of the Esk Estuary approximately 10 km south of the Sellafield site (UK National Grid SD089947). The marsh receives a component of the Sellafield discharge, is not easily accessible and hence not disturbed by the general public. The saltmarsh consists of large areas of vegetated marsh interspersed with unvegetated creeks. Five different vegetation zones were identified by Horrill (1984). The morphology of the saltmarsh is a result of sedimentation and erosion. The latter is through slumping of the vegetated marsh banks into the creeks. Comparison of the map of the marsh produced by Horrill with the situation present whilst sampling suggested that many of the creeks have widened considerably during a period of some 12 -15 years. The total area of the Ravenglass saltmarsh is approximately 55,000 m<sup>2</sup> or 0.055 km<sup>2</sup>. Although the marsh is not grazed, it is bordered by farmed fields.

### 6.2.2. *Sample collection*

The saltmarsh sediment core was collected from the Ravenglass saltmarsh on 12<sup>th</sup> July 1996. The core was collected towards the front of the marsh in a vegetated area 8m south of the sampling position identified by Horrill (1984) as X6 (Figure 6.5). A 10cm diameter PVC tube, which had been chamfered at one end, was driven into the marsh to a depth of approximately 60cm. The degree of compaction of the core was determined by measuring the difference between the height of the core in the tube relative to the surface of the marsh. 7cm of compaction was measured for a core of 56.7cm length (11% compaction). The removal of the core was aided by excavating around the core tube to permit the tube to be pushed from side-to-side, breaking the bottom of the core from the surrounding sediment. Once the core had been retrieved, both ends were wrapped in polythene and the core was transported to the Southampton Oceanography Centre for storage. The core was stored at 4°C for approximately 3 months prior to sample preparation. The core was recorded and identified in all subsequent analyses as **RC-96-007**.

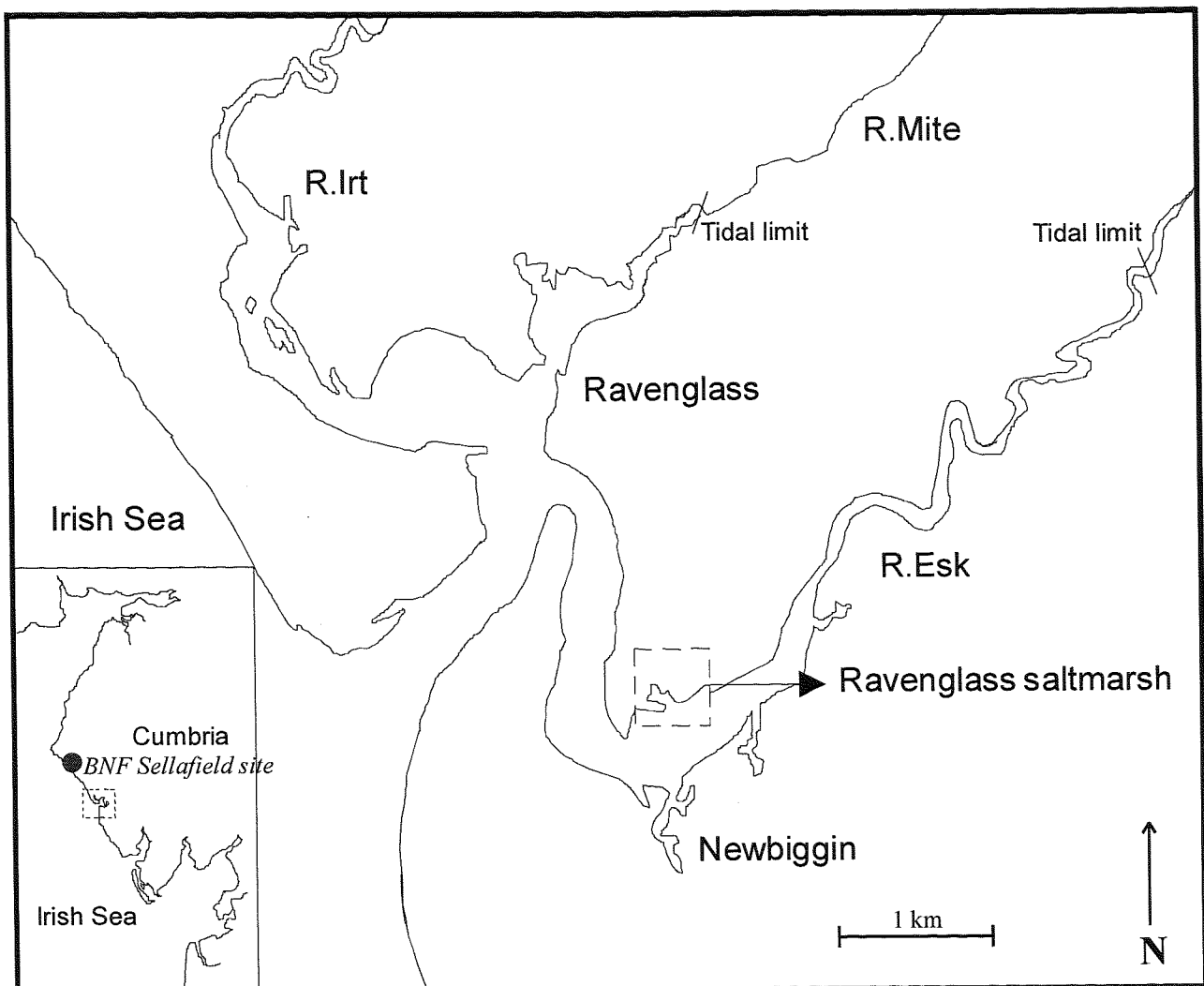


Figure 6.4 : Location of the Ravenglass saltmarsh in relation to BNF Sellafield



### 6.2.3. Physical description

The core PV-1 was cut using a chisel and wire saw. The core was relatively uniform with a diameter of 10 cm, which was the size of the metal platter used. The organic matter was very soft and friable, with a  $\sim 2.4 \text{ g cm}^{-3}$  dry density.

### 6.2.4. X-ray fluorescence

A slab of sediment was cut with a knife. The slab was then placed in a Packard Pacific 1400 sequential X-ray fluorescence spectrometer having

previously been dried in a viaduct.

Previously dried in a viaduct.

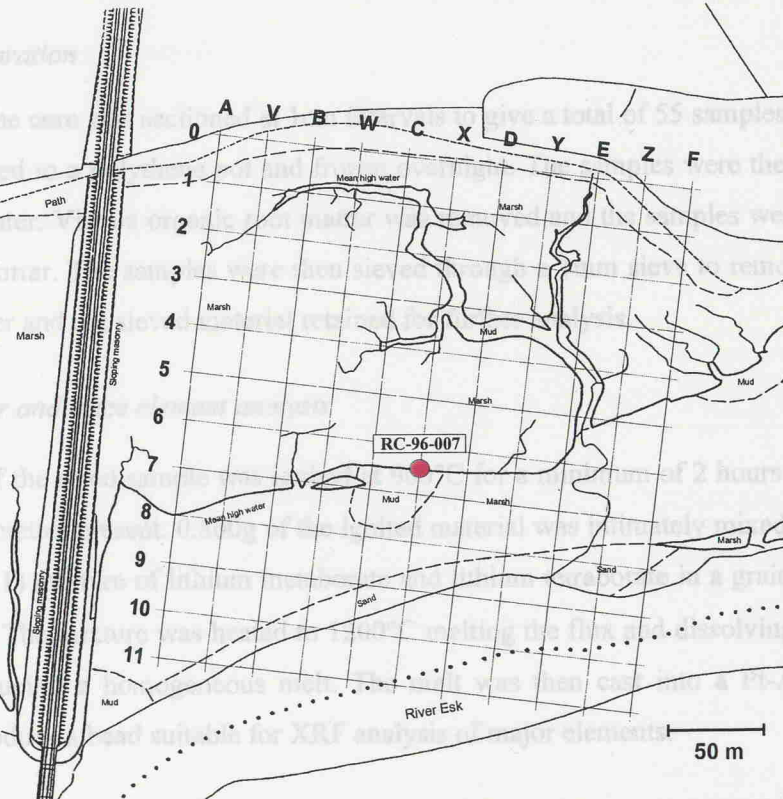
### 6.2.5. Chemical and radiochemical analysis of core RC-96-007

#### 6.2.5.1. Preparation

One half of the core was cut into 11 cm sections, giving a total of 55 samples. Each sample was transferred to a pre-weighed crucible and dried at  $60^\circ\text{C}$  to remove water. The samples were then ground in a pestle and mortar. The remaining half of the core was used to remove stones and organic matter from the sediment.

#### 6.2.5.2. Major and trace element analysis

An aliquot of the sample was dried at  $60^\circ\text{C}$  for 2 hours to decompose any organic matter. The sample was then ground in a crucible with 4.00g of n eutectic (4.00g  $\text{LiB}_4\text{AlB}_10$  and 0.005g  $\text{LiCl}$ ) and 1.00g of ground stabilised Pt.



An erucible. The sample was then dried at  $60^\circ\text{C}$  for 2 hours to decompose the sediment.

An erucible. The sample was then dried at  $60^\circ\text{C}$  for 2 hours to decompose the sediment.

10g of ground sample was pressed into a pellet. Trace elements were measured in this pellet

again using XRF. Both the major and trace element analyses were determined using a Philips

1400 sequential X-ray fluorescence spectrometer.

1400 sequential X-ray fluorescence spectrometer.

**Figure 6.5 : Aerial view of the Ravenglass saltmarsh and map showing the sampling position for core RC-96-007 (grid after Horrill, 1984)**

### 6.2.3. *Physical description of Core RC-96-007*

The core PVC tube was cut using an angle grinder and the sediment core was halved using a cheesewire. The physical appearance of the core was then recorded. The core was relatively uniform with no distinct banding or zonation. Some orange/brown mottling was observed which was most prominent in the first 29cm but was still observable below this depth. Root matter was visible again to a depth of about 29cm. Below this depth the decomposing organic matter was visible.

### 6.2.4. *X-radiography*

A slab of sediment 1cm thick was cut from one half of the core using an electro-osmotic knife. The slab was cut in half prior to X-radiography. The slab was placed in a Hewlett Packard Faxitron X-ray system and exposed for 2mins at 56 kV (the exposure time having previously been determined using test films exposed for different times at 56 kV).

### 6.2.5. *Chemical and radiochemical analysis of core RC-96-007*

#### 6.2.5.1. *Preparation*

One half of the core was sectioned at 1cm intervals to give a total of 55 samples. Each sample was transferred to a polythene pot and frozen overnight. The samples were then freeze-dried to remove water. Visible organic root matter was removed and the samples were ground in a pestle and mortar. The samples were then sieved through a 1mm sieve to remove stones and organic matter and the sieved material retained for further analysis.

#### 6.2.5.2. *Major and trace element analysis*

An aliquot of the dried sample was ignited at 900°C for a minimum of 2 hours to decompose any organic matter present. 0.800g of the ignited material was intimately mixed with 4.00g of a eutectic (4:1) mixture of lithium metaborate and lithium tetraborate in a grain stabilised Pt-Au crucible. The mixture was heated to 1200°C melting the flux and dissolving the sediment sample producing a homogeneous melt. The melt was then cast into a Pt-Au mould and cooled to produce a bead suitable for XRF analysis of major elements.

10g of ground sample was pressed into a pellet. Trace elements were measured in this pellet again using XRF. Both the major and trace element analyses were determined using a Philips 1400 sequential X-ray fluorescence spectrometer.

#### 6.2.5.3. *Carbon analysis*

Total carbon analysis was performed on a Carlo Erba CHNO-S elemental analyser. A known mass of sample was weighed into a tin capsule that was subsequently crimped. The sample was then ignited by flash pyrolysis and the gases separated by gas chromatography. Final detection of the gases was achieved using a flame ionisation detector. Standards of known elemental composition were measured to permit quantification.

#### 6.2.5.4. *Gamma spectrometric analysis*

Approximately 20g of sample were transferred to a 22ml polythene scintillation vial and the exact mass of sample recorded. The sample was then counted on a well-type high purity germanium (HPGe) detector. The resulting energy spectrum was deconvoluted and the activity of each identified radioisotope calculated using Fitzpeaks software. The gamma spectrometer was previously calibrated for both energy and efficiency against an Amersham QCY-48 mixed radioisotope standard adsorbed onto a sediment matrix using the method described by Croudace (1991).

#### 6.2.5.5. *Radiochemical analysis*

Radiochemical analysis of  $^{55}\text{Fe}$ ,  $^{63}\text{Ni}$  and  $^{90}\text{Sr}$  were performed on the freeze-dried material using the sequential separation scheme described in Chapter 5.  $^{99}\text{Tc}$  was also determined (Wigley – pers. comm.) using the method described by Wigley *et al* (1999).

### 6.3. Analytical results for core RC-96-007

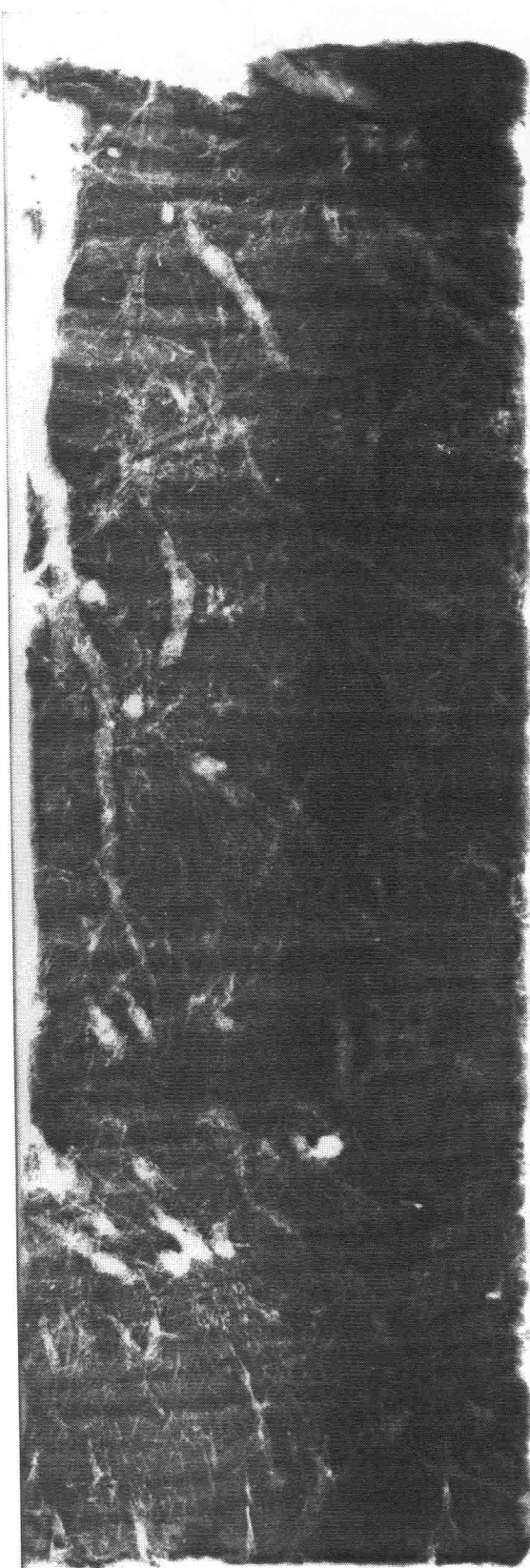
#### 6.3.1. Physical and X-radiographic description of the core

Initial observation of the sediment core showed no visible signs of banding or zonation along the core. The general appearance was uniform down the core with the exception of identifiable root material at the top of the core and decomposing organic matter at depth. However X-radiography (Figure 6.6) identified discrete light and dark banding of the core at approximately 0.5cm intervals. This banding is a result of slight compositional variation of incoming sediments at intervals probably corresponding to summer and winter months. Inspection of a thin section of sediment under a microscope has identified that the dark bands correspond to coarser-grained material containing quartz, plagioclase and feldspar whilst the light bands contain more clay minerals.

#### 6.3.2. Major and trace element composition

Geochemical analysis (Figures 6.7 & 6.8) showed that the bulk composition of the sediment was relatively uniform to a depth of about 50cm. As major and trace element analysis was performed with a resolution of 1cm, compositional changes related to the banding observed in the X-radiograph were not resolved. Al and Ti contents were uniform throughout the core at approximately 10-11 and 0.6 – 0.7 wt % respectively. Si varied between 70 and 75 wt % down to a depth of 50cm. Below 50cm the Si concentration increased to 78% as the sediment became more sandy suggesting that the underlying sand was being approached. Ca was highest at the top of the core (4.33 wt %) declining rapidly to reach a value of 1.4 wt % at a depth of 7cm. A similar exponential decrease in concentration was observed for Sr but not for Ba. The Ca/Sr ratio (Figure 6.9) varied from 186 at the top of the core to around 90 below 7cm. The Ca and Sr profiles are indicative of the dissolution of a source of calcium/strontium carbonate at the top of the core with subsequent migration of the dissolved Ca and Sr downwards. Sources of carbonate would include microfauna (e.g. forams) and shell material, which was observed in some quantity on the surface of the marsh. The maximum Ca/Sr ratio of 205 is comparable with Ca/Sr ratios of 108-248 measured in a number of mollusc shells (Bowen, 1956). Cl concentrations declined down the core reflecting the decline in seawater content with depth.

TOP



12cm

BOTTOM

**Figure 6.6 : X-radiograph image of core RC-96-007**

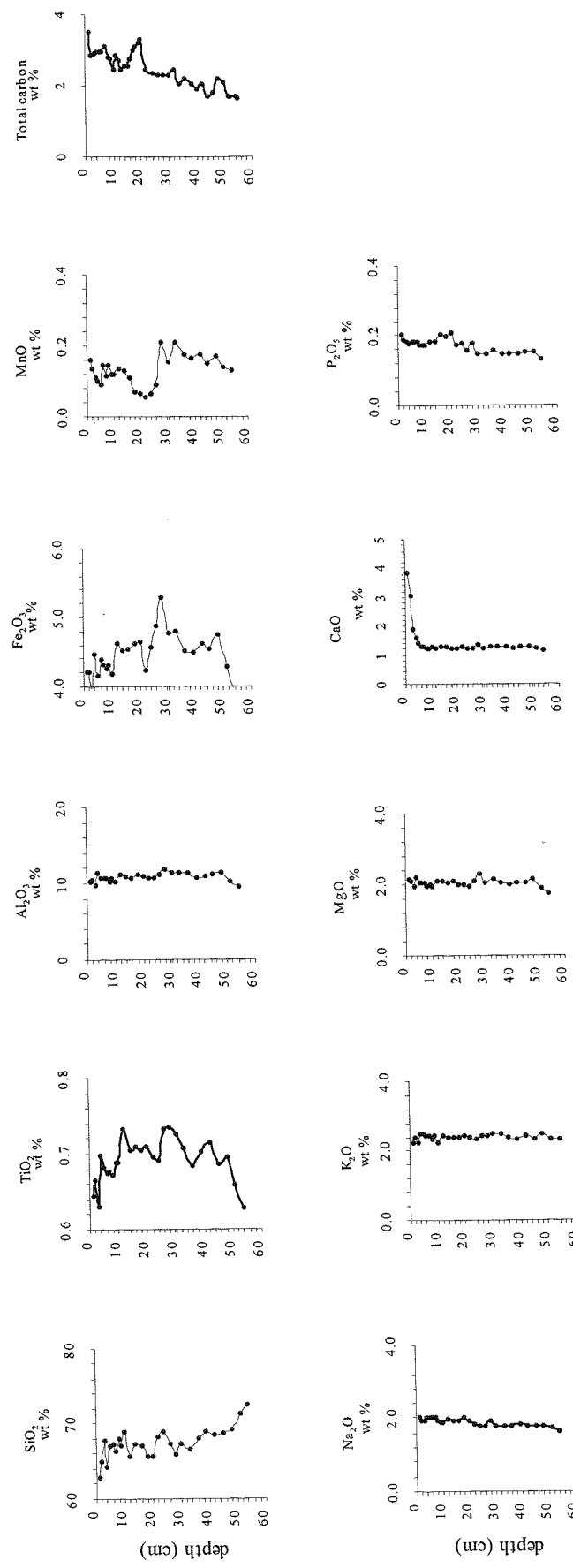


Figure 6.7 : Major element results for RC-96-007

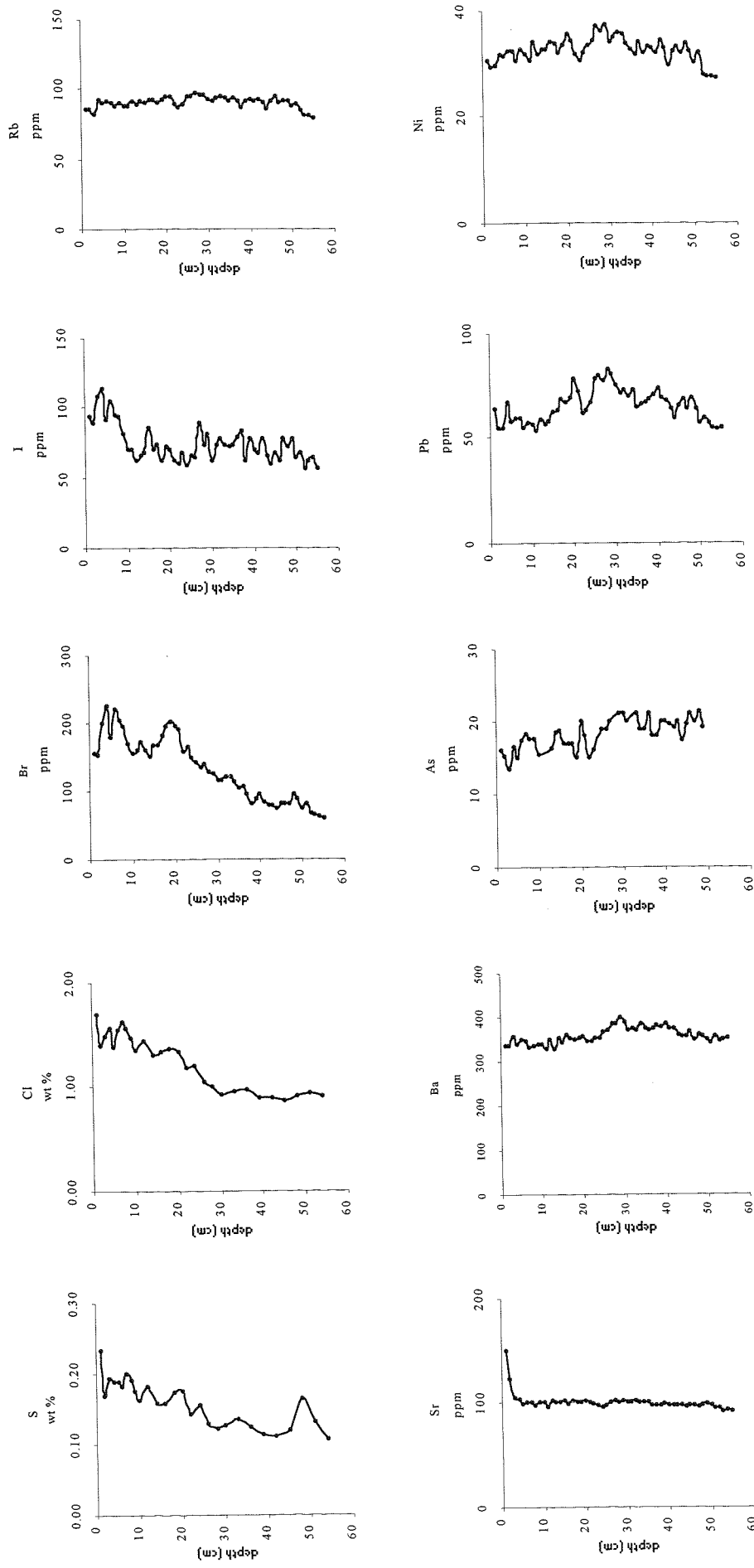


Figure 6.8 : Trace element data for core RC-96-007

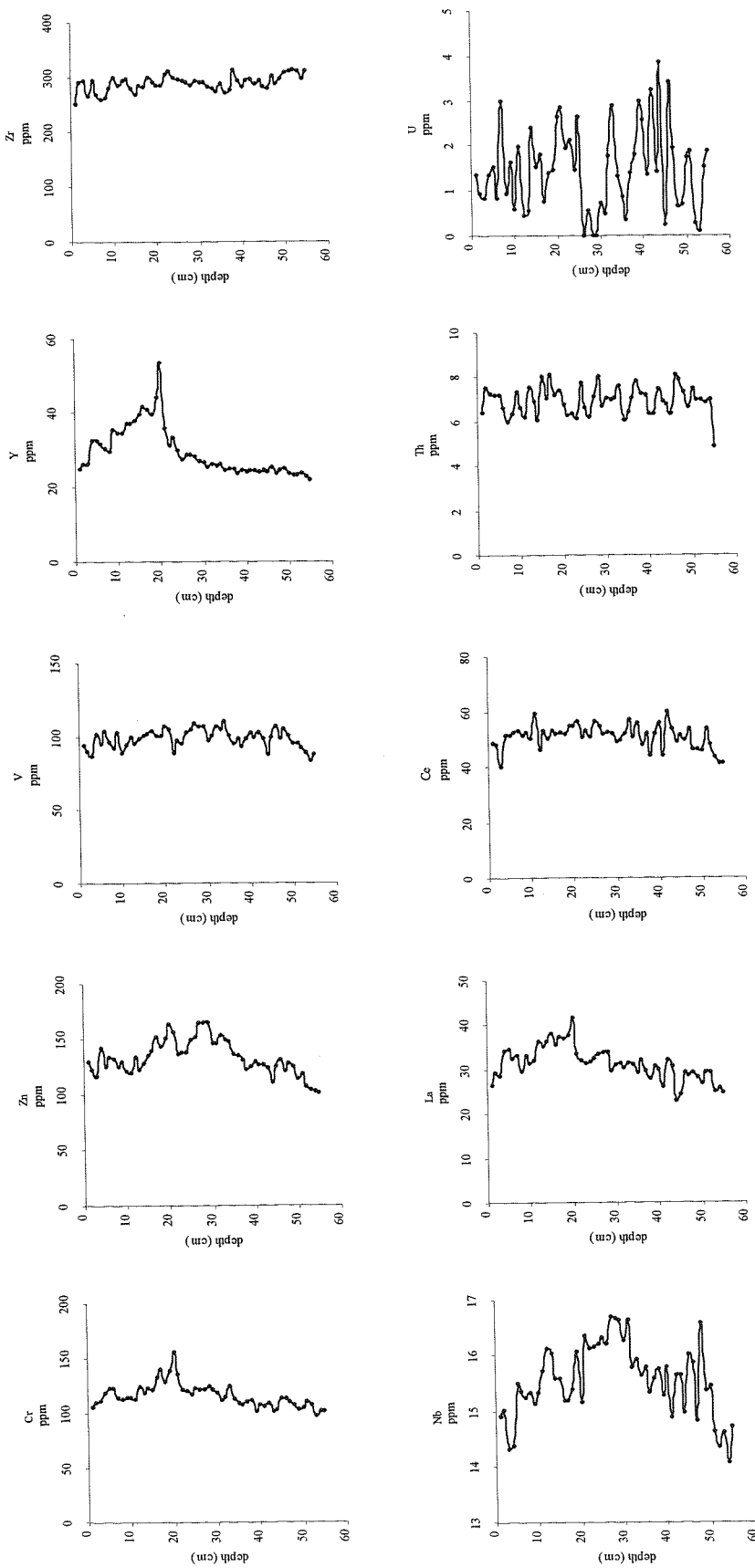


Figure 6.8 (continued) : Trace element data for core RC-96-007

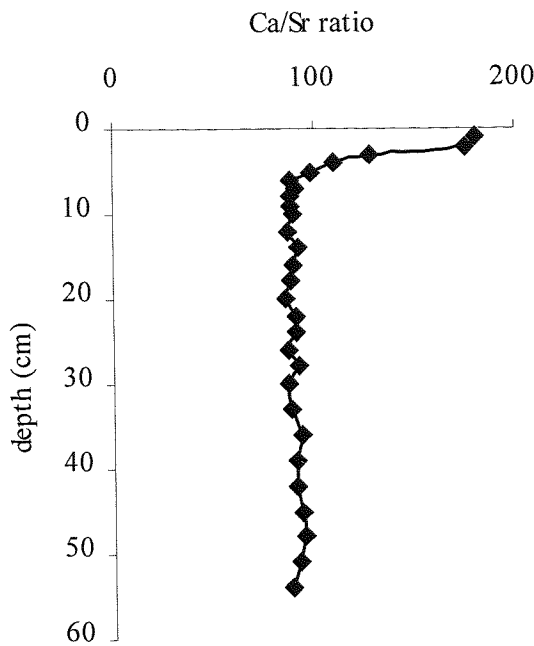


Figure 6.9 : Variation of Ca/Sr ratios with depth

Peaks in Y, La and Cr occur at 20cm indicating an influx of detrital heavy minerals. It is unlikely that this was as a result of a significant storm event as levels of Si (associated with quartz and feldspar), Al (as aluminosilicates) and Ca (associated with shell debris) did not increase accordingly.

Some evidence for diagenesis in the core was observed although this was far from conclusive. A clear drop in Mn concentration was observed at 14cm with the  $\text{MnO}_2$  concentration falling from 0.13 to 0.05 wt %. This would suggest dissolution of Mn from the particle phase presumably through the reduction of particulate-bound manganese oxyhydroxides to the soluble Mn(II).  $\text{MnO}_2$  concentrations then increased to 0.21 wt % at a depth of 28cm. The Mn peak at 28cm coincides with an apparent peak in  $\text{Fe}_2\text{O}_3$  concentration of 5.27 wt %. However, the Fe profile is quite erratic making interpretation difficult. Also the Fe and Mn peaks at 28cm do not correspond with any observable peak in S as might be expected if the Fe and Mn had re-precipitated as the sulphide. Some of the irregularity observed may be as a result of the regular flooding of the marsh and dynamic nature of the water table causing short-term variations in oxidising / reducing conditions in the core.

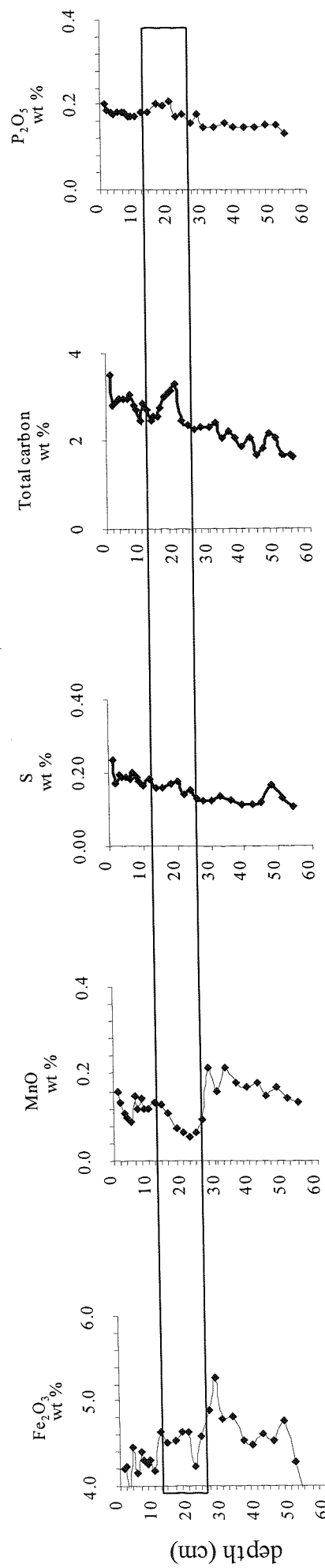


Figure 6.10 : Redox sensitive element concentrations in core RC-96-007. The boxed area indicates the zone of apparent Mn depletion.

### 6.3.3. Gamma spectrometry data

Gamma spectrometric analysis of sediment samples from core RC-96-007 detected measurable activities of  $^{60}\text{Co}$ ,  $^{137}\text{Cs}$  and  $^{241}\text{Am}$  (Figure 6.12). Low levels of  $^{57}\text{Co}$ ,  $^{154}\text{Eu}$  and  $^{155}\text{Eu}$  were also detected along with isotopes of the natural U and Th decay chains. Only  $^{60}\text{Co}$ ,  $^{137}\text{Cs}$  and  $^{241}\text{Am}$  will be considered further as they were the only isotopes consistently found above limit of detection and all isotopes have a relatively well-documented discharge history. Activities of all three isotopes varied markedly with depth. Peak activities were measured at depths of 15, 17 and 18 cm for  $^{60}\text{Co}$ ,  $^{137}\text{Cs}$  and  $^{241}\text{Am}$  respectively. The activity profile of  $^{137}\text{Cs}$  and  $^{241}\text{Am}$  with depth compared qualitatively with the discharge history of these two radioisotopes from the Sellafield site with peak discharges in 1975. A similar comparison for  $^{60}\text{Co}$  was not possible as discharges of this radioisotope were only published from 1982. If it is assumed that the  $^{60}\text{Co}$  profile in the saltmarsh core is a record of Sellafield discharge the proximity of the  $^{60}\text{Co}$  peak to the  $^{137}\text{Cs}$  and  $^{241}\text{Am}$  peaks in the core would suggest that the peak in  $^{60}\text{Co}$  discharge occurred at a similar time to that of  $^{137}\text{Cs}$  and  $^{241}\text{Am}$  and is higher than the values published post-1982 (maximum published value of  $2.3 \times 10^{12}$  Bq in 1985). However, further comparison of the core profile with discharge data requires a knowledge of the local sedimentation rate and lag-times of the radioisotopes.

The ratio of  $^{137}\text{Cs}$  and  $^{241}\text{Am}$  in the core range from 0.48 to 1.33 compared to the range in Sellafield discharge of 4.2 to 808 (Figure 6.11). This reflects the difference in distribution coefficients for  $^{137}\text{Cs}$  and  $^{241}\text{Am}$  with a significant fraction of  $^{241}\text{Am}$  being particle-associated compared with only 10% of the discharged  $^{137}\text{Cs}$ .

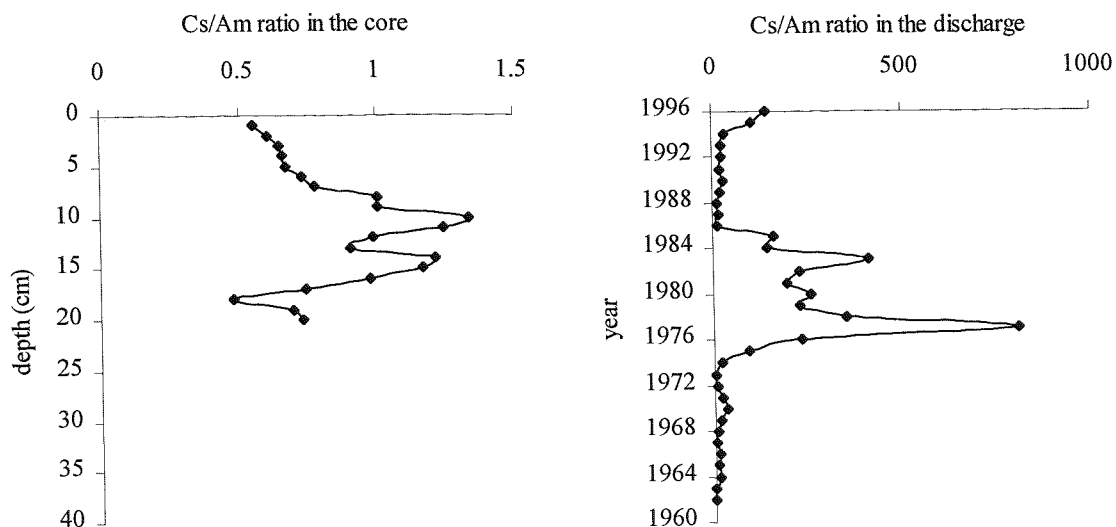


Figure 6.11 : Ratio of  $^{137}\text{Cs}/^{241}\text{Am}$  in core RC96-007 and in Sellafield discharges (data decay-corrected to 1996)

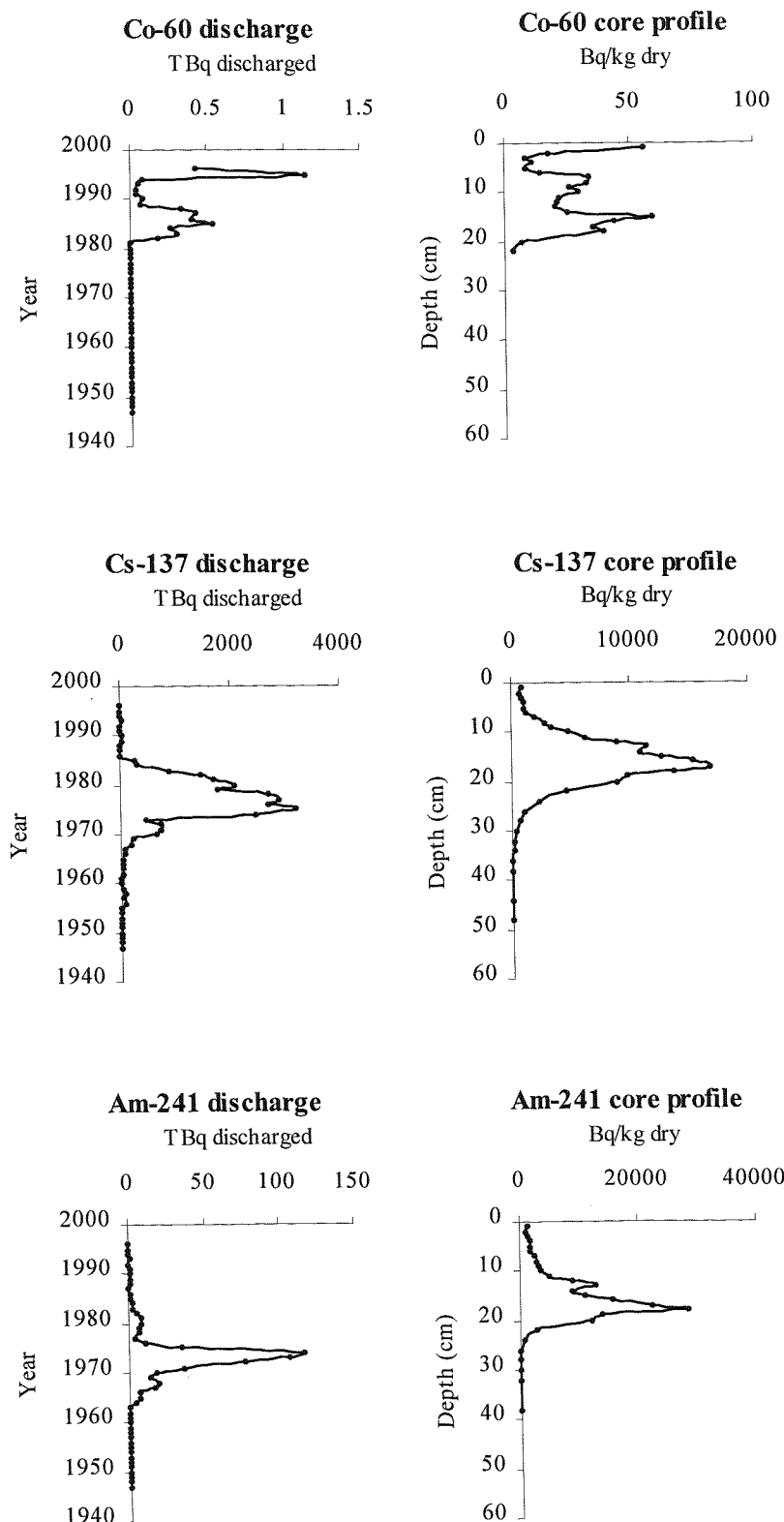


Figure 6.12 : Radioisotope data for Core RC-96-007 – gamma emitters (decay corrected to 1996)

#### 6.3.4. Beta-emitting radioisotopes

Radiochemical analysis of the sediment core for  $^{55}\text{Fe}$ ,  $^{63}\text{Ni}$ ,  $^{90}\text{Sr}$  and  $^{99}\text{Tc}$  indicated that all of the isotopes could be detected above the limit of detection for the analysis (Figure 6.13). The highest measured activities were found for  $^{99}\text{Tc}$  at 217 Bq/kg at the top of the core, related to the increase in  $^{99}\text{Tc}$  discharges in 1994 following the commissioning of EARP. The levels dropped down the core to around 20-30 Bq/kg. This is broadly comparable with  $^{99}\text{Tc}$  activities of 7.7 and 10.1 Bq/kg measured in Whitehaven Harbour in the 1980s (Koide and Goldberg, 1985) and with 18.7 Bq/kg measured in a sediment collected from the Ravenglass estuary in 1988 (Assinder *et al*, 1993). Levels of  $^{63}\text{Ni}$  were erratic down the core ranging from 13 to 53 Bq/kg. Again this broadly agrees with measurements made previously on Whitehaven sediments with  $^{63}\text{Ni}$  activities of 17 and 33 Bq/kg (Koide and Goldberg, 1985). Activities of  $^{90}\text{Sr}$  towards the top of the core were comparable with those reported by BNFL in 1996 for Maryport and Workington silts at 240 Bq/kg and 320 Bq/kg respectively (BNFL, 1997). However, activities of  $^{90}\text{Sr}$  at depth were considerably higher. No comparative data were available for  $^{55}\text{Fe}$  measurements in Cumbrian sediments

##### *Iron-55*

It is difficult to correlate the profile of  $^{55}\text{Fe}$  down the core with the reported discharge data as the latter are somewhat erratic. However there is some resemblance between the two curves. No discharge record for  $^{55}\text{Fe}$  prior to 1982 is available. Levels of  $^{55}\text{Fe}$  appear to fall at depth indicating that historic discharges of  $^{55}\text{Fe}$  have since decayed and current discharges are not migrating down the sediment core. Under aerobic marine conditions iron, as  $\text{Fe}^{3+}$ , rapidly reacts with hydroxyl ions to produce the insoluble  $\text{Fe}(\text{OH})_3$  species ( $k_{\text{sp}} = 10^{-38}$ ).  $^{55}\text{Fe}$  associated with stable Fe is unlikely to redissolve unless reduced to  $\text{Fe}^{2+}$  in an anoxic environment. If this had occurred, any post depositional migration of  $^{55}\text{Fe}$  at depth is no longer observable as this  $^{55}\text{Fe}$  has since decayed.

##### *Nickel-63*

Nickel-63 shows no profile in the core corresponding to the discharge profile. No peak in  $^{63}\text{Ni}$  in the core was observed that corresponded with the discharge peak in 1988.  $^{63}\text{Ni}$  was found throughout the core at very low levels suggesting that the radioisotope is mobile in the saltmarsh environment. However, again the discharge data is incomplete and it is possible that significant discharges of  $^{63}\text{Ni}$  have occurred throughout the operational history of the Sellafield site.

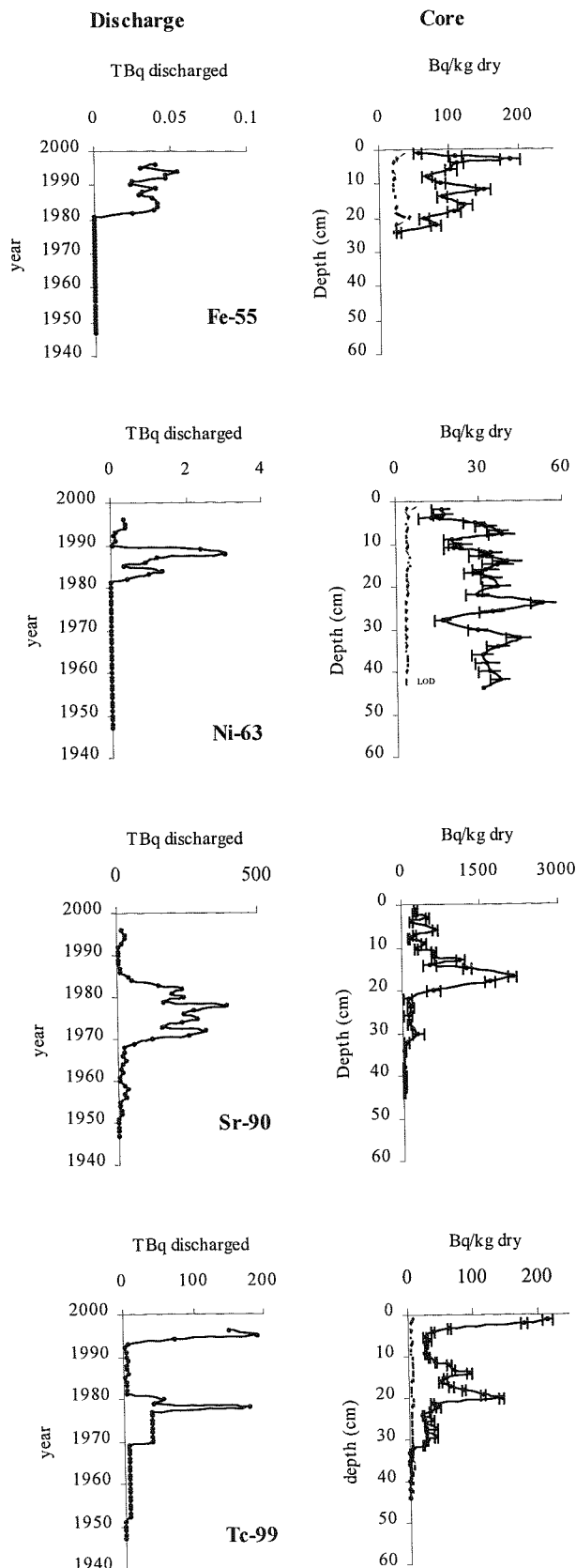


**Figure 6.13 : Radioisotope data for RC-96-007 – beta emitters (decay corrected to 1996)**  
 (method detection limits are shown as dashed lines on right hand plots)

### Strontium-90

The  $^{90}\text{Sr}$  profile shows a well-defined peak with the maximum  $^{90}\text{Sr}$  activity of 2100 Bq/kg dry present at 17cm depth. The maximum  $^{90}\text{Sr}$  discharge is unclear as discharges were consistently high (with some slight variation) between 1970 and 1982. However, the peak in  $^{90}\text{Sr}$  activity in the core does coincide with the peak in  $^{137}\text{Cs}$  at a depth of 17cm. No  $^{89}\text{Sr}$  was detected in any fraction, although any  $^{89}\text{Sr}$  originally present would most probably have decayed in the time between sampling and analysis.

### Technetium-99

Technetium-99 exhibited a core profile that approximated to the discharge profile. However, whereas the discharge record only had one significant peak (prior to the recent increase in discharges) in 1978, the core profile shows two discrete peaks at 14 and 20cm. Also, if it is assumed that the 20cm peak corresponds to the 1978 discharge and the peak at the top of the core corresponds to the 1995 discharge then the ratio of core concentrations to discharge are different (0.80 and 1.14  $\text{Bq kg}^{-1}/\text{TBq}$  for 1978 and 1995 respectively). This would suggest that either the mechanism for incorporation of  $^{99}\text{Tc}$  into the saltmarsh has varied in this time-span or that the  $^{99}\text{Tc}$  in the 20cm peak has had sufficient time to experience post-depositional migration following emplacement..

The relative activity of a radioisotope in the core will depend on the amount of the radioisotope discharged and the distribution coefficient of the radioisotope. The ratio of the core peak activity to discharge activity would therefore be expected to increase with increasing distribution coefficient (Table 6.1). This relationship appears to be systematic over a wide range of distribution coefficients (Figure 6.14), although the data available are limited and is highly dependent on the distribution coefficient appropriate to the local environment (which may not be accurately represented by the generalised  $K_D$ 's published by IAEA).

**Table 6.1 : Peak discharge activities and peak core activities for four radioisotopes**

Radioisotope	Peak Discharge TBq	Year	Peak activity in sediment core $\text{Bq/kg dry}$	Depth (cm)	Ratio, R $\text{Bq kg}^{-1}/\text{TBq}$	$k_D$
$^{90}\text{Sr}$	389	1978	2126	17	5.5	1000
$^{99}\text{Tc}$	180	1978	143	20	0.80	100
$^{137}\text{Cs}$	3200	1975	16730	17	5.2	3000
$^{241}\text{Am}$	116	1974	28690	18	247	2000000

*All activities are decay-corrected to 1996  
 $k_D$ 's are mean values quoted in IAEA (1985)*

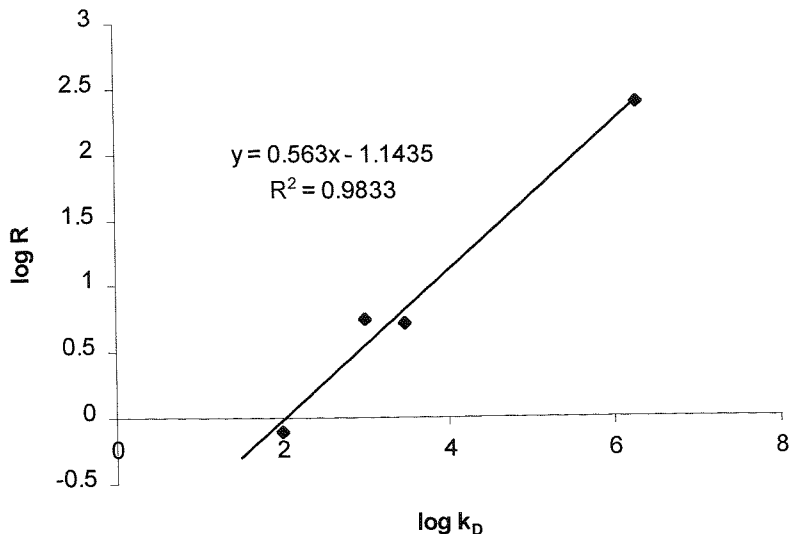


**Figure 6.14 : Potential relationship between  $\log R$  and  $\log k_D$**   
*where  $R$  is the ratio between the activity in the core (Bq/kg dry) and the discharge activity (TBq)*

### 6.3.5. Estimation of lag time and sedimentation rate

#### 6.3.5.1. Lag time

In order to interpret the core profiles more rigorously it is necessary to determine the lag-time between radioisotope release from Sellafield and arrival at the marsh and also to determine the sedimentation rate prevalent at the sampling location.

The lag-time has been calculated by a number of researchers by measuring two radioisotopes of the same element. The two isotopes must have significantly different half-lives and their ratio must be well characterised in the discharge.  $^{134}\text{Cs}$  and  $^{137}\text{Cs}$  are most commonly used.  $^{134}\text{Cs}$  has a half-life of 2.06 years whilst the half-life of  $^{137}\text{Cs}$  is 30 years. The ratio of  $^{134}\text{Cs}$  to  $^{137}\text{Cs}$  in the marsh is measured and compared with known values for the discharge. The difference in ratio results from the decay of  $^{134}\text{Cs}$  in transit and this can be used to calculate the transit time. Isotopes of different elements may also be used but any deviation may be related to chemical fractionation in the environment rather than radioactive decay of one of the elements. The lack of  $^{134}\text{Cs}$  in the measured gamma spectra was of some concern as this may suggest that the transit time has been sufficiently long for the  $^{134}\text{Cs}$  to decay to levels below limit of detection. The ratio of  $^{134}\text{Cs}/^{137}\text{Cs}$  in the discharge range between 0.04 and 0.05 making it impossible to detect  $^{134}\text{Cs}$  in the saltmarsh samples with any accuracy in the presence of the other gamma emitters.

A number of lag-times have been calculated in the literature. Kershaw *et al* (1990) quoted a lag-time of 2 years for Maryport Harbour to the north of Sellafield. A detailed discussion of lag times based on measurements of  $^{134}\text{Cs}$ : $^{137}\text{Cs}$  and  $^{106}\text{Ru}$  has been presented by Stanners and Aston (1981). Lag times were calculated for a number of marshes relative to the Ravenglass marsh. Lag times of 1.5 years were found for Maryport and Workington Harbours and the Duddon Estuary with lag times increasing to 3.9 years for the Solway Firth. By comparing the data of Kershaw *et al* (1990) and Stanners & Aston (1981) a tentative lag time of 0.5 years is calculated for the Sellafield-to-Ravenglass transit time. This is in broad agreement with the value of  $\sim 1$  year calculated by Hamilton and Clarke (1984) and this value is used in all further calculations.

Lag-times may also be radioisotope-dependent with different lag-times for conservative and non-conservative radioisotopes. The rapid increase in  $^{99}\text{Tc}$  towards the top of the core would indicate that the recent discharges of  $^{99}\text{Tc}$  have already reached the marsh suggesting transit times of less than one year. Transit times for conservative radioisotopes from Sellafield to the Clyde Sea area have been estimated as less than 8 months (Baxter *et al*, 1979) again suggesting a more rapid transport of conservative compared to non-conservative radioisotopes

#### *6.3.5.2. Calculation of sedimentation rate via excess $^{210}\text{Pb}$ dating*

Lead-210 dating has been widely used for the determination of accumulation rates in sediment cores where relatively high sedimentation rates of at least 0.5 cm/yr are prevalent. The technique relies on a constant or well-characterised input of  $^{210}\text{Pb}$  from the atmosphere with subsequent decay of the deposited  $^{210}\text{Pb}$  in the core (Appleby and Oldfield, 1992). However, sources of  $^{210}\text{Pb}$  originating from the Albright and Wilson phosphate processing plant at Whitehaven have meant that an additional, water-borne, source of  $^{210}\text{Pb}$  is present. Measurements (Croudace, pers. comm.) show that the profile of  $^{210}\text{Pb}$  in the saltmarsh core had been significantly altered by the input of this additional, uncharacterised and variable component and  $^{210}\text{Pb}$  dating was not suitable for determining the accumulation rate in this core using the conventional techniques. However, the dramatic fall in  $^{210}\text{Pb}$  activity at 4 cm can be correlated with the closure of the Albright and Wilson plant in 1992 suggesting an accumulation rate of approximately 1 cm/yr

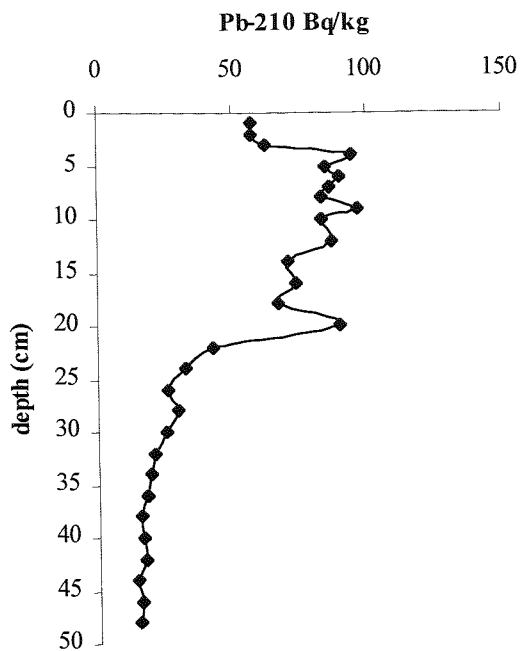


Figure 6.15 :  $^{210}\text{Pb}$  profile in core RC-96-007 (after Croudace, pers. comm.)

#### 6.3.5.3. Calculation of accumulation rate via laminations

X-radiography of the core identified alternating light and dark bands at regular intervals throughout the core. The most likely explanation for this banding is slight compositional variations of the incoming sediment in summer and winter months. This biannual stratification down the core permits the calculation of the sedimentation rate as two bands will represent the deposition in one year. By counting the number of pairs of bands over a set depth, the deposition rate per year is determined.

On closer inspection of the banding it was noted that the banding was thicker at the base of the core compare to the top of the core. This is either explained by a more rapid sedimentation rate during the early years of saltmarsh formation or by non-uniform compression of the core during sampling with the upper, higher water content, fraction of the core becoming more compressed. It was not possible from the current dataset to identify which if these processes had resulted in the thicker bands at the base of the core and an average sedimentation rate for the whole core was therefore calculated. Over the length of the core the average lamination-pair corresponded to 0.8cm in depth. If this is corrected for, the compaction of the core during sampling (at 11%) the average sedimentation rate for the whole core is 0.89 cm/yr.

#### 6.3.5.4. Calculation of sedimentation rate via $^{137}\text{Cs}$ and $^{241}\text{Am}$ profiles

The  $^{137}\text{Cs}$  and  $^{241}\text{Am}$  profiles may be used to determine the core sedimentation rate (Figure 6.16). To do this it is assumed that the maxima in the core profiles correspond to the maxima in the discharge history and that no significant post-depositional migration has occurred. The lag time must also be taken into account to correct for the time taken for the discharge signal to reach the marsh. Using this approach, sedimentation rates of 0.85 and 0.86 cm/yr are obtained from  $^{137}\text{Cs}$  and  $^{241}\text{Am}$  profiles respectively. This method is limited by the sampling resolution of the core and the estimation of the lag times for  $^{137}\text{Cs}$  and  $^{241}\text{Am}$ . Despite this, there is good agreement between the two values and between these values and those obtained from the laminations of 0.89 cm/yr.

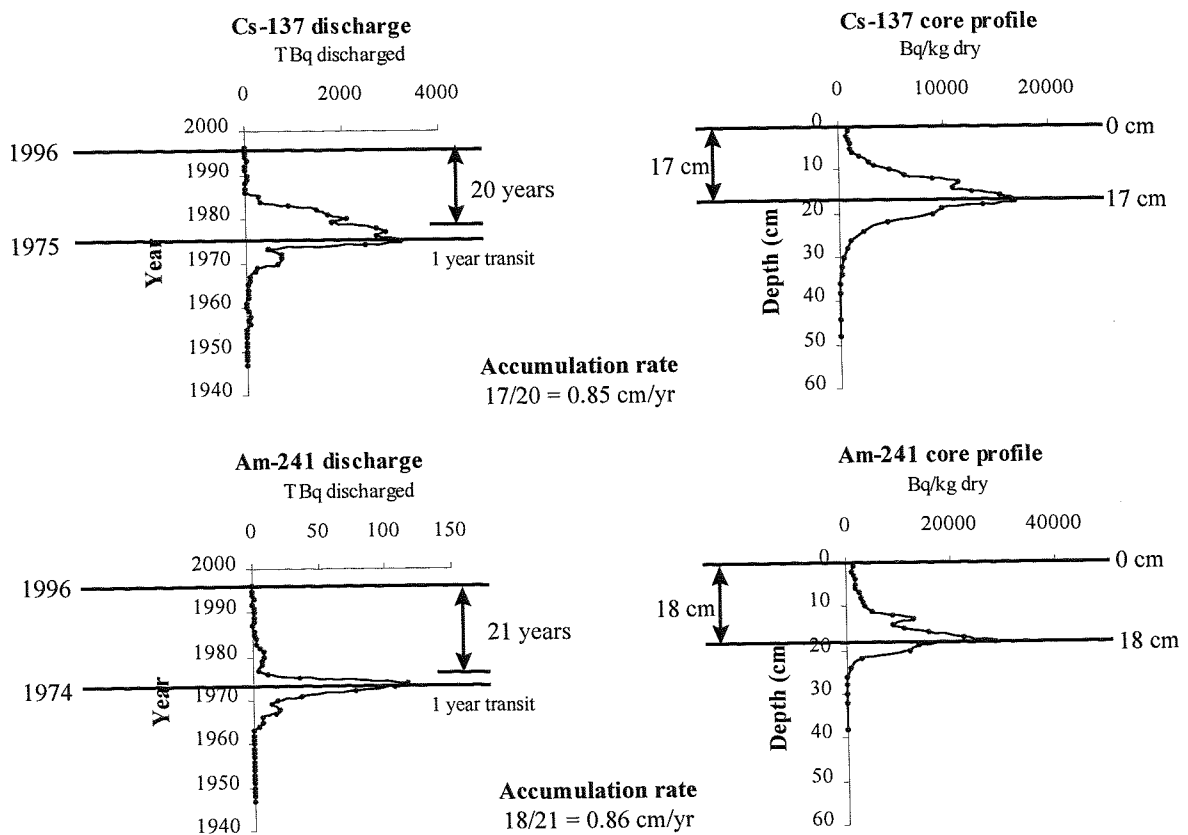
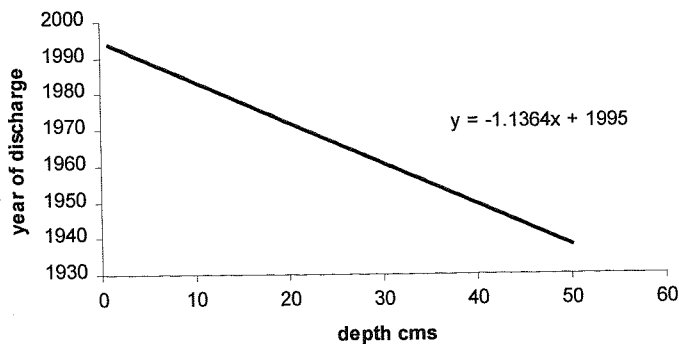


Figure 6.16 : Calculation of accumulation rate from radioisotope discharge and core profiles

#### 6.3.5.5. Overall estimate of sediment accumulation rate

The mean accumulation rate from the three methods is **0.87 cm/yr**.

The calculated accumulation rate may now be used to date the various depths of the core (Figure 6.17) and compare in more detail the discharge history and the core profiles for all the measured radioisotopes.



**Figure 6.17 : Relationship between the year of discharge and the depth that BNFL discharge would be recorded in core RC-96-007. Sedimentation rate = 0.87 cm/yr; lag time = 1 year**

### 6.3.6. Detailed discussion of core profiles

#### 6.3.6.1. Contribution of radioisotopes from sources other than Sellafield

To fully interpret the core profiles it is necessary to consider all potential sources of the radioisotopes. An assessment of the likely impact of other radioisotope sources relative to the Sellafield discharge was therefore performed. The main sources of radioactivity other than the aqueous Sellafield discharge are

1. Nuclear weapons' fallout deposited over the Irish Sea
2.  $^{137}\text{Cs}$  deposited following the Chernobyl incident
3. Airborne discharge from the Sellafield site
4. Run-off waters from the Cumbrian area, containing radioactivity from all three sources identified above.

Of these, routes (1) and (2) are likely to be the most important and are considered further.

Total deposition of fallout from nuclear weapons' testing and the Chernobyl incident onto the Irish Sea will depend on the surface area of the Irish and rainfall over the area. The total surface area of the Irish Sea has been estimated as  $1 \times 10^5 \text{ km}^2$  (McKay and Pattenden, 1993). Typical deposition rates for  $^{90}\text{Sr}$  and  $^{137}\text{Cs}$  are 1.6 and 2.4 GBq  $\text{km}^{-2}$  giving a total input of these two isotopes into the Irish Sea as 155 and 235 TBq respectively ( $^{137}\text{Cs}$  data from Playford *et al*, 1992 – data for Milford Haven.  $^{90}\text{Sr}$  calculated from  $^{137}\text{Cs}$  assuming an average ratio of 0.66 – UNSCEAR 1982 - data decay corrected to 1996). This is low compared to the total input of  $^{90}\text{Sr}$  and  $^{137}\text{Cs}$  from Sellafield at 3.8 and 26 PBq respectively (total decay corrected to 1996).  $^{63}\text{Ni}$  and  $^{99}\text{Tc}$  would also be deposited from weapons' fallout. However, it has been estimated that only 140TBq total of  $^{99}\text{Tc}$  was injected into the atmosphere through atmospheric weapons' testing (Aarkrog *et al*, 1986), which is only a fraction of the total  $^{99}\text{Tc}$  discharge from Sellafield of 1.2 PBq (estimated). Data for  $^{63}\text{Ni}$  are scarcer. Holm *et al*, (1992) estimated a  $^{63}\text{Ni}/^{137}\text{Cs}$  ratio in fallout of  $1.7 \times 10^{-4}$  giving total deposition over the Irish Sea of 0.04 TBq as compared with cumulative Sellafield discharges of 12 TBq. Iron-55 was also released in significant quantities during weapons' testing but has long since decayed and is not considered as a significant input here. Peaks from nuclear weapons' testing and Chernobyl would appear at 28 cm and 7-8cm respectively in the Ravenglass core. No peaks are apparent in these fractions suggesting that any input from these two sources is low compared with the Sellafield aqueous discharge. MacKenzie *et al* (1994) noted that  $^{137}\text{Cs}$  potentially associated with the Chernobyl incident was apparent in a saltmarsh core collected from Southwick

Marsh, South-West Scotland. Levels of  $^{137}\text{Cs}$  in the Sellafield-derived peak in the Southwick core were 1880 Bq/kg compared with the Chernobyl-derived peak of 651 Bq/kg dry. These activities are a factor of 10 lower than those found in the Ravenglass core, which peak at 16700 Bq/kg dry. Any Chernobyl-derived radioactivity has therefore been completely masked by the higher levels of Sellafield-derived  $^{137}\text{Cs}$  present in the Ravenglass marsh.

Airborne discharges from Sellafield are unlikely to have a significant direct input into the Irish Sea. Airborne releases are likely to be dispersed via the prevailing winds inland away from the Irish Sea. Deposition will occur locally and the levels of radioactivity discharged are significantly lower than that found in the aqueous discharges.

Radioisotopes deposited on land may return to the marine environment via run-off waters collecting into streams and rivers. No estimate of the input of radioisotopes via this route has been attempted in the Sellafield area. Such a calculation requires knowledge of river catchment areas and radioisotope transfer factors through the estuarine system.

#### *6.3.6.2. Mixing of radioisotopes prior to deposition*

Having determined the accumulation rate for the core, it is possible to plot the core activity profile in terms of date rather than depth and to compare this to the discharge history (Figure 6.18). Iron-55 and  $^{63}\text{Ni}$  were not included as the levels of these two radioisotopes were low, with high associated uncertainties, and the discharge histories were incomplete.

With the exception of  $^{99}\text{Tc}$ , all core profiles are comparable to the discharge history. The peak for  $^{137}\text{Cs}$  in the core corresponds exactly with the peak in  $^{137}\text{Cs}$  discharge. The core peak for  $^{241}\text{Am}$  is offset by about 1cm but this is most likely an artefact of the core dissection. The peak in  $^{90}\text{Sr}$  activity in the core broadly corresponds to the general maximum in  $^{90}\text{Sr}$  discharge although the discharge pattern is somewhat erratic and unlike  $^{137}\text{Cs}$  and  $^{241}\text{Am}$ , does not show a clear maximum. The  $^{99}\text{Tc}$  peak is significantly offset to the discharge peak. It is noteworthy that the most recent peak in  $^{99}\text{Tc}$  activity towards the top of the core appears lower than expected by the discharge ratio. This may suggest that the transit time employed in the calculation of the date of the core depth is not appropriate for  $^{99}\text{Tc}$  indicating a different transport mechanism for  $^{99}\text{Tc}$  compared with the other radioisotopes.

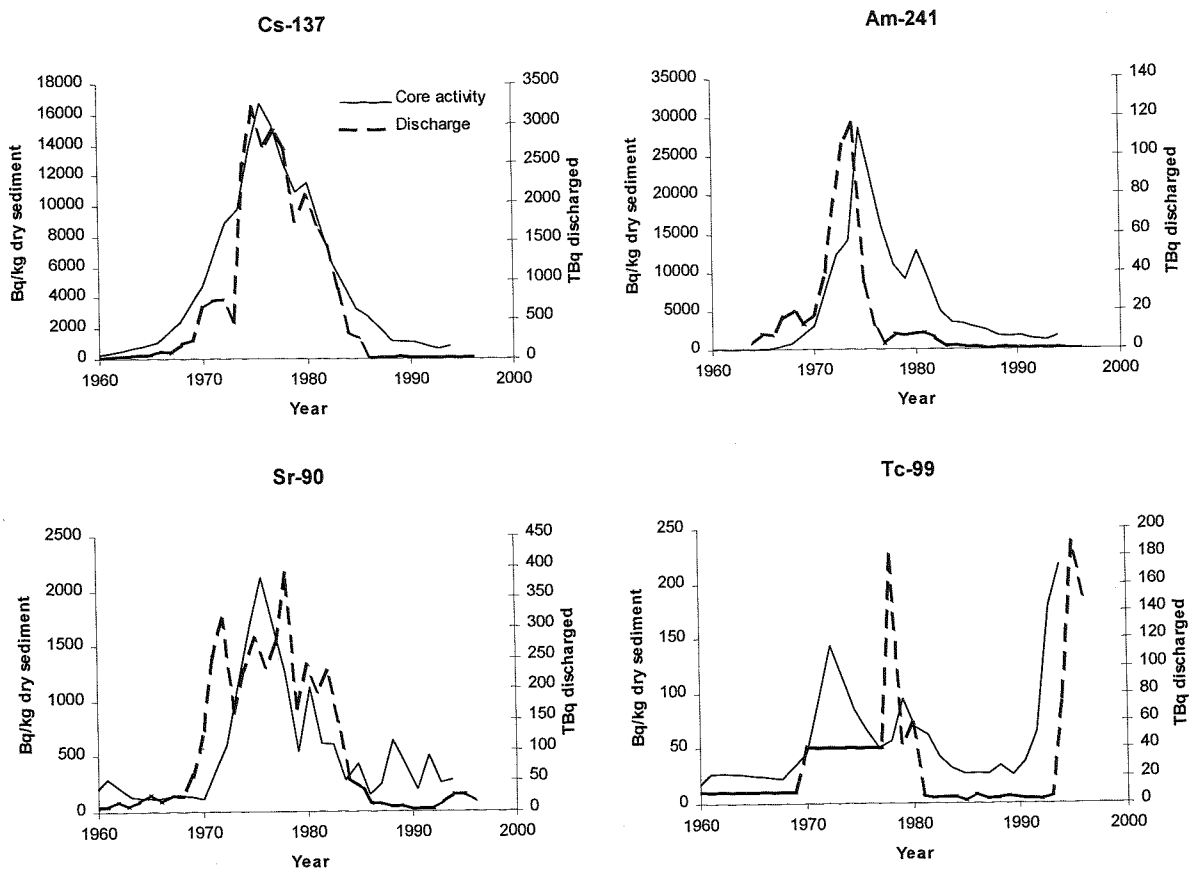


**Figure 6.18 : Comparison of core activity profiles with discharge profiles.  
All data are decay corrected to 1996**

Although the peak in discharge activity appears to be recorded in the core profile, the decline in discharge activity is not reproduced in the core record. This is apparent for  $^{90}\text{Sr}$ ,  $^{137}\text{Cs}$  and  $^{241}\text{Am}$  but is most noticeable for  $^{241}\text{Am}$ . Although  $^{241}\text{Am}$  discharges declined rapidly from 116 TBq in 1974 to 3.6 TBq in 1977 (ratio of 32:1) the core activity only falls from 28700 Bq/kg to 15700 Bq/kg (ratio of 1.8: 1) in the same period suggesting an apparent excess of 14800 Bq/kg  $^{241}\text{Am}$ . The apparent excess of  $^{241}\text{Am}$  in the core in more recent years is partially explained by the in-growth of  $^{241}\text{Am}$  from  $^{241}\text{Pu}$  following deposition. However, there is insufficient  $^{241}\text{Pu}$  present in the marsh to account for the total excess. An excess of  $^{241}\text{Am}$  of 14800 Bq/kg growing in between 1977 and 1998 (21 years to the date of measurement) would require a total  $^{241}\text{Pu}$  activity of 779000 Bq/kg  $^{241}\text{Pu}$  to be deposited. This would have subsequently decayed to leave 283000 Bq/kg  $^{241}\text{Pu}$ . Measurements by Oh (pers. comm.) show that the highest  $^{241}\text{Pu}$  activity in this core is 114000 Bq/kg and that the  $^{241}\text{Pu}$  activity at 14cm (corresponding to deposition in 1977) is 92940 Bq/kg.

It is therefore likely that the sediment deposited in more recent years is not only labelled with that year's discharge but also with a component of previous years' discharges. A significant

quantity of Am and Pu discharged are retained in the mud patch in the vicinity of the Sellafield pipeline whilst only approximately 10% of  $^{137}\text{Cs}$  is retained. Measurements of seabed cores (e.g. MacKenzie *et al*, 1998) have shown significant mixing of the sediment with the potential for resuspension and transportation in the water column. It is likely that the saltmarsh therefore records an annual signal of the resuspended seabed material that may include a time-integrated history of the Sellafield discharge. The magnitude of such an integration of the signal via adsorption onto seabed sediments, mixing and resuspension/dispersion would be dependent on the affinity of a particular radioisotope for sediment material. Hence, this time integrated signal will be more predominant for radioisotopes with high distribution coefficients. This explains why the core profiles are more anomalous for  $^{241}\text{Am}$  compared with  $^{90}\text{Sr}$  and  $^{137}\text{Cs}$ .

The relationship between the core activity record and the discharge history is more clearly seen in the plots of core activity-to-discharge ratios versus year (Figure 6.19). In these plots the activity of a given isotope in the core is divided by the discharge activity for the year. Core depth is correlated with the appropriate discharge year via the equation derived in Section 6.3.5. This equation assumes a transit time of one year, which, as discussed previously, was not deemed appropriate for  $^{99}\text{Tc}$ . No transit time was therefore included for ratios relating to  $^{99}\text{Tc}$ . For  $^{241}\text{Am}$ , there is a steady increase in the ratio to 1978 (region a) as  $^{241}\text{Am}$  discharges increased. After 1978, the discharges fell dramatically and the ratio of activity in the core compared to the discharge activity remained constant but higher than had been previously observed prior and during the peak discharge. This increase and levelling of the ratio is consistent with the theory that the saltmarsh is recording an integrated history of current and past discharge events. For  $^{90}\text{Sr}$  and  $^{137}\text{Cs}$ , the ratio starts high (zone a) and then falls during the peak discharge of these radioisotopes (zone b). Once the discharge begins to fall the ratio rises again (zone c). Zones b and c are again consistent with a time-integrated signal arriving at the saltmarsh. However, the higher ratios prior to peak discharge suggest that either historic discharges were higher than had previously been reported or that limited post-depositional migration of  $^{90}\text{Sr}$  and  $^{137}\text{Cs}$  has occurred. Madruga and Cremers (1997) have shown that the binding of  $^{90}\text{Sr}$  in estuarine sediments is reversible unlike  $^{137}\text{Cs}$ , which is only partially reversible, reflecting a difference in binding mechanism. There was, however, no evidence for enhanced mobility of  $^{90}\text{Sr}$  relative to  $^{137}\text{Cs}$  in the sediment column.

The plot of ratio versus year for  $^{99}\text{Tc}$  is even more complex although the magnitude of the ratio is lower than that observed for the other radioisotopes reflecting the lower distribution coefficient of  $^{99}\text{Tc}$ . Initially the ratio is low although a slight increase in the ratio is observed in 1961. Discharge histories are estimated for this time period and it is likely that the sudden

kick in ratio simply reflects better estimation of the discharge. There is a distinct increase in the ratio between 1980 and 1993 corresponding to a trough in  $^{99}\text{Tc}$  discharge. This could be attributed to the time-integrated signal containing some of the historic discharge or to post-depositional migration of  $^{99}\text{Tc}$  from the  $^{99}\text{Tc}$  deposited in or recent years at the top of the marsh where ratios again fall with increasing activities discharged.

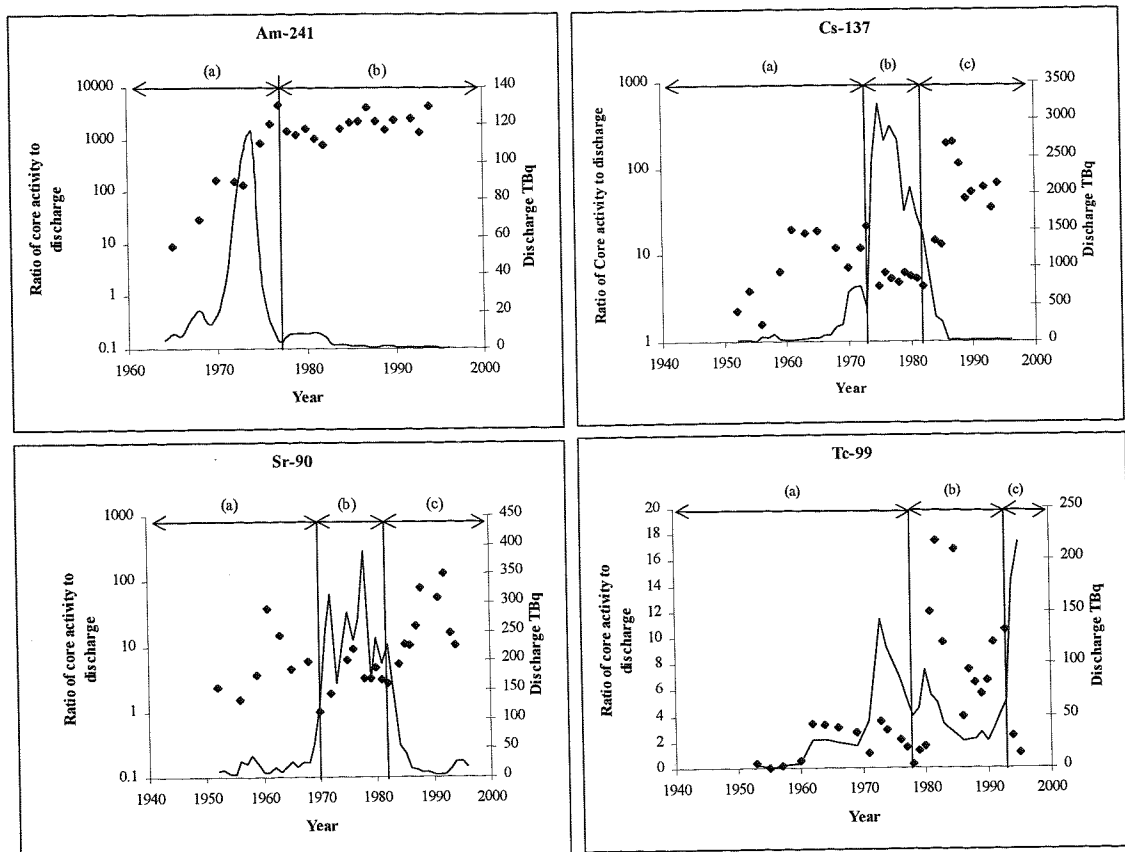


**Figure 6.19 : Core activity to discharge activity ratios versus year and discharge profile for four isotopes. Core activity/discharge ratios as  $\text{BqTBq}^{-1}\text{kg}^{-1}$ .**

*A one year transit time is assumed for all radioisotopes except for  $^{99}\text{Tc}$  where no transit time is applied.*

#### 6.3.6.3. Post depositional element migration and redox control

The profile of  $^{99}\text{Tc}$  in the core shows a poor correlation with the discharge history. A small peak in the core profile corresponds with the reported discharge peak and the higher levels of  $^{99}\text{Tc}$  at the top of the core reflect the recent increases in  $^{99}\text{Tc}$  discharge following the commissioning of EARP. However, the core profile shows a second large peak at 20cm corresponding to 1972. There is no record of a significantly elevated level of  $^{99}\text{Tc}$  being discharged around this time. Gray *et al* (1995) noted that  $^{99}\text{Tc}$  discharge records were estimated prior to 1978 and it is possible that an unrecorded elevated discharge of  $^{99}\text{Tc}$  did

occur in 1972. However, such a speculated increase in discharge cannot be linked with any reported changes in site operations in this period (Figure 6.1).

Although the second peak in  $^{99}\text{Tc}$  does not coincide with a peak in  $^{99}\text{Tc}$  discharge, the peak does coincide with a zone of lower Mn concentration between 18cm and 28cm (Figure 6.20). This trough in Mn is followed by a substantial rise at 28cm to concentrations greater than those found at the top of the marsh. This increase in Mn is unlikely to be associated with the influx of heavy minerals (see page 228) observed higher in the sediment column as indicated by a sharp increase in Y, La and Cr at around 20cm.

Post-depositional migration of Mn from one zone of the core coupled with an elevation of Mn above and below this zone is usually attributed to the reduction of particle-associated Mn(IV) to soluble Mn(II) at depth resulting from a lack of oxygen penetrating the marsh below certain levels. This solubilised Mn(II) may then migrate in the porewaters of the sediment until it encounters a more oxidising environment with subsequent re-oxidation of Mn(II) to Mn(IV) and reprecipitation as the oxyhydroxide. Alternatively, the Mn(II) may diffuse to greater depths where it will encounter a sulphidic zone and precipitate as  $\text{Mn}_2\text{S}_7$  (Figure 6.21). Such oxidation-reduction-precipitation mechanisms may also be expected to affect Tc although in this case the oxidised form of Tc, Tc(VII) is soluble whereas the reduced form, Tc(IV) is likely to be particle-associated. The coincidence of the Tc peak with the Mn trough supports the suggestion that the Mn trough is indicative of a reducing environment. The increase in Mn concentration below the trough also coincides with a slight increase in Fe concentration as would be expected if the Fe and Mn had encountered a sulphidic zone in the sediment at depth. However, sulphur does not show a characteristic increase at this point and it is highly unlikely that a sulphidic zone is present here. Other redox-sensitive elements, such as I and As (Thomson *et al*, 1999), do not show evidence of post-depositional migration as would be expected. Well defined oxic, post-oxic and sulphidic zones are not apparent at discrete depths in the marsh.

The trough in Mn does coincide with a peak in C and Br (which is often associated with organic carbon). Such a correlation may indicate that the higher levels of C in this part of the marsh have led to a localised reducing environment. Mn(IV) and Fe(III) would have been reduced in this zone and migrated upwards and downwards until a more oxic environment was encountered where the two elements would have reprecipitated. Such a localised reducing environment surrounded by one that is more oxic, would explain the reprecipitation of Mn and Fe below the reducing zone in the absence of a sulphidic zone. Any mobile Tc(VII) diffusing into this localised reducing zone would be reduced to the particle-reactive

Tc(IV) and be immobilised. This would account for the coincidence of the second Tc peak with the trough in Mn. The cause of this high carbon concentration within a distinct zone is, however, unclear although it may be due to decomposing root matter at depth.

From the data available, it is not possible to definitively link core geochemistry with  $^{99}\text{Tc}$  mobility in the saltmarsh environment. However, the data do suggest that the behaviour of  $^{99}\text{Tc}$  in the marsh may be dependent to some degree on local redox conditions prevalent within the marsh.

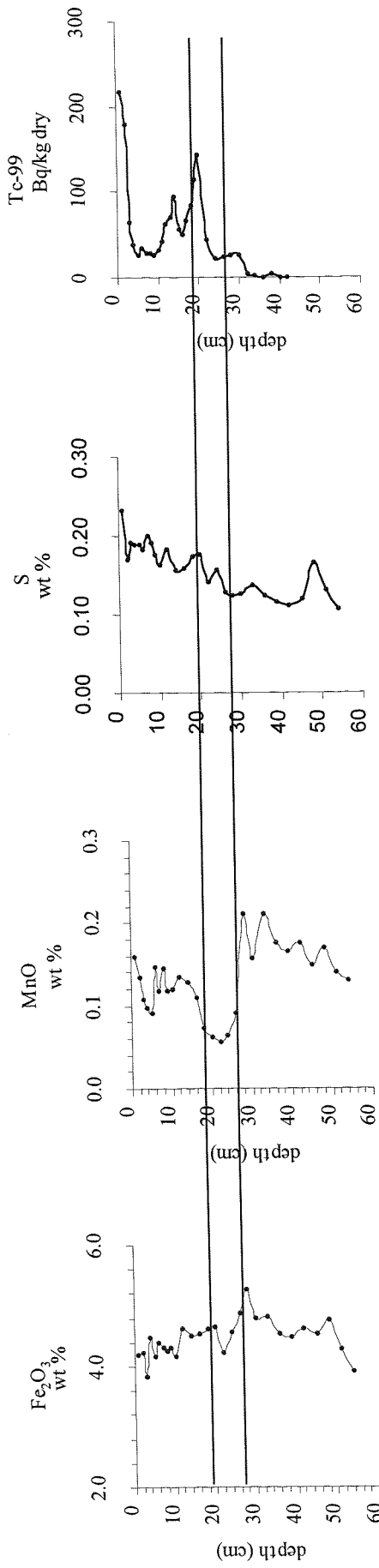


Figure 6.20 : Relationship between  $^{99}\text{Tc}$  activity and the redox-sensitive elements Mn, Fe and S

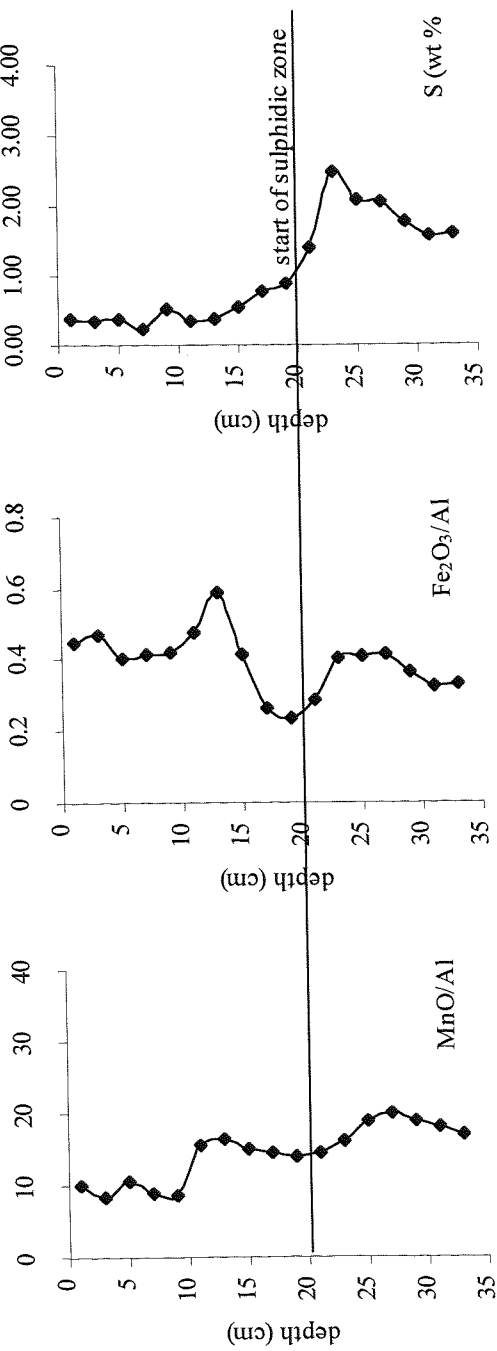


Figure 6.21 : Mn, Fe and S profiles from a saltmarsh in Hamble, southern UK showing post-depositional migration of Mn and Fe and the presence of a sulphidic zone at depth  
 (after Cundy & Croudace, 1995)

#### 6.4. Conclusions

Iron-55,  $^{63}\text{Ni}$ ,  $^{90}\text{Sr}$  and  $^{99}\text{Tc}$  were all detectable in the saltmarsh core RC-96-007 although levels of  $^{55}\text{Fe}$  and  $^{63}\text{Ni}$  were approaching the analytical limit of detection. Profiles of  $^{90}\text{Sr}$  reflected the history of discharges from the Sellafield site and were therefore comparable with the profiles of  $^{137}\text{Cs}$  and  $^{241}\text{Am}$  (as measured by gamma spectrometry). The low levels of  $^{55}\text{Fe}$  and  $^{63}\text{Ni}$  coupled with an incomplete discharge history made it impossible to thoroughly compare core profiles with the discharges from Sellafield. However, levels of  $^{55}\text{Fe}$  did fall with depth in the core and no  $^{55}\text{Fe}$  was detected below 24cm suggesting that Fe is not significantly migrating down the core following deposition.

The  $^{99}\text{Tc}$  core profile reflected a peak in discharge in 1978 and the recent increase in  $^{99}\text{Tc}$  discharges following the commissioning of the EARP plant and subsequent processing of previously stockpiled Magnox wastes. However, the  $^{99}\text{Tc}$  core profile did show a second peak corresponding to 1972. This either reflects a previously unrecorded discharge event or more likely suggests remobilisation of the  $^{99}\text{Tc}$  from the 1979 peak downwards. Mn and Fe measurements indicate the potential presence of a reducing zone that corresponds with a peak in carbon content as well as the second peak in  $^{99}\text{Tc}$  activity. It is possible that mobile Tc(VII) has migrated following deposition in the marsh. On reaching the anoxic zone, the Tc(VII) has been reduced to Tc(IV) and been immobilised resulting in the formation of a second  $^{99}\text{Tc}$  peak at depth.

When compared with the discharge history, the profiles for  $^{90}\text{Sr}$ ,  $^{137}\text{Cs}$  and  $^{241}\text{Am}$  do not reflect the rapid decline of discharges following the improvements in waste treatment. It is proposed that the slower decline in the core record is as a result of a mixing of the current year's discharge with previous years' discharges in the seabed prior to the mixed seabed material being subsequently resuspended and transported along the coastline in the water column, supporting the claims of McKenzie *et al*, 1998.

## 6.5. References

Aarkrog A., Dahlgaard H., Hallstadius L., Holm E., Mattsson and Rioseco J. (1986). Time trend of  $^{99}\text{Tc}$  in seaweed from Greenland Waters. In Desmet G. and Myttenaere C.(eds) Technetium in the environment. Elsevier Applied Science Publishers, London, UK.

Appleby P.G. and Oldfield F. (1992). Application of  $^{210}\text{Pb}$  to sedimentation studies. In M Ivanovich and R.S. Harmon (eds.). Uranium-series disequilibrium. Applications to earth, marine and environmental sciences. 2<sup>nd</sup> Edition. Oxford Science, pp731-778.

Assinder D.J., Yamamoto M., Kim C.K., Seki R., Takaku Y., Yamauchi Y., Igarashi S., Komura K. and Ueno K. (1993). Radioisotopes of thirteen elements in intertidal coastal and estuarine sediments in the Irish Sea. *J. Radioanal. Nucl. Chem. Articles*, **170**(2), 333-346.

Baxter M.S., McKinley I.G., MacKenzie A.B. and Jack W. (1979). Windscale radiocaesium in the Clyde sea area. *Mar. Poll. Bull.*, **10**, 116-120.

BNFL (1997) Annual Report, BNF Ltd, Warrington, Cheshire.

Bowden K.F. (1955). Physical oceanography of the Irish Sea. *Fish Invest. Ser. II*, **18**(8), 1-67.

Bowen H.J.M. (1956). Strontium and barium in seawater and marine organisms. *J. Mar. Biol. Assoc.*, **35**, 451-459.

Crick M.J. and Linsley G.S. (1984). An assessment of the radiological impact of the Windscale reactor fire, October 1957. *Int. J. Radiat. Biol.*, **46**, 479-506.

Croudace I.W. (1991). A reliable and accurate procedure for preparing low activity efficiency calibration standards for germanium gamma-ray spectrometers. *J. Radioanal. Nucl. Chem., Letters*, **153**(2), 151-162.

Cundy A.B. and Croudace I.W. (1994). Sedimentary and geochemical variations in a saltmarsh / mudflat environment from a mesotidal Hamble estuary, Southern England. *Mar. Chem.*, **51**, 115-132

Day J.P. and Cross J.E. (1981).  $^{241}\text{Am}$  from the decay of  $^{241}\text{Pu}$  in the Irish Sea. *Nature*, **292**, 43-45.

Dahlgaard H., Chen Q., Herrmann J., Nies H., Ibbett R.D. and Kershaw P.J. (1995). On the background level of  $^{99}\text{Tc}$ ,  $^{90}\text{Sr}$  and  $^{137}\text{Cs}$  in the North Atlantic. *J. Mar. Sys.*, **6**, 571-578.

Gray J., Jones S.R. and Smith A.D. (1995). Discharges to the environment from the Sellafield site, 1951 – 1992. *J. Radiat. Prot.*, **15** (2), 99-131.

Hamilton E.I. and Clarke K.R. (1984). The recent sedimentation history of the Esk estuary, Cumbria, UK: the application of radiochronology. *Sci. Total Environ.*, **35**, 325-386.

Holm E., Roos P. and Skwarzec B. (1992). Radioanalytical studies of fallout  $^{63}\text{Ni}$ . *Appl. Radiat. Isot.*, **43** (1/2), 371-376.

Horrill A.D. (1984). Concentration and spatial distribution of radioactivity in an ungrazed saltmarsh. In Ecological aspects of radionuclide release. Coughtrey P.J. (ed.). British Ecological Society, Special publication No3, Blackwell, Oxford pp199-215.

Jefferies D.F., Preston A. and Steele A.K. (1973). Distribution of caesium-137 in British coastal waters. *Mar. Poll. Bull.*, **4**, 118-122.

Kershaw P.J. (1986). Radiocarbon dating of Irish Sea sediments. *Estuarine. Coastal Shelf Sci.*, **23**, 295-303.

Kershaw P.J., Swift D.J., Pentreath R.J., Lovett M.B. (1983). Plutonium redistribution by biological activity in Irish Sea sediments. *Nature*, **306**, 774-775.

Kershaw P.J., Swift D.J., Denoon D.C. (1988). Evidence for recent sedimentation in the Eastern Irish Sea. *Mar. Geol.*, **85**, 1-14.

Kershaw P.J., Woodhead D.S., Malcolm S.J., Allington D.J. and Lovett M.B. (1990). A sediment history of Sellafield discharges. *J Environ. Radioact.*, **12**, 201-241.

Koide M., and Goldberg E.D., (1985). Determination of  $^{99}\text{Tc}$ ,  $^{63}\text{Ni}$  and  $^{121\text{m}+126}\text{Sn}$  in the marine environment. *J. Environ. Radioactivity*, **2**, 261-282.

Livens F.R., Horrill A.D. and Singleton D.L. (1994). Plutonium in estuarine sediments and the associated interstitial waters. *Estuarine Coastal. Shelf Sci.*, **38**, 479-489.

McDonald P., Cook G.T., Baxter M.S. and Thomson J.C. (1990). Radionuclide transfer from Sellafield to south-west Scotland. *J. Environ. Radioact.*, **12**, 285-285-298.

McKay W.A. and Pattenden N.J. (1993). The behaviour of plutonium and americium in the shoreline waters of the Irish Sea. A review of Harwell studies in the 1980's. *J. Environ. Radioact.*, **18**, 99-132.

MacKenzie A.B., Scott R.D. and Williams T.M. (1987). Mechanism for northwards dispersal of Sellafield waste. *Nature*, **299**, 613-616.

MacKenzie A.B., Scott R.D., Allan R.L., Ben Shaban Y.A., Cook G.T. and Pulford I.D. (1994). Sediment radionuclide profiles: implications for mechanisms of Sellafield waste dispersal in the Irish Sea. *J. Environ. Radioact.*, **23**, 39-69.

MacKenzie A.B., Cook G.T., McDonald P. and Jones S.R. (1998). The influence of mixing timescales and re-dissolution processes on the distribution of radionuclides in Northeast Irish Sea sediments. *J. Environ. Radioact.*, **39 (1)**, 35-53.

Madruga M.J. and Cremers A. (1997). On the differential binding mechanisms of radiostrontium and radiocaesium in sediments. In Desmet G. (ed) *Freshwater Estuarine Radioecology*, Elsevier Science, Netherlands.

Nelson D.M. and Lovett M.B. (1978). Oxidation state of plutonium in the Irish Sea. *Nature*, **276**, 599-601.

Pentreath R.J., Harvey B.R. and Lovett M.B. (1986). Chemical speciation of transuranium nuclides discharged into the marine environment. In Bulman R.A. and Cooper J.R. (eds). *Speciation of fission and activation products in the environment*. Elsevier Applied Science, London, UK.

Stanners D.A. and Aston S.R. (1981).  $^{134}\text{Cs}$ : $^{137}\text{Cs}$  and  $^{106}\text{Ru}$ : $^{137}\text{Cs}$  ratios in intertidal sediments from the Cumbria and Lancashire coasts, England. *Estuar. Coast. Shelf Sci.*, **13**, 409-417.

Thomson J., Mercone D., de Lange G.J. and van Santvoort P.J.M. (1999). Review of recent advances in the interpretation of eastern Mediterranean sapropel S1 from geochemical evidence. *Mar Geol.*, **153**, 77-89.

UNSCEAR (1982). Sources and effects of ionising radiation. United Nations Scientific Committee on the Effects of Atomic Radiation. United Nations, New York, USA.

Wigley F., Warwick P. E., Croudace I.W., Caborn J., Sanchez A.L (1999). An optimised method for the routine determination of technetium-99 in environmental samples by liquid scintillation counting. *Analyt. Chim. Acta.*, **380**, 73-82

## Chapter 7

### **Overall conclusions**

**More detailed conclusions are presented at the end of each chapter**

## 7. Overall conclusions

### 7.1 Radioanalytical study

Anthropogenic radionuclides that decay via the emission of beta particles or via electron capture are of considerable importance both in assessing the total radioactive inventory of wastes arising from nuclear operations and when determining the potential radiological impact of stored nuclear waste. In addition, quantities of beta emitting radioisotopes are routinely released via authorised discharges from nuclear power stations, nuclear reprocessing facilities and during atmospheric nuclear weapons' testing in previous years. In particular, the commissioning of EARP has resulted in a significant increase in  $^{99}\text{Tc}$  being discharged into the Irish Sea.

The determination of beta emitters is hindered by the distribution of beta energies emitted for a given decay energy and hence the lack of any spectrometric approach for identification and quantification of a mixture of beta emitting radioisotopes. This has meant that the determination of beta emitters requires the separation and purification of the element prior to measurement of the beta activity. Once a single element has been purified, it is possible to use relatively simple spectrometric techniques to deconvolute two or possibly three isotopes of the same element. The success of such a deconvolution will depend on the difference in decay energies of the isotopes.

Of the range of beta emitters present in nuclear wastes,  $^{55}\text{Fe}$ ,  $^{63}\text{Ni}$ ,  $^{90}\text{Sr}$  and  $^{99}\text{Tc}$  were chosen for further study. These isotopes are routinely analysed in reactor effluents and discharges of these radioisotopes are recorded for many nuclear facilities. Liquid scintillation counting was chosen for all measurements. In general, counting efficiencies were higher for liquid scintillation counting compared with any other radiometric technique. The use of a Wallac Quantulus liquid scintillation counter provided very low backgrounds and correspondingly high figures of merit through the use of a guard chamber and anti-coincidence circuitry coupled with considerable shielding. A range of source preparation techniques were investigated including counting of organic extracts, acidic solutions and precipitates. Optimised techniques were then developed for all radioisotopes. Although precipitation of  $^{63}\text{Ni}$  as Ni pyridine thiocyanate was investigated as a source preparation technique, the precision of measurement was not as good as for an acidic solution mixed with commercial scintillant. Iron-55 was also counted as an acidic solution, although  $\text{H}_3\text{PO}_4$  was used to produce a colourless ferriphosphate complex that overcame the colour quench normally associated with the yellow Fe(III) ion.  $^{90}\text{Sr}$  was best determined by Cerenkov counting of the  $^{90}\text{Y}$  daughter using the liquid scintillation counter. The absence of liquid scintillant reduced

the counting efficiency but this was compensated for by a significant reduction in background count rates with correspondingly higher figure of merit. A mathematical deconvolution technique was assessed for determination of a mixture of  $^{89}\text{Sr}$  and  $^{90}\text{Sr}$  as measured by Cerenkov counting.  $^{99}\text{Tc}$  was determined either by mixing a tri-n-octylamine extract with scintillant or by adding  $^{99}\text{Tc}$  on TEVA resin directly into scintillant. The addition of TEVA resin directly to scintillant resulted in slightly lower counting efficiencies compared with the organic extract and hence was only incorporated into techniques specifically developed for low level waste applications where ultimate limits of detection are not required. Optimisation of all counting techniques was undertaken.

Non-radiometric techniques such as ICP-MS and TIMS often offer a more sensitive alternative to radiometric techniques for the determination of long-lived radioisotopes. Of the isotopes studied, only  $^{99}\text{Tc}$  had a half life sufficiently long to be considered for mass spectrometric measurement. However, practical considerations meant that radiometric measurement was preferable.

Suitable counting techniques were developed for the determination of the four radioisotopes. Additionally selective chemical separation procedures were devised to isolate the radioisotopes of interest and purify them from any potential interferences. Although ion exchange chromatography has been widely used in radioanalytical chemistry, solvent extraction-based techniques are often more specific. If the organic extractant is loaded onto an inert support, the benefit of high specificity associated with solvent extraction is combined with the high separation factors and ease of handling associated with a column based technique, giving rise to the technique of extraction chromatography. The techniques of solvent extraction and extraction chromatography were therefore investigated for the purification of the beta emitters. Solvent extraction of Tc(VII) into tri-octylamine and Fe(III) as the  $\text{FeCl}_4^-$  anion into a range of solvents was investigated. Both extraction systems were then developed into extraction chromatographic procedures. In addition, commercially available TEVA resin and Sr resin were investigated for the purification of  $^{99}\text{Tc}$  and  $^{90}\text{Sr}$  respectively. Extraction chromatographic separation of  $^{55}\text{Fe}$  on a diisobutyl ketone based extraction column was found to work well for samples containing low levels of Fe. For many samples, the Fe concentration was too high to permit an extraction chromatographic separation on a practically sized column and solvent extraction was the preferred procedure. In all other cases extraction chromatography was suitable for effective purification of the radioisotopes of interest. As well as improving the purification of the radioisotopes, extraction chromatography also considerably reduced the volume of organic wastes produced during an analysis. However, in the case of  $^{99}\text{Tc}$  in environmental samples, better limits of detection

were achievable by extracting Tc(VII) into tri octylamine and mixing this directly with scintillant. This acted as both a chemical separation and source preparation procedure and was adopted in preference to extraction chromatography for environmental samples.

To shorten analytical times and permit the analysis of all radioisotopes on samples of limited mass, sequential separation schemes were developed. Sequential separation of  $^{55}\text{Fe}$ ,  $^{63}\text{Ni}$ ,  $^{90}\text{Sr}$  and  $^{99}\text{Tc}$  from low level waste materials was achieved using a series of extraction chromatography columns. For environmental samples, the high concentrations of stable Fe required the solvent extraction purification of  $^{55}\text{Fe}$ .  $^{63}\text{Ni}$  and  $^{90}\text{Sr}$  were analysed using the extraction chromatographic separation technique. Specific pretreatment steps for  $^{99}\text{Tc}$  also meant that  $^{99}\text{Tc}$  was analysed on a separate sub-sample. Final purification of  $^{99}\text{Tc}$  was achieved using solvent extraction into trioctylamine with the extract being added directly to scintillant in order to obtain lowest limits of detection. Again, the sequential separation schemes were optimised.

## 7.2 Environmental application

The separation schemes developed for environmental samples were used to assess the levels of beta emitters in a saltmarsh environment. The Ravenglass saltmarsh at the mouth of the Esk estuary was chosen for the investigation as the marsh has been thoroughly studied in the past. The marsh is also routinely exposed to discharges from the reprocessing plant at Sellafield, Cumbria. Levels of major and trace elements were determined using XRF analysis and gamma emitting radioisotopes were measured using gamma spectrometry to provide supporting information in the interpretation of the data for beta emitters.  $^{55}\text{Fe}$ ,  $^{63}\text{Ni}$ ,  $^{90}\text{Sr}$  and  $^{99}\text{Tc}$  were all detectable in the marsh although levels of  $^{55}\text{Fe}$  and  $^{63}\text{Ni}$  were only just above the limit of detection. Interpretation of  $^{55}\text{Fe}$  and  $^{63}\text{Ni}$  was also complicated by the limited discharge data available. The profiles of  $^{90}\text{Sr}$ ,  $^{137}\text{Cs}$  and  $^{241}\text{Am}$  broadly reflected the discharge history of the site. There was evidence for significant radionuclide mixing between current and previous years' discharges prior to deposition in the marsh. Post depositional migration appeared to be limited although the profile of  $^{99}\text{Tc}$  in the core did suggest migration of  $^{99}\text{Tc}$  had occurred. There was some geochemical evidence for a reducing zone in the core and this may play a part in the post depositional migration and subsequent immobilisation of Tc.

Although the levels of  $^{55}\text{Fe}$  and  $^{63}\text{Ni}$  were too low in the core to permit a more thorough evaluation it is suggested that this approach could be used on larger sample sizes to improve the sensitivity of the technique and evaluate the post depositional behaviour of these two radioisotopes. In addition, such an approach could provide valuable information on the

behaviour of Fe and Ni in the marine environment. The measurement of  $^{90}\text{Sr}$  in the saltmarsh environment is of potential importance in assessing the long-term impact of discharges as the relatively high levels of  $^{90}\text{Sr}$  held within the saltmarsh coupled with the high energy beta emission of the  $^{90}\text{Y}$  daughter may make this an important consideration in calculating future radiation doses to local critical groups in the future. Likewise,  $^{99}\text{Tc}$  bound in the saltmarsh may be re-released in the future and must therefore be considered as a potential sink and source when assessing future doses to the general public.

## **Appendices**

---

**Appendix 1 : Conferences/meetings/courses attended/publications**
**A 1.1 Conferences/meetings since 1988**

1988 (5 days)	Radioisotopes techniques short course, Loughborough University, UK
1990 (5 days)	4th International Symposium on Environmental Radioactivity, Manchester, UK (Poster/paper : The separation of actinides from lanthanides by anion exchange in methanol/hydrogen chloride medium, and its application to routine separation)
1990 (1 day)	The Young Radiochemists Meeting (Presentation : as above)
1992 (1 day)	IRDG meeting, NRPB, Chilton, UK (Presentation : The effect of uncertainty on the estimate of dose using the DREAMS database)
1992 (3 days)	Radiotoxicology working group meeting, Aix-en-Provence, France
1993 (3 days)	Radiotoxicology working group meeting, La Hague, France
1993 (4 days)	Analytical Quality Control, Chester, UK
1994 (1 day)	Quality systems in NAMAS laboratories, Manchester, UK
1994 (3 days)	5th International Symposium on Environmental Radiochemistry, Bournemouth, UK
1995 (4 days)	Eichrom Workshop, MAFF, Weybridge, UK.
1995 (5 days)	ICRM '95, Seville, Spain (Presentation/Paper : A review of analytical techniques for the determination of <sup>241</sup> Am in soils and sediments)
1996	Geochemistry group meeting, SOC, Southampton, UK (Presentation : Behaviour of pure beta emitters in the marine environment)
1996 (1 day)	Young Environmental Chemist meeting, Leicester, UK (Poster : as above)
1996 (1 day)	Eichrom User Group meeting, Brussels, Belgium (Presentation : The use of tritium columns and Ni-SPEC in effluent analysis)
1997 (1 day)	SERMG seminar, Southampton, UK
1997 (1 day)	Radiochemical methods group, RSC. Harwell, UK. Radionuclide measurements : developments in high sensitivity methods (Presentation – Analysis of U isotopes by TIMS)
1997	Societe Jersiaise (invited lecture on the impact of the nuclear industry on the environment)
1997 (1 day)	Emergency procedures for the rapid determination of radionuclides. NPL, Teddington, UK (Presentation – Sequential separation of pure beta emitting radioisotopes)
1998 (3 day)	Organised the 'Technetium 1998' conference at Southampton Oceanography Centre
1998 (1 day)	Nottingham-Trent University (invited lecture – Greenham Common Survey)
1998 (1 day)	AEA Technology, Harwell (invited lecture – Analysis of pure beta emitting radioisotopes)
1998 (2 day)	International workshop on the application of extraction chromatography in radionuclide measurement, Geel, Belgium (Presentation/paper – Development of extraction chromatographic techniques for the separation of pure beta emitting radioisotopes in low-level wastes).
1999 (1 day)	MAFF RADREM-TESC meeting on sea-to-land transfer of radionuclides (London)

## A 1.2 Papers in refereed journals

### A 1.2.1 Accepted / published

1. Bains M.E.D. and Warwick P.E. (1993). The separation of actinides from lanthanides by anion exchange in methanol/hydrogen chloride medium and its application to routine separation. *Sci. Total Environ.*, **130/131**, 437-445.
2. Warwick P.E., Croudace I.W. and Carpenter R. (1996). Review of analytical techniques for the determination of americium-241 in soils and sediments. *Appl. Radiat. Isot.*, **47**(7), 627-642.
3. Dale C.J., Warwick P.E. and Croudace I.W. (1996). An optimised method for technetium-99 determination in low level waste by extraction into tri-n-octylamine. *Radioact. Radiochem.*, **7**(3), 23-31,
4. Croudace I.W., Warwick P.E. and Dee S.J. (1997). Greening the Common. *Chem Brit*, 26-29
5. Toole J., Adsley I., Hearn R., Wildner H., Montgomery N., Croudace I., Warwick P. & Taylor R. (1997). Status of analytical techniques for the measurement of uranium isotopic signatures. Workshop on the status of measurement techniques for the identification of nuclear signatures, 25-27 February 1997, Geel Belgium. Report EUR 17313.
6. Warwick P.E., Croudace I.W. and Bains M.E.D. (1998). An optimised method for the measurement of  $^{55}\text{Fe}$  using liquid scintillation analysis. *Radioact. Radiochem.*, **9**(2), 19-25.
7. Taylor R.N., Croudace I.W. and Warwick P.E. (1998). Optimised method for the measurement of Uranium by TIMS - *Chem Geol*, **144**, 73-80.
8. Dale C.J., Warwick P.E. and Croudace I.W. (1998). An optimised method for the determination of Tc-99 by solvent extraction used at the Waste Quality Checking Laboratory. In Odoj R., Baier J., Brennecke P. and Kühn K. (eds). Radioactive waste products 1997, Forschungszentrum Jülich GmbH, Germany.
9. Croudace I.W., Warwick P.E., Taylor R.N. and Dee S.J. (1998). Rapid procedure for plutonium and uranium determination in soils using a borate fusion followed by ion-exchange and extraction chromatography - *Analyt. Chim. Acta*, **371**, 217-225.
10. Bahaj A.S., Croudace I.W., James P. Moeschler F.D. & Warwick P.E. (1998). Continuous radionuclide recovery from wastewater using magnetotactic bacteria. *J. Magnetism Magnetic Mat.*, **184**, 241-244.
11. Warwick P.E., Croudace I.W., Dale C.J. and Howard A.G. (1998). Extraction chromatographic techniques in the sequential separation of pure beta emitting radionuclides in low-level waste. Conference proceedings for the International workshop on the application of extraction chromatography in radionuclide measurement, Geel, Belgium
12. Croudace I.W., Warwick P.E., Taylor R.N., Dee S.J., Milton J.A. and Oh J. (1998). Borate fusion followed by ion-exchange/extraction chromatography for the rapid determination of Pu and U in environmental samples. *Radioact. Radiochem.*, **9**(3), 41-48
13. Warwick P.E., Croudace I.W. & Dale A.A. (1999) An optimised method for the determination of uranium and plutonium in aqueous samples - *Appl. Radiat. Isot.*, **50**, 579-583
14. Wigley F., Warwick P. E., Croudace I.W., Caborn J., Sanchez A.L. (1999) An optimised method for the routine determination of technetium-99 in environmental samples by liquid scintillation counting - *Analyt. Chim. Acta*, **380**, 73-82

15. Warwick P.E., Croudace I.W. & Howard A.G. (1999) An improved technique for the routine determination of tritiated water in aqueous samples. *Analyt Chim Acta*, **382**, 225-231

#### **A 1.2.2 Papers submitted**

1. Cundy A.B., Croudace I.W and Warwick P.E. Environmental decline of radionuclides following nuclear reactor closure:  $^{60}\text{Co}$  and  $^{65}\text{Zn}$  from the Winfrith Reactor, southern England – *Environmental Science and Technology*

### A 1.3 Official reports

1. Warwick P.E. (1989) The uptake and distribution of cobalt in *Fucus serratus*. AEA Internal Report RSD Tech Memo 89/1
2. Bains M.E.D. & Warwick P.E. (1991) The separation of strontium from large amounts of calcium during radiochemical analysis. A study of a modified approach. AEA Internal Report HSD Tech. Memo. 91/07.
3. Warwick P E & Bains M.E.D. (1991) Review of analytical techniques for the determination of tritium in urine AEA Internal Report HSD Tech Memo 91/11.
4. Warwick P.E. (1992) Analysis of glass fibre smears for tritiated water. AEA Internal Report EE/92/03.
5. Warwick, P.E. & Smith, M.M. (1993) Action levels for radionuclides in environmental samples. AEA Internal Report HPD/93/01.
6. Warwick, P.E. (1993) Report on investigation of sewage sludge heaps next to SGHWR. AEA Internal Report HPD/93/02.
7. Croudace I.W., Sanderson D.C.W., Warwick P.E. and Allyson J.D. (1997). A regional study of the radiation environment of Greenham Common, Newbury District and surrounding areas. Available from West Berkshire Council, Berks UK
8. Croudace I.W., Warwick P.E., Taylor R.N. and Dee S. (1997) An investigation of radioactive contamination at Greenham Common, Newbury District and surrounding areas. Final Report. Available from West Berkshire Council, Berks UK.
9. Wigley F., Warwick P.E. and Croudace I.W. (1998). Technetium-99 in fucoid seaweeds and other marine biota. Study commissioned by the Greenpeace Research Laboratories, University of Exeter, Exeter, UK.
10. Croudace I., Warwick P., Taylor R., Bradshaw K. and Warneke T. (1999) An assessment of radioactive contamination in the environment as a result of operations at the AWE sites in Berkshire. Study commissioned by AWE Hunting-BRAE Ltd, Aldermaston, UK

**A 2 : Major and trace element results for core RC-96-007**  
**(all results refer to dry material)**

<i>Depth</i> <i>cm</i>	1	2	3	4	5	6	7	8	9	10	11	12	13	14	15
<i>Major elements wt %</i>															
<i>SiO<sub>2</sub></i>	62.75	64.83	67.65	64.25	67.08	67.23	66.32	67.89	67.14	68.99		65.68		67.26	
<i>TiO<sub>2</sub></i>	0.64	0.67	0.63	0.70	0.68	0.67	0.68	0.67	0.69	0.69		0.73		0.70	
<i>Al<sub>2</sub>O<sub>3</sub></i>	10.14	10.46	9.69	11.31	10.76	10.77	10.66	10.32	10.71	10.29		11.24		11.02	
<i>Fe<sub>2</sub>O<sub>3</sub></i>	4.19	4.22	3.84	4.47	4.16	4.40	4.32	4.25	4.30	4.17		4.62		4.51	
<i>MnO</i>	0.16	0.13	0.11	0.10	0.09	0.15	0.12	0.15	0.12	0.12		0.14		0.13	
<i>MgO</i>	2.16	2.11	1.95	2.20	2.04	2.05	2.07	1.93	2.02	1.93		2.08		2.08	
<i>CaO</i>	3.82	3.03	1.89	1.59	1.38	1.26	1.28	1.22	1.24	1.26		1.24		1.29	
<i>Na<sub>2</sub>O</i>	2.02	1.92	1.93	2.03	2.05	2.04	2.03	1.95	1.89	1.86		1.97		1.94	
<i>K<sub>2</sub>O</i>	2.22	2.36	2.23	2.48	2.47	2.44	2.45	2.35	2.42	2.23		2.44		2.38	
<i>P<sub>2</sub>O<sub>5</sub></i>	0.20	0.19	0.18	0.18	0.18	0.18	0.18	0.17	0.17	0.17		0.18		0.18	
<i>LOI</i>	11.70	10.10	9.90	10.70	9.10	8.80	9.90	9.10	9.30	8.30		9.70		8.50	
<i>Cl</i>	1.70	1.40	1.49	1.56	1.37	1.54	1.63	1.56	1.47	1.35		1.44		1.30	
<i>S</i>	0.23	0.17	0.19	0.19	0.19	0.18	0.20	0.19	0.18	0.16		0.18		0.16	
<i>Trace elements ppm</i>															
<i>Rb</i>	85	85	83	92	90	91	90	88	90	88		88		91	91
<i>Sr</i>	151	124	105	103	100	101	100	98	100	101		97		102	100
<i>Ba</i>	335	337	357	340	349	347	330	336	338	340		329		351	330
<i>Br</i>	157	154	200	226	179	220	204	196	170	156		159		172	159
<i>I</i>	93	89	109	114	91	105	95	93	81	70		70		62	66
<i>As</i>	16	15	13	17	15	17	18	18	18	15		15		16	19
<i>Pb</i>	64	55	55	67	58	59	59	55	57	57		54		59	57
<i>Ni</i>	30	29	29	32	31	32	32	30	33	32		31		34	32
<i>Cr</i>	106	110	112	119	123	122	115	112	115	115		112		124	119
<i>Zn</i>	129	123	117	142	125	134	133	125	129	121		119		134	123
<i>V</i>	94	90	87	101	96	104	96	92	103	89		95		99	96
<i>Y</i>	25	26	26	33	32	32	31	30	36	35		35		37	38
<i>Zr</i>	253	291	293	266	293	268	259	262	280	301		285		294	297
<i>Nb</i>	15	15	14	14	16	15	15	15	15	15		16		16	16
<i>La</i>	26	29	28	34	34	32	33	30	33	31		32		36	35
<i>Ce</i>	49	48	41	52	52	53	53	52	53	51		59		46	53
<i>Th</i>	6	8	7	7	7	7	6	6	7	7		6		8	7
<i>U</i>	1	1	1	1	2	1	3	1	2	1		2		0	1

## A2 - continued

Depth cm	16	17	18	19	20	21	22	23	24	25	26	27	28	29	30
<b>Major elements wt %</b>															
<i>SiO<sub>2</sub></i>	67.03		65.76		65.64		68.15		68.83		67.22		65.86		67.18
<i>TiO<sub>2</sub></i>	0.71		0.70		0.71		0.70		0.69		0.73		0.74		0.73
<i>Al<sub>2</sub>O<sub>3</sub></i>	10.81		11.09		11.01		10.76		10.59		11.06		11.78		11.40
<i>Fe<sub>2</sub>O<sub>3</sub></i>	4.54		4.63		4.64		4.23		4.57		4.88		5.27		4.78
<i>MnO</i>	0.11		0.07		0.06		0.05		0.06		0.09		0.21		0.16
<i>MgO</i>	2.05		2.12		2.02		1.99		1.95		2.10		2.28		2.05
<i>CaO</i>	1.26		1.24		1.23		1.26		1.23		1.24		1.32		1.22
<i>Na<sub>2</sub>O</i>	1.94		2.01		1.92		1.82		1.76		1.81		1.93		1.76
<i>K<sub>2</sub>O</i>	2.36		2.37		2.44		2.37		2.33		2.44		2.43		2.47
<i>P<sub>2</sub>O<sub>5</sub></i>	0.20		0.20		0.21		0.17		0.18		0.16		0.17		0.15
<i>LOI</i>	9.00		9.80		10.10		8.50		7.80		8.30		8.00		8.10
<i>Cl</i>	1.33		1.36		1.34		1.18		1.20		1.04		1.00		0.93
<i>S</i>	0.16		0.17		0.18		0.14		0.16		0.13		0.12		0.13
<b>Trace elements ppm</b>															
<i>Rb</i>	92	93	91	92	94	94	89	87	89	95	94	97	96	96	92
<i>Sr</i>	100	102	100	101	103	101	99	98	97	98	101	103	101	102	101
<i>Ba</i>	362	352	349	355	356	348	347	353	352	367	371	385	386	400	390
<i>Br</i>	167	182	195	201	195	190	158	166	148	142	136	140	127	125	116
<i>I</i>	70	74	62	72	70	62	60	68	58	66	64	89	74	81	62
<i>As</i>	17	17	17	15	20	18	15	16		19	19	20		21	21
<i>Pb</i>	63	68	67	69	78	72	62	63	67	78	80	78	82	81	75
<i>Ni</i>	34	34	32	33	35	34	32	31	32	34	34	37	36	37	34
<i>Cr</i>	133	140	129	138	156	136	121	119	117	123	122	122	125	121	119
<i>Zn</i>	139	152	144	150	164	156	136	138	138	149	152	165	164	165	146
<i>V</i>	101	104	101	100	108	105	89	97	96	102	105	109	108	108	98
<i>Y</i>	42	41	40	44	53	36	31	33	30	27	29	29	28	27	27
<i>Zr</i>	286	284	299	293	287	284	306	312	301	298	296	291	284	293	293
<i>Nb</i>	15	15	15	16	15	16	16	16	16	16	16	17	17	17	16
<i>La</i>	36	37	37	38	41	33	32	31	32	33	34	34	34	29	31
<i>Ce</i>	52	53	52	55	55	57	51	53	51	57	55	52	53	52	49
<i>Th</i>	7	8	7	7	7	6	6	6	8	7	6	7	8	7	7
<i>U</i>	2	1	1	1	3	3	2	2	1	3	0	1	0	0	1

## A2 - continued

Depth cm	31	32	33	34	35	36	37	38	39	40	41	42	43	44	45
<b>Major elements wt %</b>															
<i>SiO<sub>2</sub></i>		66.66			67.99			68.85			68.51			68.68	
<i>TiO<sub>2</sub></i>		0.71			0.68			0.70			0.71			0.69	
<i>Al<sub>2</sub>O<sub>3</sub></i>		11.50			11.44			10.73			10.93			11.06	
<i>Fe<sub>2</sub>O<sub>3</sub></i>		4.81			4.52			4.48			4.61			4.54	
<i>MnO</i>		0.21			0.18			0.17			0.18			0.15	
<i>MgO</i>		2.14			2.07			2.02			2.06			2.05	
<i>CaO</i>		1.27			1.28			1.27			1.24			1.28	
<i>Na<sub>2</sub>O</i>		1.77			1.80			1.81			1.77			1.77	
<i>K<sub>2</sub>O</i>		2.49			2.38			2.34			2.44			2.35	
<i>P<sub>2</sub>O<sub>5</sub></i>		0.15			0.16			0.15			0.15			0.15	
<i>LOI</i>		8.30			7.50			7.50			7.40			7.30	
<i>Cl</i>		0.96			0.97			0.90			0.90			0.86	
<i>S</i>		0.14			0.12			0.11			0.11			0.12	
<b>Trace elements ppm</b>															
<i>Rb</i>	92	94	95	94	92	94	91	87	91	92	91	93	91	86	92
<i>Sr</i>	101	102	101	101	101	97	98	98	100	98	98	98	98	96	98
<i>Ba</i>	371	376	372	386	376	370	375	383	380	386	375	375	362	358	357
<i>Br</i>	116	121	121	115	105	106	95	82	88	95	84	79	79	75	80
<i>I</i>	74	78	74	72	74	79	83	62	78	70	68	78	66	60	68
<i>As</i>	20		21	19	19	21	18	18	20	20	20	19	20	17	20
<i>Pb</i>	71	73	70	73	65	66	67	68	71	74	69	68	64	60	65
<i>Ni</i>	35	36	36	34	33	32	34	32	33	33	32	34	33	30	32
<i>Cr</i>	111	114	124	113	108	107	110	111	101	107	106	108	102	103	113
<i>Zn</i>	147	153	150	148	137	135	130	122	126	129	126	126	123	112	125
<i>V</i>	101	107	105	110	101	95	99	93	98	103	99	103	99	88	100
<i>Y</i>	25	26	26	26	24	25	25	24	24	24	25	25	24	24	24
<i>Zr</i>	291	284	281	274	290	270	278	313	295	283	295	296	290	294	284
<i>Nb</i>	17	16	16	16	16	15	16	16	15	16	15	16	16	15	16
<i>La</i>	31	30	31	31	29	32	30	28	31	30	26	32	31	23	24
<i>Ce</i>	50	52	57	51	56	48	52	44	52	56	44	60	54	49	52
<i>Th</i>	7	7	8	6	6	7	8	7	7	6	6	7	7	7	6
<i>U</i>	0	2	3	1	1	0	1	2	3	3	1	3	1	4	0

## A2 - continued

<i>Depth cm</i>	<i>46</i>	<i>47</i>	<i>48</i>	<i>49</i>	<i>50</i>	<i>51</i>	<i>52</i>	<i>53</i>	<i>54</i>
<i>Major elements wt %</i>									
<i>SiO<sub>2</sub></i>		69.16			71.19			72.48	
<i>TiO<sub>2</sub></i>		0.70			0.66			0.63	
<i>Al<sub>2</sub>O<sub>3</sub></i>		11.37			10.32			9.64	
<i>Fe<sub>2</sub>O<sub>3</sub></i>		4.76			4.27			3.90	
<i>MnO</i>		0.17			0.14			0.13	
<i>MgO</i>		2.14			1.89			1.77	
<i>CaO</i>		1.30			1.22			1.16	
<i>Na<sub>2</sub>O</i>		1.79			1.72			1.65	
<i>K<sub>2</sub>O</i>		2.47			2.34			2.31	
<i>P<sub>2</sub>O<sub>5</sub></i>		0.15			0.15			0.13	
<i>LOI</i>		6.00			6.10			6.20	
<i>Cl</i>		0.91			0.95			0.91	
<i>S</i>		0.17			0.13			0.11	
<i>Trace elements ppm</i>									
<i>Rb</i>	95	90	91	91	88	89	85	81	82
<i>Sr</i>	98	96	98	99	97	94	94	92	94
<i>Ba</i>	367	349	361	359	349	343	356	345	350
<i>Br</i>	82	80	95	89	74	80	67	64	62
<i>I</i>	62	78	72	78	64	68	56	62	64
<i>As</i>	21	20	21	19					
<i>Pb</i>	69	64	69	64	57	60	57	55	54
<i>Ni</i>	33	32	34	32	30	32	28	28	28
<i>Cr</i>	113	110	106	103	105	110	107	97	101
<i>Zn</i>	131	121	128	126	114	119	107	104	102
<i>V</i>	107	99	105	100	96	96	92	89	83
<i>Y</i>	25	24	24	25	24	23	23	23	23
<i>Zr</i>	281	304	289	296	309	310	316	311	297
<i>Nb</i>	16	15	17	15	15	15	14	15	14
<i>La</i>	29	28	29	28	27	29	29	25	26
<i>Ce</i>	50	54	47	46	46	54	48	44	41
<i>Th</i>	8	8	7	7	7	7	7	7	7
<i>U</i>	3	2	1	1	2	2	0	0	2

**A 3 : Detection Limits in routine XRF analysis at Southampton using a Rh anode X-ray tube**

Element	X-Ray	Possible interferences*	L.L.D. (ppm) **
As	As K	Pb	2 (200 s)
Ba	Ba L	Ce, high As	10
Bi	Bi L	W	5
Br	Br K		30
Ce	Ce L		10
Cl	Cl K		50
Cr	Cr K	V	4
Cu	Cu K	Cu from the tube	3
Ga	Ga K		1.5
I	I K		3 (200 s)
La	La K		5
Mo	Mo K		5
Ni	Ni K		1.5
Nb	Nb K	Y	1.5
P	P K		30
Pb	Pb L	Bi	1.5
Rb	Rb K	high U	1.5
S	S K		50
Sb	Sb K		5
Sn	Sn K		4
Sr	Sr K		1.5
Th	Th L	High Pb	2
U	U L	High Rb	1.4 (400s)
V	V K		4
W	W L	High Zn, Ga	8
Y	Y K	Rb	1.5
Zn	Zn K		1.5
Zr	Zr K	Sr	1.5

The detection limits are calculated assuming a count-time of 100 seconds on the background unless otherwise stated.

\* Note that most of these interferences are already dealt with automatically.

\*\* Better DLs may be obtained by using longer count times.

**A4 : Results for gamma emitters in core RC-96-007**

<i>Depth</i>	<i>Am-241</i>	<i>Co-57</i>	<i>Co-60</i>	<i>Cs-134</i>	<i>Cs-137</i>	<i>Eu-154</i>	<i>Eu-155</i>	<i>K-40</i>
<i>1</i>	1590		56.2		882	17	4.1	1045
<i>2</i>	1168		17.8		711	12.8	4.8	829
<i>3</i>	1291	9	8.2		837		6.8	730
<i>4</i>	1695	10.5	10.8		1117		11.8	970
<i>5</i>	1663	12	8.5		1113		10.3	880
<i>6</i>	1672	13	14.3		1219			820
<i>7</i>	2555		34		1989	29.4	13.5	911
<i>8</i>	2784		32.8		2788	36.8	15.7	829
<i>9</i>	3298		26		3307	48.9	25.3	847
<i>10</i>	3535	9.6	29.3		4735	42.2	26.7	861
<i>11</i>	4983		21.7		6200	82	43.3	800
<i>12</i>	9026		21.5		8909	103.7	54.5	928
<i>13</i>	12740	22.8	20.2		11498	137.2	89.4	1037
<i>14</i>	9052	21.4	25.8		10970	110	69.2	970
<i>15</i>	10900	13.1	59.2		12743	88	48.2	915
<i>16</i>	15710		43.7		15350	147.7	69.9	910
<i>17</i>	22580	22.8	35.8		16730	138	72.4	964
<i>18</i>	28690		39.5		13780	158.3	59.6	1010
<i>19</i>	14070				9763	112.3	45.2	810
<i>20</i>	12200		6.5		8885	58.4	15.7	978
<i>21</i>								
<i>22</i>	2951	4.3	3.8		4716			998
<i>23</i>								
<i>24</i>	600				2332			1030
<i>25</i>								
<i>26</i>	67.5				1006			945
<i>27</i>								
<i>28</i>	28.1				689			997
<i>29</i>								
<i>30</i>	10				347.2			936
<i>31</i>						200		993
<i>32</i>	4.9							
<i>33</i>					98.8			900
<i>34</i>								
<i>35</i>					67.3			913
<i>36</i>								
<i>37</i>					37.8			880
<i>38</i>	3.5							
<i>39</i>								
<i>40</i>								
<i>41</i>								
<i>42</i>								

**A4 continued**

<i>Depth</i>	<i>Am-241</i>	<i>Co-57</i>	<i>Co-60</i>	<i>Cs-134</i>	<i>Cs-137</i>	<i>Eu-154</i>	<i>Eu-155</i>	<i>K-40</i>
43								
44					10.6		869	
45								
46								
47								
48					3.7		1004	
49								
50							863	
51								
52							945	
53								
54							902	
55	11.5				11.8		806	

All results are in Bq/kg dry

## A5 : Results for beta emitters in core RC-96-007

All results are in Bq/kg dry decay corrected to July 1996

Depth	Fe-55			Ni-63			Sr-90			Tc-99		
	Bq/kg	2 s.d	LOD	Bq/kg	2 s.d	LOD	Bq/kg	2 s.d	LOD	Bq/kg	2 s.d	LOD
1	56	6	38				284	41	n.d.	217	8	8
2	109	9	24	17	4	9	252	25	n.d.	180	5	4
3	188	13	26	17	4	7	505	42	n.d.	64	3	4
4	113	9	21	13	4	9	200	29	n.d.	37	3	5
5				29	4	6				26	2	4
6	103	8	19	33	4	8	648	49	n.d.	34	2	4
7				37	4	7	243	31	n.d.	27	2	4
8	69	6	20	38	5	9	147	23	n.d.	27	2	4
9				21	3	7	432	43	n.d.	26	2	3
10	88	7	19	23	4	8	287	23	n.d.	32	2	4
11				21	4	7	616	47	n.d.	42	2	4
12	149	11	20	34	4	8	606	47	n.d.	63	3	4
13				31	5	9	1124	76	n.d.	69	4	5
14	91	8	21	40	5	10	538	138	n.d.	95	4	4
15				37	6	12	1260	82	n.d.	56	3	5
16	123	10	24	32	5	9				50	3	4
17				28	4	7	2126	91	n.d.	66	3	4
18	107	9	23	34	4	7	1696	90	n.d.	85	3	3
19										115	4	4
20	65	7	44	36	5	10	594	125	n.d.	143	5	4
21										36	2	4
22	80	7	23	30	4	8	120	79	n.d.	45	3	4
23										32	2	3
24	27	3	20	53	5	8	152	58	n.d.	22	2	3
25										36	2	3
26				35	5	11	117	77	n.d.	25	2	4
27										41	3	3
28				17	3	7	131	32	n.d.	27	2	3
29										42	2	3
30				29	4	6	290	112	n.d.	27	2	3
31										22	2	3
32				44	4	8	84	56	n.d.	5	1	4
33										1	0	3
34				36	4	9	42	19	n.d.	2	0	4
35										0	0	3
36				31	4	8				0	0	4
37												
38				33	5	9	27	19	n.d.	3	0	3
39												
40				33	4	7	35	24	n.d.	1	0	3
41												
42				37	4	7	31	17	n.d.	0	0	3
43												
44				31	4	8	31	17	n.d.	0	0	4

**A6 : Sellafield aqueous discharge data (all values in Bq)**

Year	H-3	Sr-90	Zr/Nb-95	Ru-106	Cs-134	Cs-137	Ce-144	Pu-238	Pu-239	Pu-241	An-241	Tc-99	Pm-147	Co-60	Fe-55	Ni-63	I-129	Np-237
1952	2.50E+14	3.30E+13	2.00E+14	9.10E+13	1.20E+12	4.60E+13	6.60E+13	2.00E+10	5.40E+11	2.00E+12								
1953	2.50E+14	3.60E+13	2.00E+14	1.80E+14	1.20E+12	4.60E+13	6.60E+13	2.00E+10	5.00E+11	1.00E+12								8.00E+12
1954	2.50E+14	1.90E+13	2.00E+14	2.70E+14	1.20E+12	4.60E+13	6.60E+13	2.00E+10	6.00E+11	2.30E+12								8.00E+12
1955	2.50E+14	9.30E+12	2.40E+14	2.10E+14	5.20E+11	2.10E+13	3.50E+13	2.00E+10	7.00E+11	1.90E+12								8.00E+12
1956	2.50E+14	7.10E+13	2.40E+14	1.60E+15	4.40E+12	1.60E+14	4.70E+13	6.00E+10	1.80E+12	3.70E+12								8.00E+12
1957	2.50E+14	6.10E+13	2.60E+14	9.90E+14	3.50E+12	1.40E+14	9.60E+13	5.00E+10	1.60E+12	3.40E+12								8.00E+12
1958	2.50E+14	9.30E+13	3.20E+14	1.60E+15	5.70E+12	2.30E+14	2.20E+14	6.00E+10	1.90E+12	3.90E+12								8.00E+12
1959	2.50E+14	5.70E+13	5.60E+14	1.30E+15	2.70E+12	7.30E+13	2.60E+14	6.00E+10	2.10E+12	4.40E+12								8.00E+12
1960	2.50E+14	1.90E+13	3.20E+14	1.50E+15	1.40E+12	3.40E+13	3.30E+13	8.00E+10	2.70E+12	6.20E+12								8.00E+12
1961	2.50E+14	1.80E+13	3.30E+14	9.30E+14	1.80E+12	4.00E+13	8.00E+13	1.40E+11	4.60E+12	1.80E+13								8.00E+12
1962	2.50E+14	3.80E+13	1.90E+14	8.50E+14	3.90E+12	7.40E+13	8.90E+13	2.00E+11	6.60E+12	3.70E+13								8.00E+12
1963	1.40E+14	2.00E+13	1.40E+14	1.20E+15	6.10E+12	8.50E+13	5.20E+13	2.50E+11	8.10E+12	5.50E+13								8.00E+12
1964	2.90E+14	3.60E+13	1.60E+15	9.10E+14	6.10E+12	1.00E+14	1.20E+14	2.20E+11	5.50E+12	6.20E+13								8.00E+12
1965	3.30E+14	5.60E+13	1.80E+15	7.50E+14	1.00E+13	1.10E+14	1.40E+14	3.00E+11	6.90E+12	8.10E+13								8.00E+12
1966	4.60E+14	3.40E+13	1.40E+15	9.20E+14	1.60E+13	1.80E+14	2.50E+14	6.60E+11	1.30E+13	1.70E+14								8.00E+12
1967	5.90E+14	5.20E+13	1.70E+15	6.40E+14	1.50E+13	1.50E+14	5.10E+14	1.20E+12	1.70E+13	2.90E+14								8.00E+12
1968	7.90E+14	5.00E+13	2.40E+15	9.00E+14	4.80E+13	3.70E+14	3.70E+14	2.10E+12	2.80E+13	6.30E+14								8.00E+12
1969	8.70E+14	1.10E+14	2.30E+15	8.50E+14	6.20E+13	4.40E+14	5.00E+14	2.80E+12	2.70E+13	7.30E+14								8.00E+12
1970	1.20E+15	2.30E+14	7.10E+14	1.00E+15	2.20E+14	1.20E+15	4.60E+14	3.80E+12	3.10E+13	1.00E+15								8.00E+12
1971	1.20E+15	4.60E+14	1.30E+15	1.40E+15	2.40E+14	1.30E+15	6.40E+14	9.30E+12	4.60E+13	1.80E+15								8.00E+12
1972	1.20E+15	5.60E+14	1.80E+15	1.10E+15	2.20E+14	1.30E+15	5.00E+14	9.90E+12	4.70E+13	1.90E+15								8.00E+12
1973	7.40E+14	2.80E+14	1.60E+15	1.40E+15	1.70E+14	7.70E+14	5.40E+14	1.10E+13	5.40E+13	2.80E+15								8.00E+12
1974	1.20E+15	3.90E+14	3.50E+14	1.10E+15	1.00E+15	4.10E+15	2.40E+14	8.00E+12	3.80E+13	1.70E+15								8.00E+12
1975	1.40E+15	4.70E+14	3.20E+14	7.60E+14	1.10E+15	5.20E+15	2.10E+14	8.80E+12	3.50E+13	1.80E+15								8.00E+12
1976	1.20E+15	3.80E+14	3.40E+14	7.70E+14	7.40E+14	4.30E+15	1.50E+14	8.80E+12	3.80E+13	1.30E+15								8.00E+12
1977	9.10E+14	4.30E+14	2.90E+14	8.20E+14	6.00E+14	4.50E+15	1.50E+14	7.50E+12	2.90E+13	9.80E+14								8.00E+12

Year	H-3	Sr-90	Zr/Nb-95	Ru-106	Cs-134	Cs-137	Pu-144	Pu-238	Pu-239	Pu-241	An-241	Tc-99	Pm-147	Co-60	Fe-55	Ni-63	I-129	Np-237
1978	1.00E+15	6.00E+14	2.30E+14	8.10E+14	4.00E+14	4.10E+15	1.00E+14	1.20E+13	4.60E+13	1.80E+15	7.90E+12	1.80E+14						
1979	1.20E+15	2.50E+14	1.60E+14	3.90E+14	2.40E+14	2.60E+15	8.30E+13	1.20E+13	3.80E+13	1.50E+15	7.80E+12	4.30E+13						
1980	1.30E+15	3.50E+14	1.60E+14	3.40E+14	2.40E+14	3.00E+15	3.70E+13	6.90E+12	2.00E+13	7.30E+14	8.20E+12	5.70E+13						3.00E+11
1981	2.00E+15	2.80E+14	3.30E+14	5.30E+14	1.70E+14	2.40E+15	1.70E+13	5.00E+12	1.50E+13	6.00E+14	8.80E+12	5.80E+12						3.00E+11
1982	1.80E+15	3.20E+14	5.20E+14	4.20E+14	1.40E+14	2.00E+15	2.20E+13	4.70E+12	1.60E+13	4.80E+14	6.40E+12	3.60E+12	3.20E+12	1.10E+12	9.00E+11	5.00E+11		
1983	1.80E+15	2.00E+14	6.00E+14	5.50E+14	8.90E+13	1.20E+15	2.40E+13	2.90E+12	8.70E+12	3.30E+14	2.20E+12	4.40E+12	2.50E+12	1.70E+12	1.10E+12	1.10E+12		
1984	1.60E+15	7.20E+13	4.70E+14	3.50E+14	3.50E+13	4.30E+14	9.00E+12	2.60E+12	8.30E+12	3.50E+14	2.30E+12	4.30E+12	7.70E+12	1.30E+12	9.00E+11	1.50E+12		3.00E+11
1985	1.10E+15	5.20E+13	4.60E+13	8.10E+13	3.00E+13	3.30E+14	5.00E+12	8.00E+11	2.60E+12	8.10E+13	1.60E+12	1.90E+12	5.90E+12	2.30E+12	7.00E+11	4.00E+11		2.00E+11
1986	2.20E+15	1.80E+13	1.50E+13	2.80E+13	1.30E+12	1.80E+13	1.30E+12	6.20E+11	2.00E+12	6.30E+13	1.30E+12	6.60E+12	2.70E+12	1.50E+12	5.00E+11	1.00E+12	1.20E+11	4.00E+11
1987	1.40E+15	1.50E+13	1.30E+13	2.20E+13	1.20E+12	1.20E+13	3.90E+12	3.50E+11	9.70E+11	3.20E+13	6.50E+11	3.60E+12	3.10E+12	1.40E+12	3.00E+11	1.30E+12	1.00E+11	2.30E+11
1988	1.70E+15	1.00E+13	9.80E+12	2.40E+13	9.50E+11	1.30E+13	3.20E+13	3.80E+11	1.00E+12	3.60E+13	7.50E+11	4.20E+12	2.30E+12	9.60E+11	2.50E+12	3.20E+12	1.30E+11	2.80E+11
1989	2.10E+15	9.20E+12	1.10E+13	2.50E+13	1.70E+12	2.90E+13	3.80E+12	3.10E+11	9.00E+11	3.00E+13	1.10E+12	6.10E+12	3.60E+12	1.70E+11	2.40E+11	2.50E+12	1.70E+11	4.00E+11
1990	1.70E+15	4.20E+12	6.80E+12	1.70E+13	1.20E+12	2.40E+13	2.00E+12	2.90E+11	8.40E+11	3.20E+13	7.50E+11	3.80E+12	3.10E+12	1.70E+12	1.70E+11	3.00E+11	1.10E+11	2.30E+11
1991	1.80E+15	4.10E+12	1.20E+13	1.90E+13	7.60E+11	1.70E+12	2.60E+11	8.20E+11	3.00E+13	7.40E+11	3.00E+13	7.40E+11	3.90E+12	1.30E+12	9.00E+10	1.20E+11	1.60E+11	2.90E+11
1992	1.20E+15	4.20E+12	1.00E+13	1.30E+13	8.30E+11	1.50E+13	1.70E+12	2.40E+11	6.90E+11	2.50E+13	5.40E+11	3.20E+12	1.20E+12	7.00E+10	1.30E+11	8.00E+10	7.00E+10	1.80E+11
1993	2.30E+15	1.70E+13	6.30E+12	1.70E+13	1.20E+12	2.20E+13	2.50E+12			3.80E+13	8.70E+11	6.10E+12	1.70E+12	9.00E+10	1.00E+11	1.30E+11	1.60E+11	3.90E+11
1994	1.70E+15	2.90E+13	2.10E+12	6.70E+12	6.10E+11	1.40E+13	8.40E+11			1.40E+13	3.80E+11	7.20E+13	5.40E+11	1.10E+11	9.00E+10	4.00E+11	4.00E+11	3.30E+11
1995	2.70E+15	2.80E+13	3.40E+11	7.30E+12	5.10E+11	1.20E+13	1.10E+12			7.70E+12	1.10E+11	1.90E+14	6.10E+11	1.30E+12	4.00E+10	4.10E+11	2.50E+11	1.80E+11
1996	3.00E+15	1.60E+13	5.20E+11	9.00E+12	2.70E+11	1.00E+13	7.80E+11			4.40E+12	7.00E+10	1.50E+14	4.20E+11	4.30E+11	4.00E+10	3.40E+11	4.10E+11	4.00E+10

Discharge activities refer to the year of discharge and are not decay-corrected

**A 7 : Table of principle decay energies for the Nirex priority radioisotopes**

Isotope	Half Life	Alpha energy MeV	Beta E <sub>ave</sub> keV	Gamma energy keV	Other
<sup>3</sup> H	12.28 y		5.7 (100)		
<sup>10</sup> Be	1.6 x 10 <sup>6</sup> y		203 (100)		
<sup>14</sup> C	5730 y		49 (100)		
<sup>35</sup> S	87.44 d		48.8(100)		
<sup>36</sup> Cl	3.01 x 10 <sup>5</sup> y		251 (99)		
<sup>41</sup> Ca	1.3 x 10 <sup>5</sup> y				E.C.
<sup>51</sup> Cr	27.20 d			320 (9.8)	E.C.
<sup>54</sup> Mn	312.7 d			835 (100)	
<sup>55</sup> Fe	2.7 y				E.C.
<sup>58</sup> Co	70.80 d			811 (99.4)	$\beta^+$
<sup>60</sup> Co	5.27 y		95.8 (99.9)	1173 (100)	
				1332 (100)	
<sup>59</sup> Ni	7.5 x 10 <sup>4</sup> y				E.C.
<sup>63</sup> Ni	100 y		17.1 (100)		
<sup>65</sup> Zn	244.4 d			1116 (50.7)	$\beta^+$
<sup>79</sup> Se	6.5 x 10 <sup>4</sup> y		52.2 (100)		
<sup>89</sup> Sr	50.6 d		583 (100)		
<sup>90</sup> Sr	28.6 y		196 (100)		
<sup>91</sup> Y	58.51 d		604 (99.7)		
<sup>93</sup> Zr	1.53 x 10 <sup>6</sup> y		19.5 (100)		
<sup>95</sup> Zr	64.02 d		109 (55.4)	724 (43.7)	
			120 (43.7)	757 (55.3)	
<sup>93m</sup> Nb	14.6 y				i.t.
<sup>94</sup> Nb	2.03 x 10 <sup>4</sup> y		146 (100)	871 (100)	
				703 (100)	
<sup>95</sup> Nb	35.06 d		43.4 (100)	766 (99.8)	
<sup>93</sup> Mo	3.5 x 10 <sup>3</sup> y				E.C.
<sup>99</sup> Tc	2.13 x 10 <sup>5</sup> y		84.6 (100)		
<sup>103</sup> Ru	39.35 d		30 (6.4)	497 (88.9)	
			63.2 (90.0)	610 (5.6)	
			239(3.5)		

Isotope	Half Life	Alpha energy MeV	Beta E <sub>ave</sub> keV	Gamma energy keV	Other
<sup>106</sup> Ru	368.2 d		10.0 (100)		& from Rh-106
<sup>107</sup> Pd	6.5 x 10 <sup>6</sup> y		9.27 (100)		
<sup>108m</sup> Ag	127 y			434 (89.9) 614 (90.4) 723 (90.5)	
<sup>121m</sup> Sn	55 y		27.2 (22.4)		
<sup>126</sup> Sn	1 x 10 <sup>5</sup> y		70 (100)		γ from daughter
<sup>129</sup> I	1.57 x 10 <sup>7</sup> y		40.9 (100)	39.6 (7.5)	
<sup>131</sup> I	8.04 d		192 (89.4)	numerous	
<sup>134</sup> Cs	2.06 y		2.3 (27.4) 12.3 (2.5)	605 (97.6) 796 (85.4)	
			210 (70.1)		
<sup>135</sup> Cs	2.3 x 10 <sup>6</sup> y		56.3 (100)		
<sup>137</sup> Cs	30.2 y		157 (94.6)		γ from daughter
<sup>144</sup> Ce	284.3 d		50.2 (19.6) 91.1 (77.2)	134 (10.8)	+ high energy β from daughter
<sup>147</sup> Pm	2.62 y		62.0 (100)		
<sup>151</sup> Sm	90 y		19.7 (99.1)		
<sup>154</sup> Eu	8.8 y		176 (36.5) 276 (17.4) 695 (11.4)	123 (40.5) + others	
<sup>182</sup> Ta	115 d		129 (21.0) 157 (40.0) 181 (3.2)	100 (14.0)	
<sup>210</sup> Pb	22.3 y		4 (80) 16 (20)	46.5 (4.1)	
<sup>210</sup> Po	138.4 d	5.30 (100)			
<sup>226</sup> Ra	1600 y	4.78 (94.6)		186 (3.28)	
<sup>229</sup> Th	7340 y	4.85 (56.3) + others		numerous low yield	
<sup>230</sup> Th	7.7 x 10 <sup>4</sup> y	4.62 (23.4) 4.69 (76.2)			

Isotope	Half Life	Alpha energy MeV	Beta E <sub>ave</sub> keV	Gamma energy keV	Other
<sup>232</sup> Th	$1.41 \times 10^{10}$ y	3.95 (23) 4.01 (77)			
<sup>231</sup> Pa	$3.28 \times 10^4$ y	5.01 (25) + numerous other			
<sup>233</sup> U	$1.59 \times 10^5$ y	4.78 (13) 4.83 (80.4)			
<sup>234</sup> U	$2.45 \times 10^5$ y	4.72 (27.4) 4.78 (72.4)			
<sup>235</sup> U	$7.02 \times 10^8$ y	4.36 (11) 4.40 (55.0)			
<sup>236</sup> U	$3.42 \times 10^6$ y	4.46 (26.0) 4.49 (74.0)			
<sup>238</sup> U	$4.47 \times 10^9$ y	4.15 (27.0) 4.20 (76.7)			
<sup>237</sup> Np	$2.14 \times 10^6$ y	4.77 (25) 4.79 (47.1)			
<sup>238</sup> Pu	87.75 y	5.46 (28.3) 5.50 (71.6)			
<sup>239</sup> Pu	$2.4 \times 10^4$ y	5.10 (12) 5.14 (15) 5.16 (73.3)			
<sup>240</sup> Pu	6537 y	5.12 (26.4) 5.17 (73.4)			
<sup>241</sup> Pu	14.4 y		5.23 (100)		
<sup>242</sup> Pu	$3.76 \times 10^5$ y	4.86 (22.4) 4.90 (78.5)			
<sup>241</sup> Am	432.2 y	5.44 (12.8) 5.49 (83.2)		59.8 (35.7)	
<sup>242m</sup> Am	152 y				i.t.
<sup>243</sup> Am	7380 y	5.28 (87.9)			
<sup>242</sup> Cm	163.2 d	6.07 (25.9) 6.11 (74.1)			
<sup>243</sup> Cm	28.5 y	5.74 (11.5) 5.79 (72.9)			

Isotope	Half Life	Alpha energy MeV	Beta E <sub>ave</sub> keV	Gamma energy keV	Other
<sup>244</sup> Cm	18.11 y	5.76 (23.6) 5.81 (76.4)			
<sup>245</sup> Cm	8500 y	5.30 (5.0) 5.36 (93.2)			
<sup>246</sup> Cm	4750 y	5.34 (21.0) 5.39(79.0)			

From Radioactive Decay Tables, D.C. Kocher (1981)

DOE/TIC - 11026 Technical Information Centre U.S. Department of Energy, Washington D.C.

E.C. - electron capture       $\beta^+$  - positron emission

i.t. - isomeric transition

SOUTHAMPTON UNIVERSITY LIBRARY

USER'S DECLARATION

AUTHOR: *Wauk P.E.*

**TITLE:**

1998-02-24 10:00:00

1920-1921

DATE:

I undertake not to reproduce this thesis, or any substantial portion of it, or to quote extensively from it without first obtaining the permission, in writing, of the Librarian of the University of Southampton.

To be signed by each user of this thesis